

An Integrated Approach for Paleo-Ice Stream Determination in Mid Continental Prairies, Saskatchewan, Canada

by

Roberta S. Adams

A thesis
presented to the University of Waterloo
in fulfillment of the
thesis requirement for the degree of
Master of Science
in
Earth Sciences

Waterloo, Ontario, Canada, 2009

© Roberta S. Adams 2009

Author's Declaration

I hereby declare that I am the sole author of this thesis. This is a true copy of the thesis, including any required final revisions, as accepted by my examiners.

I understand that my thesis may be made electronically available to the public.

Abstract

Ice stream research has gained momentum in the last decade due to the increased need to understand ice sheet dynamics and instability and, by extension, the role ice streams have on climate change and sea level rise. Although significant progress has been made recently in understanding the role of ice streams in ice sheet dynamics, much remains to be done for documenting and understanding paleo-ice stream records. This is especially true for terrestrial paleo-ice streams like those that operated in the southwest Laurentide Ice Sheet. In previous studies evidence was shown for at least two large paleo-ice stream systems in southern Saskatchewan and a model was proposed involving major glacial dynamics shifts during the Late Wisconsinan linked to ice streaming in the Prairies. The goal of this research is to further characterize drift provenance and to verify sediment-landform assemblages that are central to the proposed reconstruction. This is done through spatial analysis of sediment and landform characteristics (e.g. compositional data, till fabric, landform identification). Provenance is also investigated using radiometric data and $^{40}\text{Ar}/^{39}\text{Ar}$ dating of hornblende grains. All of the data are geo-referenced in GIS to examine the spatial relationships. Results show spatially consistent patterns that fit within the structure of the proposed ice stream model. Ten assemblages were delineated, some showing landform evidence of southwestern and southeastern flow, while others show an older western signature through compositional data. The ice flow dynamics were characterized by a combination of landform evidence and compositional data, where three distinct ice flow phases can be seen. Of these three flow phases, two can be characterized by paleo-ice streams. The older south westward Maskwa system flowed against the regional slope, creating a large area of mega-scale glacial lineations, as well as transverse ridges, and was bound on either side by hummocky terrain. The preservation of the southwest Maskwa system was due to the abrupt shift to the southeastward Buffalo system. The Buffalo system captured the subglacial water from the Maskwa causing its shutdown, which fed the James Lobe until it collapsed. The Buffalo paleo-ice stream was the youngest and least stable of the two systems, as shown in the cross-cutting landform evidence. This approach combines multiple methods of analysis to go beyond the geomorphologic evidence to test the main underlying assumptions of paleo-ice stream landsystem models. This is critical if we are to understand the processes involved in the formation of paleo-ice streams and to reconstruct their evolution. Further

characterization of the paleo-ice stream systems in the Prairies is critical to improve our understanding of how large ice sheets, like the Laurentide Ice Sheet, evolved and eventually collapsed.

Acknowledgements

I would like to thank my supervisor Martin Ross for his guidance and feedback over the course of this Master's thesis. I would like to acknowledge the help of Janet Campbell (formerly of the Northern Saskatchewan Geological Survey) for her extensive help and guidance in local knowledge and research, as well as her generous help in the field. I would also like to thank my thesis committee members, Dr. Sidney Hemming and Dr. Tom Edwards.

Dedication

I would like to dedicate this to my family and friends, who have been supportive over the whole Masters processes, especially the writing of the thesis. Thank you:

- Mom and Dad (Marty and Helene)
- Steve
- Josh and Alisha
- Sarah, Jackie and Amanda
- Rm 1007: Dale, Lily, Eric and Matt

Table of Contents

Table of Contents	vii
List of Figures.....	xi
List of Tables.....	xx
Chapter 1 Introduction.....	1
1.1 Modern ice streams.....	1
1.1.1 Ice stream types and their links to climate change and sea level	3
1.2 Paleo-ice stream research	4
1.2.1 Mega-scale glacial lineations (MSGs)	6
1.2.2 Sticky spots	6
1.3 Paleo-ice stream record of Saskatchewan	7
1.3.1 Previous work in the Prairies.....	7
1.4 Thesis objectives and hypothesis	11
Chapter 2 Methodology	14
2.1 Surficial Landscape Analysis	14
2.2 Fabric and Striation Measurements	15
2.3 Pebble Lithology	16
2.4 Grain Size and Hydrometer Analysis	17
2.5 Geochemistry	19
2.6 ⁴⁰ Ar/ ³⁹ Ar Hornblende Dating.....	19
2.7 Geodatabase.....	20
Chapter 3 Sediment-Landform Assemblages	21
3.1 Previous Glacial Geomorphology Research in Saskatchewan	21
3.1.1 The role of Bedrock Geology	21
3.1.2 Landforms	22
3.1.3 Internal characteristics	26
3.2 Paleo-ice Stream (PIS) Criteria.....	27
3.2.1 Application to Saskatchewan	29
3.3 Sediment Fabrics	54
3.4 Striations and Beddings	60

3.5 Summary of the landscape analysis	61
3.5.1 Characteristic Shape and Dimensions.....	61
3.5.2 Rapid Velocity	63
3.5.3 Abrupt Lateral Margins and Shear Margin Moraines	64
3.5.4 Inter-Ice Stream Areas	64
Chapter 4 Till Provenance: Compositional Data and Detrital Ages	65
4.1 Till Composition	65
4.1.1 Carbonate Chemistry	69
4.1.2 Ca/Al and Mg/Al ratios.....	73
4.1.3 Pebble Lithology.....	73
4.2 Airborne Radiometric Survey.....	75
4.3 ⁴⁰ Ar/ ³⁹ Ar dating.....	78
4.4 Summary	83
Chapter 5 Interpretation and Discussion	84
5.1 Westward Ice Flow Phase	84
5.1.1 Dispersal of Omars	84
5.1.2 Dispersal of Carbonates	86
5.1.3 Other Evidence and Supporting Data	87
5.2 Southwestward Ice Flow Phase	88
5.2.1 Summary of evidence	88
5.2.2 The Maskwa paleo-ice stream	88
5.3 Southeastward Ice Flow Phase	93
5.3.1 The Buffalo paleo-ice stream	93
5.4 Shift between Maskwa and Buffalo Systems	98
Chapter 6 Conclusion	102
6.1 The subglacial landscape of the southern Interior Plains	102
6.2 Thesis Contributions	105
6.3 Implications of Work.....	107
References	109

Appendix

Appendix A Site Data	130
Site # 1 RD 642 01.....	130
Site # 2 Battleford 01.....	132
Site # 3 Birch Lake 01.....	133
Site # 4 Cutknife 01.....	135
Site # 5 Dana 01.....	137
Site # 6 Glaslyn 01	137
Site # 7 Hepburn 01.....	139
Site # 8 Hwy 02 01	141
Site # 9 Hwy 13 01	141
Site # 10 Hwy 14 to Biggar.....	143
Site # 11 Hwy 15 02	145
Site # 12 Hwy 21 01	147
Site # 13 Hwy 52 01	149
Site # 14 Maymont 01	149
Site # 15 Moose 01A.....	150
Site # 16 Moose 02	150
Site # 17 Moosomin 01.....	151
Site # 18 North B 01.....	153
Site # 19 Qu'Appelle 01	155
Site # 20 RD 304 01.....	155
Site # 21 RD 602 01.....	157
Site # 22 RD 687 01.....	159
Site # 23 RD 734 01.....	159
Site # 24 RD 787 02.....	161
Site # 25 RD 26 Good Sect	163
Site # 26 RD 26 Cln Rd Cut.....	163
Site # 27 St Benedict 01.....	165
Site # 28 Sweetgrass 01	167

Site # 29 West of 6	168
Site # 30 Yorkton 01	169
Site # 31 Griffin B and F.....	170
Appendix B Laboratory Data	172
Appendix C Bedrock Geology.....	201
Appendix D Methodology	203

List of Figures

Figure 1.1: Digital Elevation Model of Saskatchewan, showing the location of various cities within the province. The simple unaltered DEM image shows a very dynamic landscape.	8
Figure 1.2: Numbered field site locations (yellow dots) over DEM image of Saskatchewan.....	12
Figure 3.1: Names and locations of potential paleo-ice stream corridors in Saskatchewan.	23
Figure 3.2: Topographic controls in Saskatchewan. Manitoba Escarpment and Missouri Coteau form a series of steps in Prairies, towards the Rocky Mountains. The Buffalo paleo-ice stream was bound by these features at certain times over its life cycle. Blue dashed lines delineate the boundaries of these features.	24
Figure 3.3: MSGs are naturally subdued features. Some areas of MSGs are even more subdued because they are buried by younger sediments, for example, the MSGs in the western limb of the Buffalo Corridors is buried by Glacial Lake Regina glaciolacustrine sediments. These are best seen with DEM images and are not readily visible in air photos (Slimmon, 2007).....	25
Figure 3.4: Maskwa Paleo-ice Stream is delineated by red dashed lines, and inter-ice stream areas (or assemblages) are delineated in white dashed lines. The Maskwa system is over 900 km long, and the MSGs are concentrated and preserved between the red boundaries. The system is discontinuous due to cross-cutting by younger paleo-ice streams (discussed later). It is hummocky terrain, and black numbers are assemblage numbers.....	30
Figure 3.5: Maskwa paleo-ice stream along assemblages 6 and 7. Red arrows point to landform evidence of a continuation of the Maskwa southwest flow across the Battleford Corridor between assemblages 6 and 7, that was later cross cut by the Battleford paleo-ice stream system. Black arrows point to ice flow convergence into the Maskwa system.....	31
Figure 3.6: Assemblage 5's transverse ridges (blue lines) are evidence of the terminal zone of Maskwa system. These are glacial thrust features that may be moraines. MSGs are found in the northern portion of the assemblage, but are discontinuous like those of assemblages 6 and 7.....	34

Figure 3.7: Siple Coast Ice Streams, West Antarctica. Tributaries (blues and purples, slower velocities) can be seen feeding wide corridors of ice streams (reds and pinks, higher velocities). This morphology is analogous to Buffalo paleo-ice stream system. Letters indicate Ice Stream name (Joughin and Tulaczyk, 2002). 35

Figure 3.8: Smaller and narrower corridors feed into the larger and wider Buffalo Corridor. Black arrows represent ice flow from tributaries to main corridor. Continuous streamlined features are evidence of convergent flow, as tributaries enter into the Buffalo system. This is consistent with PIS criteria of tributary-type flow patterns and convergent flow patterns. 37

Figure 3.9: Lateral shear margin moraines (as outlined by the black arrows) are found along the boundary of the Buffalo Corridor, and were previously mapped as ridged moraines. Classical lateral shear margin shape is narrow, so their genesis as lateral shear margin moraines is either polymodal or time-transgressive. Polymodal genesis suggests the moraine was originally pristine but surging of the Weyburn lobe (western limb of the Buffalo system, that later became Glacial Lake Regina) reworked the margin. Time-transgressive genesis is due to the dynamics of the Buffalo system, its instability resulted in changing ice flow margins and this feature could be due to multiple margin formations. 38

Figure 3.10: Basin Lake Ridge is a lateral shear margin moraine that spans over 170km, and is delineated by the black arrows. The neighboring "palimpsest" terrain (transverse ridges) is outlined in orange, and is likely a "sticky spot" along the Buffalo Corridor, due to the large amount of erosion that took place (older landforms are most likely not preserved). Assemblage 2 is outlined, showing southwest-trending landforms. This is most likely the oldest relict landscape in the area. Basin Lake Ridge migration is found in this assemblage as well (red arrows)..... 39

Figure 3.11: Transverse ridges similar in morphology, found along the Buffalo Corridor (orange outlines). These are most likely "sticky spots" caused by increased friction along the subglacial bed, rather than palimpsest terrain, which would not have been possible with the high erosion that took place along the Buffalo Corridor..... 41

Figure 3.12: (a) Assemblage 3a and (b) Assemblage 3b. Both are topographic highs and show little to no landform evidence suggest ice flow direction. These may have been inter-ice stream sticky spots. 42

Figure 3.13: Red Deer Hill (with boulder striation measuring 225°, purple arrow) and Prince Albert late glacial lobes. The Red Deer Hill (-hole pair) does not suggest ice streaming but is consistent with ice flow, just like the boulder striations are consistent with surrounding landform evidence in the Buffalo Corridor. 43

Figure 3.14: Red dashed lines show ice margin migration of the Buffalo Corridor. Most likely migrated to the west as the paleo-ice stream became thinner. Like the Basin Lake Ridge, these features are consistent with PIS criteria of abrupt lateral margins. 45

Figure 3.15: Dirt and Cactus Hills are ice thrust features found along the Missouri Coteau, formed during multiple lateral ice thrust events by the Buffalo paleo-ice stream. Yellow line outlines the thrust structures. 46

Figure 3.16: Assemblage 1, bound between Churchill Corridor and the Molanosa Corridor. There are two sets of lineations; the older set trends southwest (consistent with Maskwa) and the younger trends southeast (consistent with Buffalo). 47

Figure 3.17: Assemblage 4 is an assemblage of genetically unrelated features, which are mostly bedrock-controlled, and were likely preserved due to stagnant ice when the Buffalo system was active. 48

Figure 3.18: Assemblage 8 shows southwest trending ice flow, possibly ice streaming, along the Primrose and Cold Lake area (black arrows). This area is also a topographic high. 49

Figure 3.19: Assemblage 9 and 10, show little landform evidence of ice flow, save a few in Assemblage 9, which suggest the Buffalo paleo-ice stream was unstable and shifted between its topographic bounds (Manitoba Escarpment and Missouri Coteau). Both are topographic highs covered in hummocky terrain. 50

Figure 3.20: Google Maps photo of North Battleford. Fluting field is easily recognized from air photos. From Google Maps (2009)..... 52

Figure 3.21: Battleford fluting fields, delineated in red, within the Battleford Corridor. Streamline features exist throughout the corridor when seen in the DEM. Black arrows are Stauffer et al. (1990) air photo measurements and boulder striations (127° and 115° , respectively) and the blue is the fluting direction determined from DEM analysis (132°). The directions are very similar, with difference in fluting direction being a factor of site selection..... 53

Figure 3.22: (a) Example of fabric classification based on A-axis and AB plane directions; (b) Field site ‘Rd 304-01’ classified as strong fabric but fabric direction is inconsistent with surrounding landforms, and maybe be remnant of older flow, or due to poor pebble conditions; (c) Field site ‘Hepburn 01’ is classified as a good fabric, but is inconsistent with landform evidence. .. 57

Figure 3.23: AB plane data for all field sites where ‘strong’ and ‘good’ fabric measurements were taken. Black arrows indicate ‘strong’ fabric classification/direction, and dash-lines indicate ‘good’ fabric classification/direction. AB plane data is used to avoid transverse orientations of pebbles. 58

Figure 3.24: A-axis data for all field sites where ‘strong’ and ‘good’ fabric measurements were taken. Black arrows indicate ‘strong’ fabric classification/direction, and dash-lines indicate ‘good’ fabric classification/direction. 59

Figure 3.25: Striations data from literature; Stauffer et al. (1990) for the Maymont area (115°) and Christiansen and Sauer (1993) for the Red Deer Hill (225°). 60

Figure 3.26: Striation measurements from field work. Samples are more consistent with landform evidence than till fabrics, because till fabric conditions throughout the province are not ideal whereas boulder measurements are only selected if boulder is elongated, flat-topped and lodged. 61

Figure 3.27: Boulder pavement found at field site Rd 642 01, west of Regina. 11 boulders were freshly exposed along the youngest till, with an average direction of $114\pm 10^{\circ}$; this is consistent with the landform evidence along the Buffalo Corridor. 62

- Figure 4.1: Carbonate source in Manitoba and northeastern Saskatchewan, and the carbonate distribution from the Thorleifson and Garrett (1993) database. There is a stronger carbonate signal with proximity to the source. There is a lower carbonate signature in Alberta and in corridors with western source regions, such as the Battleford paleo-ice stream system..... 69
- Figure 4.2: Site #31 (Griffin 01), with two visible till units within the Buffalo paleo-ice stream corridor. Younger Battleford till lacks staining and jointing, where the older Floral Formation is weathered and jointed..... 72
- Figure 4.3: Site #21 (Rd 602 01), also within the Buffalo Corridor. Only one till was exposed. Based on field observations (no jointing or staining) and local boreholes, this is Battleford Till at this location..... 72
- Figure 4.4: Ca/Al ratios used to determine crystalline to carbonate sources. Higher ratios suggest carbonate sources, to the west and preserved in assemblages 2, 9 and 10. Ca/Al ratio is consistent with the Mg/Al ratio, where the higher ratios are preserved in assemblages 2, 9 and 10, as well as along the eastern limb of the Buffalo Corridor..... 74
- Figure 4.5: Pebble lithology from 2mm+ fraction. Higher concentration of crystalline pebbles to the north and more clastic pebbles to the south. Carbonate pebble distribution is consistent with carbonate content and geochemistry ratios..... 75
- Figure 4.6: The distribution of eTh/K (ppm/%) values over the Canadian Shield and the SRTM elevation model over the Interior Plains. Two regional dispersal trains are clearly visible. The approximate centre-line of the Maskwa paleo-ice stream is indicated by the thick black dashed line with the arrow indicating ice flow direction (Ross et al., 2009). 77
- Figure 4.7: Geological provinces used for provenance determination of hornblende grains. Superior Province is Archean in age and the Churchill province is Paleoproterozoic. 78
- Figure 4.8: Field sites (numbered) where samples had hornblende grains $^{40}\text{Ar}/^{39}\text{Ar}$ dated. Some Archean aged grains are found within the Maskwa Corridor but are mostly Paleoproterozoic in age. Minimal to no Archean aged grains are found within Assemblage 2, the Battleford and Buffalo Corridors. The difference in the amount of Archean-aged grains in the southeastern

portion of the province between sites #16 and 21 demonstrates potential for preservation of previous ice flow in inter-ice stream areas.	80
Figure 4.9: Assemblages where an Archean signature is possible due to known ice flow directions (from the Keewatin ice dome) are those found south of the extended boundary between the Churchill and Superior provinces, as delineated by red dashed line.	81
Figure 5.1: Westward dispersal of carbonates from source area in Manitoba.	86
Figure 5.2: Westward shift of Archean-aged grains from Superior Province. Signature preserved in assemblages with more abundant Archean-aged grains.	87
Figure 5.3: Southwest-trending MSGs in Primrose and Cold Lake area, cross-cut by Battleford Corridor and extending into Alberta. More work needs to be done to delimit extent but initial observations suggest the possibility it is contemporaneous to the Maskwa paleo-ice stream. Black arrows follow MSGs.....	89
Figure 5.4: Conceptual Model where Maskwa paleo-ice stream created transverse ridges north of the Cypress Hills. (a) In the terminal zone of the Maskwa system (Assemblage 5), transverse ridges are perpendicular to ice flow, and are created when ice thrusts till to create stacks; (b) Continuous surging creates thick sequences of stacked tills throughout the assemblage; (c) A simplified bird's eye view of the Maskwa system shows similarities to the time-transgressive model for terrestrial ice streams in Stokes and Clark (1999). However this new model expects there to be thrust ridges due to the regional slope and surges, while hummocky terrain represents almost stagnant conditions outside of the corridor during ice streaming.....	92
Figure 5.5: Fan-shaped dispersal of carbonates due to reworking of till by two separate ice flow events. The first was the westward flow, and then followed by the south-eastward flow, that decreased the carbonate content along the western limb of the Buffalo paleo-ice stream....	95
Figure 5.6: Similar fan dispersal pattern as seen with the carbonate content, the carbonate pebble lithology is higher in the southeast due to proximity to source and reworking of the till. High abundance of crystalline lithology is found along the Maskwa paleo-ice stream.	96

Figure 5.7: Lack of Archean-aged grains found within the Battleford Corridor is consistent with landform evidence suggesting southeastern flow along the corridor, into the Buffalo system. Yellow area shows ice flow direction along Battleford Corridor based on landform evidence. 97

Figure 5.8: Conceptual model of the shift between Maskwa and Buffalo paleo-ice stream systems. (a) at LGM the Maskwa paleo-ice stream was flowing southwest, and the James Lobe was fed by a system in Manitoba; (b) around 14 ¹⁴C ka BP the ice sheet had thinned and regional flow patterns changed to the southeast, changing the catchment area for the James Lobe, thus initiating the Buffalo system in Saskatchewan; (c) by 13.5 ¹⁴C ka BP, inter-ice stream areas had developed and the Maskwa system was shut off due to the Buffalo system capturing its subglacial water, and thus stagnating it and preserving the landscape; (d) the last major surge of the James Lobe happened around 12.5 ¹⁴C ka BP, and at this time the eastern limb had captured most of the subglacial water from the western limb, causing it to develop into a outlet lobe, while the western tributaries continued to feed the whole Buffalo system. 100

Figure A. 1: RD 642 01, linear feature, west of Regina SK. Boulder pavement divides younger Battleford till from older Floral Formation. 130

Figure A. 2: One of eleven boulders, creating a pavement, with striations in the 114° direction..... 130

Figure A. 3: Linear feature along the Maskwa Corridor. 132

Figure A. 4: Subdued feature along the Maskwa Corridor..... 133

Figure A. 5: Linear feature along the Maskwa Corridor, few kilometers long. 135

Figure A. 6: Large exposure within Assemblage 2..... 137

Figure A. 7: Subdued linear feature transverse to flow along the Maskwa Corridor. 137

Figure A. 8: Long attenuated landforms along the Buffalo Corridor..... 139

Figure A. 9: Subdued landform, part of extensive field in Assemblage 2, trending southwest..... 141

Figure A. 10: Exposure along road, in southeastern limb of Buffalo Corridor. 141

Figure A. 11: Railway cut through lineation in Maskwa Corridor.	143
Figure A. 12: Subdued landform west of Assemblage 9 in the Buffalo Corridor.	145
Figure A. 13: Located on the edge of Assemblage 7 boundary with Battleford Corridor.	147
Figure A. 14: Subdued landforms along Assemblage 9.	149
Figure A. 15: Elongated features along the Battleford Corridor.	149
Figure A. 16: Hummocky terrain on Moose Mountain.	150
Figure A. 17: Large exposure of hummocky terrain, Moose Mountain.	150
Figure A. 18: Dugout outside of Moosomin, SK, south eastern limb of Buffalo Corridor. Some exposed boulders were found and striations measured.	151
Figure A. 19: Dugout outside of North Battleford, SK.	153
Figure A. 20: Large exposure at top of Qu'Appelle Valley, southwest of Melville.	155
Figure A. 21: Northern most field site, along Maskwa Corridor in Assemblage 7.	155
Figure A. 22: Subdued landforms along southwestern limb of Buffalo Corridor.	157
Figure A. 23: Large exposure along Maskwa Corridor.	159
Figure A. 24: Subdued ridges north of Regina.	159
Figure A. 25: Elongated ridge along Maskwa Corridor.	161
Figure A. 26: Large exposure along the Maskwa Corridor.	163
Figure A. 27: Subdued elongated feature along Maskwa Corridor.	163
Figure A. 28: Exposure west of Basin Lake Ridge in Assemblage 2.	165
Figure A. 29: Exposure along Maskwa Corridor.	167
Figure A. 30: Shale bedrock fragments (yellow arrows) found in till, southwestern Buffalo Corridor.	168

Figure A. 31: Drumlinoid feature in Buffalo Corridor with large sand deposits.	169
Figure A. 32: Two exposed tills along Buffalo Corridor.	170
Figure B. 1: Modality Classification Curve, from Evans et al. (2007)	181
Figure B. 2: Ternary Plot classification for fabrics, from Evans et al. (2007).	181
Figure B. 3: A/B Plane Modality.	182
Figure B. 4: A-axis modality.	182
Figure B. 5: Ternary Plot of A/B plane data.	183
Figure B. 6: Ternary Plot of A-axis data.	183
Figure C. 1: Bedrock Geology of Saskatchewan.....	201

List of Tables

Table 1.1: Geomorphological criteria for identifying former ice streams. Modified from Stokes and Clark (1999).....	5
Table 3.1: Saskatchewan Stratigraphy and associated Carbonate Content. Modified from Barendregt et al (1998), Christiansen and Sauer (2001).	27
Table 3.2: Paleo-ice Stream Criteria, Characteristic Dimensions of Mega-scale Glacial Lineations found in southcentral Saskatchewan. (E) Eastern limb of the Buffalo Corridor, (W) Western limb of the Buffalo Corridor, (N) north of Assemblage 9.	51
Table 3.3: Paleo-ice Stream Criteria, Characteristic Dimensions of Ice Stream Corridors found in southcentral Saskatchewan. (E) Eastern limb of the Buffalo Corridor, (W) Western limb of the Buffalo Corridor, (S) south of the Canada-U.S. Border. Width varies across the ice stream and thus given as a range from largest to smallest.	54
Table 4.1: Till composition, pebble lithology and geochemistry ratios for all field sites.....	67
Table 4.2: $^{40}\text{Ar}/^{39}\text{Ar}$ field site data. Amount of grains tested and their ages, as well as their ratios and average ages.	82
Table 5.1: Regional chronology based on geomorphology, Dyke (2003) radiocarbon chronology, and mosaic landsystem model.	85
Table A. 1: Fabric data for field site #1.	131
Table A. 2: Fabric data for field site #3.	133
Table A. 3: Fabric data for field site #4.	135
Table A. 4: Fabric data for field site #6.	138
Table A. 5: Fabric data for field site #7.	139
Table A. 6: Fabric data for field site #9.	142

Table A. 7: Fabric data for field site #10.....	143
Table A. 8: Fabric data for field site #11.....	145
Table A. 9: Fabric data for field site #12.....	147
Table A. 10: Fabric data for field site #17.....	151
Table A. 11: Fabric data for field site #18.....	153
Table A. 12: Fabric data for field site #20.....	156
Table A. 13: Fabric data for field site #21.....	157
Table A. 14: Fabric data for field site #23.....	160
Table A. 15: Fabric data for field site # 24.....	161
Table A. 16: Fabric data for field site #26.....	164
Table A. 17: Fabric data for field site #27.....	165
Table A. 18: Fabric data for field site #29.....	168
Table A. 19: Fabric data for field site #31, Battleford till.	171
Table A. 20: Fabric data for field site # 31, Floral Formation till.	171
Table B. 1: Grain size curve values for all sampled sites. Values were determined from seive and hydrometer analysis.	173
Table B. 2: Summary of Fabric Data for all field sites where fabric measurements were taken.	175
Table B. 3: Field sites where only samples were taken.	177
Table B. 4: Field sites where bedding plane measurements or boulder striations were taken. Yorkton and Qu'Appelle field sites do not have samples.	178
Table B. 5: Modality classification from fabric data. Numerical values related to graphing.	179

Table B. 6: Geochemistry Set (1).....	184
Table B. 7: Geochemistry Set (2).....	186
Table B. 8: Geochemistry Set (3).....	188
Table B. 9: Geochemistry Set (4).....	190
Table B. 10: Geochemistry Set (5).....	192
Table B. 11: $^{40}\text{Ar}/^{39}\text{Ar}$ dated hornblend grains, bath results.....	194

Chapter 1 Introduction

1.1 Modern ice streams

Ice streams are areas of fast moving ice within an ice sheet. They have been considered the arteries of an ice sheet, moving large quantities of ice and debris to the ice margin (Bennett, 2003), yet their role in ice sheet stability and dynamics is still not fully understood. Most contemporary ice streams are classified as either “pure” or topographic ice streams. Topographic ice streams (ice streams in deep subglacial valleys or other geologically controlled conditions) flow rapidly due to thermo-mechanical feedback mechanisms (Bamber, 2000). “Pure” ice streams (those not controlled by topography) require a layer of soft deformable sediment or a thin sheet of water to lubricate the ice-bed interface (Bennett, 2003; Stokes and Clark, 1999). Depending on where the ice streams terminate, they can also be classified as either being terrestrial or marine-based.

In Antarctica many ice streams have been identified and it is thought they may contribute to as much as 90% of its drainage (Bamber, 2000). The location and vigor of ice streams is one of the most important controls on the stability of ice sheets (Bennett, 2003). They are typically several hundred kilometers long, tens of kilometers wide and are characterized by rapid flow surrounded by slower flowing ice (Bennett, 2003). Although there have been over two decades of research into ice stream behaviour and mechanisms, some features are still not fully understood, such as rapid changes in ice stream velocity and configuration. However, because direct observation of the ice-bed interface underneath ice streams is not currently possible, many insights may come from the study of formerly glaciated areas. Ice streams in both Antarctica and Greenland have similar characteristics and tributary-type flow systems (Bamber, 2000). It can thus be assumed that former ice sheets also exhibited analogous flow characteristics. By assuming this, analogies between paleo and contemporary ice streams can be made. The accessibility to the subglacial bed of paleo-ice streams makes this a worthwhile endeavour. Stokes and Clark (1999) offered four reasons why finding the locations of former ice streams is important:

- The large ice flux would have had a profound effect on ice sheet configurations, including drainage basins and ice divide locations. This is of great importance with respect to reconstructing ice sheet geometries.

- It is difficult and expensive to study the beds of contemporary ice streams. Former ice stream tracks provide an ideal opportunity to gain information about the processes occurring beneath ice streams.
- Paleo-ice stream interactions with climate are important for both reconstructing past climate change and predicting ice sheet response to future climate change.
- The large sediment flux is comparable with the today's largest fluvial systems. Very large sedimentary submarine fans were often produced at ice stream termini. The structure and stability of these fans have implications for mineral exploration as well as potential geohazards.

Since the early 1980s, there has been a focus on understanding ice stream behaviour. This began because regions of the West Antarctic Ice Sheet were found to have collapsed in the past and “that its retreat since the LGM [Last Glacial Maximum] has been, and may continue to be brought about, by ice streaming” (Stokes et al., 2007). And although many people believe in the significance of ice streams, the comprehension of their behaviour is still a challenge. Researchers noted early on that fast-flowing ice streams could move up to 1000 meters every year despite having no sources of surface water and having a much smaller gravitation pull than most slower moving ice (Clark, 1995). Two mechanisms have been considered to explain such behavior: subglacial “soft” bed deformation and sliding. The process of subglacial deformation was demonstrated by Boulton and Hindmarsh (1987) and further developed by Boulton (1996). R.B. Alley and others (e.g. Alley et al. 1987) demonstrated that this process could account for the fast flow of Ice Stream B in the West Antarctic Ice Sheet. Very weak till was later recovered providing support to this idea (Engelhardt et al. 1990). Laboratory test confirmed that the till is weak enough to deform even under the low shear stresses of Ice Stream B (Kamb, 1991). However, Kamb (1991) argued that, given the highly non-linear till rheology and meltwater production, ice stream velocities must be controlled by “sticky spots” at the bed, otherwise they could flow catastrophically.

Sliding occurs when subglacial porewater pressures are high enough to support the glacier causing extensive decoupling of the ice from its bed (Iverson et al., 1995). A thin distributed drainage system develops at the ice-bed interface. This process leads to a reduction of basal deformation rates and

fast flow is achieved by efficient lubrication and sliding. But the question of how sliding was controlled was still unanswered. It has been shown recently that ice stream shear margins contribute significantly to the overall frictional drag and therefore can control sliding to a certain extent (Raymond et al., 2001)

1.1.1 Ice stream types and their links to climate change and sea level

The majority of paleo-ice streams that are known today, were found by using either satellite imagery or geophysical techniques, and were quantified by one or more forms of research (i.e. geomorphology, sedimentology or modeling). Table 1.1 is some former ice streams and the main lines of evidence used in their identification from Stokes and Clark (1999). The main difference between terrestrial and marine ice streams is the environment in which they terminate. This difference is reflected in their geomorphology (marine ice streams produce offshore sediment accumulation fans). Once the grounding-line of a marine ice streams is inland it is then classified as terrestrial. The hypothetical life cycle of marine and terrestrial ice streams include inception, growth, mature and declining phases. These can be rejuvenated unless ice sheet collapse exceeds a critical threshold (Hughes, 1992). There are four types of land-system signatures produced by paleo-ice streams; isochronous and time-transgressive for both marine and terrestrial ice streams. Currently the majority of paleo-ice streams identified are marine-based. There are few documented paleo-ice streams that are strictly terrestrial. An increase in knowledge and understanding of these terrestrial-based ice streams can provide a more robust example for modern systems. Ice streams have an effect on sea level when they are discharging into the ocean and change the amount of water reserved as ice on land. The relation to climate change is a function of sea level change, but also iceberg release, Heinrich Events and ocean water circulation.

There were other moments which brought ice streaming to the forefront of research; the Andrews et al (1987) and Andrews and Tedesco (1992) papers that discussed the Hudson Strait Ice Stream and how it linked with North Atlantic Heinrich Events were the first to link the importance of ice streaming to climate systems. Other papers soon followed such as Oppenheimer (1998), with stability and climate change scenarios. From this, research regarding effect of ice streaming on ice

sheet stability became in high demand. But to understand what is going on under current ice sheets, we need to understand what went on under previous ice sheets. One advantage of paleo-ice stream research is that it can potentially provide insights into evolution of ice stream systems on a much longer period of time (millennia) than direct observations of modern systems (few decades). And this is where paleo-ice stream research can contribute.

1.2 Paleo-ice stream research

Over the past decade there has been a strong drive not only to find and understand contemporary ice streams, but also to recognize and reconstruct paleo-ice streams from geomorphologic and geologic records. In 2001, the INQUA Commission on Glaciations organized the first Paleo-Ice Stream International Symposium, which was held in late October at the University of Aarhus in Denmark (Clark et al., 2003). This was the first time that researchers were brought together to discuss ice streams- “interaction occurred between Quaternary scientists working on terrestrial evidence; geophysicists working on investigations of marine signatures; and with numerical modelers investigating the significance of ice streams and the fundamentals of basal ice-stream processes” (Clark et al, 2003). Because it is difficult to directly observe contemporary ice streams and the ice-bed interface, many researchers use published geophysical and ice coring investigations of Antarctic ice streams along with their own theories and observations of paleo-ice streams to try to build models of what the record of ice streaming should look like.

In what can be argued as a landmark paper in paleo-ice stream research, Stokes and Clark (1999) developed a set of geomorphological criteria for identifying paleo-ice streams. In this paper they identified eight geomorphic signatures that could identify former ice streams and how these signatures are related to contemporary ice stream characteristics. Since the publication of these criteria, other more refined criteria for mega-scale glacial lineations (Clark et al., 2003), hereafter named MSGLs, and ice stream “sticky” spots (Stokes et al., 2007), have also been published. These reviews and classification criteria have generally been used to unify paleo-ice stream research.

Table 1.1: Geomorphological criteria for identifying former ice streams. Modified from Stokes and Clark (1999).

Contemporary ice stream characteristic	Proposed geomorphological signature	Explanation
Characteristic shape and dimension	Characteristic shape and dimensions	Ice streams are large features and are characteristically greater than 20km wide and 150km long, but they may be larger or smaller, especially if the shape is consistent with contemporary ice streams.
	Highly convergent flow patterns	In contemporary ice streams, the onset of streaming is characterized by a large convergence zone where slower moving ice is generally incorporated into ice stream. Thus the bedforms produced by an ice stream may exhibit a large degree of convergence at the head of the postulated former ice stream track.
Rapid velocity	Highly attenuated bedforms (length-to-width >10:1)	Streamlined bedforms are known to vary in their elongation ratio. Highly attenuated bedforms (i.e. with a large length to width ratio, usually >10:1) could arise from either fast ice flow over a short duration or slower moving ice over a longer duration. Many researchers argue that a high elongation ratio is indicative of fast ice flow. One line of argument is that as the flow geometry of ice sheets are known to vary rapidly then it is unlikely that highly attenuated bedforms such as mega-scale lineations were formed by slow moving ice over very long time periods. Thus, it is suggested that swarms of highly attenuated drumlins and mega-lineations may record the flow direction and spatial extent of former ice streams.
	Boothia-type erratic dispersal trains	Dyke and Morris (1988) recognized two types of dispersal train; only the boothia-type dispersal train is indicative of ice stream activity, as the Dubawnt-type can be formed by slow sheet flow. Hence it is important to identify the spatial extent of the source area from which the distinctive till is transported. There is not necessarily a blatant connection between ice streams and dispersal trains, but when found in conjunction with other criteria, it may be highly suggestive of streaming activity. This is because ice streams have the ability to transport sediment in a very distinctive fashion.
Sharply delineated shear margin	Abrupt lateral margins	Ice streams are characterized by their abrupt lateral margins bordered by slower-moving ice. The image to the left shows the characteristic lateral variation in velocity across an ice stream and it can be seen that the crevassed marginal area is only around one-tenth of the ice stream width. Thus, the characteristic geomorphology inscribed by a former ice stream would be expected to exhibit a sharp zonation of landforms at the margin.
	Lateral shear moraine	Abrupt lateral margins, of fast ice contacting slower ice, may also produce characteristic landforms. Dyke and Morris (1988) identified a single narrow ridge of till that delineated the western side of the drumlin field. This ridge is approximately 68 km long but less than 1 km in width. The ridge was interpreted as being a lateral shear moraine. It marked a shear zone at the side of an ice stream separating fast flowing ice from slower flowing cold based ice.
Deformable bed conditions	Glaciotectionic and geotechnical evidence of pervasively deformed till	Subglacial till deformation has been associated with fast flow and because it has been detected beneath Ice Stream B on Siple Coast of West Antarctica evidence of pervasively deformed till has been linked to former ice stream activity. Thus, areas of highly deformable till may predispose parts of an ice sheet to fast flow.
	Submarine till delta or sediment fan	Although not necessarily indicative of ice stream activity, focused accumulations of substantial sediment on a continental shelf may provide compelling evidence for ice stream activity. Their formation is thought to be attributable to a deformable till layer being deposited at the grounding line by rapidly moving ice streams. As a stable ice sheet margin (i.e. without an ice stream) would not deliver such concentrated accumulations of sediment to the continental shelf over short time periods, it is clear that offshore sediment accumulations can provide a clue to the former existence of ice streams. However substantial sediment may be accumulated at a stable margin if the ice sheet focuses small amounts of sediment over very long time periods. This may occur for example in topographic troughs which are not prone to ice streaming. Thus it is very important to constrain the timing of the sediment deposition in order to correctly ascertain the glaciological setting.

1.2.1 Mega-scale glacial lineations (MSGs)

Clark et al. (2003) illustrates the known first-order distribution of MSGs (and therefore inferred paleo-ice streams) in Canada. These mega-scale glacial lineations are longitudinally aligned narrow ridge-groove structures, 6-100 km long, in subglacial sediment (Clark et al, 2003). The exact processes involved in the development of this landscape are not clearly understood but lineations are thought to form in association with fast-moving ice, possibly through a groove-ploughing mechanism (Tulaczyk et al. 2001; Clark et al. 2003). Some of the most compelling evidence indicating a relationship with ice streams is that fields of MSGs have been mapped on the Antarctic shelf in continuity with currently active ice streams (e.g. Larter et al., 2009; O’Cofaigh et al., 2002).

1.2.2 Sticky spots

Ice stream beds have been thought to contribute to the forward motion of ice, and have raised the possibility that sediment properties have the potential to exert some form of control over ice sheet behaviour and stability. By understanding the sediment properties, we may be able to understand how the subglacial system functions. “Sticky” spots were first proposed by Kamb (1991) as the cause of flow resistance, providing the necessary drag to prevent ice streams from flowing catastrophically. These patches are thought to vary in space and time owing to changes in subglacial conditions such as the quantity and distribution of water. Bennett (2003) shows the stick-slip cycle of basal motion, emphasizing the importance of subglacial water pressure, between stick, slip and deformation. Stokes et al. (2007) have determined four primary causes for “sticky spots”, that can lead to changes in base conditions: (i) bedrock bumps; (ii) till-free areas; (iii) areas of strong/well-drained till; and (iv) freeze-on of subglacial meltwater. If there is an increase in the amount of one or more of these base conditions, there is a possible increased chance of ice stream shut-down (Stokes et al., 2007). Other possible reasons for ice stream shut-down include the change from ‘canalized’ to ‘channelized’ system, surging, ice shelf back stress, ice piracy, water piracy and thermal processes (Bennett, 2003).

1.3 Paleo-ice stream record of Saskatchewan

The DEM images produced from the SRTM data by NASA (USGS 2008, <http://srtm.usgs.gov/>.) revealed previously unrecognized and extensive tracks of crosscutting fields of MSGs. This new generation of DEMs has had a tremendous impact on our view and understanding of the glacial landscape of the Canadian Prairies. These images provided new geomorphologic information at a scale that could not be previously captured efficiently by air photos and surficial mapping alone. Figure 1.1 is the DEM image of central and southern Saskatchewan.

Previous work done in the Canadian Prairies with respect to ice sheet deglaciation and dynamics has focused on the reconstruction of the ice margin and chronology of ice retreat (Christiansen, 1979; Clayton and Moran, 1982; Dyke, 2004). Ice flow lines have remained loosely constrained and uniform ice flow models have been widely used. In addition, the relationships between till stratigraphy, ice flow indicators, and Wisconsinan ice sheet dynamics have yet to be established. Jennings (2006) emphasized the need to change flow pattern models based on field evidence from the James and Des Moines lobes in North Dakota and Minnesota. The evidence suggests that these lobes were fed by ice streams similar to those found in the West Antarctic Ice Sheet. If true, there are important implications for modeling LIS dynamics in the prairies and for addressing ice sheet stability issues. More recently, models involving ice streaming over the Canadian Prairies have been proposed (Evans et al., 2008, Ross et al., 2009) and tend to support Jennings' proposition. The work presented here is a detailed expansion of the work presented in Ross et al. (2009), where the main focus was to propose a mosaic landsystem model consistent with ice stream flow in Saskatchewan.

1.3.1 Previous work in the Prairies

In the Mid-Continental Prairies, there are well-defined tracks of elongated landforms and their associated features. This has lead some researchers to postulate that this area could have been the site of the large scale ice streaming and configuration changes that would have impacted the stability and deglaciation history of this area. The interesting array of landform assemblages in Saskatchewan have been noted since the 19th century (e.g. the Dirt Hills and Qu'Appelle Valley). They were not studied in great detail until the 1950s when interest into the South Saskatchewan

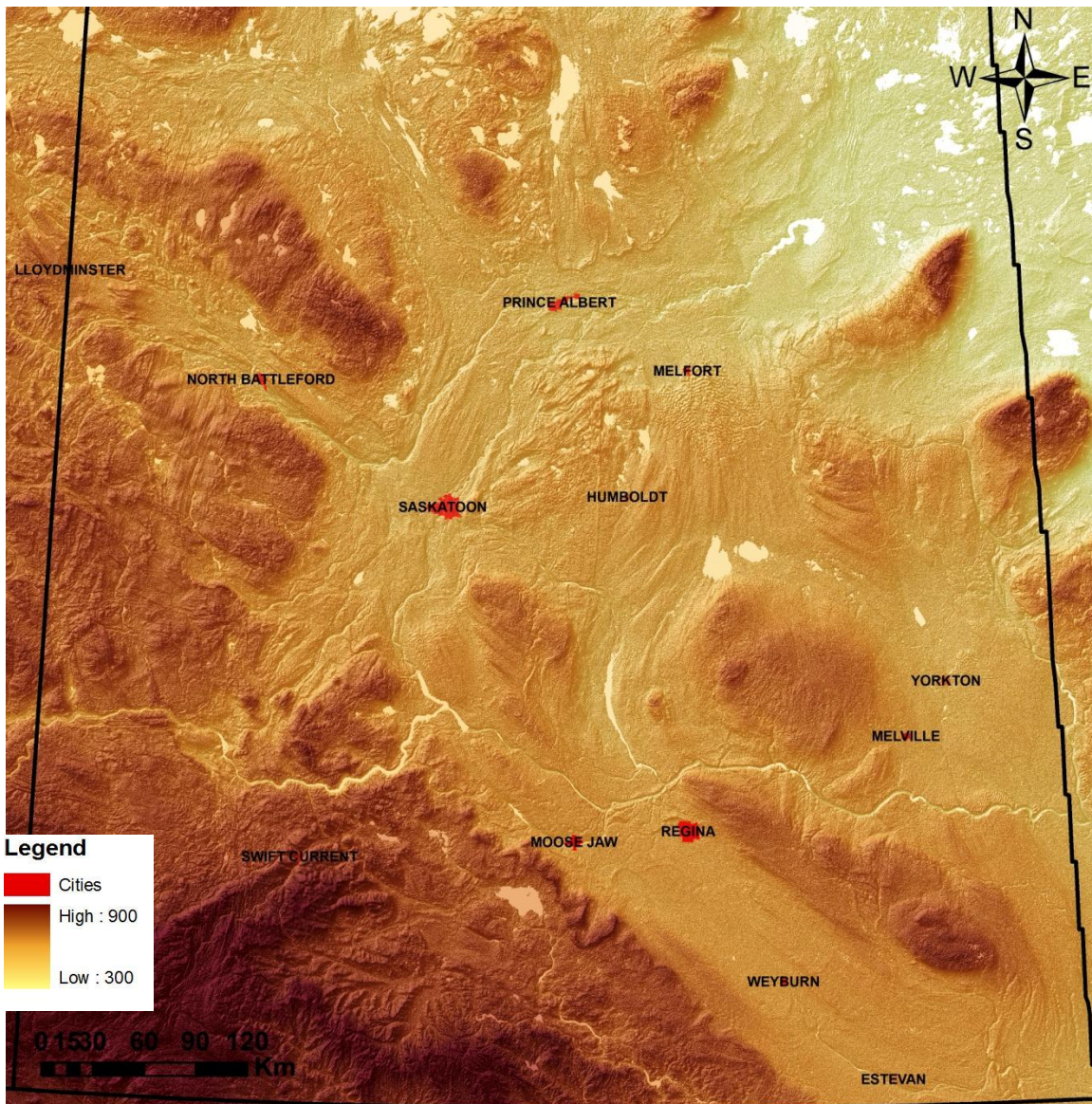


Figure 1.1: Digital Elevation Model of Saskatchewan, showing the location of various cities within the province. The simple unaltered DEM image shows a very dynamic landscape.

Dam project and energy resources became the driving force for industry and government funded research (Sauer, 1973). Drift stratigraphy (and Quaternary based) research after 1965 increased due to the groundwater research program. In the 1980s the industry and government funding became more focused in the north, leaving few geologists to continue to research the Quaternary history of the south. Since the 1950s, there was a steady stream of research papers released by a select group

of researchers that dealt with the geology, geochemistry and engineering properties of the southern Saskatchewan Quaternary history.

Christiansen (1979) was the first to discuss the deglacial history of Saskatchewan in detail. He used extensive geomorphologic evidence, deposits and stratigraphy with the few radiocarbon dates that were available at the time, to delineate a possible history of deglaciation. He broke up the deglaciation into 9 phases and then calculated the rate of deglaciation from Cypress Hills in the southwest corner of Saskatchewan to the center of deglaciation west of Hudson Bay.

In the *Chronology of Late Wisconsinan Glaciation in Middle North America*, Clayton and Moran (1982), proposed a chronology of glacial fluctuations from Alberta to Wisconsin based on radiocarbon dates from only wood samples. The downside was that there are fewer wood sample dates and only four of the sixteen fluctuations (they proposed) are accurate- none of the fluctuations in the western part of the region are accurately dated. Because the chronology of glaciation is for a large area (Alberta to Wisconsin) there is very little detail in specific areas and the model is based mainly on wood-sample radiocarbon dates, and very little on any other medium such as geomorphologic evidence. Klassen (1983) remarked that “a number of regional chronologies [were] rather summarily abandoned by Clayton and Moran (1982)” and the chronology was based mainly from sites in central Iowa, Minnesota and North Dakota, with limits extrapolated from these sites. These extrapolations disregarded research from other provinces. It was also noted that their assumptions were based on the single ice center over Hudson Bay model, as opposed to the new (at the time) paradigm shift that introduced multiple ice centers that need not be synchronous (Klassen, 1983).

In Dyke et al. (2002), the deglaciation of Saskatchewan is limited to a brief paragraph that discuss mostly the Laurentide and Cordilleran ice coalescence and refers back to Clayton and Moran (1982) for the not-well-defined oscillations of the margin after 20 ¹⁴C ka BP. The paper is well written as an overview to the Laurentide and Innuitian ice sheets during the Last Glacial Maximum, without going into great regional detail. The database of dates associated with Dyke (2003) is the most comprehensive one for Canada and includes parts of the United States. Dyke’s reconstruction is

more detailed than either of the previous models because it contains more data points (20 more years worth of radiocarbon date collection) as well as it takes into account the previous work done by regional experts and the geomorphologic evidence. To date, it is the most comprehensive deglaciation model for specific regions and North America as a whole.

We also know from previous studies (Klassen, 1989) that a first westward and southwestward flow system brought carbonates from Manitoba far into Saskatchewan. The till was later re-entrained by a southeastward flow system. This will have an effect on dispersion of material and will be discussed in a later chapter.

As mentioned before, present day models have many factors to account for in order to make a more realistic model. Unfortunately there currently are no successful models that can capture the fast-flowing outlets and ice streams that are responsible for much of the ice drainage in the Mid-Continent. This is not to say that they are unable to model ice streams, but just that few ice streams have been significant enough to be encompassed into a continent-wide model.

The Digital Elevation Models (DEMs) for Saskatchewan show long and well-defined tracks of elongated landforms and their associated features. These features and similar features elsewhere have been associated with ice streams, which has led researchers to postulate this as a site of ice streaming and configuration changes that would have affected the stability of the Laurentide Ice Sheet and deglaciation history of this area. No research has previously been done in Saskatchewan that has suggested ice streaming until recently. Surrounding areas such as Alberta, North Dakota and Minnesota have found evidence for ice streaming, and it only seems logical that these features in Saskatchewan are part of the deglacial system that created these neighboring features.

It was proposed that the Laurentide Ice Sheet (LIS) created two glacial landscapes and it was the lowland landscapes where there was intense glacial erosion and thin till where ice streams flowed and pushed outlet glaciers beyond the ice sheet (Patterson, 1998). This is the case for

the Des Moines Lobe. Later on, Jennings (2006) discussed the geomorphology of the Minnesota area and how it explains similar features, also found in the Dakotas and the Canadian Prairies, as products of lobate extensions of ice streams that issued from various ice sheds within the LIS. Using a DEM of the Minnesota area, Jennings was able to show how mapping Laurentide landscapes can give new insight into contemporary ice streams and their behavior because of the accessibility and continuity of the deposits of the paleo systems (Jennings, 2006).

Evans et al. (2008), as well as others, show examples within the Canadian landscape of paleo-ice streams (i.e. Stokes and Clark, 2003, 2004). Through preliminary interpretation of DEMs of Alberta, ice streaming in the southwest LIS is identified by geomorphology and sedimentology. Evans et al. (2008) drew reference between the properties, characterization and the features within the province. Detailed footprints, ice stream chronology and other questions remain unanswered (Evans et al., 2008).

One reason why ice stream research in Saskatchewan can help to better define the deglaciation history of Saskatchewan and the Laurentide Ice Sheet as a whole is because no current North American deglacial model includes ice streams in the southwestern margin of the LIS even though it has been demonstrated by previous research that they could exist. The result of this is that glacial dynamics affect ice thickness and extent, sea level changes, climate variability and more, therefore altering the results of climate modeling on both regional and global scale.

1.4 Thesis objectives and hypothesis

There were multiple sites of investigation for this thesis, the approximate study area is 49°N 110°W to 49°N 101°W by 56°N 110°W to 56°N 101°W (southern to central Saskatchewan between the Alberta and Manitoba borders). Figure 1.2 is the field site locations.

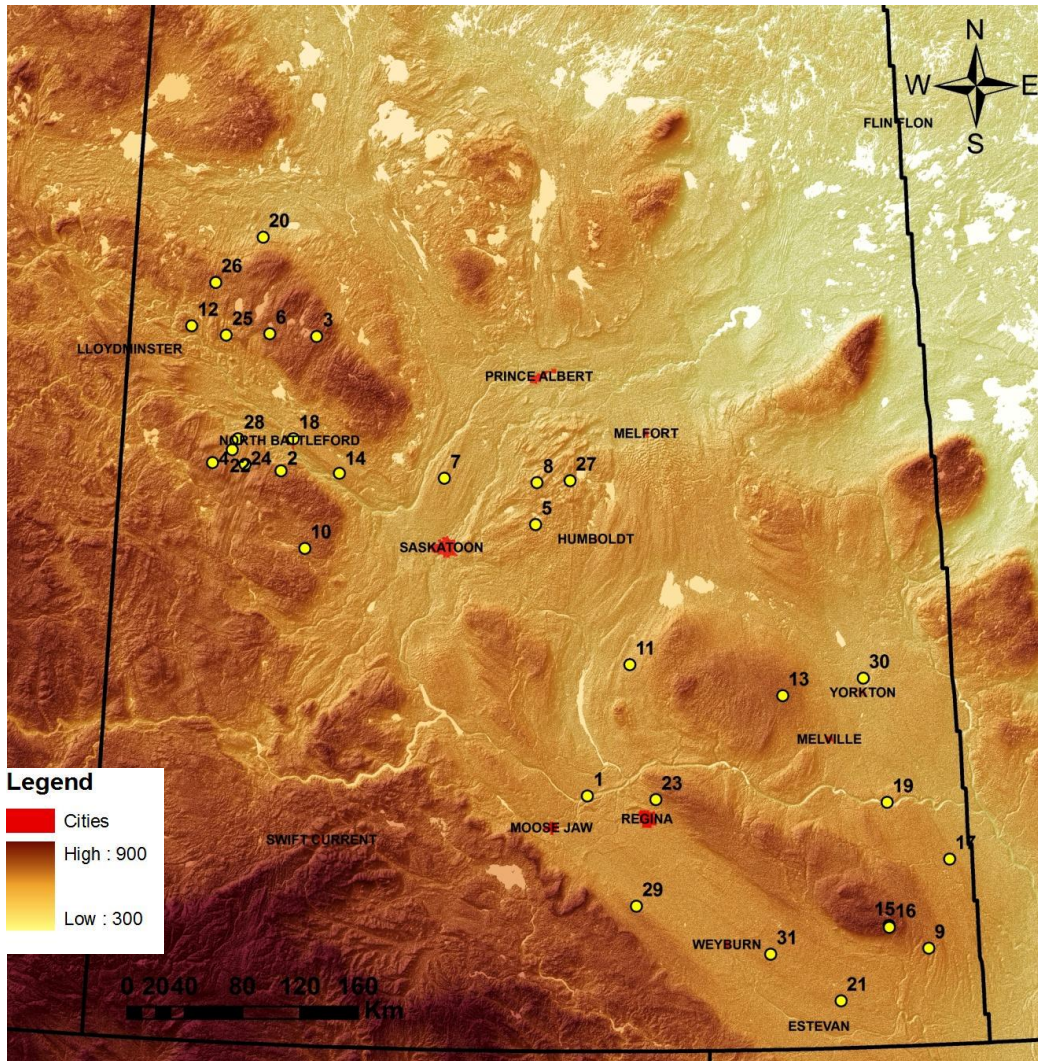


Figure 1.2: Numbered field site locations (yellow dots) over DEM image of Saskatchewan.

The thesis hypothesis is as follows: Fields of MSGLs in southern Saskatchewan represent paleo-ice stream corridors with older fields preserved between younger systems due to limited erosion in inter-ice stream zones. The latter may also include other subglacial landforms that are not associated with ice streaming such as hummocky terrain. This implies that a relationship must exist between surficial sediments and landforms forming discrete assemblages. For example, the composition of the surface till within an inferred paleo-ice stream corridor should be spatially consistent, predictable to some degree, and be distinct from the composition of adjacent terrains formed by contrasting ice-flow dynamics. Till fabric, composition, and the provenance of minerals

should thus vary throughout the research area according to the assemblages and their inferred glacial dynamics. Such sediment-landform relationship is not predicted by previous uniform ice sheet flow models (e.g. Klassen, 1987) or the mega-scale outburst flood hypothesis (e.g. Shaw, 2002, 2009).

The main thesis objectives are as follows:

- 1) Update and refine the subglacial landscape mosaic assemblage map of Ross et al. (2009)
- 2) Test the paleo-ice stream model and the landscape reconstruction of Ross et al. (2009)

In order to achieve these goals, new data are needed as well as additional analyses. The following specific objectives are designed to address those needs:

- 1) Complete the delineation of subglacial assemblages using digital elevation models and other datasets.
- 2) Describe the surface till, its fabric, and measure striations on lodged boulders (where possible) in assemblages
- 3) Document the composition of the till in the key assemblages
 - Record the main lithologies of the framework grains in the till
 - Add geochemical data to the existing database (Thorleifson and Garrett, 1993) in critical areas (e.g. small assemblages that were under-sampled)
 - Date hornblende grains in the till to further establish the compositional 'signature' of the surface till of key assemblages and to test provenance predictions

Chapter 2 Methodology

In order to update and refine the mosaic landscape model from Ross et al. (2009), and to further test the model, various methods were used and are outlined below. First the landscape is analyzed using existing map compilations and Digital Elevation Models, and then field sites are selected based on these interpretations, and field data are collected to test these interpretations. Field and laboratory results are integrated and analyzed within ArcGIS to provide a spatial context for the data. Outlined in the following sections is the description of the various methods used. Areas of potential inaccuracy and alternative methods, if appropriate, are noted.

2.1 Surficial Landscape Analysis

Surficial landscape analysis consists of two parts, Digital Elevation Model interpretation and map compilations. The Digital Elevation Model (DEM) interpretation identifies features using the Satellite Radar Topography Mission (SRTM) data of 3 arc-second, 90m resolution initially provided by NASA and now released by the USGS (USGS 2008, <http://srtm.usgs.gov>). The ability to use ArcGIS allows the scale of the image to change frequently, zooming in and out as needed, but the smallest scale in which features were identified was the 1:100,000 due to the resolution of the images. Of particular interest to this project are subglacial features that seem genetically-related and contemporaneous, as well as features that are consistent with the geomorphological criteria put forth by Stokes and Clark (1999). These features were outlined or grouped together in ArcGIS to be used in addition with the surficial geology map compilation. These map compilations are provided by the Geological Survey of Canada, Northern Geological Survey of Saskatchewan and other provincial surveys (AGS, 2009; GSC, 2008; MGS, 2009; NDGS, 2009, SGS, 2009). These interpretations were used to aid in directing field work locations.

Some site selection was based on the identification of features and assemblages from the DEM. These sites were then used to collect samples and to make fabric and striation measurements. Other sites were selected because of their good exposure and accessibility, found during field investigations.

2.2 Fabric and Striation Measurements

Till fabric measurements (the orientation and dip of particles in a till matrix) are used to determine sedimentological history such as ice flow direction during deposition (Andrews, 1971). Till fabrics, bedding plane measurements and striations on boulders can all be used in conjunction with till compositional data and geomorphologic data to better constrain ice flow direction at time of deposition. Saskatchewan has clay-rich tills attributed to underlying bedrock characteristics (Klassen, 1989). Pebbles found in the pebble-poor till also can range in size but are generally small (approximately < 1.5cm). In addition, the clasts are frequently equivilant with elongated ones difficult to find. Till fabric measurements can therefore be time-consuming and measurements are more prone to errors and uncertainties than in other areas. Because of this, till fabric data are complementary to other data collected. In the field, sites were prepared by excavating into undisturbed material approximately 60cm or more down to avoid weathering and frost effects, as well as avoiding boulders and roots. Once a flat horizontal surface has been cleaned off, selected pebbles that are tabular in shape and have an elongation ratio of approximately 3:2, have their dip and dip direction measured with a compass equipped with a clinometer. The a-axis and b-axis are measured and will later be used to determine the A/B plane.

Due to the multiple sites throughout the province, the declination is set to zero and corrected for in the office based on the date, time and location recorded for the site in the GPS unit. An exact declination for each site and the date it was collected was determined by using the declination calculator provided online by the Geological Survey of Canada (<http://geomag.nrcan.gc.ca/apps/mdcal-eng.php>). Once all measurements have been taken and a sample removed from the site for further analysis, the hole is restored. Back in the lab, the measurements are corrected for declination and are inputted into stereonet software, StereoStat (Rockware, 2008), where equal-area Schmidt and rose diagrams are produced, as well as contour plots for each site. Eigenvectors and values are calculated in the stereonet program and a random site was double checked by hand calculations as well. A/B planes were used to avoid the potential problem of transverse orientations observed for clast A-axis. They also provide poles-to-plane data,

strengthen modality plots and provide a clear visual impression of stress directions (Evans et al., 2007).

Striations on elongated, flat topped boulders firmly lodged in the underlying till, sometimes within shallow (near-surface) boulder pavements, were measured for flow direction. This type of measurement is done with the boulders in-situ, and provides stronger, more coherent data than till fabrics. The striations found on boulders throughout the province were measured using a compass after the top was cleaned off the boulder exposing multiple striations. Older sets of striations (over printed) were also noted. In select locations, boulder pavements were found and each boulder's striations were measured and recorded. Striations approximately parallel to the long axis of the boulder provide a robust measurement.

Once all the measurements are complete, analysis of rose diagrams, stereonet, contour plots, ternary diagrams, modality plots and directions on ArcGIS map are done. These results are found in the following chapters and appendices.

Sources of error for till fabric measurements include possible human error in measuring the pebble's dip and dip direction, which can happen especially with small clasts.

2.3 Pebble Lithology

Pebble count is the collection and identification of pebbles found within a sediment, to be used for provenance and other sedimentological studies. For tills, clast lithology has commonly proved to be a reliable indicator of glacier flow patterns in space and time, subglacial transport distances, and of buried mineralized outcrops of economic value. Considerable success has been achieved in determining the source areas of individual till sheets in glaciated North America (e.g. Gwyn and Dreimanis, 1979; Shetsen, 1987). The identification of the pebbles was based on the methodology used in the University of Waterloo Earth Science class Quaternary Geology (University of Waterloo, 2007b). The original methodology uses 105 pebbles of 1-2" diameter found in the field, but due to the small clast size and low pebble content in the Saskatchewan tills, all clasts from the 2mm or

greater fraction were used (See Appendix D for the methodology). This was also done to better characterize the dispersal patterns of carbonate clasts as they are much less abundant in the coarse fractions. Clast lithology was categorized as crystallines, carbonates (limestones and dolostones), and clastics (shale, siltstone and sandstone).

Once the sample was selected, the pebbles were washed with water in a sieve to remove any mud or calcareous cement. Lithology identification was done by visual inspection using a hand lens, knife for scratching and 10% HCl. Limestones were identified when they strongly effervesce with HCl, and are easily scratched by knife. They were not subdivided further into categories i.e. fossiliferous etc., because that amount of detail was not necessary. Dolostones show little to no effervescence until powdered by scratching with a knife. After each site's sample was complete, the results were tabulated and summarized as percentage of sample for each category. The categories used in the summary are dependent on lithologies encountered, as there are sites that do not include all the lithologies set out in the methodology. The accuracy of this method is dependent upon the ability of the identifying person to correctly identify the lithologies of the pebbles.

Other methods could be used for pebble lithology identification, such as breaking open of the pebbles with a hammer, rather than washing the pebbles. This method would be appropriate if the pebbles were of larger size. Another method is petrography, making thin sections of the pebbles but this would prove to be expensive and unnecessary for this type of identification.

2.4 Grain Size and Hydrometer Analysis

Grain size and hydrometer analysis are two methods used in conjunction with one another, in order to determine the grain size distribution of a sample. This information is useful in characterizing tills and analyzing geochemistry. As with the pebble lithology, this method is based on the methodology used in the University of Waterloo Earth Science class Quaternary Geology (Earth 440), and can be found in Appendix D (University of Waterloo, 2007a). However, due to visibly large amount of clay size particles in the tills in Saskatchewan, an extra step had to be added to the methodology. In the original methodology, set out in Earth 440, the till samples are to be prepared for hydrometer

analysis then saved and re-analyzed with the sieve method. In the new methodology, for the sieve portion, 250 grams of homogenized sample was dried in an oven at a temperature of approximately 50°C, for 24 hours (or more if needed). Throughout the drying process, larger pieces were occasionally broken up as they dried, to prevent the “baking” of the sample. Other methods for clay rich tills were explored (e.g. wet sieving) but found them to be ineffective due to sample loss and the amount of samples for this project. Once the samples were dried, they were weighed to determine the % moisture loss, which is used in the curve calculations later on. Once the sample is dried and weighed, it is placed in the top of a predetermined series of sieves. Due to the smaller nature of the grains, and to increase the amount of values for the grain size curves, nine sieves (8mm, 4mm, 2mm, 1mm, 0.5mm, 0.25mm, 125µm, 105µm, and 63µm) and a pan were used. Once the sample was inside the sieve structure it was placed in a shaking column for 30 min intervals until the entire sample had been sieved. Once the sample is sieved, sample from each sieve is weighted and recorded. Sources of error for this portion of the method have to do with loss of sample within the shaking column, sample loss in sieve mesh and possible incomplete sieving.

For the hydrometer portion of the grain analysis, 50 grams of homogenized sample is dried at 50°C for a few hours occasionally breaking up larger pieces as they dry, until completely dry. Once the sample is dry it is added to a 250 mL beaker with 125 mL sodium hexametaphosphate 4% solution, stirred and stands overnight. The next day the solution is mixed with a mechanical mixer and poured into a 1000 mL hydrometer cylinder, topped and shake vigorously. Once the cylinder has been shaken it is topped up to the 1000 mL mark and a hydrometer is inserted, where readings are taken for the next 24 hours (15 s., 30 s., 1 min, 2, 4, 8, 15, 30 mins, 1 hour, 2, 4, 8, 24 hours). Once all the readings have been taken in the sample cylinder (as well as the reference cylinder), hydrometer calculations are done and entered into a spreadsheet. These values are combined with the grain size values to create a grain size curve, and therefore % sand, silt and clay. Error can occur in this method because of sample loss during mixing and column shaking.

Another method that can be used in place of the hydrometer and sieves is grain size analysis via laser measurements. However this method is currently not available at University of Waterloo.

2.5 Geochemistry

After grain size analysis was done, a 60 gram split was prepared for geochemistry and sent to Becquerel Labs in Mississauga ON. The geochemistry was done in order to have the ability to create elemental ratios that can be used as proxies to compare tills as well as note various changes in till composition across the province. The “Geological Characterization” package was selected because it analyzes over 50 elements and is sensitive down to parts per billion for some. The samples were analyzed using the Neutron Activation Analysis (NAA) as well as ICP-MS for total analysis, overlapping some elements to reduce method uncertainty. NAA packages samples that become irradiated in a research reactor, and the samples become radioactive when the neutrons interact with the nuclei of the elements’ atoms. The radioisotopes formed begin to decay and the energy signature of the gamma rays emitted and this signature is proportional to the concentration of that element. A total digestion was used which means that the sample is digested at a high temperature in an acid mixture for over 24 hours. After the samples are cool and diluted, the samples are run on an inductive coupled plasma- mass spectrometer (ICP-MS) where the sample is put through a nebulizer and becomes an aerosol as it enters the instrument and the spectrometer measures the elements and their concentration are recorded. Like most methods there are sources of error. For NAA it would be an incomplete irradiation of samples, but Becquerel takes additional precautions by re-analyzing with ICP-MS. Errors for ICP-MS include sample loss during digestion (it is removed at set time intervals for centrifuging and additional acid mixture), and cross contamination within the spectrometer (if the rinse cycle was interrupted or incomplete due to mechanical means, between samples). Quality assurance for the samples was done by both myself and the laboratory. The samples submitted were numbered and a duplicate was submitted blindly to the lab. In the lab, duplicates were run throughout the sample set.

2.6 $^{40}\text{Ar}/^{39}\text{Ar}$ Hornblende Dating

The $^{40}\text{Ar}/^{39}\text{Ar}$ dating method for hornblende grains was used to aid in the determination of provenance and flow history. The $^{40}\text{Ar}/^{39}\text{Ar}$ dating method for hornblende was used because the K-Ar clock can be reset during times of high temperature (>450°C, either metamorphism or igneous formation). It has been shown that hornblende grains from different Canadian Shield domains (e.g.

Churchill, Superior) have distinctive ages and can thus be used as a tracer in regional provenance studies (Hemming et al., 2000, Roy et al., 2007). Tills produced by ice flow systems coming from various sectors of the Canadian Shield should thus contain a mixture of grains that is representative of the lithologies incorporated during transport, including the source Shield region (Roy et al., 2007). Once the grain size analysis was complete, a 30 gram split of size 150 – 500 μm was made and sent to Sidney Hemming at Columbia University at Lamont-Doherty Earth Observatory, in Palisades NY. Samples were washed, dried and weighted. Hornblende was hand-picked from the sample, selecting black to dark green minerals with cleaved surfaces. Single-step laser fusion $^{40}\text{Ar}/^{39}\text{Ar}$ analysis for individual grains was made in the Ar geochronology lab. Samples were irradiated at the Oregon State reactor. Single grains were then heated with a CO_2 laser at Lamont. Ages were calculated from isotope ratios and corrected for mass discrimination, interfering nuclear reactions, and atmospheric Ar contamination (Hemming et al., 2002). To further refine the test, the Ca/K ratios were measured for each grain. Ratios less than one or greater than 60 were not considered as they could be biotite or pyroxene (felsic or mafic), respectively (S. Hemming, pers. comm., 2009). Ages can be obtained from biotite as well but they will tend to be younger and have a lower closing temperature (300°C). A Ca/K ratio of 0.6-0.9 can be interpreted as an alkaline hornblende rather than biotite, so reanalysis of grains would have to occur. A possible problem would be having grains of low % radiogenic Ar yields, which could be a sign of an alteration product in the grain such as intergrowths, which would produced a mixed age.

Another method that could be used is Pb isotopes and feldspars to further refine the difference between metamorphosed Archean grains versus early Proterozoic grains.

2.7 Geodatabase

A geodatabase was constructed in ArcGIS by compiling all the data collected from the above techniques into Excel files and converting them to shape or database files in ArcGIS. By doing so, the results for each method could be analyzed in their spatial context, as well as compared to other methods. In creating a geodatabase, the samples and their associated results are georeferenced (under NAD 1983 projection) and can be visualized as layers and compiled into maps.

Chapter 3 Sediment-Landform Assemblages

3.1 Previous Glacial Geomorphology Research in Saskatchewan

Previous work done in the Canadian Prairies with respect to Quaternary geology focused on the development of a Quaternary stratigraphic framework, and the chronology and pattern of ice retreat during the deglaciation (Christiansen and Sauer, 1983, 1988, 1992, 1997, 2001, 2002). Aspects of glacial dynamics have been investigated mainly through more local studies (e.g. Klassen, 1992; Aber, 1993). Proposed regional ice flow reconstructions do not satisfactorily explain the complexity of the subglacial landscape (e.g. Klassen 1989). But it was difficult to realize this before the advent of remote sensing and GIS analysis techniques applied to glacial dynamics reconstructions (e.g. Boulton and Clark 1990; Stokes 2002). More recently, however, work on terrestrial paleo-ice streams in Alberta (Evans et al., 2008) and Minnesota (Jennings, 2006) has caused renewed interest in the regional-scale subglacial geomorphology of the region. Ross et al. (2009) recently presented a regional-scale analysis of the subglacial landscape of Saskatchewan. The research presented herein has emerged from this latter analysis.

The glacial landscape of southern and central Saskatchewan was analyzed using geographical information system ArcGIS, fully integrating all topographical and surficial geological data that was available. It is estimated that before Landsat images of Canada, only 30-40 percent of paleo-ice flow indicators such as drumlins and megaflutes, were recorded (Clark, 1993). Based on DEM interpretation, Ross et al. (2009) introduced potential corridors of ice streaming and associated chronology. Figure 3.1 is the location and names of the corridors. They are further described and analyzed in following sections.

*All collected data discussed, in part or full, can be found for each site in **Appendices A and B**.*

3.1.1 The role of Bedrock Geology

Landscape evolution is strongly influenced by the nature of the underlying bedrock in both physical processes and sedimentary development. Shown in detail in Appendix C, the bedrock geology of Saskatchewan is composed of Cretaceous-age, fine-grained clastic sediments that border up to the

thin belt of Paleozoic carbonate rock that run along the Precambrian Shield in the central to northern part of Saskatchewan. The clastic sediments are mostly shales and siltstones deposited by shallow Cretaceous seas, and in some areas can contain bentonite (montmorillonite) which collectively account for the clast-poor, fine-grained tills throughout the province. Tertiary sandstones and siltstones are relatively widespread and are more resistant to weathering than the Cretaceous beds and are found at higher elevations. The fine-grained material was eroded by glacial events, producing a high proportion of silts and clays in the tills, which later influenced ice stream formation and production.

The interior plains generally rise to the west south-west. Preglacial rivers and valleys shaped the flat sedimentary rocks, but are now buried by Quaternary sediments. An example of one of the large preglacial valleys is the Hatfield Valley which spans across a large portion of Saskatchewan (Meneley, 1967; Christiansen, 1977). The gradual rise of the interior plains consists of a series of 'steps' that include the Missouri Coteau and the Manitoba Escarpment (Figure 3.2). These steps run northwest to southeast and bisect the borders of Alberta and Manitoba, with the Saskatchewan Plain (400-800 m.a.s.l.) between the two steps (Klassen, 1989). The Buffalo paleo-ice stream system, shown on Figure 3.1, is loosely bound within the Missouri Coteau and the Manitoba Escarpment, most likely shifted between these bounds over its life cycle.

3.1.2 Landforms

The subglacial landforms of Southern Saskatchewan mainly consist of drumlins, mega-scale glacial lineations (MSGSL), ribbed moraines, shear margin moraines, hill-hole pairs, and eskers. It is generally agreed upon that these types of landforms have a direct relationship to ice flow direction on various scales. MSGSLs and shear margin moraines are among the landforms generally used to recognize ice streaming from the landform record.

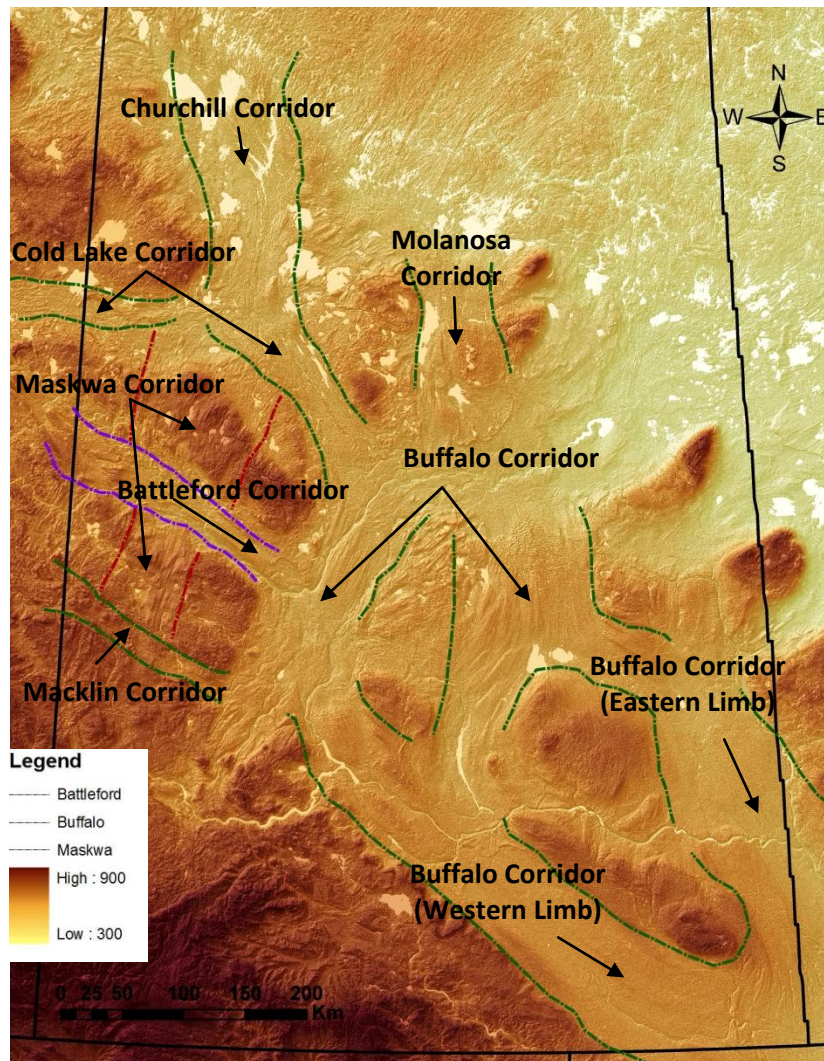


Figure 3.1: Names and locations of potential paleo-ice stream corridors in Saskatchewan.

Streamlined till ridges, and MSGLs in particular, are the most common landforms in the paleo-ice stream corridors. Large fields or areas of ridges are found in previous maps, but due to absence of SRTM technology and DEMs, many subdued landforms within the corridors have not been previously mapped (Ross et al, 2009). By definition, MSGLs are subdued features due to their long and narrow shape, having a height that is often lower than drumlins. However, within the Buffalo Corridor these till ridges are even more subdued in some places because they were buried by later events and sediments, such as the till ridges outside of Regina which were buried by Glacial Lake Regina's glaciolacustrine sediments (Figure 3.3). The direct cause of MSGL formation has several

hypotheses (erosion, deposition, or a combination), but current research emphasizes subglacial sediment deformation due to various factors such as ice sheet velocity, basal shear stress, porewater pressure, effective pressure and geotechnical properties of the subglacial material (Hubbard and Reid, 2006). These factors influence the flow of the material and the morphology of the deformed ice-bed interface (Hubbard and Reid, 2006).

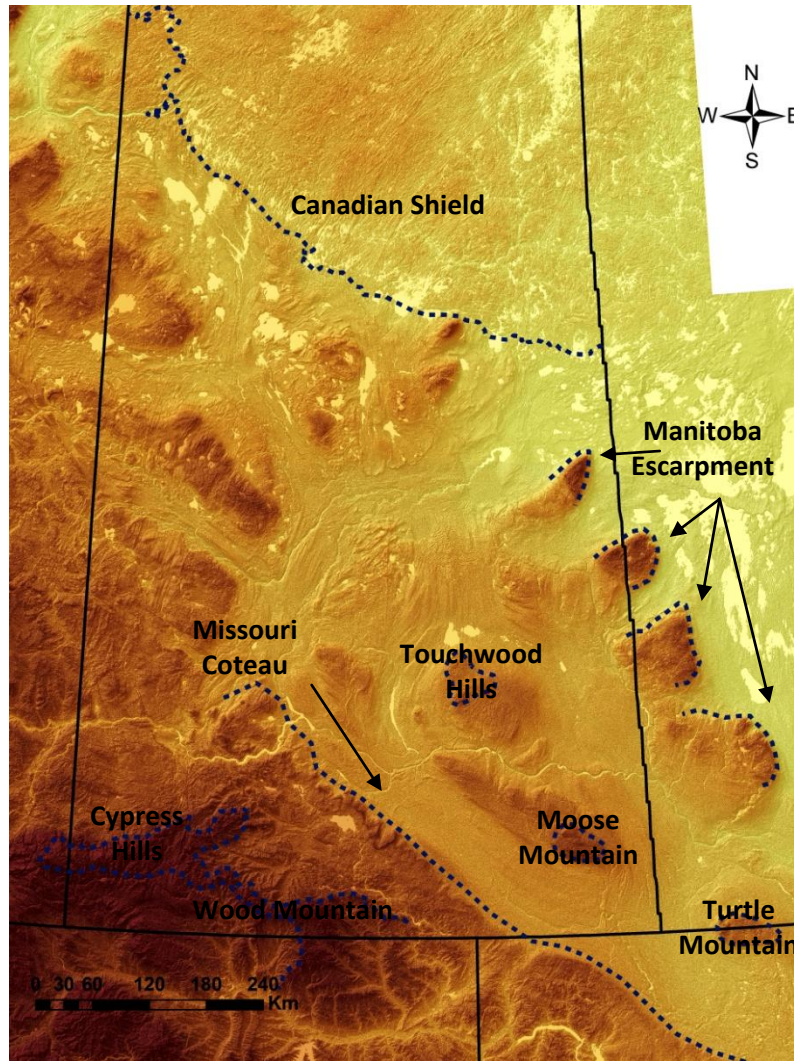


Figure 3.2: Topographic controls in Saskatchewan. Manitoba Escarpment and Missouri Coteau form a series of steps in Prairies, towards the Rocky Mountains. The Buffalo paleo-ice stream was bound by these features at certain times over its life cycle. Blue dashed lines delineate the boundaries of these features.

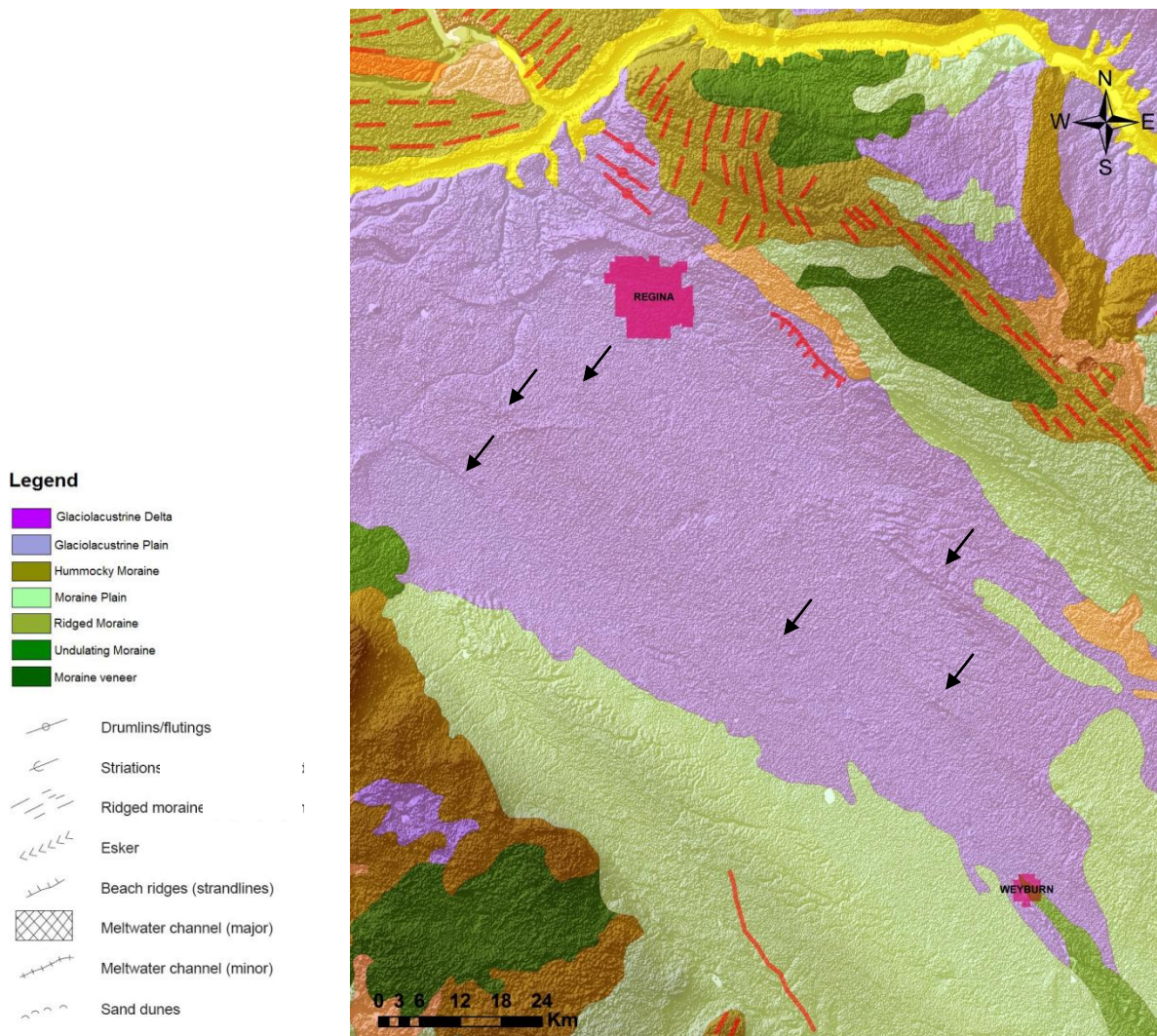


Figure 3.3: MSGLs are naturally subdued features. Some areas of MSGLs are even more subdued because they are buried by younger sediments, for example, the MSGLs in the western limb of the Buffalo Corridors is buried by Glacial Lake Regina glaciolacustrine sediments. These are best seen with DEM images and are not readily visible in air photos (Slimmon, 2007).

The streamlined terrain in the prairie regions of North America (Saskatchewan, Alberta, North Dakota) are known for having glacially streamlined forms that are low and have large length-to-width ratios, as well as small areas of drumlins or flutes (Moran et al., 1978). The proposed corridors (Buffalo, Battleford and Maskwa) are consistent with the streamlined landforms mentioned in Moran et al. (1978) and associated ice flow directions (Christiansen, 1956, 1960, 1972; Kupsch, 1955; Langford, 1973; Parizek, 1964).

Existing mapped landforms were found in literature and maps. The Northern Geological Survey of Saskatchewan, as well as other national and provincial surveys, provided free online GIS map downloads that were used in the help of interpretation (SGS, 2009). Potential bedrock and topographic controls are outlined in Figure 3.2.

3.1.2.1 Assemblages

By grouping streamlined and other associated features together, we get assemblages of discrete terrain elements, defined by a set of internal geomorphological characteristics, distinguishable from adjacent terrain (Ross et al., 2009). The landforms in the assemblage are assumed to be genetically related, and are defined by sharp boundaries from other landforms that are not related. Areas outside of ice streams, based on the Stokes and Clark (1999, 2001) criteria, should reflect slow basal motion to stagnant ice (e.g. hummocky terrain). However, older landforms created by active ice can also be preserved by limited erosion under these “stagnant” conditions.

3.1.3 Internal characteristics

The internal characteristics of landforms have an effect on the formation of the landform, such as resistance to erosion or other formation processes. It is possible that within the context of this project, the internal characteristics can be used to differentiate between different systems. When looking at landforms in the field, it was noted when possible, what till unit the landform was composed of. However, samples were taken in the uppermost till to allow establishment of any potential relationship with the landform record. In Saskatchewan the tills are of very similar colour and texture, and can be differentiated based on consolidation pressure or carbonate content. Table 3.1 is the stratigraphy of tills in Saskatchewan. Total carbonate content, expressed in mL CO₂/g has been found to be sufficient in separating and tracing tills in southern Saskatchewan (Christiansen and Sauer, 2002). However, Ross et al. (2009) demonstrated the importance of placing this into a spatial context. Tills in Saskatchewan can also be differentiated by their weathering, staining and preconsolidation pressures (Christiansen, 1992).

Table 3.1: Saskatchewan Stratigraphy and associated Carbonate Content. Modified from Barendregt et al (1998), Christiansen and Sauer (2001).

Time			Saskatchewan Stratigraphy		Lithology	Carbonate Content (mL CO ₂ /g)				
						Mean	SD			
Quaternary	Late Pleistocene	Wisconsinan	Holocene	Saskatoon group	Unnamed, surficial stratified deposits	sand, silt, clay				
			Late		Battleford Formation	till	37.3	8.2		
			Middle		Weathered Zone					
			Early		Floral Formation	till	34.6	2.2		
		Sangamonian	Riddell Member		stratified deposits					
	Middle Pleistocene	Illinoian	Pre-Illinoian	Sutherland Group	Floral Formation	till and stratified deposits	35.3	4.9		
					Warman Formation	tills and stratified deposits	11.4	2.9		
					Dundurn Formation	tills and stratified deposits	24.5	4.0		
	Early			Empress Group	Mennon Formation	tills and stratified deposits	9.5	0.8		
					Stewart Valley sediments	stratified deposits				
Tertiary (Late Pliocene)					Unnamed	stratified deposits				
Cretaceous			Montana Group	Bearpaw Formation	Snakebite Member	silts and clays				
					Ardkenneth Member					
					Beechy Member					
					Demaine Member					
					Sherrard Member					
					Metador Member					
					Unnamed, Outlook, Broderick Members					
				Judith River Formation						

3.2 Paleo-ice Stream (PIS) Criteria

Stokes and Clark (1999) introduced a list of criteria and developed a paleo-ice stream landsystem model that has been used extensively in paleo-ice stream and ice sheet dynamics research, as well as tested within contemporaneous ice stream research (for verification of criteria viability). Stokes and Clark (1999) used a relatively simple ice stream and catchment area model for their criteria. They did not provided criteria for paleo-ice stream tributaries or inter-ice stream zones. Other

researchers have described remnant landscapes between ice stream corridors, however most examples are in the Canadian Arctic and generally invoke cold-based ice to explain the lack of erosion (Dyke et al., 1992; Piotrowski et al., 2004; Stokes et al., 2005; De Angelis and Kleman, 2007; Kleman and Glasser, 2007; Stokes et al., 2009). There is no clear understanding of the subglacial thermo-mechanical conditions for inter-ice stream areas in the prairies yet. However, it is assumed that these areas have contrasting sediment and landform characteristics relative to their contemporaneous paleo-ice stream. Below is a proposed modified list of criteria to identify paleo-ice streams and their inter-ice stream areas in Saskatchewan (new criteria from Ross et al. (2009) and this study is indicated by an asterisk*):

- Characteristic shape and dimensions of fields of streamlined landforms
 - Convergent flow patterns,
 - Tributary-type flow pattern*
- Rapid velocity
 - Attenuated bedforms (mainly MSGs)
 - Boothia-type dispersal train
- Abrupt lateral margins
 - shear margin moraines,
 - sharp topographic steps*
- Inter-ice stream areas characterized by contrasting terrain characteristics relative to their contemporaneous paleo-ice stream corridor*
 - Fragmented record of previous ice flow preserved due to possibly stagnant ice,
 - Distinct geochemical signature

Many criteria listed above are based on geomorphological evidence and in the following subsections; they are used to refine the delineation of the subglacial assemblages map (specific thesis objective 1) and to further characterize the geomorphologic imprint of paleo-ice streams. Structural information (fabrics, striations) is then used to establish the conceptual degree of fit with the landform assemblage map. In Chapter 4, the compositional data will be used to further test and verify the concept of sediment-landform assemblages and the distinct boundary between paleo-ice stream corridors and inter-ice areas.

3.2.1 Application to Saskatchewan

Ross et al. (2009) recognized two paleo-ice stream corridors in Saskatchewan and a number of inter-ice stream areas: The Maskwa and the Buffalo paleo-ice streams. The Maskwa paleo-ice stream was relatively straight and was not topographically confined. The second system (the Buffalo paleo-ice stream) was topographically confined by the Manitoba escarpment and the Missouri Coteau (Figure 3.1). However, the ice stream was able to migrate laterally inside these limits. In Ross et al. (2009), the Buffalo paleo-ice stream was fed by various tributaries during its life cycle.

3.2.1.1 Maskwa Corridor

This paleo-ice stream corridor is defined by discontinuous fields of MSGs extending approximately 900 km, from the Athabasca Basin on the Canadian Shield to the southwest corner of Saskatchewan. The corridor width varies but is approximately 60-120 km wide from one side of the glacial lineations to the other (Figure 3.4). The Maskwa Corridor represents a single, curvilinear, paleo-ice stream that extended up to the northern flank of the Cypress Hills.

The MSGs of the Maskwa Corridor (Figure 3.4) are oriented south-southwest and consist of till ridges, some as long as 80 km (Ross et al., 2009). Discontinuities are seen within this corridor, and are due to erosion and crosscutting by later ice flows linked to ice stream reconfigurations (Ross et al., 2009). These areas of preserved till ridges are over multiple assemblages, bounded by hummocky terrain. This type of terrain is not part of the original list of paleo-ice stream criteria. However, the sharp contact relationship with MSGs indicates that these landforms developed subglacially. The proposed interpretation is that they record ice sheet stagnation in inter-ice stream areas. They are thus considered coeval and genetically-related to the MSGs, forming together a consistent terrain assemblage. Three assemblages of this type have been identified and delineated (Assemblages 5, 6, and 7). The Maskwa paleo-ice stream flowed over and across the North Saskatchewan River valley (the Battleford Corridor) with little modifications in flow direction. This can be seen in Figure 3.5, where the till ridges slightly bend into and out of the Maskwa Corridor from Assemblages 7 to 6.

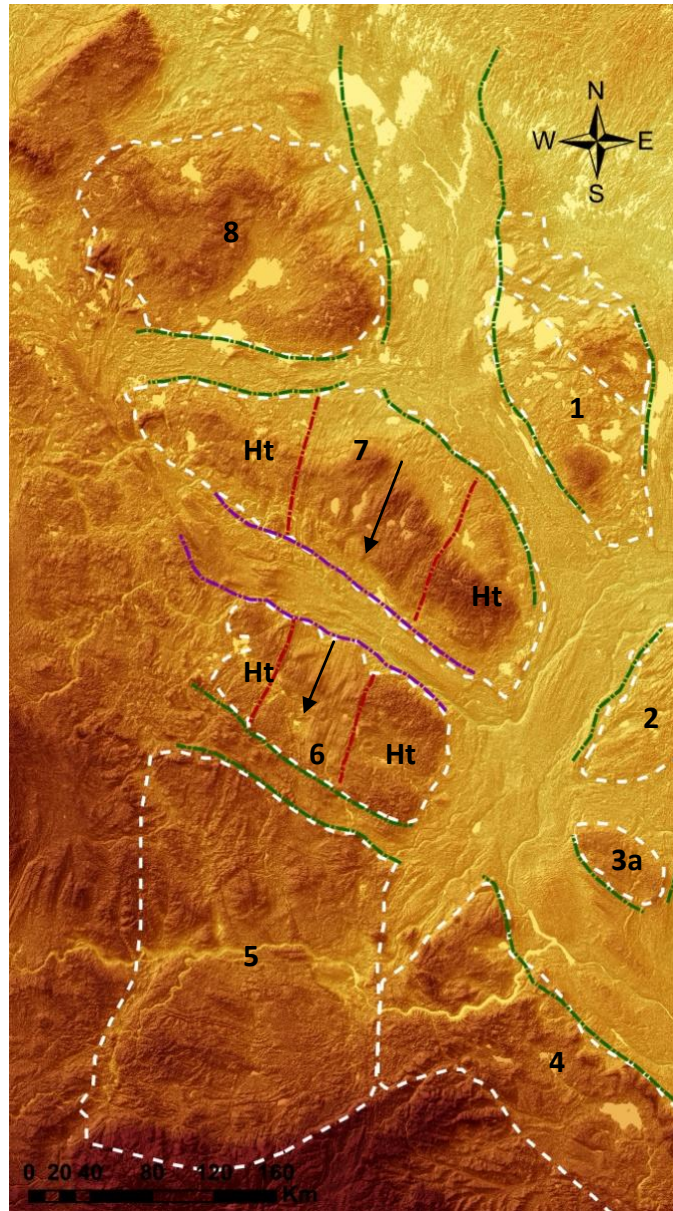


Figure 3.4: Maskwa Paleo-ice Stream is delineated by red dashed lines, and inter-ice stream areas (or assemblages) are delineated in white dashed lines. The Maskwa system is over 900 km long, and the MSGLs are concentrated and preserved between the red boundaries. The system is discontinuous due to cross-cutting by younger paleo-ice streams (discussed later). Ht is hummocky terrain, and black numbers are assemblage numbers.

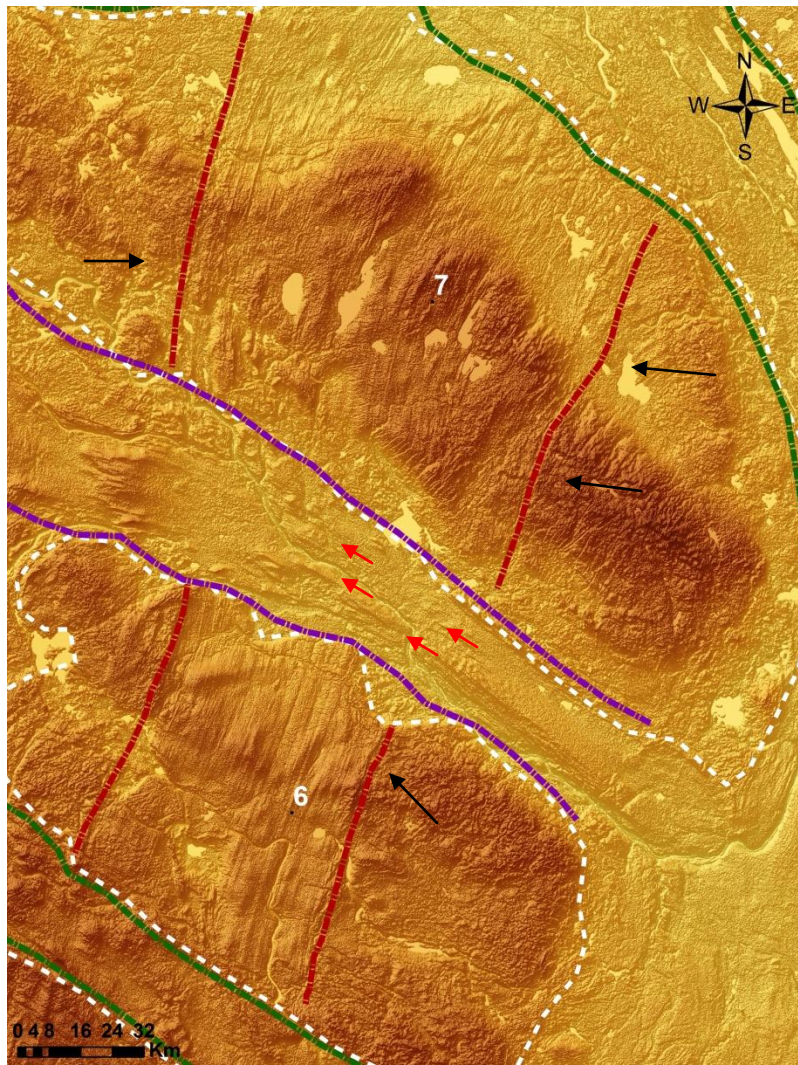


Figure 3.5: Maskwa paleo-ice stream along assemblages 6 and 7. Red arrows point to landform evidence of a continuation of the Maskwa southwest flow across the Battleford Corridor between assemblages 6 and 7, that was later cross cut by the Battleford paleo-ice stream system. Black arrows point to ice flow convergence into the Maskwa system.

Assemblage 6 is located west-southwest of North Battleford, and is bounded on the north by the Battleford Corridor, on the south by the Macklin Corridor, and on the east by the Buffalo Corridor (Figure 3.4). The assemblage is relative topographic high compared to its surrounding corridors, with its boundaries being determined by topography and opposing linear features. This assemblage contains the Maskwa paleo-ice stream, which is sharply defined on either side by hummocky moraines, while the corridor is moraine plain with strong long linear features trending south-

southwest. Striations on boulders and lineations found in the hummocky moraine area suggest previous westward flow not contemporaneous to the Maskwa paleo-ice stream. The hummocky moraine and MSGs are thought to be contemporaneous because they form a consistent paleo-ice stream landsystem with the hummocks representing the inter-ice stream stagnant zone, and the MSGs representing the fast-flowing ice stream. The sharp boundary between the two landform types precludes use of the traditional interpretation that hummocky terrains are late deglacial features.

Assemblage 7 is located north of North Battleford and is bounded by the Battleford Corridor to the south, and the Cold Lake Corridor to the north. This assemblage contains the south-southwest-trending Maskwa Corridor and, similar in nature to Assemblage 6, there is a sharp boundary between the Maskwa Corridor and the surrounding hummocky moraine. However, there are DEM mapped features within the hummocky terrain that converge towards the Maskwa Corridor. Onset of ice streaming is characterized by a convergence zone where slower-moving ice is 'captured' or incorporated into the faster-moving ice (Stokes and Clark, 1999). However, this convergence is not limited to the onset zone, as seen in Figure 3.5, where there is convergent flow into the Maskwa ice stream system along the corridor. The onset zone for the Maskwa paleo-ice stream has yet to be defined due to its northern extent, which remains to be explored. This convergent pattern into the Maskwa paleo-ice stream may indicate a slightly different Maskwa configuration prior to the development of the final hummocky-MSG landsystem.

The set of unnamed moraines and transverse ridges in Saskatchewan that continues into Alberta's Lethbridge Moraine, outlined in Assemblage 5, is where it is believed that the Maskwa track terminated (Figure 3.6). Assemblage 5 is located west-southwest of Saskatoon, and extends west across the Alberta-Saskatchewan border. It is bordered by the Buffalo Corridor to the east, and the Macklin Corridor to the north, and is bisected by the South Saskatchewan River. This assemblage represents the terminal zone of the Maskwa system. Its northern portion includes the southernmost MSGs that can be confidently correlated with those in Assemblage 6. The southernmost portion consists of large transverse ridges, and this series of transverse ridges extend from the South Saskatchewan River to the Cypress Hills. These features are not part of the list of criteria for

paleo-ice stream identification, but form a consistent paleo-ice stream track (onset zone, trunk and terminal zone, see Figure 1.2). Transverse ridges are ridges formed parallel to the front of the glacier that formed them, due to glacial thrusting, and can be composed of bedrock ridges or drift material or a combination. Researchers have noted multiple sets of thrust ridges throughout Saskatchewan, Alberta and North Dakota, some forming frontally and others laterally in the vicinity of the Missouri Coteau (Christiansen, 1959; Kupsch, 1962; Bluemle and Clayton, 1984; Klassen, 1994). Christiansen (1959) and Kupsch (1962) describe glacial-thrust ridges, covered in ablation till, west-northwest of Swift Current, SK, and the ridges are composed of mostly till and little bedrock. These ridges are found in Assemblage 5, once the MSGs can no longer be traced, and are developed along the regional slope, deforming material southward towards Cypress Hills.

The Maskwa ice stream travelled against the regional slope, and crossed over preglacial valleys such as the Battleford valley (area encompassed by the current North Saskatchewan River valley), from Lloydminster to Saskatoon (Christiansen, 1967). By crossing over preglacial valleys, this indicates that the ice sheet was thick over the Interior Plains while Maskwa paleo-ice stream was active (Ross et al., 2009). Since the Maskwa paleo-ice stream was thick and its flow direction is consistent with the LGM southwest trending ice flow, an LGM age for this system is quite likely. This suggests that the southwestern portion of the Laurentide Ice Sheet had one or more large and relatively straight ice streams delivering ice to the margins at the LGM (Evans et al., 2008; Ross et al., 2009) as opposed to uniform ice flow systems (Christiansen, 1979; Klassen, 1989, 1994; Clayton and Moran, 1982).

3.2.1.2 Buffalo Corridor

Early estimations before the release of SRTM, predicted topographic ice stream boundaries such as the Missouri Coteau, Moose Mountain, and Manitoba Escarpment, with the uplands most likely marking the boundaries between fast and slow ice (Patterson, 1997). Truncated stratigraphies at escarpment edges indicate that erosion is increased in areas of ice streaming (Patterson, 1997).

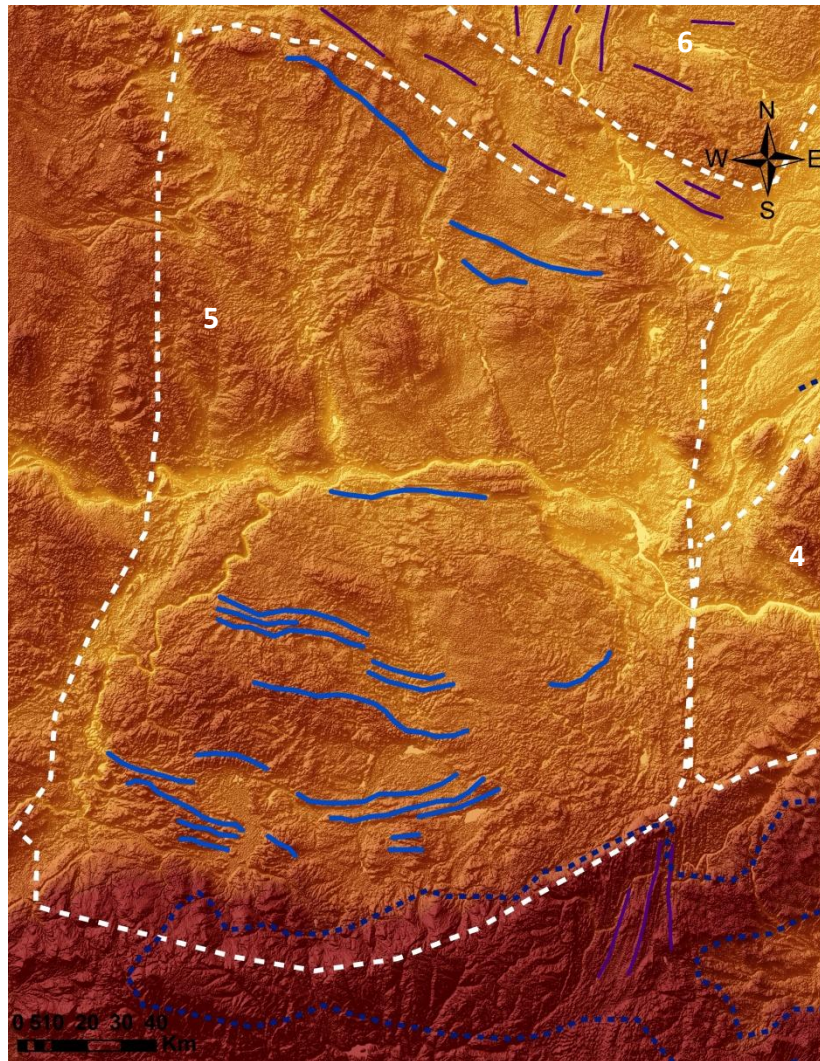


Figure 3.6: Assemblage 5's transverse ridges (blue lines) are evidence of the terminal zone of Maskwa system. These are glacial thrust features that may be moraines. MSGLs are found in the northern portion of the assemblage, but are discontinuous like those of assemblages 6 and 7.

The Buffalo system is a wide and extensive tributary-type corridor, similar to the contemporaneous ice stream systems seen in Antarctica today (Figure 3.7). The broad corridors consist of curvilinear ridges, bounded in some areas by the Canadian Shield, Manitoba Escarpment, Moose Mountain and Missouri Coteau. These wide corridors are fed by smaller and narrower corridors (such as the Battleford Corridor) from the west and the north (Figure 3.8). From this smaller corridor we see streamline features entering into the larger Buffalo Corridor. This is consistent with Paleo-ice Stream

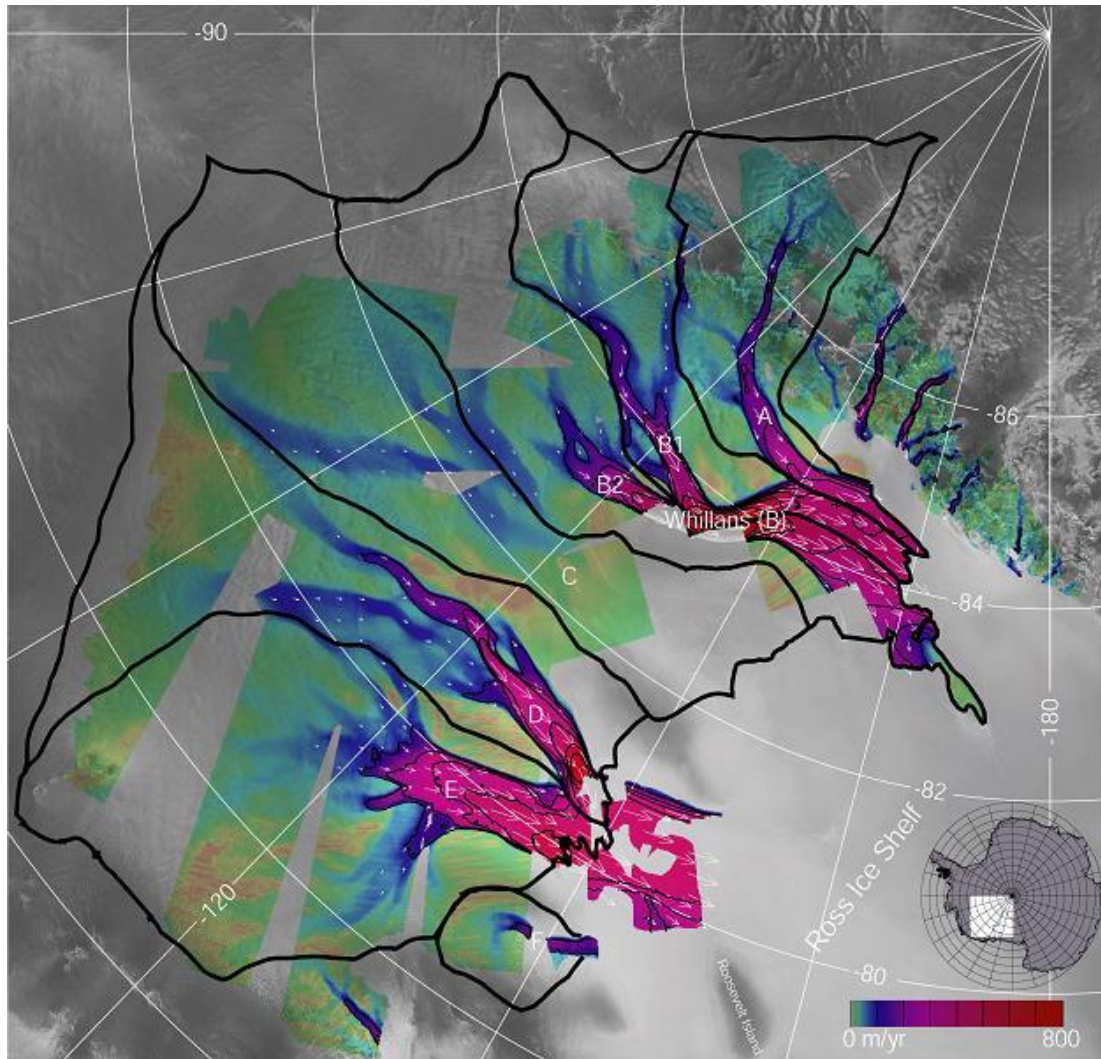


Figure 3.7: Siple Coast Ice Streams, West Antarctica. Tributaries (blues and purples, slower velocities) can be seen feeding wide corridors of ice streams (reds and pinks, higher velocities). This morphology is analogous to Buffalo paleo-ice stream system. Letters indicate Ice Stream name (Joughin and Tulaczyk, 2002).

Criteria of convergent flow patterns, as well as attenuated bedforms, like MSGs. Looking at the areas outside of the Buffalo Corridor, the assemblages identified show both preservation of landforms as well as hummocky terrain. As mentioned earlier in Paleo-ice Stream Criteria, other researchers have also shown that areas between ice streams can have potential to preserve evidence of ice flow direction (Dyke et al., 1992; Piotrowski et al., 2004; Stokes et al., 2005; De Angelis and Kleman, 2007; Kleman and Glasser, 2007; Stokes et al., 2009). The Buffalo system

formed inter-ice stream areas from the Maskwa system but only the remaining assemblages will be discussed (Assemblages 1, 2, 3, 4, 8, 9 and 10) since the Maskwa landscape has already been described.

The Buffalo Corridor is in some areas bounded by discontinuous ridges interpreted as lateral shear margin moraines (Figure 3.9). A lateral shear margin moraine is defined as a lateral margin between fast ice flow and slower ice that forms characteristic landform (Stokes and Clark, 1999; Hindmarsh and Stokes, 2008). Multiple modes of formation have been proposed: differential erosion rates, meltwater processes depositing sediment, melt-out and deposition of entrained debris, downstream sediment recycling from a step at margin or lateral advection of sediment towards margin (Hindmarsh and Stokes, 2008). Characteristically, these margins are long and narrow, and for the Buffalo system, we see two types, where one type is wider than traditionally seen elsewhere. This is due to one of two possibilities. The internal migration and instability of the Buffalo system, and the eventual width decreases of the ice stream within its corridor, would produce a long succession of lateral shear margin moraine formations, most likely from the differential erosion rates between the fast ice flow and the slow or stagnant ice that bordered it (time-transgressive). The other possibility is that the margins are polygenic, where a traditional shear margin was created subglacially but during deglaciation, it was reworked into a lateral moraine because of the surging Weyburn outlet glacier (lobe). The location of the lateral shear margin moraine is where it is expected, but cannot say for certain its genesis.

The Basin Lake Ridge is a narrow till ridge that trends due south, west of Melfort, Saskatchewan, then slightly curves west, running a total length of approximately 170 km (Figure 3.10). The internal structure of the ridge is unknown, but it is possibly a lateral shear margin moraine as it is characteristically similar to those found on Prince of Wales and Victoria Island in the Arctic (Dyke and Morris, 1988) and it is found on the edge of a field of MSGLs. It was first named and initially mapped by W.A. Meneley in the 1960s but is still not fully understood today (Meneley, 1964; Meneley, 1967; J. Campbell, pers. comm., 2009). This feature is prominent within the landscape but its full extent was unknown and unmapped until seen in the DEM images. The ridge is partially located over the ancient buried Hatfield Valley but is not bedrock controlled (the Hatfield Valley

later trends eastward) (Meneley, 1967). The Basin Lake Ridge is consistent with PIS criteria of an abrupt lateral margin.

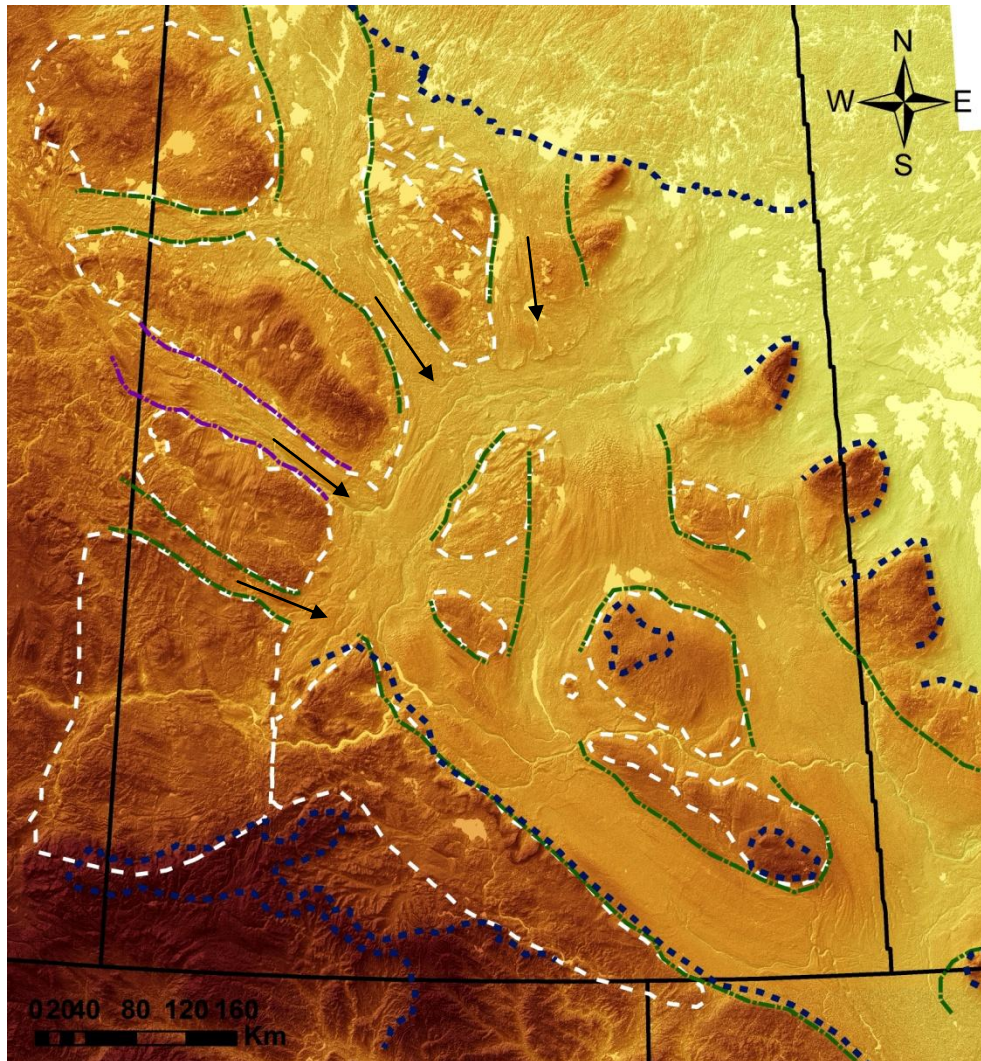


Figure 3.8: Smaller and narrower corridors feed into the larger and wider Buffalo Corridor. Black arrows represent ice flow from tributaries to main corridor. Continuous streamlined features are evidence of convergent flow, as tributaries enter into the Buffalo system. This is consistent with PIS criteria of tributary-type flow patterns and convergent flow patterns.

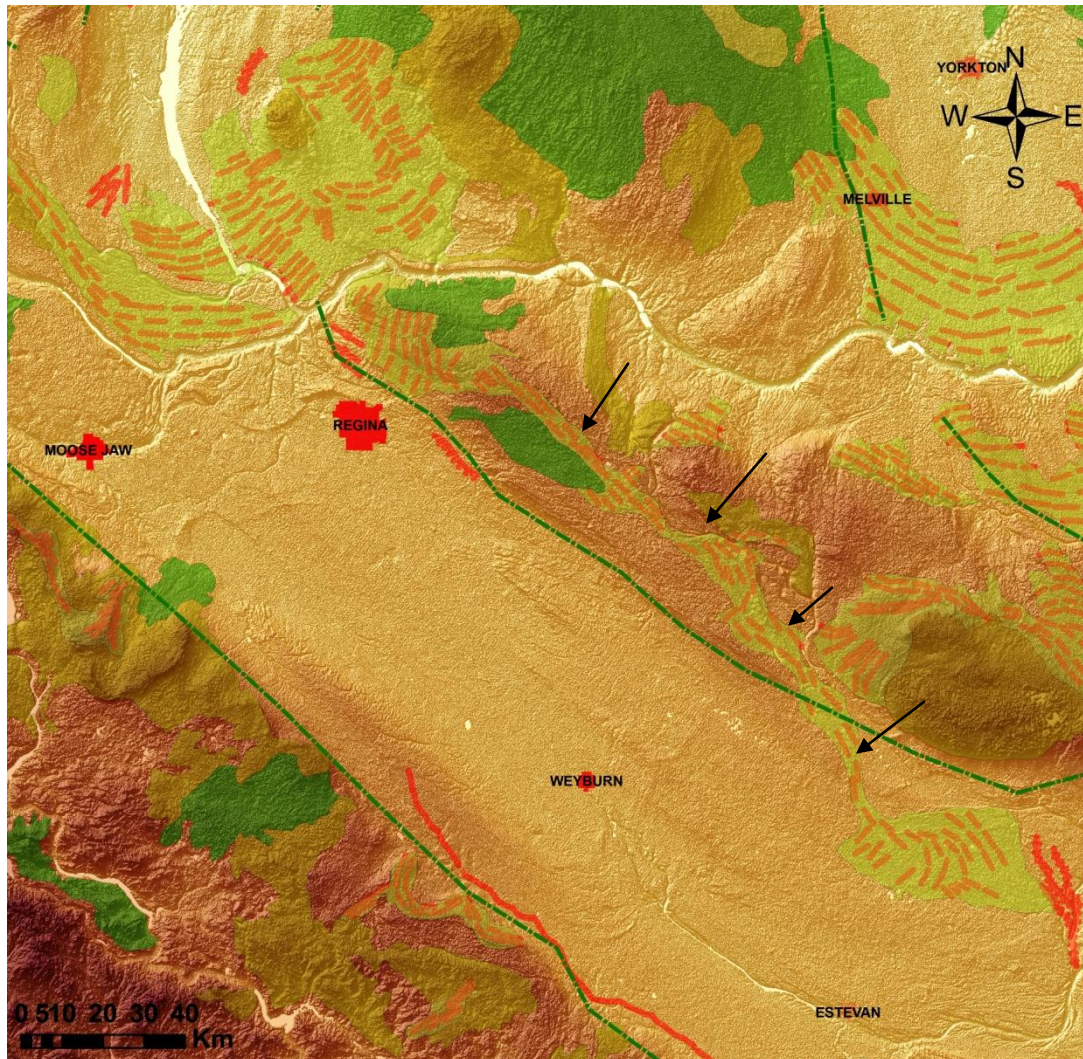


Figure 3.9: Lateral shear margin moraines (as outlined by the black arrows) are found along the boundary of the Buffalo Corridor, and were previously mapped as ridged moraines. Classical lateral shear margin shape is narrow, so their genesis as lateral shear margin moraines is either polymodal or time-transgressive. Polymodal genesis suggests the moraine was originally pristine but surging of the Weyburn lobe (western limb of the Buffalo system, that later became Glacial Lake Regina) reworked the margin. Time-transgressive genesis is due to the dynamics of the Buffalo system, its instability resulted in changing ice flow margins and this feature could be due to multiple margin formations.

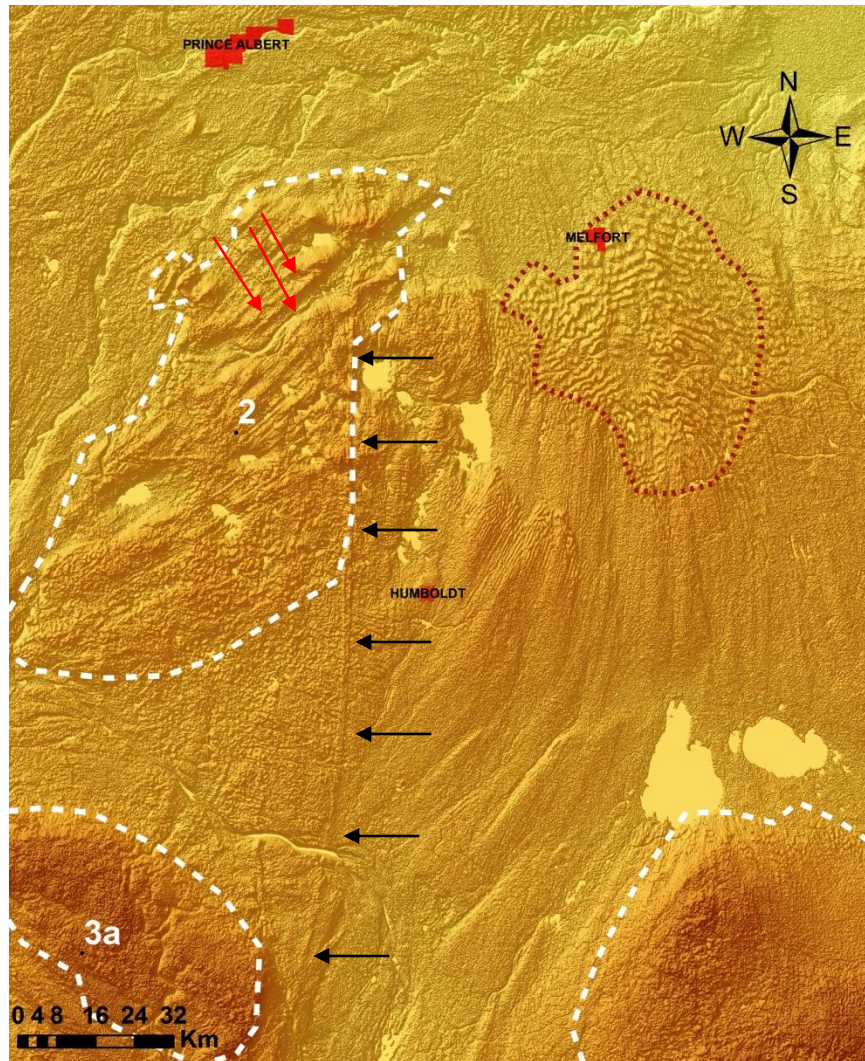


Figure 3.10: Basin Lake Ridge is a lateral shear margin moraine that spans over 170km, and is delineated by the black arrows. The neighboring "palimpsest" terrain (transverse ridges) is outlined in orange, and is likely a "sticky spot" along the Buffalo Corridor, due to the large amount of erosion that took place (older landforms are most likely not preserved). Assemblage 2 is outlined, showing southwest-trending landforms. This is most likely the oldest relict landscape in the area. Basin Lake Ridge migration is found in this assemblage as well (red arrows).

To the west of the ridge is an assemblage of hummocky terrain and southwest trending till ridges (Assemblage 2), and to the east are transverse till ridges, as well as roughly parallel curvilinear ridges within the Buffalo Corridor (Figure 3.10). These transverse ridges are only found within the Buffalo Corridor and maybe due to compressive ice flow regime linked to a steeper slope gradient (Ross et

al., 2009). Meneley (1964) determined that they are not bedrock controlled but maybe similar to ridges found in Ohio, called Palimpsest terrain. The term palimpsest terrain is used to describe visible underlying morphology where a thin veneer of till has been deposited, either by retreating glacier or a later readvance (Meneley, 1964). The youngest till, the Battleford Till, is known for being thin and discontinuous throughout Saskatchewan (Christiansen, 1968). The area and extent of these ridges are substantial and resemble ripple patterns. Meneley believes that the terrain was created during a previous glaciation, possibly a moraine or glacial thrusting, that was later overridden and eroded, and then a thin till was deposited, allowing the original terrain to still be visible beneath the younger sediments (Meneley, 1964). Boreholes are absent in this area so the original terrain genesis is speculative (J. Campbell, pers. comm. 2009). These ridges are located in four separate areas within the Buffalo Corridor (Figure 3.11). Due to the large amount of erosion that took place along the Buffalo Corridor, these features are not likely palimpsest terrain (from previous glaciations), and are most likely sticky spots. These sticky spots were due to reduced lubrication and longitudinal stress causing thrusting and stacking of pre-existing sediments and/or bedrock by the Buffalo paleo-ice stream (evidence of friction).

Assemblage 2 (Figure 3.10) is located east of Saskatoon, southwest of Melfort and south of Prince Albert, and is partly defined by the Basin Lake Ridge and includes ice marginal ridges, striated boulders and one set of flow directions. It forms an isolated and distinctive patch within the Buffalo Corridor. The flow direction based on DEM mapping and till fabric measurements is southwest, and is not believed to be associated with the flow system of the Maskwa Corridor which is south-southwest trending. One set of striated boulders suggest a flow direction of due south and is inconsistent with other flow direction indicators. The Basin Lake Ridge provides the eastern border of the assemblage. Ice marginal ridges suggest previous movement of the current Basin Lake ridge. The assemblage is a topographic high and is preserved under glaciolacustrine sediments and hummocky terrain, and could be the older relict landscape of the study area.

Assemblage 3a is located southeast of Saskatoon within the Buffalo Corridor. It is a topographic high covered by hummocky sediments. Assemblage 3b is located southeast of Melfort, and is also within the Buffalo Corridor. It is a topographic high, associated with the Manitoba escarpment to the east,

covered in hummocky moraine and glaciolacustrine deposits. No field sampling was done within either assemblage and there are no previous or DEM mapped features at these locations. Both Assemblages 3a and 3b (Figure 3.12) are possible ice stream sticky spots, localized areas of basal friction due to bedrock bumps, till-free areas, well-drained till or subglacial meltwater freeze-on.

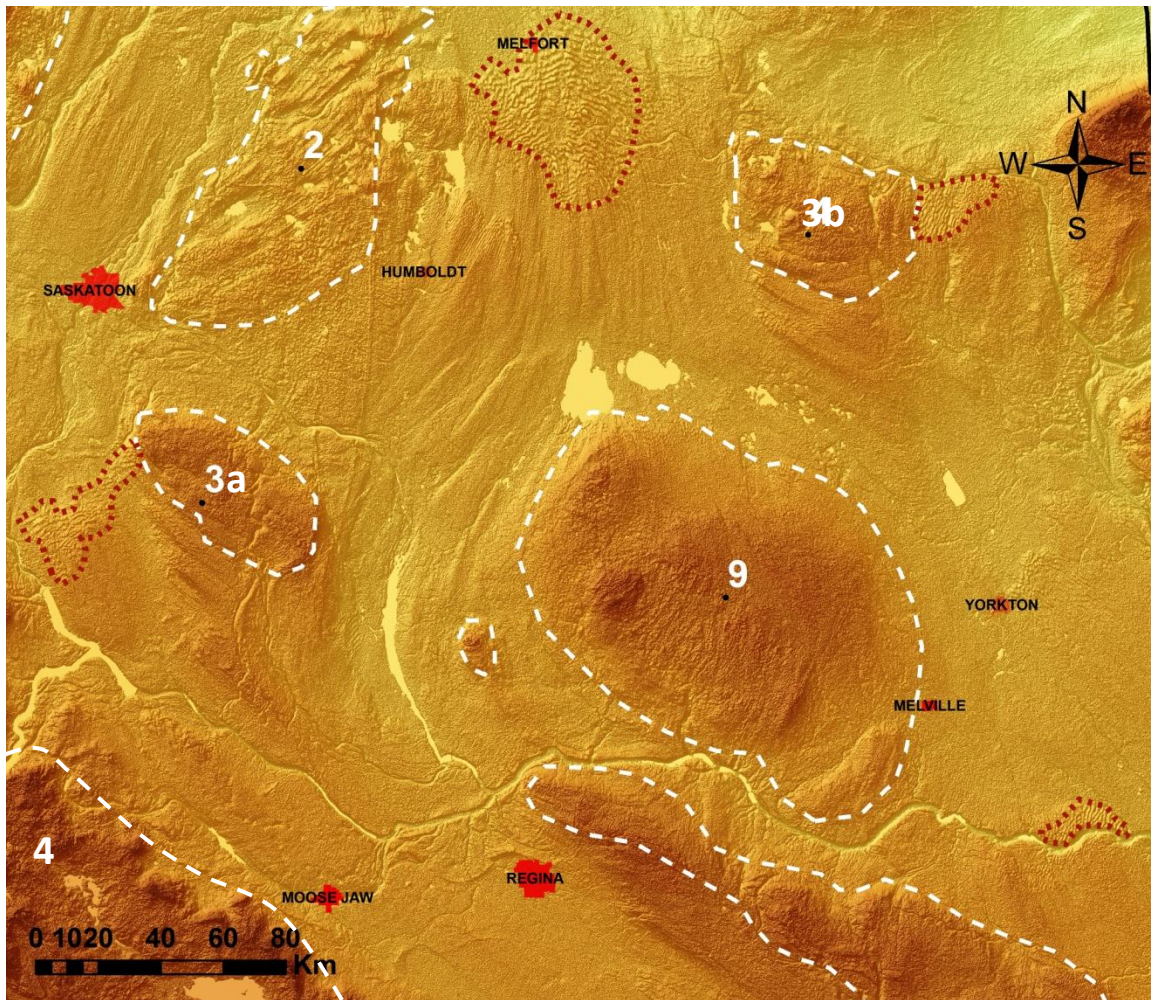


Figure 3.11: Transverse ridges similar in morphology, found along the Buffalo Corridor (orange outlines). These are most likely “sticky spots” caused by increased friction along the subglacial bed, rather than palimpsest terrain, which would not have been possible with the high erosion that took place along the Buffalo Corridor.

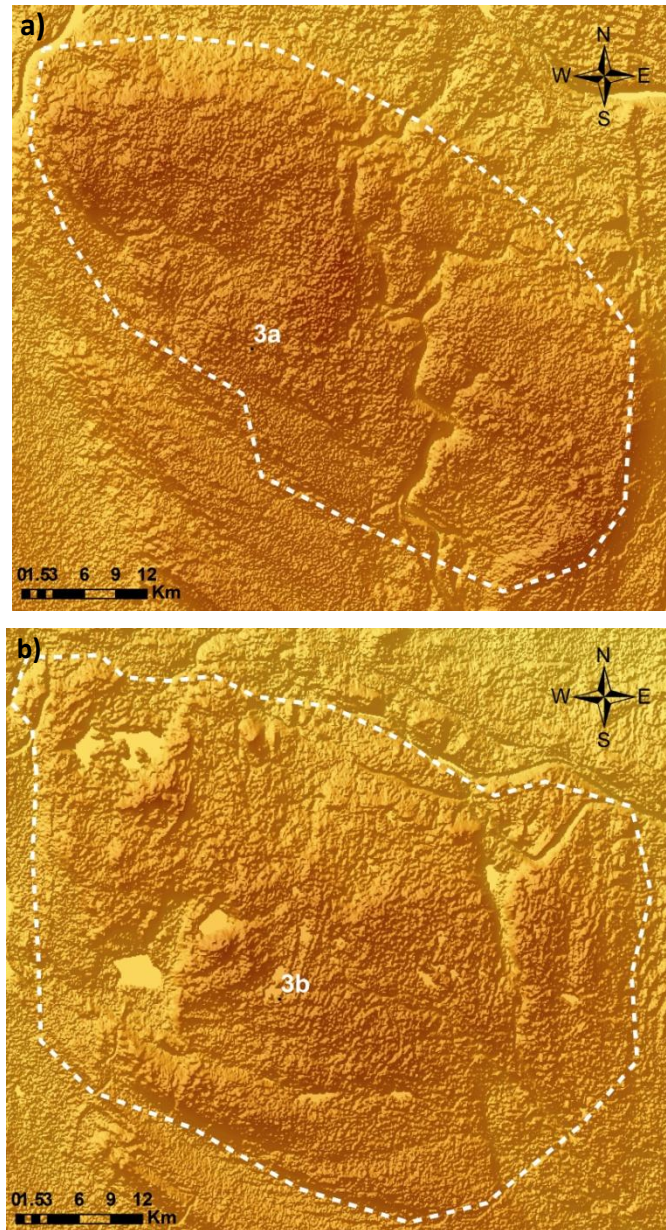


Figure 3.12: (a) Assemblage 3a and (b) Assemblage 3b. Both are topographic highs and show little to no landform evidence suggest ice flow direction. These may have been inter-ice stream sticky spots.

Red Deer Hill southwest of Prince Albert is part of a hill-hole pair with the Holmes depression. The hill-hole pair and an associated boulder (7.3m long x 6.4m wide x 1.1m high) show evidence of southwestern flow (Figure 3.13). The boulder has a scoured stoss side, plucked lee side, crescentic

gouge, and glacial striae showing glacier flow direction was 225° (Christiansen and Sauer, 1993). Hill-hole pairs do not constitute evidence of ice streaming, however, they are features that indicate frictional drag (sticky spots), and are part of the stick-slip cycle and therefore not inconsistent with the ice stream model (Figure 1.4). These are evidence of local resistance to flow followed by failure and perhaps smearing of the hill.

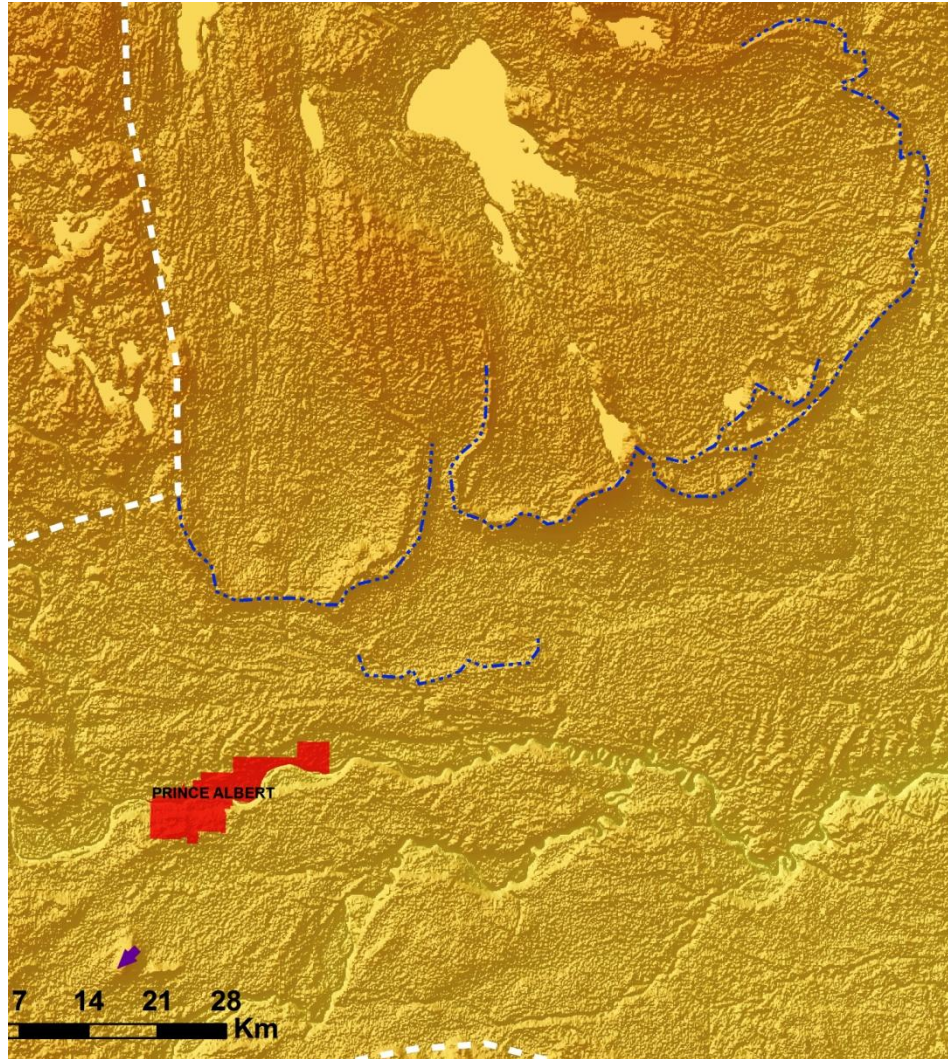


Figure 3.13: Red Deer Hill (with boulder striation measuring 225° , purple arrow) and Prince Albert late glacial lobes. The Red Deer Hill (-hole pair) does not suggest ice streaming but is consistent with ice flow, just like the boulder striations are consistent with surrounding landform evidence in the Buffalo Corridor.

Another notable feature within the Buffalo Corridor is the presence of well defined late stage thin ice lobes north of Prince Albert (Figure 3.13). These are thin ice lobes that are topographically controlled by the surrounding 100m higher terrain, which have preserved till ridges of Buffalo ice flow orientation. This indicates that part of the Buffalo landscape has been overprinted by younger events.

Contemporary ice streams generally have basal flow speeds as great as 1000m per year, which is greater than the surrounding ice, thus creating a narrow shear margin between the two ice flows (Stokes and Clark, 1999, 2002b). These margins are recognized by their zonation of landforms (fast versus slow ice landforms) and width. Changes in corridor width during ice stream activity can be seen in various areas of the corridor, with migration of ice stream shear margins (Figure 3.10, 3.14). These positions indicate overall shrinkage of the Buffalo ice stream over time during the deglaciation.

Dirt Hills and Cactus Hills in southern Saskatchewan are ice thrust features located south-southwest of Regina at the base of the Missouri Coteau (Figure 3.15). They were formed during the last deglaciation, when under compressive flow the glacier readvanced on to the Missouri Coteau escarpment and stacked the subglacial slabs of bedrock and drift creating subparallel, arcuate ice-thrust ridges (Christiansen and Sauer, 1996). The Dirt Hills are composed of three glacial thrust events, and two of the three events were later covered by till, without discontinuous erosion. The Dirt Hills were not completely overridden based on preconsolidation pressures, so part of them became a nunatak between the active northern ice and stagnant southern ice, approximately 13,000 to 11,000 years BP (Aber, 1993; Christiansen and Sauer, 1996). Thrusting most likely took place at the lateral margin of the Weyburn ice tongue during the last glaciation based on geomorphic and structural features (Aber, 1993). One possible scenario of formation is that glacier thrusting occurred at the boundary between active ice north of the Missouri Coteau and stagnant ice on the Coteau (Aber, 1993). In terms of its relation to ice streaming in this area, I speculate that stagnant ice of the Missouri Coteau may have preserved these Hills, with minimal erosion, after they were formed by three separate glaciotectionic events cause by the unstable Buffalo ice stream system. These thrust features are consistent with features associated with other paleo-ice streams.

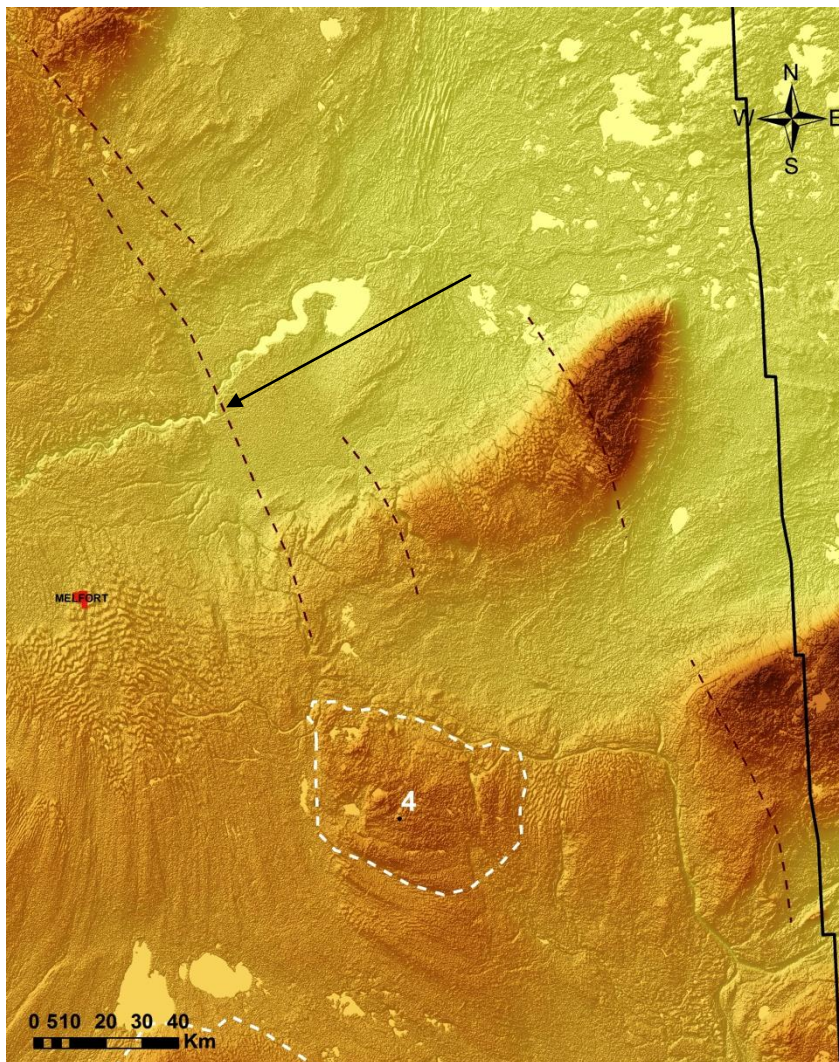


Figure 3.14: Red dashed lines show ice margin migration of the Buffalo Corridor. Most likely migrated to the west as the paleo-ice stream became thinner. Like the Basin Lake Ridge, these features are consistent with PIS criteria of abrupt lateral margins.

Assemblage 1 is a Buffalo system inter-ice stream area located northeast of the Cold Lake Corridor, north of Prince Albert (Figure 3.16). There are two sets of landform orientations in this assemblage: one set indicate ice flow to the south-southwest and is consistent with the Maskwa Corridor and the other indicates ice flow to the southeast. This southwest set appears to be older, being overprinted by the southeastern flow. The southeast flow is preserved well and may be a short-term phase

during the beginning of the Buffalo system, as ice flow shifted from the southwest Maskwa system to the southeast-trending Buffalo system. Previous mapping and new DEM mapping show these two sets. This assemblage includes two topographic highs but is not limited to higher topography. The previous and new DEM mapping on either side of the assemblage suggest different ice flow direction from both sets within the assemblage.

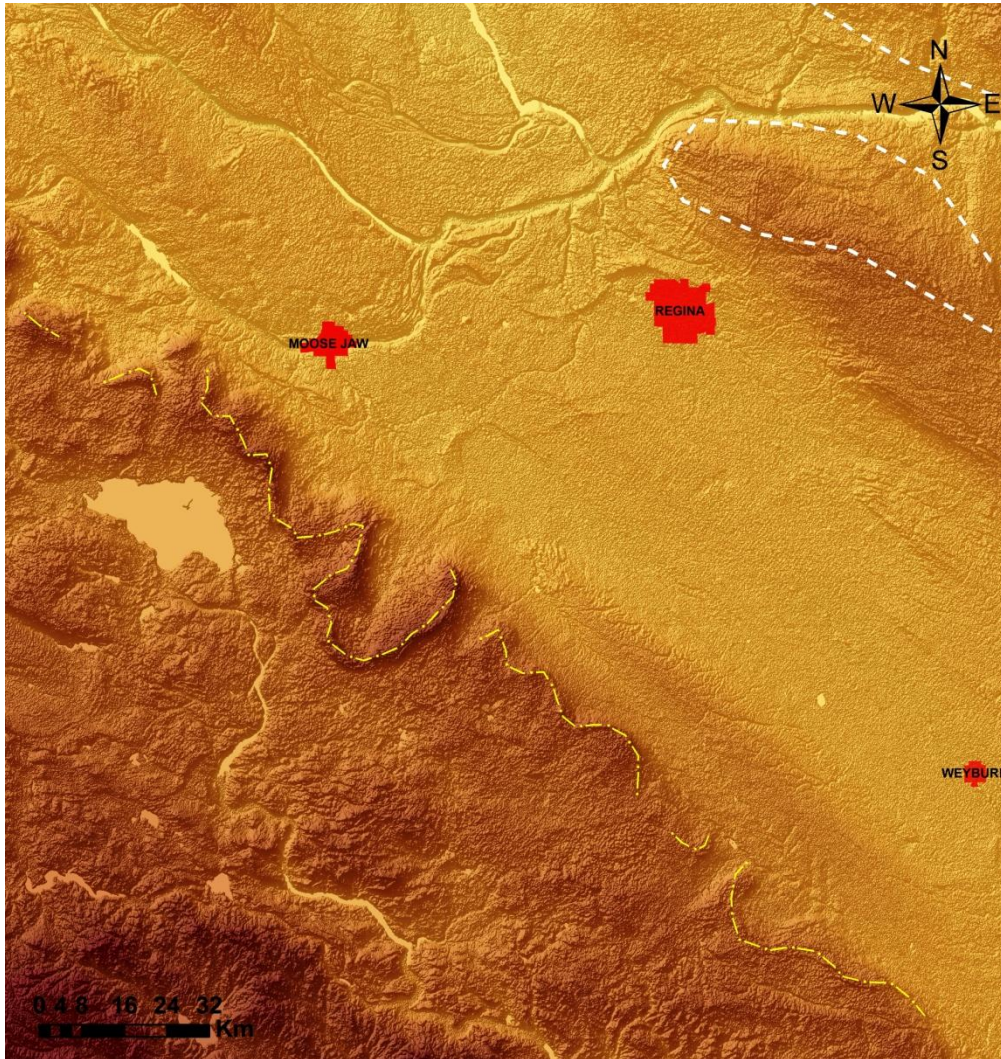


Figure 3.15: Dirt and Cactus Hills are ice thrust features found along the Missouri Coteau, formed during multiple lateral ice thrust events by the Buffalo paleo-ice stream. Yellow line outlines the thrust structures.

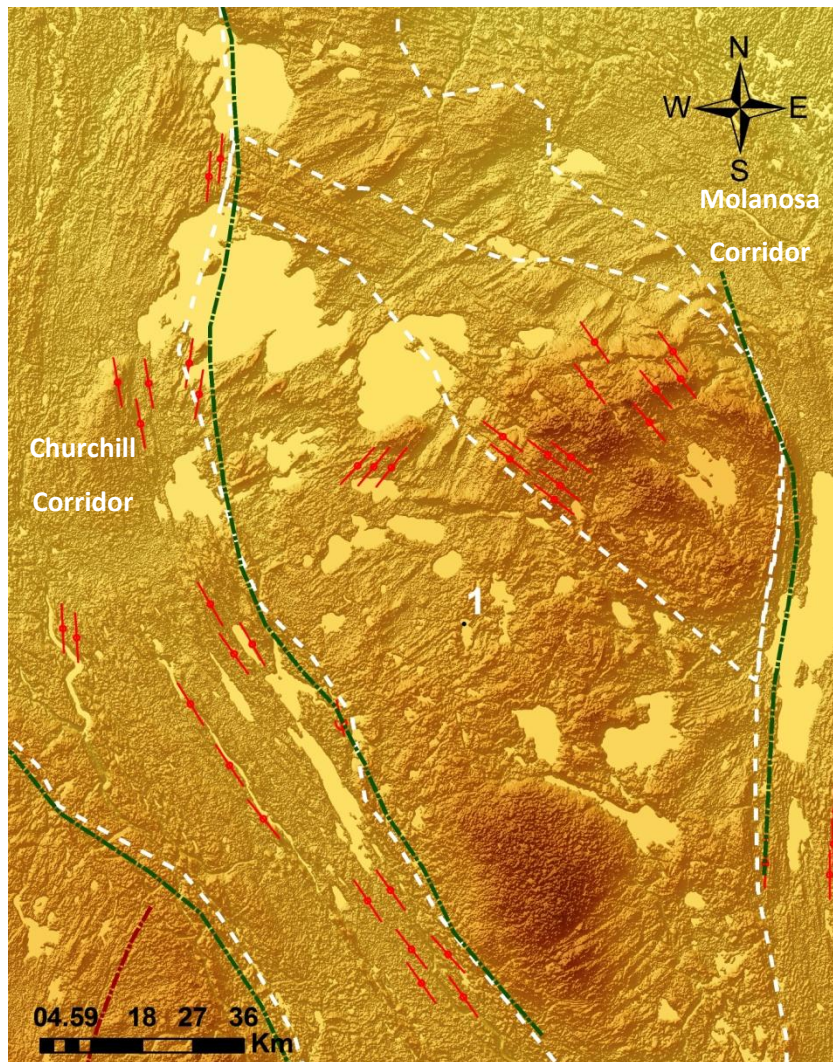


Figure 3.16: Assemblage 1, bound between Churchill Corridor and the Molanosa Corridor. There are two sets of lineations; the older set trends southwest (consistent with Maskwa) and the younger trends southeast (consistent with Buffalo).

Assemblage 4 (Figure 3.17) is unlike the others, as its features are not genetically related to each other, but all are preserved during the Buffalo paleo-ice stream system due to stagnant ice over the Missouri Coteau at that time. Most of the features within this assemblage are bedrock features.

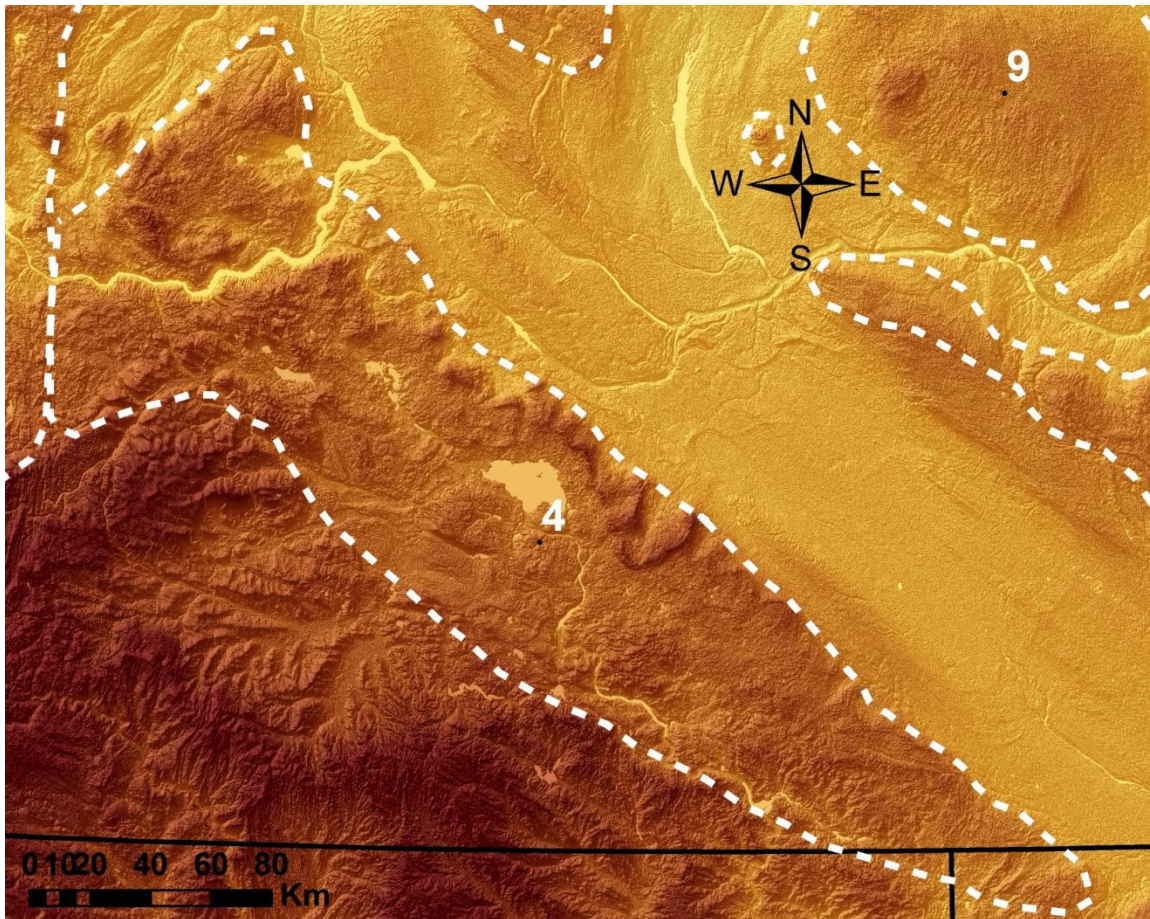


Figure 3.17: Assemblage 4 is an assemblage of genetically unrelated features, which are mostly bedrock-controlled, and were likely preserved due to stagnant ice when the Buffalo system was active.

Assemblage 8, located west of Churchill Corridor and north of Cold Lake Corridor, is a topographic high of moraine and streamlined terrains (Figure 3.18). Mapped features suggest a southwest ice flow direction, but are not consistent with the Maskwa paleo-ice stream system. However, these features suggest that they were formed under similar Maskwa dynamics but the relation is unknown.

Assemblage 9 is located northeast of Regina, the assemblage is a topographic high surrounded by the Buffalo Corridor (Figure 3.19). There are few mapped features, and the assemblage is mostly hummocky moraine. DEM mapped features are curvilinear southwest but show little surficial

expression in the field. This assemblage for most of the time during the activity of Buffalo system, was an inter-ice stream zone that was occasionally overridden by the ice stream during intervals of lateral migrations and shifting due to ice stream instabilities. The south border is bounded by the Qu'Appelle River and may be contemporaneous to Assemblage 10. Assemblage 10 is bounded in the north by the Qu'Appelle River, and the Buffalo Corridor elsewhere, this is the most linear assemblage in the province. It is east of Regina, stretching southeast to Carlyle, where Moose Mountain is its terminating feature and topographic high. Its surficial material is hummocky moraine to plain moraines, with ridge moraines dominating the outline of the assemblage. There are no mapped features, save the ridge (lateral shear margin) moraines, within this assemblage. The hummocky moraines of Moose Mountain are interpreted from its stagnant ice history (Christiansen, 1958).

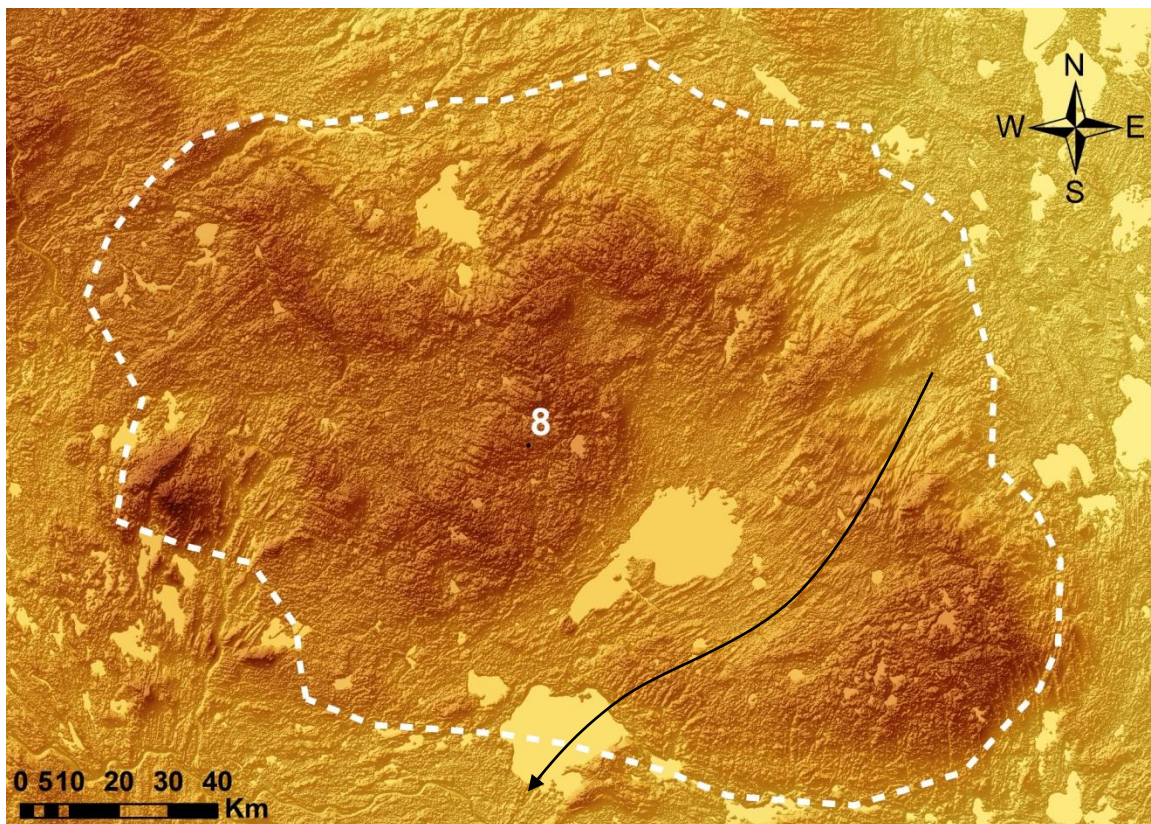


Figure 3.18: Assemblage 8 shows southwest trending ice flow, possibly ice streaming, along the Primrose and Cold Lake area (black arrows). This area is also a topographic high.

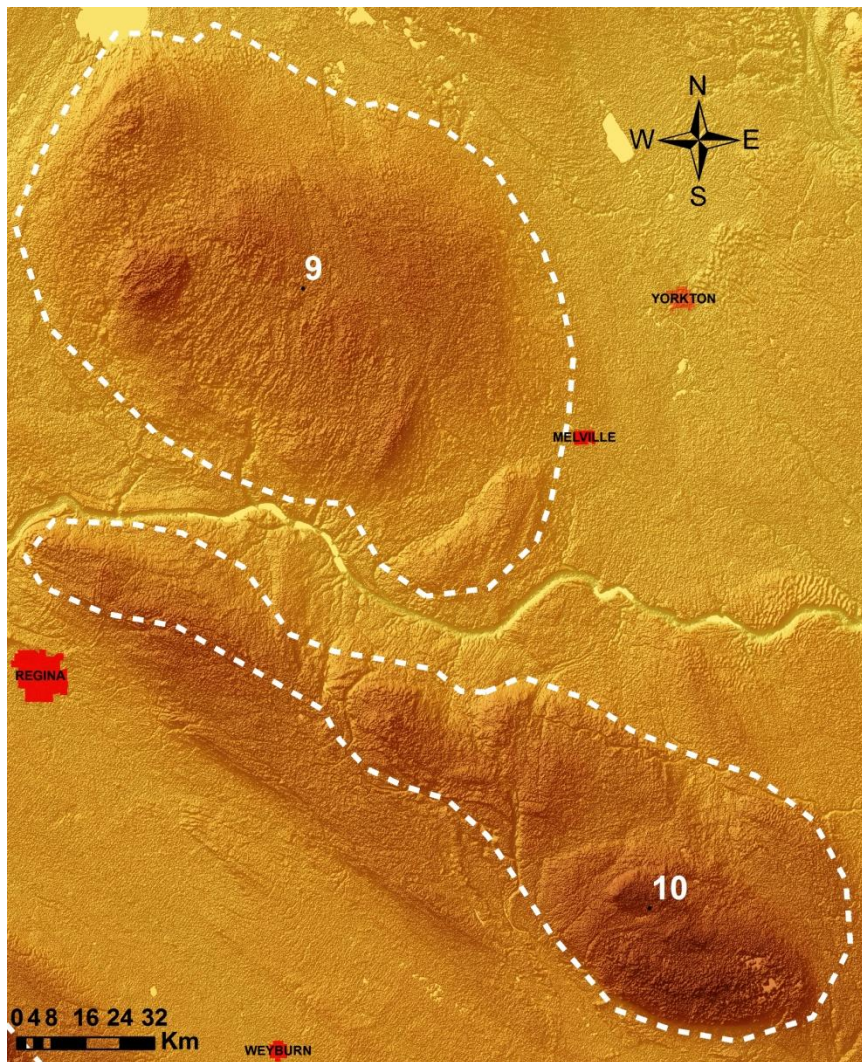


Figure 3.19: Assemblage 9 and 10, show little landform evidence of ice flow, save a few in Assemblage 9, which suggest the Buffalo paleo-ice stream was unstable and shifted between its topographic bounds (Manitoba Escarpment and Missouri Coteau). Both are topographic highs covered in hummocky terrain.

3.2.1.3 Battleford Tributary

The current North Saskatchewan River valley is within the Battleford Corridor, and is believed to have been formed during late stage deglaciation at the earliest. The Battleford Fluting field is not apparent from the ground level despite their obvious appearance on aerial photographs due to its

shallow relief of less than 1m (Stauffer et al., 1990). The fluting does show a curving and streaming flow to the southeast in the North Saskatchewan River valley, for over 300km, and southwesterly flow on the upland (Stauffer et al., 1990). This SW-trending flow system is part of the Maskwa Corridor described in the previous section. Figure 3.20 is an aerial photograph of the Battleford fluting field, and Figure 3.21 shows the previously mapped drumlin and fluting fields.

Clark (1993) concluded that when trying to determine what promotes the development of MSGs versus drumlin fields or megaflutes, the reasoning could be one of the following: (i) greater sediment supply, (ii) variations in sediment rheology, (iii) faster ice velocity, or (iv) greater time for development. Bamber et al. (2000) showed that ice stream tributaries in Antarctica are characterized by velocities that are intermediate between inland sheet flow and ice stream flow. If the Battleford Corridor is indeed a tributary of the Buffalo paleo-ice stream, as suggested by Ross et al. (2009), then the length to width ratio of subglacial bedforms along the Battleford Corridor should be lower than for the Buffalo Corridor. Table 3.2 contains the length to width ratios of ice flow features within the tributaries and corridors of the Buffalo system. The results are in good agreement with the predictions. Faster ice velocity is likely the reason why the larger corridors like the Buffalo Corridor have MSGs instead of fields of drumlins and flutes, like in the Battleford Corridor.

Table 3.2: Paleo-ice Stream Criteria, Characteristic Dimensions of Mega-scale Glacial Lineations found in south-central Saskatchewan. (E) Eastern limb of the Buffalo Corridor, (W) Western limb of the Buffalo Corridor, (N) north of Assemblage 9.

Ice Stream Corridor	Length (km)	Width (km)	Ratio (L:W)
Battleford	8 - 17	1	13:1
Buffalo	19 - 28(E), 45-56(W), 45-55(N)	1	24:1 (E), 51:1 (W), 50:1 (N)
Churchill	20 - 33	1	27:1
Cold Lake	18 - 34	1	26:1
Macklin	8 - 21	1	15:1
Maskwa	30 - 48	1	39:1



Figure 3.20: Google Maps photo of North Battleford. Fluting field is easily recognized from air photos. From Google Maps (2009)

The cross-cutting relationships between the till ridges in the Maskwa and Battleford Corridors can be seen in previous maps, but the DEMs provide a more detailed look at the relationship. These relationships are examined as well as the relative chronology proposed by Ross et al. (2009) based on the landforms and their associated assemblage. There are two forms of relative age indicators, superimposition and pre-existing linear deformation (Clark, 1993). In the case of the Battleford drumlin and fluting fields, one can see the superimposition of the Battleford Corridor features over the older Maskwa features in Figure 3.21.

Previous work in the Battleford area was done by Christiansen (1968) who explained the cross-cutting relationship in this area by means of a decreasing topographic influence during ice build-up. Christiansen proposed that ice was initially flowing to the southwest, then when it entered the Battleford area it flowed southeast until the ice sheet grew in height enough to over spill the valley

and continued its flow to the southwest. By looking at the landform record at more detailed resolution the overprinting of the Battleford Corridor over the older Maskwa features is obvious. The relative age relationship is thus opposite to Christiansen's chronology: the Battleford Corridor is younger than the Maskwa features.

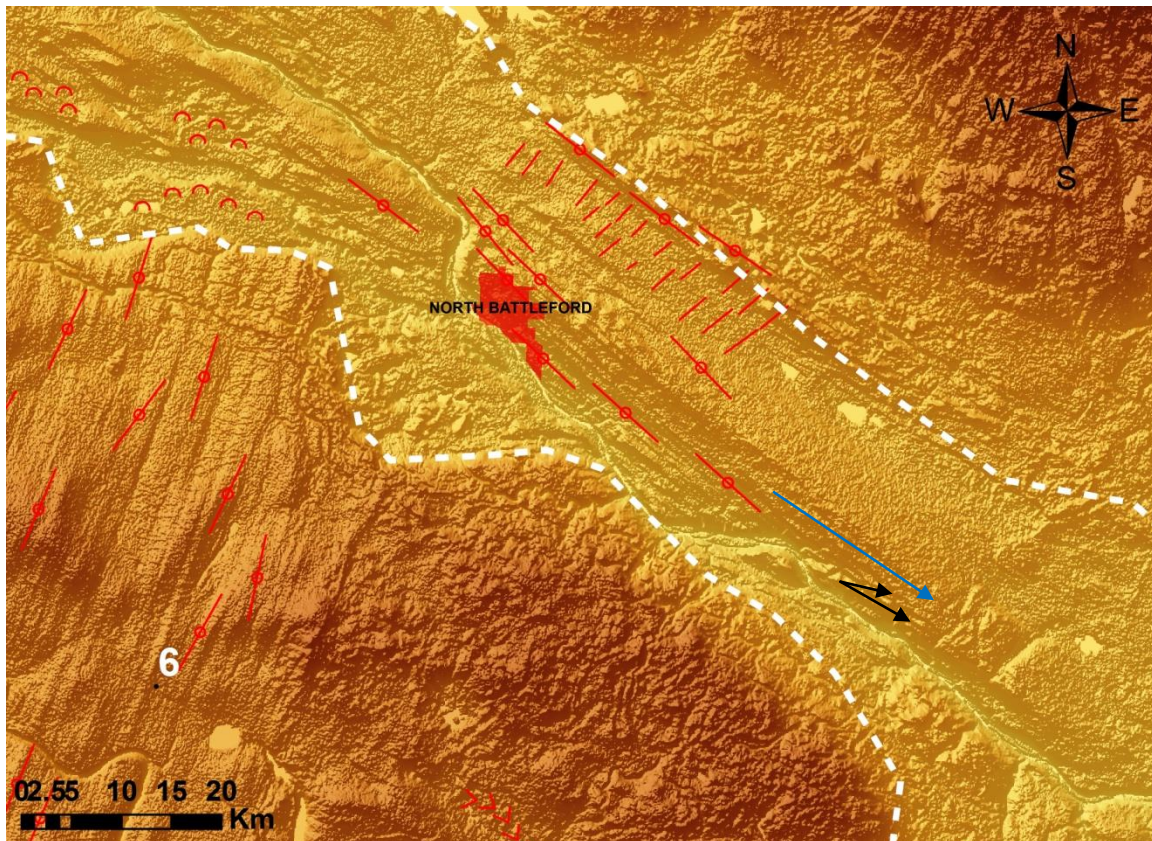


Figure 3.21: Battleford fluting fields, delineated in red, within the Battleford Corridor. Streamline features exist throughout the corridor when seen in the DEM. Black arrows are Stauffer et al. (1990) air photo measurements and boulder striations (127° and 115°, respectively) and the blue is the fluting direction determined from DEM analysis (132°). The directions are very similar, with difference in fluting direction being a factor of site selection.

The other tributary ice streams (Macklin, Cold Lake and Churchill) are very similar to each other, generally originating from the west (Alberta). No field sampling occurred in the other tributaries, and are delineated based on DEM and surficial mapping compilations. These tributaries, just like the Buffalo paleo-ice stream, have characteristic landforms and dimensions (Table 3.2 and 3.3). The

Macklin tributary ice stream is approximately 25km wide and 180km long and has east southeast trending lineations. The Cold Lake tributary ice stream is approximately 33km wide and 350 long. It has east then southeast trending lineations (an elbow shaped corridor). This corridor is described in more details in Ross et al. (2009). The till ridges are continuous and bend down-ice as they enter into the Buffalo Corridor. Some features close to the elbow could be interpreted as ice stream shear margin moraines. The Churchill tributary ice stream is approximately 75km wide and 225km long. It has almost due south trending lineations that meet and are continuous as it enters into the Cold Lake Corridor at the elbow.

Table 3.3: Paleo-ice Stream Criteria, Characteristic Dimensions of Ice Stream Corridors found in south-central Saskatchewan. (E) Eastern limb of the Buffalo Corridor, (W) Western limb of the Buffalo Corridor, (S) south of the Canada-U.S. Border. Width varies across the ice stream and thus given as a range from largest to smallest.

Ice Stream Corridor	Length (km)	Width (km)
Battleford	335	28-46
Buffalo	725(E) - 900(W) - 800(S)	70-110
Churchill	225	75
Cold Lake	350	33
Macklin	180	25
Maskwa	900	60-120

3.3 Sediment Fabrics

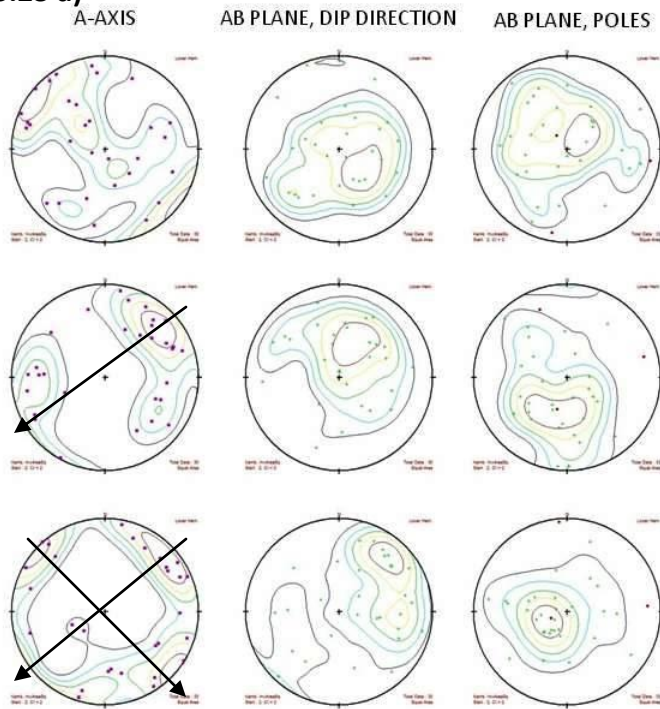
Fabric data have been used for decades to determine ice flow direction (Andrews, 1971). It is only recently that A/B planes were used to avoid the potential problem of transverse orientations observed for clast A-axis. They also provide poles-to-plane data, strengthen modality plots and provide a clear visual impression of stress directions (Evans et al., 2007). Given A/B plane data, A-axis can thus appear to be transverse to ice flow. This is interpreted as resulting from a compressive flow regime. Determining sediment fabrics is associated with specific thesis objective 2.

Determining if there are strong or good fabric data, or that the data are not to be used to determine ice flow direction, is dependent upon the number of samples, and the modality and spread of the fabric. Modality is the mode of till formation recorded as one of five fabric categories: unimodal

cluster, spread unimodal, bimodal cluster, spread bimodal, polymodal or girdle-like. When an eigenvector is used to determine ice flow direction, it can be misleading depending on the strength of the till fabric. In order to have a more accurate representation, the modality of the fabric and their eigenvectors are used together to infer subglacial till genesis, where the modality-isotropy diagram helps to distinguish till-forming processes (Hicock et al., 1996). A strong-good fabric is unimodal or bimodal (clusters or spread) whereas weak fabric is usually polymodal to girdle-like. Figure 3.22a is a comparison between different sites' fabrics to show the difference between strong, good and weak fabrics for ice flow determination. However, good is a relative term, as good fabric data may not necessarily be useful for ice flow. The last example, Rd 304 shows that the a axis is transverse to flow, because of compression, the clasts can turn yet keep the same up-glacier dipping angle, and thus the AB plane shows consistent flow direction but with two different populations. Alternatively, some of the 'transverse' clasts could record an earlier ice flow phase or more than one deposition or deformation event (Hicock et al., 1996; Hicock, 2009). Figures 3.22b and 3.22c shows the locations of the good and strong fabrics. These fabrics are, however, not consistent with the landform evidence, as are a fair size portion of the other fabric sites. This was a probability due to the poor pebble conditions.

The fabric data collected for this research are good in most cases, few being unusable, but it should be noted that the conditions in which the fabrics are taken, i.e. clay-rich, small pebbles and pebble poor till, is not ideal for fabric analysis (Andrews, 1971). Because of this, fabric data are used in conjunction with other data and should not be used to draw conclusions independent of other data, it is complementary. Figure 3.23 is all the sites where till fabric measurements were taken and their ice flow direction, based on AB plane data, and Figure 3.24 is based on the A-axis data.

3.23 a)



RD 734 01:
 •N= 30
 •S1= 0.44, 0.51
 •V1= 09-315, 75-323

WEAK

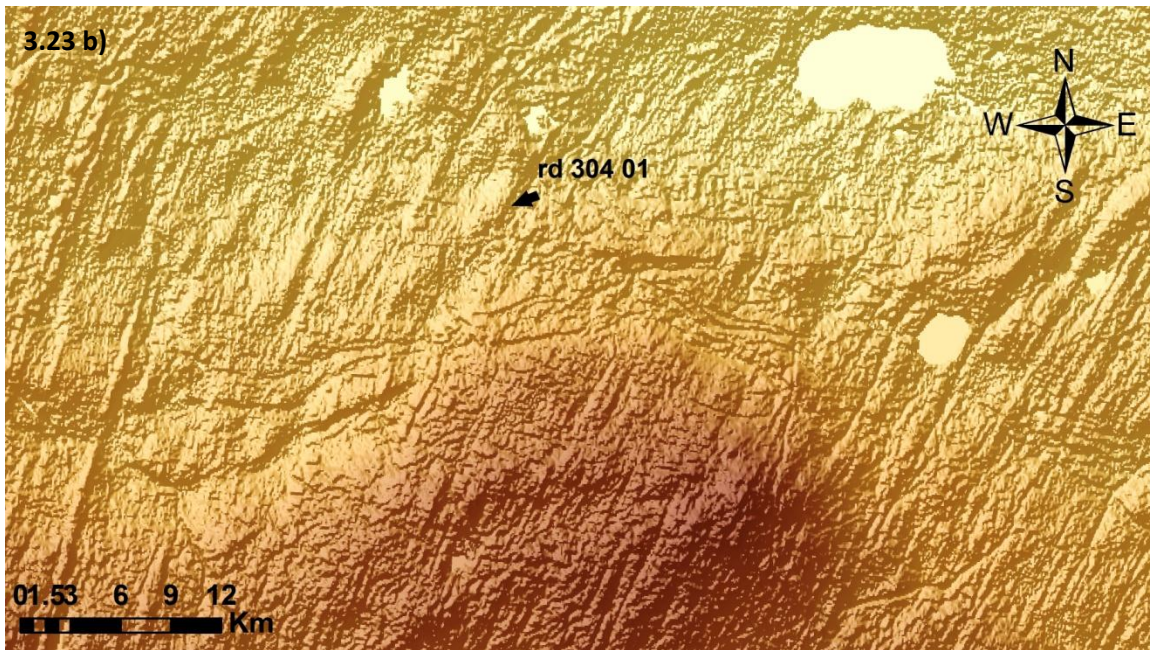
Hepburn 01:
 •N= 30
 •S1= 0.48, 0.68
 •V1= 21- 256, 66-079

GOOD

RD 304 01:
 •N= 30
 •S1= 0.44, 0.68
 •V1= 12-137, 75-248

STRONG

3.23 b)



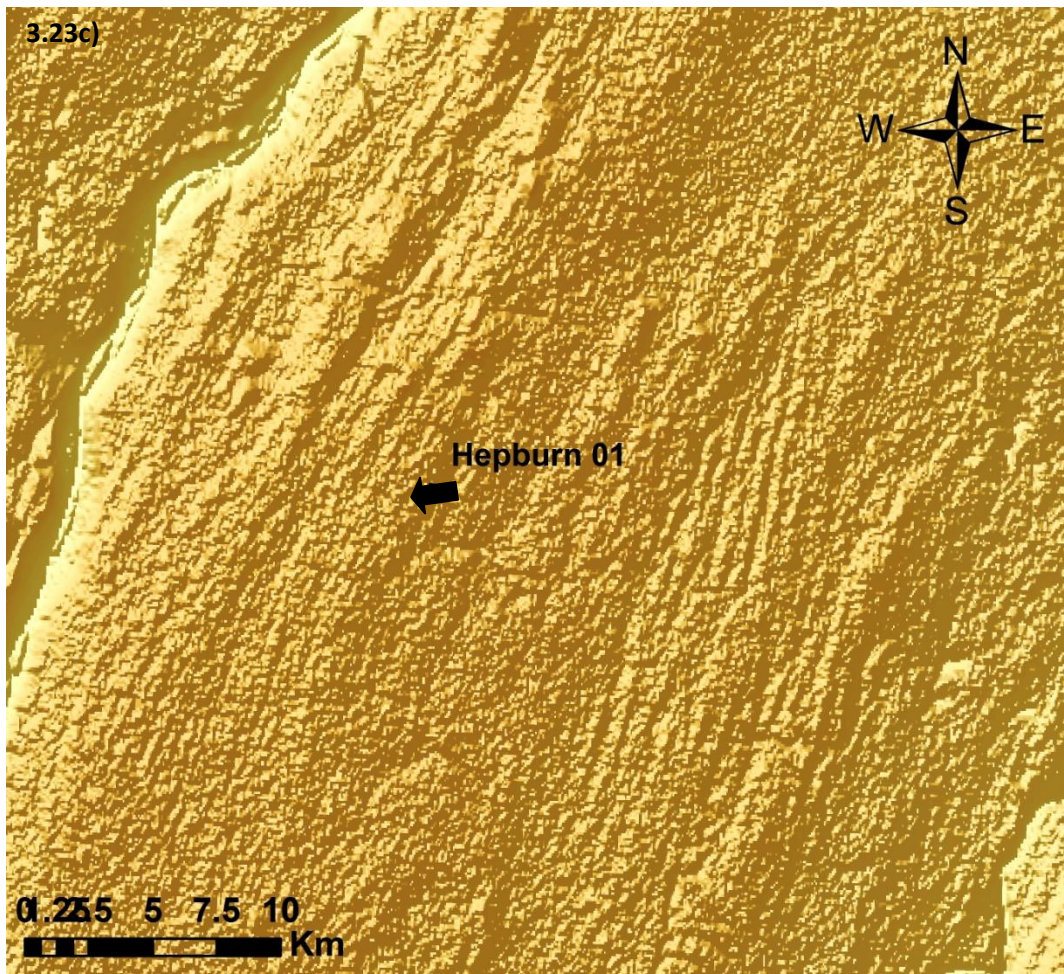


Figure 3.22: (a) Example of fabric classification based on A-axis and AB plane directions; (b) Field site 'Rd 304-01' classified as strong fabric but fabric direction is inconsistent with surrounding landforms, and maybe be remnant of older flow, or due to poor pebble conditions; (c) Field site 'Hepburn 01' is classified as a good fabric, but is inconsistent with landform evidence.

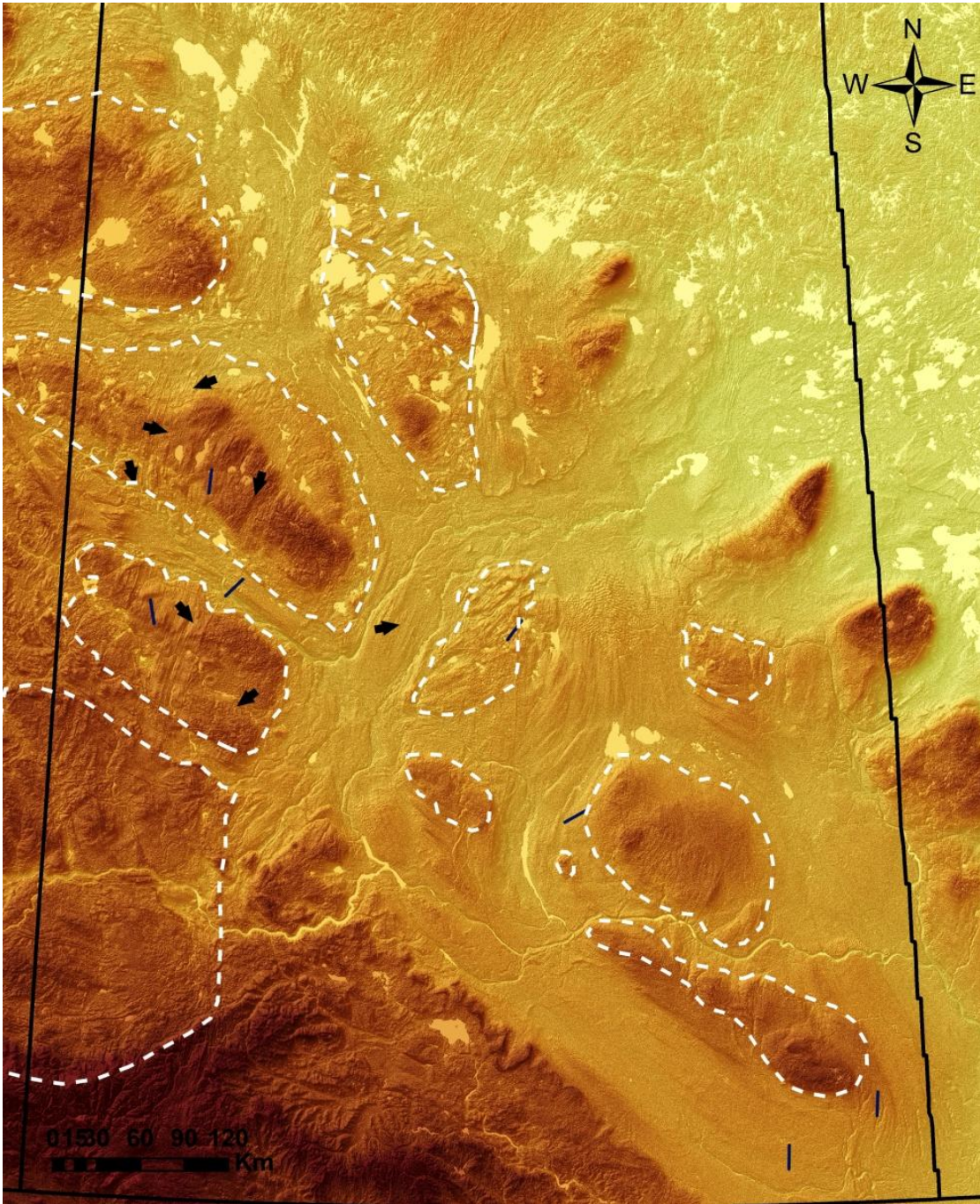


Figure 3.23: AB plane data for all field sites where 'strong' and 'good' fabric measurements were taken. Black arrows indicate 'strong' fabric classification/direction, and dash-lines indicate 'good' fabric classification/direction. AB plane data is used to avoid transverse orientations of pebbles.

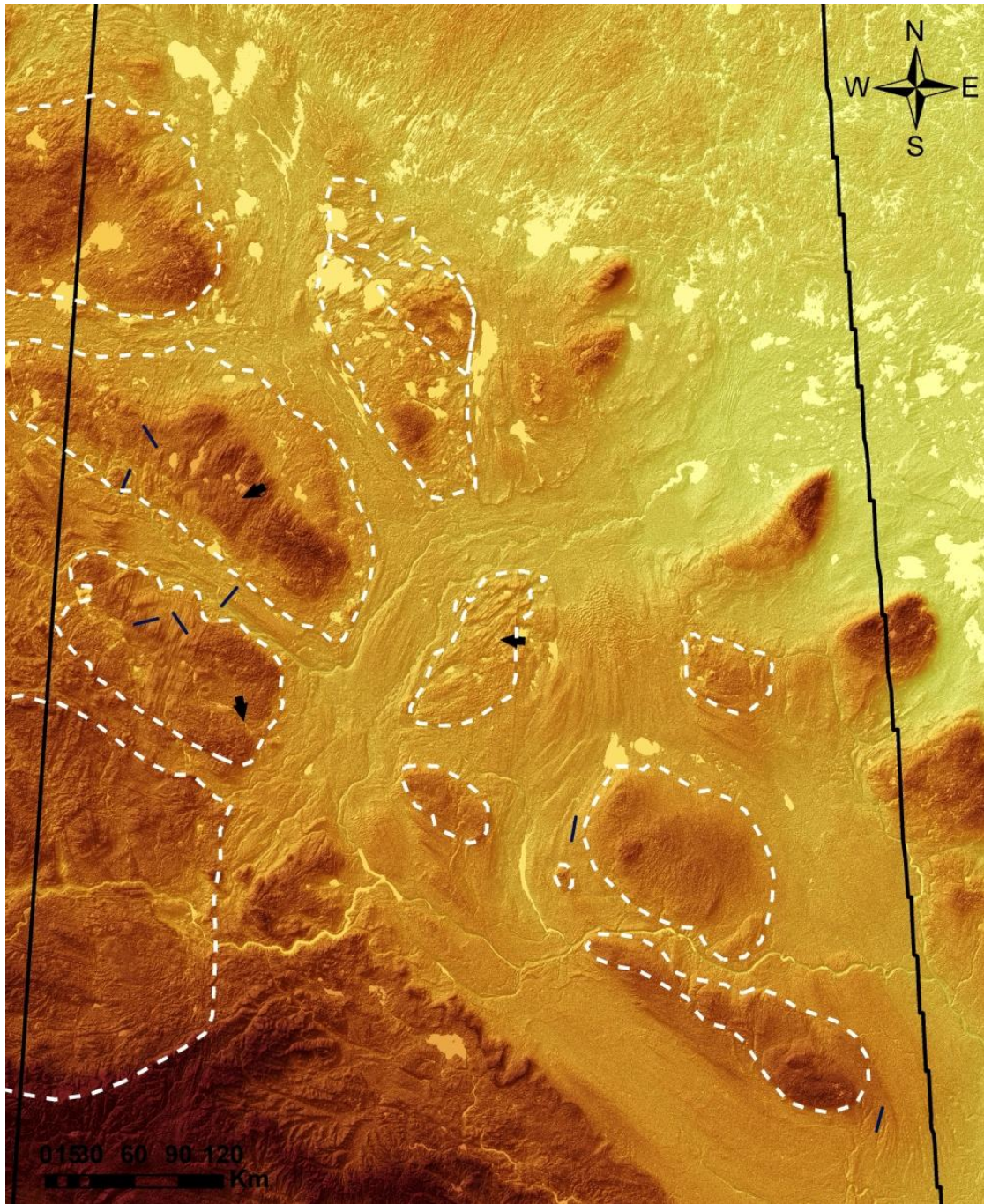


Figure 3.24: A-axis data for all field sites where 'strong' and 'good' fabric measurements were taken. Black arrows indicate 'strong' fabric classification/direction, and dash-lines indicate 'good' fabric classification/direction.

3.4 Striations and Beddings

Previous research in Saskatchewan has found multiple sites of boulder striations, boulder pavements and bedding plane measurements. Figure 3.25 shows all the sites within the research areas that have these measurements. These types of measurements are more robust as they are direct measurements that have little human involvement and therefore less interpretation and error. New sites were found throughout Saskatchewan, and can be found in Figure 3.26. Unlike the till fabric measurements, the striation measurements can be used independently of other data for ice flow direction. For example, site Rd 642-01, has a boulder pavement with 11 boulders showing an average striation direction of $114\pm 10^\circ$, this is consistent with the landforms within the Buffalo Corridor (Figure 3.27).

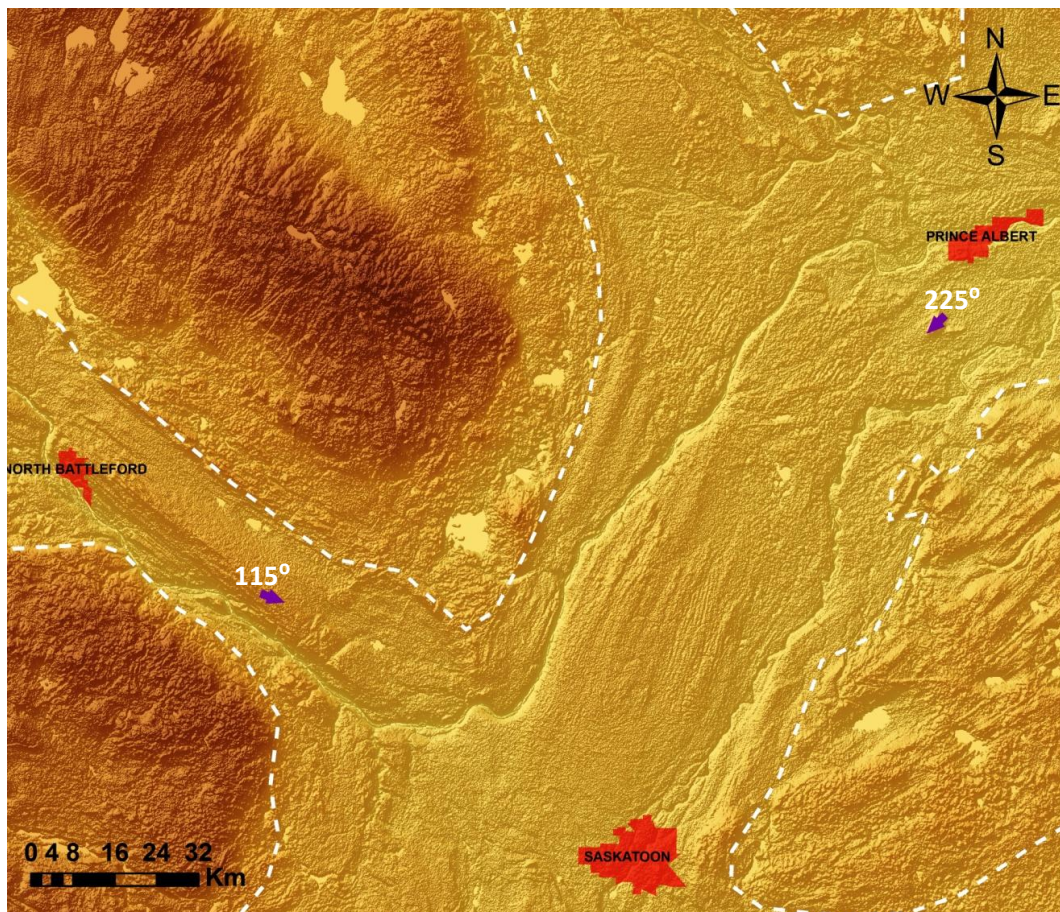


Figure 3.25: Striations data from literature; Stauffer et al. (1990) for the Maymont area (115°) and Christiansen and Sauer (1993) for the Red Deer Hill (225°).

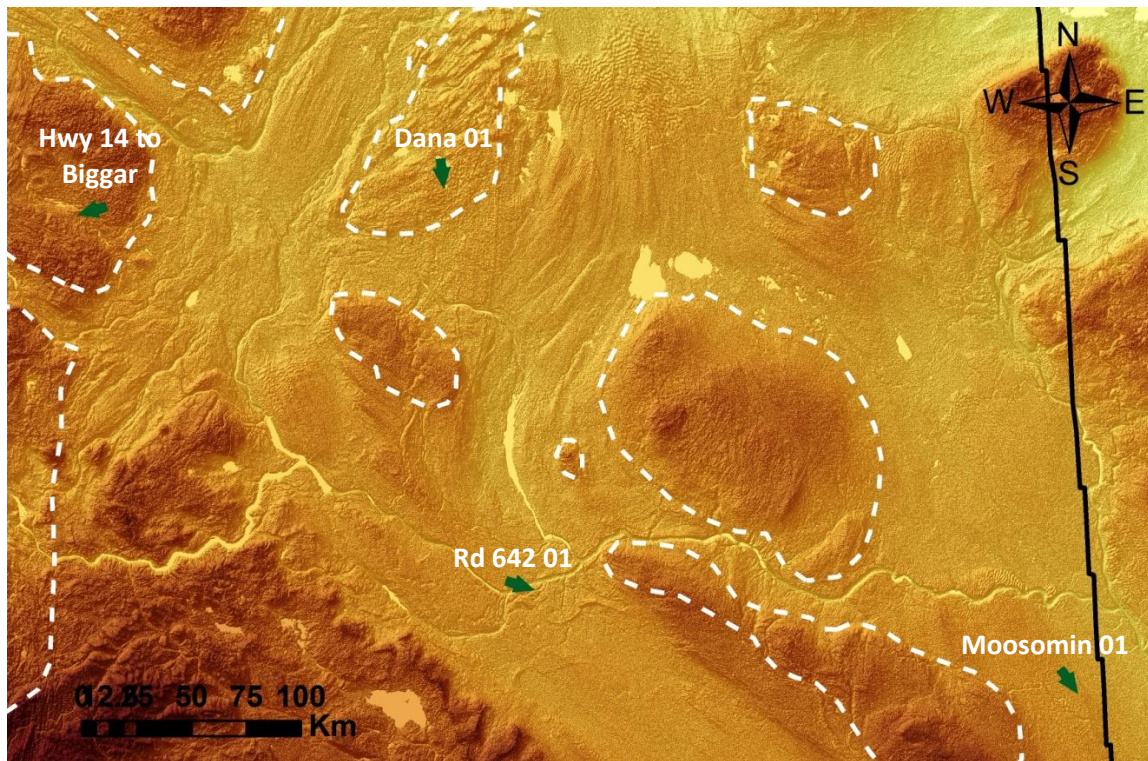


Figure 3.26: Striation measurements from field work. Samples are more consistent with landform evidence than till fabrics, because till fabric conditions throughout the province are not ideal whereas boulder measurements are only selected if boulder is elongated, flat-topped and lodged.

3.5 Summary of the landscape analysis

Below is a summary of the Paleo-ice Stream Criteria and how the subglacial landscape of Saskatchewan meet them.

3.5.1 Characteristic Shape and Dimensions

Contemporary ice streams are characterized by large dimensions, typically >20km wide and >150km long, with a convergent onset zone, and thus are the most obvious clue to ice streaming (Stokes and Clark, 1999). Table 3.3 has the dimensions for each corridor. Since contemporary ice streams are being used analogously, it is possible to have larger or smaller dimensions when the corridor-shape is consistent with contemporary ice streams (Stokes and Clark, 1999). The Table demonstrates that various paleo-ice streams, and their associated sizes, can be found over a relatively small region.

This understanding can be used to further characterize other areas of potential ice streaming, not limiting them to specific dimensions.

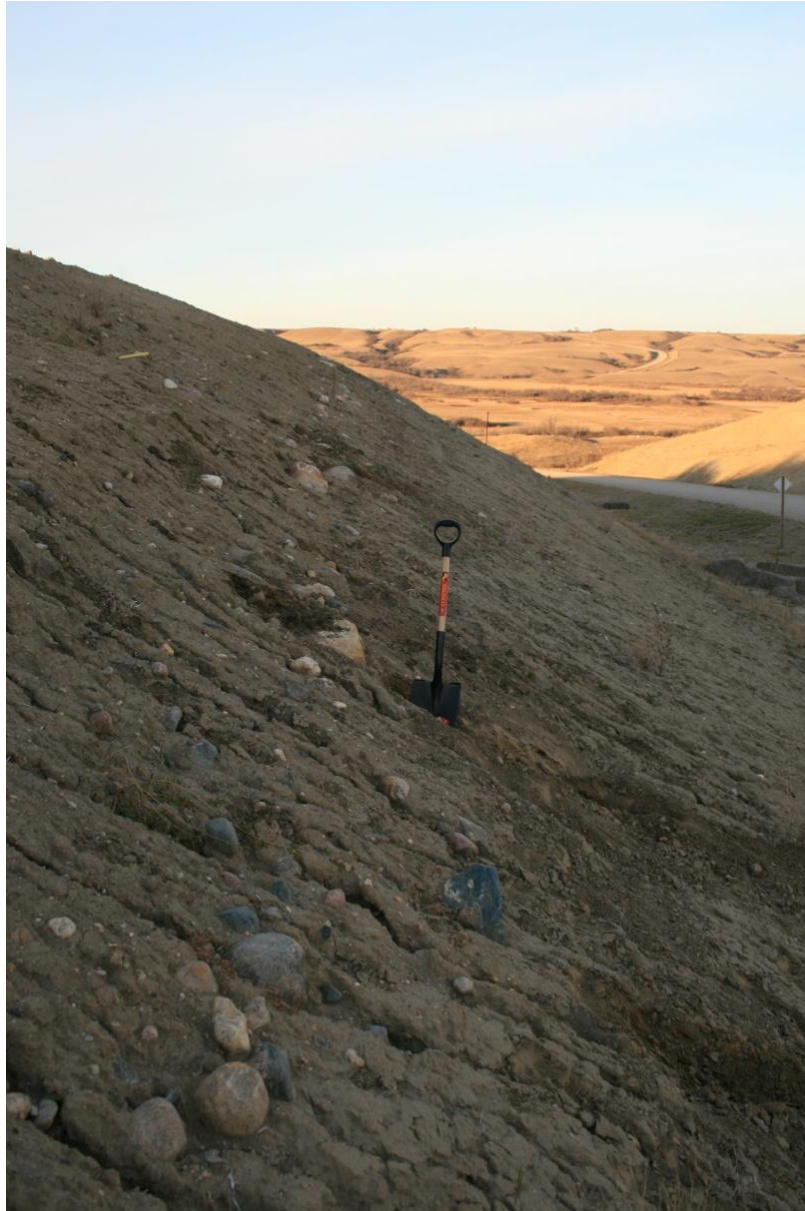


Figure 3.27: Boulder pavement found at field site Rd 642 01, west of Regina. 11 boulders were freshly exposed along the youngest till, with an average direction of $114\pm 10^\circ$; this is consistent with the landform evidence along the Buffalo Corridor.

3.5.1.1 Convergent Flow Patterns

Figure 3.5 demonstrates the convergent flow into the Maskwa ice stream system along the corridor. Another example of convergent flow is shown in Figure 3.8 where tributaries from the west are entering into the Buffalo Corridor, without truncation.

3.5.1.2 Contemporaneous tributaries

The continuity and convergence of landforms from the Cold Lake Corridor, Churchill Corridor, Battleford Corridor, and Macklin Corridor into the main Buffalo Corridor are used to argue that these features formed contemporaneously to each other forming a large Buffalo paleo-ice stream system. If they were not contemporaneous to the Buffalo Corridor such continuity would not be possible. Also, the reduction in length to width ratios from the main trunk (Buffalo Corridor) to the tributaries as well as the absence of shear margin moraines except near the coalescence is consistent with glaciological observations showing reduced velocities inside the tributaries and disappearance of shear margins.

3.5.2 Rapid Velocity

3.5.2.1 Attenuated Bedforms

Mega-scale glacial lineations are foundational bedforms for paleo-ice stream identification. MSGs are found in various locations throughout the Buffalo system, as well as the Maskwa and Battleford systems. These highly attenuated bedforms (length to width ratio $> 10:1$) are more likely only from fast ice flow over short periods than slow ice flow over long periods due to variations in ice sheet geometry (Stokes and Clark, 1999, 2002a). These features are also useful in identifying the spatial extent of former ice streams, in addition to flow direction. Examples of these features are found throughout the province (Figures 3.3, 3.16, 3.21).

3.5.3 Abrupt Lateral Margins and Shear Margin Moraines

There are two examples of lateral and shear margins in the Buffalo systems, Figures 3.10 and 3.14. Lateral margins tend to be abrupt, and narrow, and can delimit the former ice stream track. Figure 3.10 shows the Basin Lake Ridge, a lateral margin for the Buffalo Corridor. Figure 3.9 is the shear margin moraines, currently mapped as ridged moraines, as the eastern boundary of the western limb of the Buffalo paleo-ice stream, and is consistent with the criteria (Stokes and Clark, 1999; Hindmarsh and Stokes, 2008).

3.5.4 Inter-Ice Stream Areas

Similar to lateral margins, the boundaries of inter-ice stream areas (assemblages) are sharp and distinct, and exhibit zonation of landforms on either side of the margin (Stokes and Clark, 1999). These can be seen at the boundaries of all of the assemblages, however, Figure 3.10 is just one example of the distinct boundaries between the corridor and the assemblages. Another important characteristic of inter-ice stream areas is the isolated and contrasting internal landforms. Assemblages are not limited to inter-ice stream zones, and can contain MSGs, such as those of the Maskwa paleo-ice stream in assemblages 5, 6 and 7.

In the research presented herein, compositional characteristics of the surface till (e.g. geochemistry, age of mineral grains) are used to further constrain the sediment-landform analysis. The goal is to further analyze the terrain elements presented in this Chapter and to determine whether their internal compositional signature is also distinguishable from adjacent terrain elements.

Chapter 4 Till Provenance: Compositional Data and Detrital Ages

The current understanding of ice stream systems suggests that areas outside of ice stream corridors may have developed under sluggish or stagnant basal ice conditions, or are preserved landforms due to limited erosion. This would create a landscape mosaic consisting of a young paleo-ice stream corridor and remnant portions of older landscapes representing the inter-ice stream areas. For example, the discontinuous assemblages described in Chapter 3 would represent the inter-ice stream areas of the Buffalo paleo-ice stream. Some of them include evidence of non-streaming flow or other ice streaming phases with their own inter-ice stream areas (e.g. the Maskwa assemblages). These remnant patches may thus record different glacial dynamics histories. According to this mosaic landsystem model, the till composition and dispersal patterns are expected to vary between the various assemblages. The compositional data can also be useful in identifying Boothia-type dispersal patterns, which is a criterion to recognize rapid ice flow velocity in the geologic record (Table 1.1). The southerly flow pattern during the Wisconsinan of the Plains Ice of the Keewatin Sector of the Laurentide Ice Sheet (Klassen, 1989), now appears to be a gross simplification of the extremely detailed flow pattern that occurred according to the landscape analysis described in Chapter 3. In this Chapter, the composition of the till in key assemblages is described (specific objective 3) to further establish the signature of these assemblages (main objective 1), and to test the reconstruction of Ross et al. (2009) (main objective 2). *All collected data discussed, in part or full, can be found for each site in **Appendices A and B**.*

4.1 Till Composition

Till texture generally reflects the nature of bedrock lithologies from which it is derived. In the Prairies, the sand in the till matrix is largely derived from Tertiary sandstones, and the fines (silt and clay) are derived from the Cretaceous beds. The geochemistry of the till matrix should thus be largely controlled by the lithology composition of Cretaceous formations. Pebbles and clasts of prairie tills are also known to contain carbonates and crystalline rocks indicating glacial transport from carbonate and Shield areas (Klassen, 1989). The bedrock geology seen in Appendix C shows the

carbonate source to the east and northeast. Shield erratics, mostly Proterozoic erratics would indicate a more northern provenance.

A number of distinctive types of erratics have been reported from prairie tills, two of which are relevant to this study. Concretion-bearing greywackes have been found in tills from Manitoba, Saskatchewan to southeastern Alberta (Klassen, 1989). The Proterozoic Omarolluk Formation within the Belcher Group in eastern Hudson Bay is the only known source for these erratics (Prest et al., 2000). They indicate westward glacial transport of over 2000km, thus providing information on continental-scale glacial dispersal patterns. Current knowledge of the distribution of these erratics and of the major shift in regional ice flow systems suggest these erratics were transported westward during an early ice flow phase and later reworked by southward ice flow (Prest et al., 2000). Another type of indicator is the ferruginous oolitic erratics found at Cypress Hills approximately 1100km and 1500km due south of the two possible source areas, Lake Athabasca and Great Slave Lake area, respectively (Klassen, 1989).

The use of carbonate data, major and trace element geochemistry, and pebble lithology thus provides a means of determining till composition signature to investigate provenance and to establish relationships with ice flow direction indicators. These methods are well known and established in the Prairies, and show a regional westward and southwestward flow system that brought carbonates from Manitoba into Saskatchewan and Alberta (Thorleifson and Garrett, 1993). The till was later re-entrained by a south and southeastward flow system. Previous analyses did not consider the potential spatial relationships between compositional data and the landform record at the provincial-scale. Ross et al. (2009) provided a preliminary assessment suggesting that there is a potentially strong spatial relationship between landscape assemblages and till composition. This relationship is viewed as supportive evidence for the proposed paleo-ice stream model developed for this region first in Ross et al. (2009) and expanded and further defined in this research. As mentioned earlier, one of the goals of this research is to provide more constraints and to verify this hypothesis (i.e. that a spatial relationship does exist between the landscape and compositional data). Additional till samples were taken at strategic locations to supplement available data. Table 4.1 summarizes the till composition and pebble lithology for each site within Saskatchewan.

Table 4.1: Till composition, pebble lithology and geochemistry ratios for all field sites.

Site #	Site	Location		Till Composition			Pebble Lithology			Geochemistry (ratio)	
		Lat	Long	Sand	Silt	Clay	Crystalline	Carbonate	Clastic	Ca/Al	Mg/Al
1	642 Rd 01 above	50.59596	-105.19902	35%	33%	32%	50%	13%	37%	0.581	0.272
2	Battleford 01	52.58025	-108.35225	29%	34%	37%	54%	16%	29%	0.980	0.361
3	Birch Lake 01	53.42852	-108.04555	43%	30%	27%	67%	11%	22%	0.858	0.356
4	Cutknife 01	52.60952	-109.05846	53%	24%	23%	68%	8%	25%	0.562	0.286
5	Dana 01	52.28966	-105.73654	40%	34%	26%	47%	14%	39%	1.429	0.671
6	Glaslyn 01	53.43168	-108.53693	48%	25%	27%	83%	6%	11%	0.727	0.267
7	Hepburn 01	52.57002	-106.67542	38%	33%	29%	49%	19%	32%	1.482	0.495
8	Hwy 02 01	52.55090	-105.72492	38%	34%	28%	49%	14%	37%	2.798	1.242
9	Hwy 13 01	49.60349	-101.91140	42%	32%	26%	59%	17%	24%	1.771	0.553
10	Hwy 14 To Biggar	52.10304	-108.07569	48%	32%	20%	25%	27%	47%	0.977	0.382
11	Hwy 15 02	51.41646	-104.77922	35%	39%	26%	34%	29%	37%	1.252	0.518
12	Hwy 21 01	53.45351	-109.35652	32%	37%	31%	44%	14%	42%	0.875	0.238
13	Hwy 52 01	51.21027	-103.25893	46%	35%	19%	40%	19%	41%	2.381	0.548
14	Maymont 01	52.58053	-107.75542	46%	27%	27%	68%	8%	25%	0.546	0.187
15	Moose 01 A	49.75452	-102.28353	42%	32%	26%	22%	39%	39%	1.331	0.508
15	Moose 01 B	49.75452	-102.28353	42%	27%	31%	70%	15%	15%	1.112	0.471
16	Moose 02	49.74369	-102.28125	35%	30%	35%	32%	12%	57%	1.758	0.602
17	Moosomin 01	50.15380	-101.67263	5%	48%	47%	33%	14%	53%	1.646	0.541
18	North B 01	52.78370	-108.24214	52%	22%	26%	41%	11%	47%	0.705	0.345
20	Rd 304 01	54.03195	-108.65835	43%	34%	23%	31%	14%	55%	0.672	0.243
21	Rd 602 01	49.29416	-102.76859	40%	31%	29%	53%	12%	36%	1.167	0.469
22	Rd 687 01	52.69628	-108.86569	52%	22%	26%	66%	5%	29%	0.280	0.147

23 Rd 734 01	50.57171	-104.52784	28%	36%	36%	49%	14%	36%	1.898	0.352
24 Rd 787 02	52.60954	-108.72448	65%	21%	14%	99%	1%	0%	0.768	0.284
25 Rd26 GOOD SECT	53.40942	-108.99109	42%	33%	25%	37%	20%	43%	0.535	0.289
26 Rd26 Cln rd CUT	53.73349	-109.13298	48%	26%	26%	78%	7%	15%	0.138	0.117
27 St Benedict 01	52.56521	-105.38622	29%	45%	26%	72%	7%	21%	1.526	0.633
28 Sweetgrass 01	52.76709	-108.81116	50%	23%	27%	96%	0%	4%	0.497	0.207
29 West Of 6 01	49.90649	-104.72139	50%	31%	19%	41%	17%	42%	0.377	0.214
31 Griffin B	49.59666	-103.43098	39%	30%	31%	70%	10%	21%	0.862	0.352
31 Griffin F	49.59666	-103.43098	34%	37%	29%	59%	18%	23%	0.530	0.281

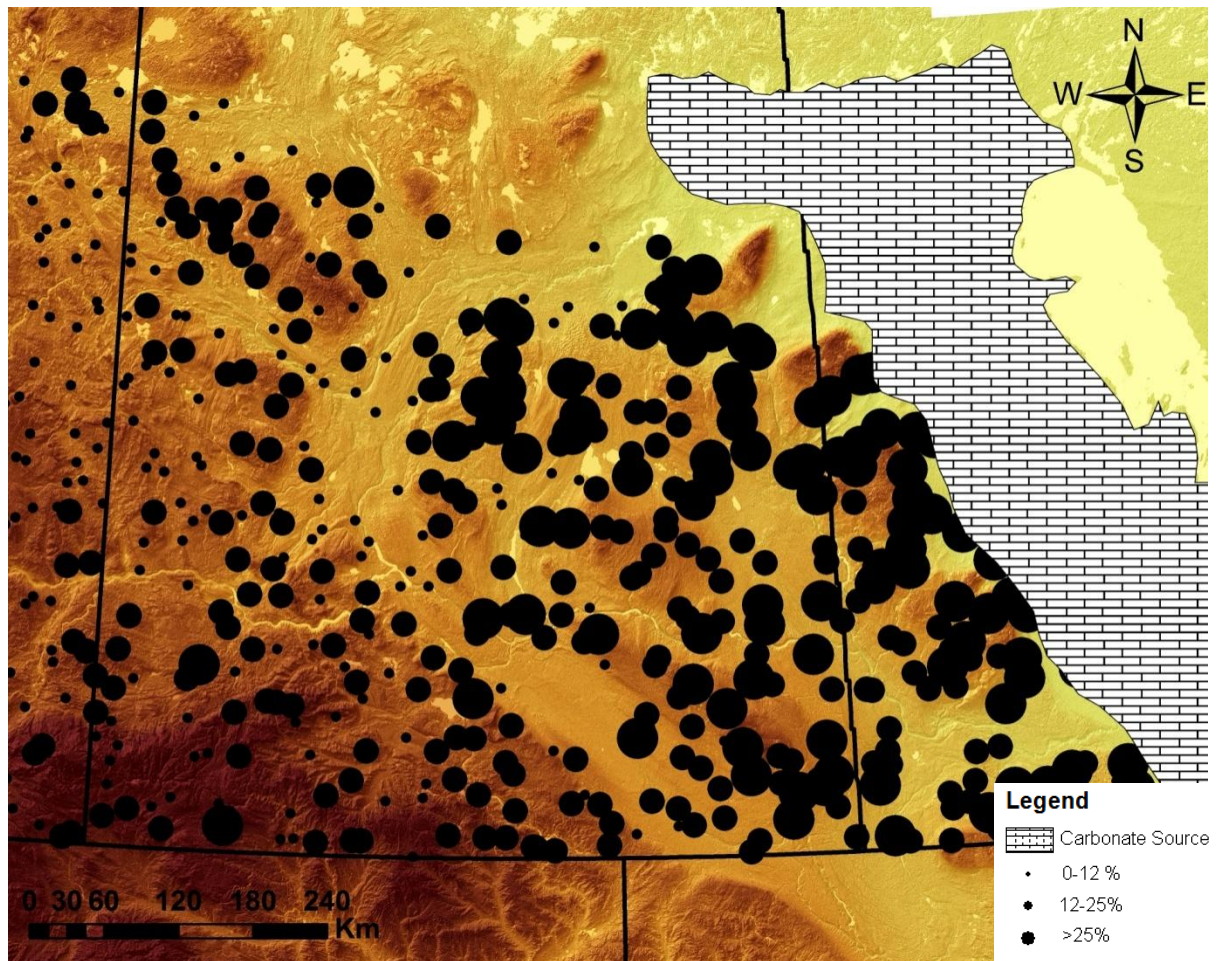


Figure 4.1: Carbonate source in Manitoba and northeastern Saskatchewan, and the carbonate distribution from the Thorleifson and Garrett (1993) database. There is a stronger carbonate signal with proximity to the source. There is a lower carbonate signature in Alberta and in corridors with western source regions, such as the Battleford paleo-ice stream system.

4.1.1 Carbonate Chemistry

Tills in Saskatchewan have been differentiated mainly from lithology, carbonate content, texture, weathering, preconsolidation pressures, jointing, staining and stratigraphic relationship criteria set out by Christiansen (1992). Since the matrix of most of the tills deposited in Saskatchewan is largely-derived from similar sedimentary rocks, the colour and texture of tills are very similar. It is because of this that for simple correlations, using carbonate content to differentiate between tills is accepted

by most researchers in the area. Carbonate content in the till is a compositional tracer, used extensively in the Prairies (Christiansen, 1968). The closest carbonate rocks are located in Manitoba and northeast Saskatchewan (Figure 4.1). The carbonate content of till has been shown to decrease westward due to previous westward ice flow (Klassen, 1989). This general trend is clearly visible from the Thorleifson and Garrett (1993) geochemical dataset (Figure 4.1). This regional distribution of carbonate data has generally been assumed to reflect ice sheet flow dynamics, and not specifically ice streaming. However, Ross et al. (2009) argued that the carbonate content of the surface till shows a strong spatial continuity along the Buffalo Corridor. For example, it was shown that low concentrations are found in the Battleford track and the western Buffalo Corridor relative to the other assemblages in the same area (Maskwa assemblages) probably indicating provenance from carbonate-poor Alberta.

The till along the Battleford and Buffalo corridors is Battleford till (the youngest till in Saskatchewan) because it is not oxidized and does not contain any jointing. Boreholes located near the field sites show the till as Saskatoon Group (without staining or jointing, it is believed to be Battleford Till, as opposed to Floral Till). The proposed interpretation was that of an ice stream system (Buffalo paleo-ice stream) fed by western tributaries (i.e. Battleford) bringing material characterized by low carbonate content into Saskatchewan. However, more control points were needed in the western Buffalo Corridor and along the Battleford track to confirm this pattern. In order to validate the sediment-landform relationship, new field work was needed to verify that the surface till of that area is not an old till (an old till would not be related to the surface landforms). For example, there is a notable increase in carbonate content and decrease in clay content in younger tills. This is thought to be due to progressive stripping of Upper Cretaceous clay beds, and therefore decreasing the source area for clayey sediments and increasing the area of Paleoproterozoic sediments available for glacial erosion (Christiansen, 1971). Therefore, the same pattern (low carbonate content) could be observed due to erosion into old tills (as opposed to glacial transport and deposition of a new till) along the Battleford Corridor and Buffalo Corridor. In addition, errors within the carbonate analysis need to be taken into account, such as the partial leaching of carbonates to a depth of 40 feet as observed in the Saskatoon area (Christiansen, 1971).

Based on field observations, I am confident that the till sampled along the Buffalo Corridor is the youngest Battleford Till and not an older, carbonate-poor till. This has also been well demonstrated around Saskatoon and Regina (Christiansen, 1992; Christiansen and Sauer, 2002), two localities within the Buffalo Corridor. Some site locations were not extensive enough to have more than one visible till unit, and therefore the till unit determination was done based on known visible evidence (no oxidation or jointing in Battleford Till, but seen in all other tills), as well as comparison to boreholes from the Saskatchewan Watershed Authority (<http://www.swa.ca/WaterManagement/Groundwater.asp?type=Mapping>). Lack of oxidation and jointing is an important Battleford Till indicator due to weathering that took place during the Mid-Wisconsinan, after the deposition of the Floral Formation (the other Saskatoon Group till).

Preconsolidation measurements for the tills would also be a good till indicator but that was not available for this project. Figure 4.2 is from site # 31 (Griffin 01), where more than one till unit is visible, so the youngest till (the surficial till for non deformed structures) is sampled for composition. Figure 4.3 is another site, #21 (Rd 602 01), also along the Buffalo Corridor. At this site there was only one till unit exposed but it again showed no sign of jointing or staining, and the associated borehole was marked as Saskatoon Group. By determining the till until analyzed, this can confirm that the geochemical data can be used to determine the relationship with the landform record.

The amount of data is well spread and can be overwhelming when looked at the provincial scale therefore it was analyzed on more regional, or corridor-assemblage, scale.

Since the westward ice flow phase, which brought the “Omars” into Saskatchewan, the till has been re-entrained by south-westward (e.g. Maskwa phase), as well as by south and south-eastward flow systems (the Buffalo system) and changes in carbonate composition can be seen, especially when comparing within and outside of assemblage areas (Figure 4.1).Based on these observations, carbonate content should be and is higher in older assemblages containing westward or south westward flutings and generally lower in others. The exception is in the eastern portion of the Buffalo system because the carbonates were continuously supplied even after shift in ice flow because of proximity to source location.

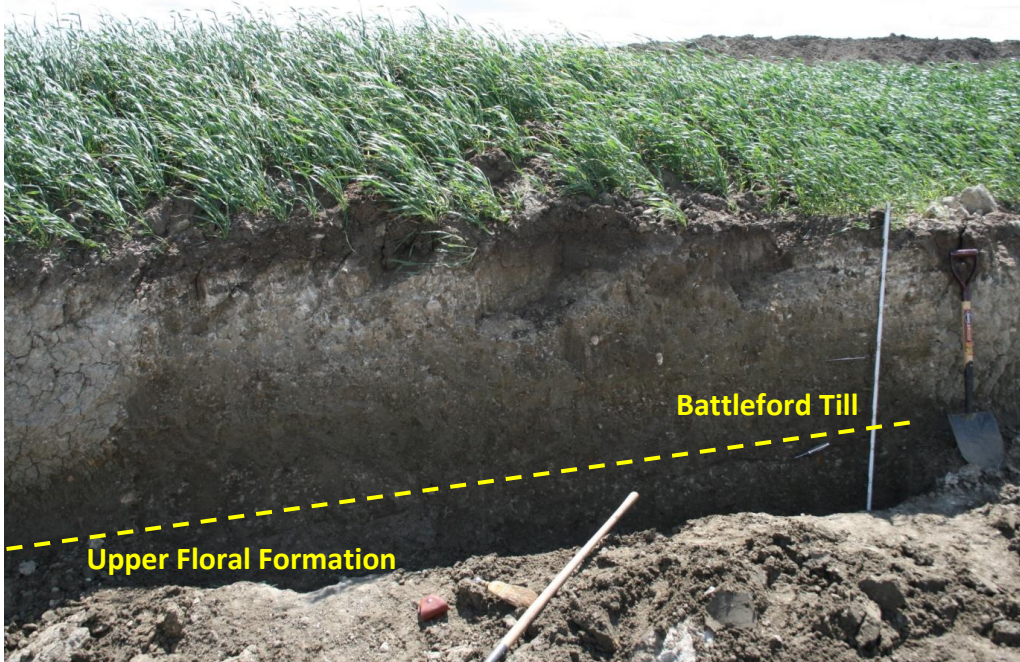


Figure 4.2: Site #31 (Griffin 01), with two visible till units within the Buffalo paleo-ice stream corridor. Younger Battleford till lacks staining and jointing, where the older Floral Formation is weathered and jointed.



Figure 4.3: Site #21 (Rd 602 01), also within the Buffalo Corridor. Only one till was exposed. Based on field observations (no jointing or staining) and local boreholes, this is Battleford Till at this location.

4.1.2 Ca/Al and Mg/Al ratios

Geochemical ratios, more specifically Mg/Al and Ca/Al ratios were used as proxies for dolostone/silicate and limestone/silicate proportions, respectively. A low ratio suggests a high proportion of silicate material (with some of the Ca potentially from a silicate source) and a high ratio indicates a high proportion of carbonates and confidently links the Ca to a sedimentary carbonate source. The new geochemical data are consistent with the Thorleifson and Garrett (1993) data. Lower ratios along the Maskwa Corridor suggest a higher proportion of crystalline material from the Canadian Shield, whereas the high values found along the southern portion of the Buffalo system indicate a greater input of carbonates from Manitoba, which is consistent with the location of these samples (Figure 4.4). High ratios are also found in small assemblages containing SW-trending till ridges such as in Assemblage 2. Results are thus consistent with the mosaic landsystem model.

4.1.3 Pebble Lithology

Pebble lithology provides a physical account of material transported, and were classified as crystalline, carbonate or clastic when observed in the lab (Table 4.1). Figure 4.5 shows the distribution of pebble lithology throughout the province. There is a higher percentage of crystalline rocks along the Maskwa Corridor, which is expected because its catchment area is located on the Shield. There is a lower percentage of crystalline rocks along the Buffalo Corridor, relative to the Maskwa, but also a higher percentage of clastic rocks. Other than a few sites, the carbonate lithology in the tills is less than 25%. The distribution of carbonate pebbles is relatively consistent with the geochemistry of the till, a higher percentage of carbonate pebbles in the tills to the east than the tills to the west. Some areas may be slightly different from the carbonate content but that is expected because of the differences in both the preservation potential and transport processes between pebbles and matrix with respect to reworking and re-entrainment. The sample size range also needs to be taken into account when analyzing pebble lithology. When the pebble lithology was performed, the sizing went to 2mm due to the poor clast content of the tills. Some rock types break apart faster during transport, and this could account for their abundance in the small fractions. This could explain the increased clastic content to the south where there is no exposed source, due to

the tendency of the shale material to break into many smaller pieces. However, it should be noted that most of southern Saskatchewan is underlain by shales.

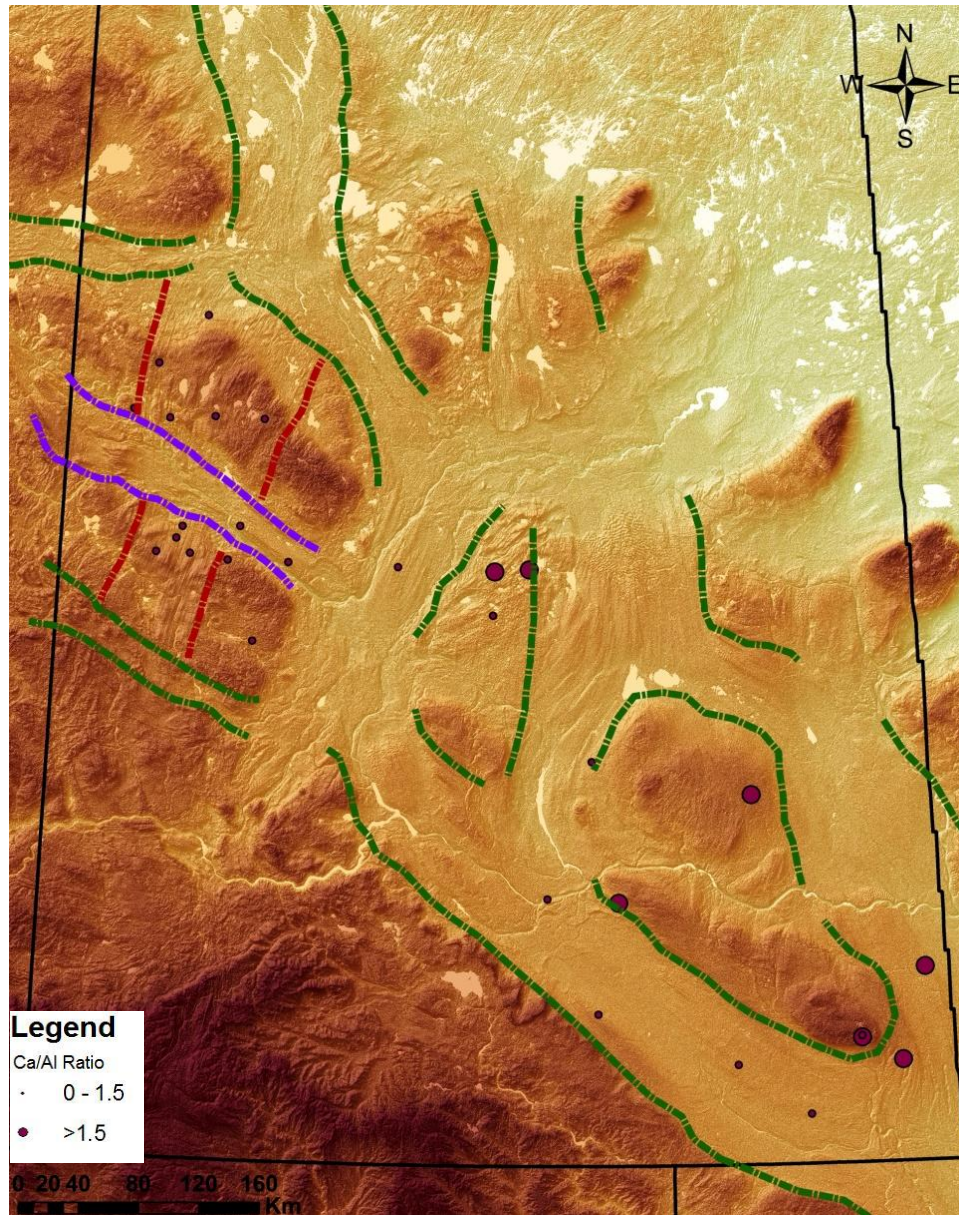


Figure 4.4: Ca/Al ratios used to determine crystalline to carbonate sources. Higher ratios suggest carbonate sources, to the west and preserved in assemblages 2, 9 and 10. Ca/Al ratio is consistent with the Mg/Al ratio, where the higher ratios are preserved in assemblages 2, 9 and 10, as well as along the eastern limb of the Buffalo Corridor.

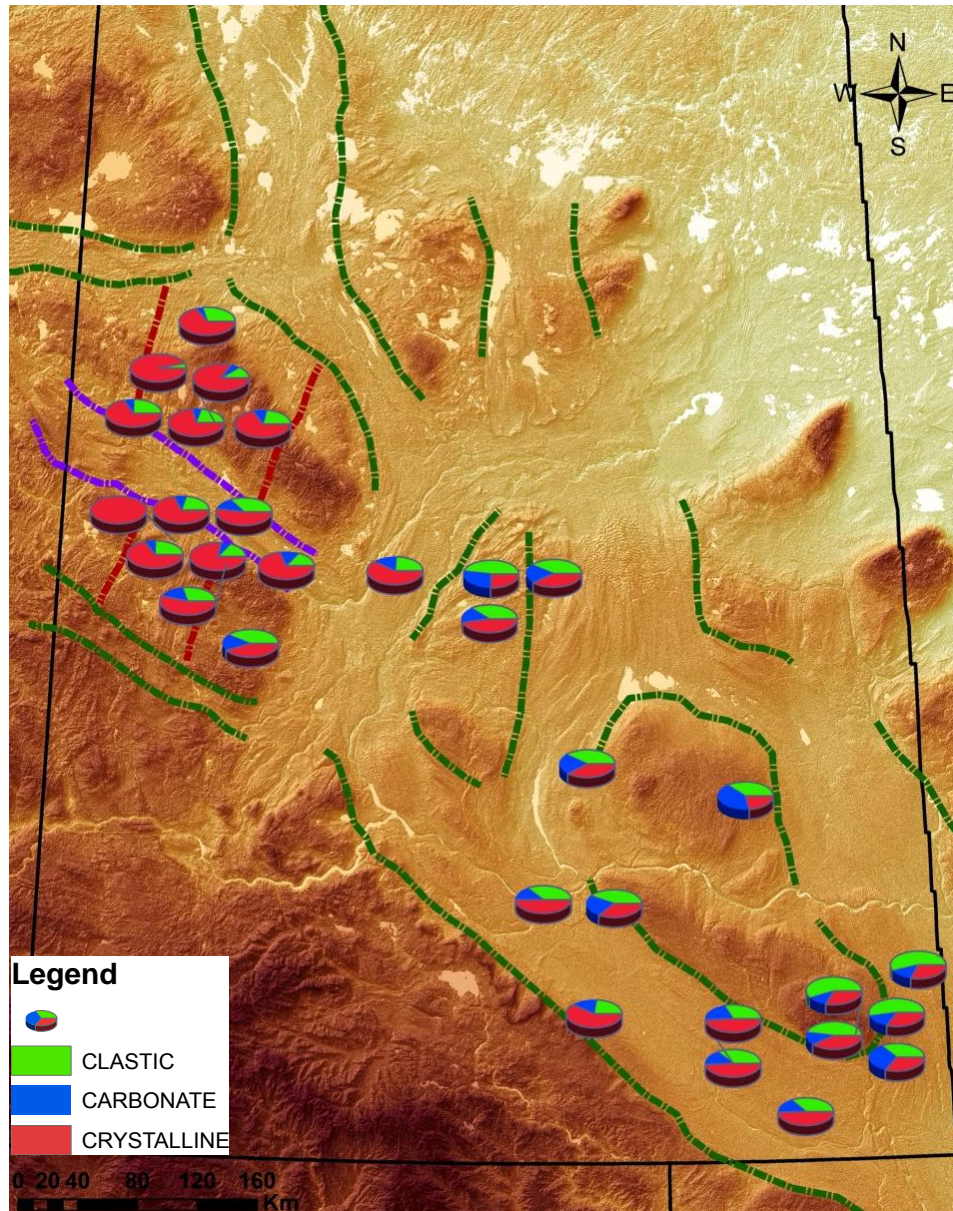


Figure 4.5: Pebble lithology from 2mm+ fraction. Higher concentration of crystalline pebbles to the north and more clastic pebbles to the south. Carbonate pebble distribution is consistent with carbonate content and geochemistry ratios.

4.2 Airborne Radiometric Survey

Due to the sparse glacial landform record over the Canadian Shield in Saskatchewan, the extent to which the Maskwa paleo-ice stream can be traced is limited to compositional data. Ross et al. (2009)

demonstrated how radiogenic signatures can be used to delineate potential dispersal trains of crystalline detritus for regional glacial transport. Campbell et al. (2007) used radiometric data and till composition to assess transport over the Athabasca Basin. In absence of glacial dispersal, a clear dispersal pattern of equivalent Thorium (eTh ppm) relative to K (%) in the surface sediments over the Athabasca Basin is apparent on the regional Th/K radiometric map, as it is underlain by quartzarenites of the Manitou Falls Formation (Ross et al., 2009). Debris derived from the felsic gneisses of the Mudjatik Domain which lie to the northeast were dispersed over the quartzarenites of the Manitou Falls Formation. This is also supported by field observations where the surface till within the dispersal train contains abundant erratic material derived from the felsic gneisses while west of the dispersal train, local sandstone is the dominant lithology in the till (Campbell et al., 2007). It is not a true Boothia-type dispersal pattern but the dispersal train over the Athabasca Basin is over 200 km long and it extends southwestward beyond the Athabasca Basin, in alignment with the Maskwa paleo-ice stream system. Figure 4.6 shows the alignment of the major palimpsest dispersal train with the Maskwa Corridor. That was used to extend the Maskwa paleo-ice stream further up-ice onto the Canadian Shield (Ross et al. 2009).

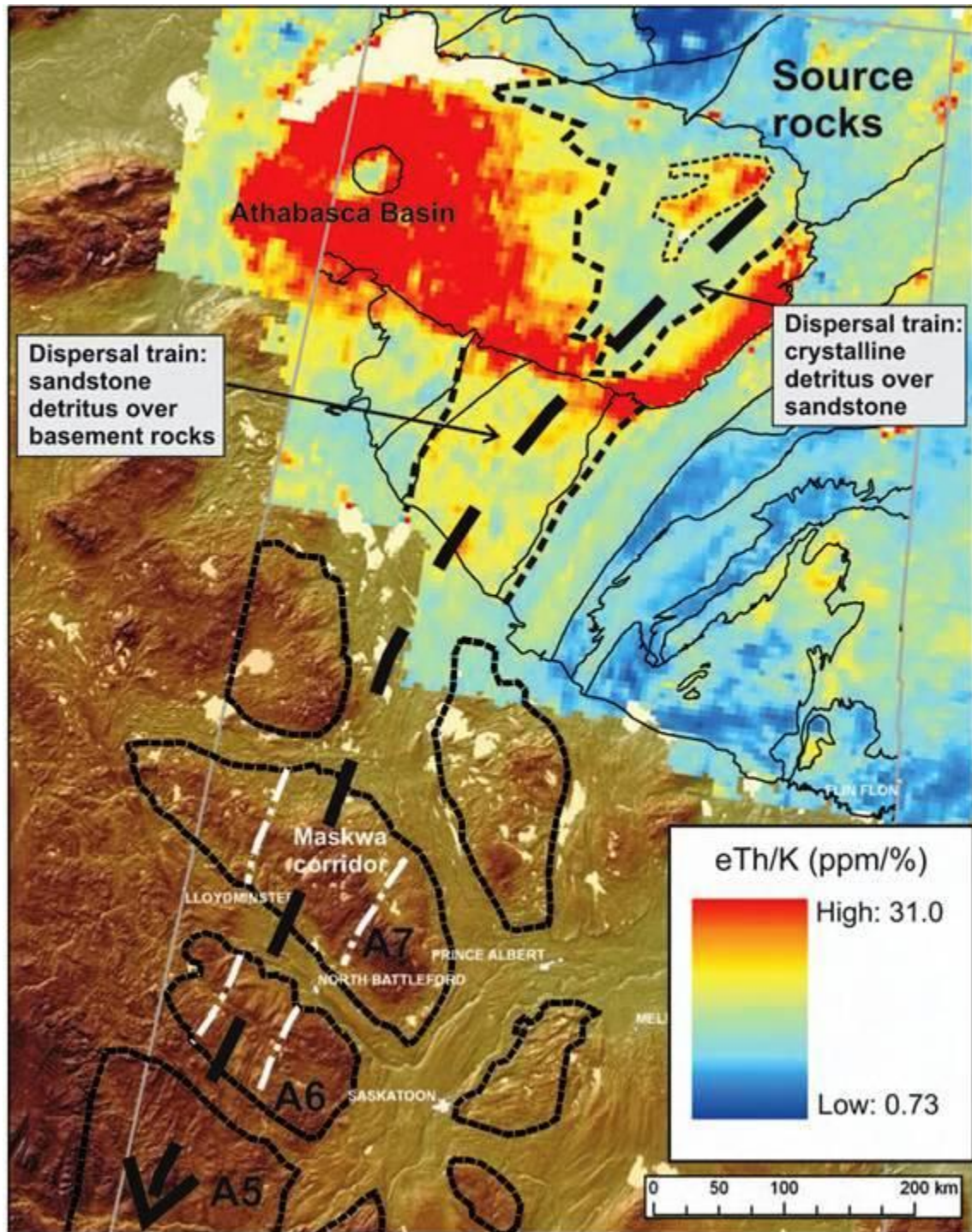


Figure 4.6: The distribution of eTh/K (ppm/%) values over the Canadian Shield and the SRTM elevation model over the Interior Plains. Two regional dispersal trains are clearly visible. The approximate centre-line of the Maskwa paleo-ice stream is indicated by the thick black dashed line with the arrow indicating ice flow direction (Ross et al., 2009).

4.3 $^{40}\text{Ar}/^{39}\text{Ar}$ dating

The $^{40}\text{Ar}/^{39}\text{Ar}$ dating method for hornblende grains was used to aid in the determination of provenance and flow history. Tills produced by ice flow systems coming from various sectors of the Canadian Shield should contain a mixture of grains that is representative of the lithologies incorporated during transport, including the source region (Roy et al., 2007). It has been shown that hornblende grains from different Canadian Shield domains (e.g. Churchill, Superior) have distinctive ages and can thus be used as a tracer in regional provenance studies (Hemming et al., 2000, Roy et al., 2007).



Figure 4.7: Geological provinces used for provenance determination of hornblende grains. Superior Province is Archean in age and the Churchill province is Paleoproterozoic.

The Canadian Shield southern boundary is located approximately 200 km north of the northern most sample site. The Canadian Shield consists of various geological provinces and smaller structural provinces within them, however, a general comparison between Superior and Churchill provinces is done for this project. The Superior province is located to the east-northeast of Saskatchewan, covering most of Manitoba and the Churchill province is to the north-northeast (Figure 4.7). Both provinces contain Archean basement rocks. However, Churchill terrains have been involved in several orogenies during the Paleoproterozoic and are characterized by a distinct Paleoproterozoic radiometric overprint. This overprinting is what the $^{40}\text{Ar}/^{39}\text{Ar}$ measures. According to Roy et al. (2007), hornblende grains derived from source rocks located within the Superior Province should record the Kenoran orogenic overprint and have $^{40}\text{Ar}/^{39}\text{Ar}$ ages > 2.6 Ga, whereas grains derived from the Churchill Province should yield $^{40}\text{Ar}/^{39}\text{Ar}$ ages ranging from 2.0 to 1.7 Ga.

By taking random hornblende grains in till samples from field sites, the dates can be used to test the predicted contrasting glacial dynamics between corridors and assemblages. Figure 4.8 outlines all the field sites whose samples were submitted for dating. It should be noted that the use of $^{40}\text{Ar}/^{39}\text{Ar}$ dating was determined before field work began, but specific sites for dating had not been chosen until after fieldwork had been completed, and only a few samples were selected due to time and financial constraints. The result of this initial work has prompted future expansion. Table 4.2 is the ratios of $^{40}\text{Ar}/^{39}\text{Ar}$ dated grains, as well as their mean ages, for all samples.

The lower right hand corner of Figure 4.8 shows field site 21 in what is believe to be the longest area of sustained flow (Buffalo Corridor), having a low Archean signature, with an overall Proterozoic date of 1.8 Ga, due to the reworking of the till (Archean to Proterozoic ratio of 1:13). Field site 16, however, is mapped as hummocky terrain and is within Assemblage 10, and has a preserved signature of Archean aged grains (1:2). This is an example of a proxy for southwestern flow older than that of the Buffalo Paleo-ice Stream. The actual distance between the two sites is 62km.

It is known from the “Omars” and erratics found in Saskatchewan and Alberta, there was an older westward flow system before ice flowed to the southwest prior and up to 14k ^{14}C years ago. The occurrence of a few Archean grains in western assemblages (Figure 4.8) supports this. In addition, a

high proportion of Churchill ages should be seen more to the northwest of the province and Superior ages to the southeast. The assemblages for which an Archean signature is to be expected are those found south of the extended boundary between the Churchill and Superior provinces (Figure 4.9). In order to use this method as a provenance indicator for this study, more dating at other sites would need to be done. Due to the contrast seen in field sites 16 and 21, this technique does hold promise for future research, where more sites and more grains should be taken in the south to better define the signatures between the assemblages and the Buffalo Corridor.

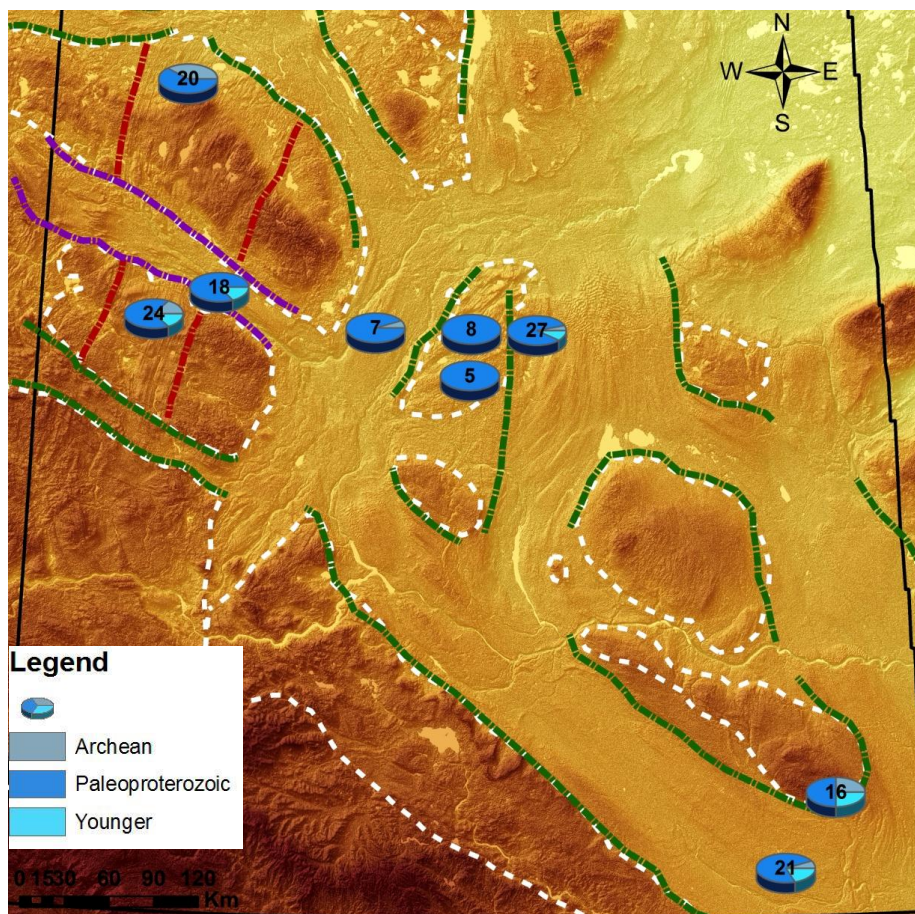


Figure 4.8: Field sites (numbered) where samples had hornblende grains $^{40}\text{Ar}/^{39}\text{Ar}$ dated. Some Archean aged grains are found within the Maskwa Corridor but are mostly Paleoproterozoic in age. Minimal to no Archean aged grains are found within Assemblage 2, the Battleford and Buffalo Corridors. The difference in the amount of Archean-aged grains in the southeastern portion of the province between sites #16 and 21 demonstrates potential for preservation of previous ice flow in inter-ice stream areas.

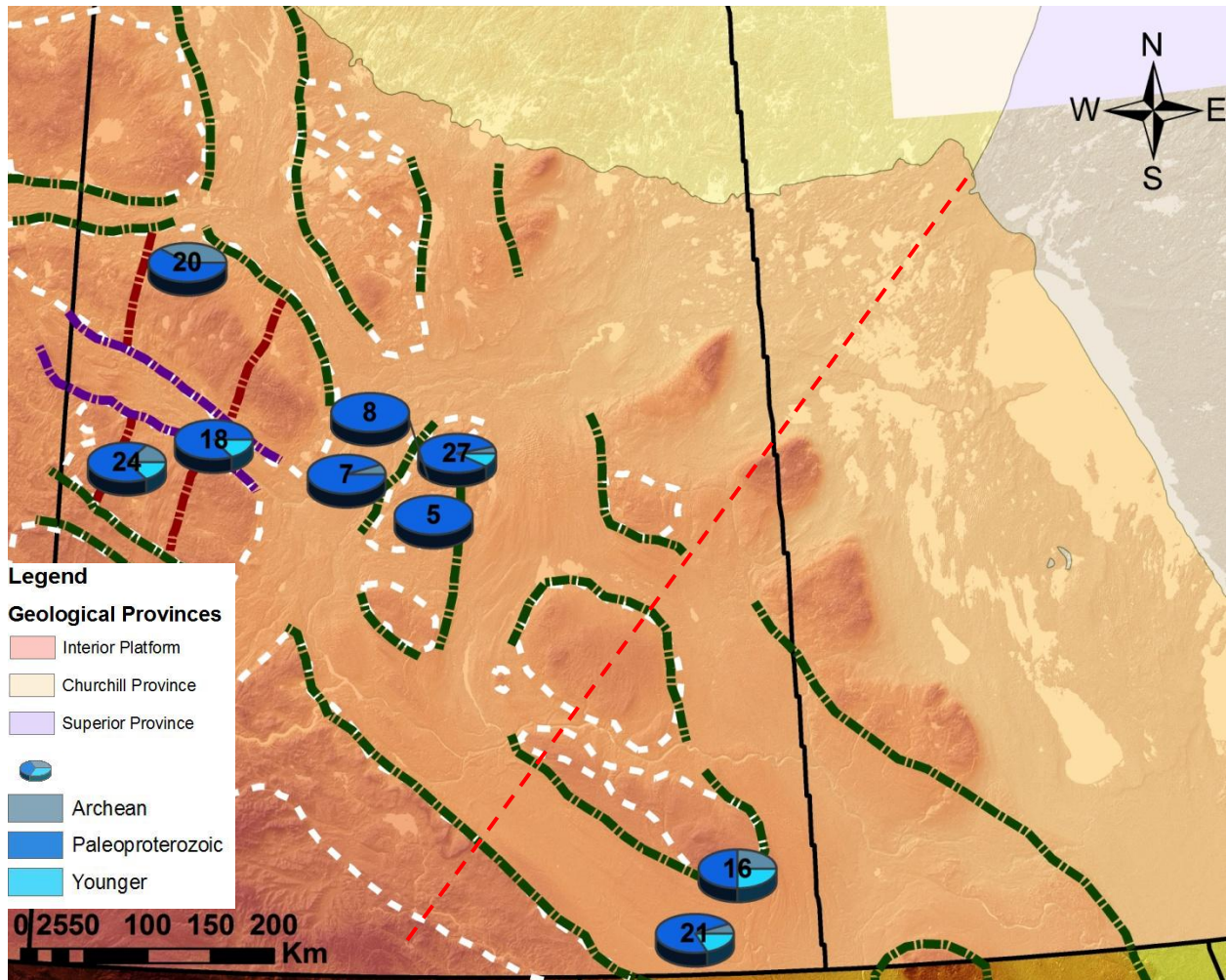


Figure 4.9: Assemblages where an Archean signature is possible due to known ice flow directions (from the Keewatin ice dome) are those found south of the extended boundary between the Churchill and Superior provinces, as delineated by red dashed line.

Table 4.2: $^{40}\text{Ar}/^{39}\text{Ar}$ field site data. Amount of grains tested and their ages, as well as their ratios and average ages.

Site #	Site Name	Count	Archean (4-2.5 Ga)	Proterozoic (2.5-.57 Ga)	Younger (<570 Ma)	A:P:Y ratio	Average (Ma)	Average Archean (Ma)	Average Proterozoic (Ma)	Average Younger (Ma)	Median (Ma)	Stdev (Ma)
5	Dana 01	5	0	5	0	0:5:0	1822.99	0	1800.11	0	1745.27	116.14
7	Hepburn 01	17	1	16	0	1:16:0	1686.05	2569.77	1630.82	0	1687.47	281.66
8	Hwy 2 01	8	0	8	0	0:8:0	1687.67	0	1687.67	0	1713.05	123.08
16	Moose 02	12	3	6	3	1:2:1	2127.62	2706.73	1573.60	151.70	1676.23	1005.84
18	North B 01	20	0	17	3	0:17:3	1687.53	0	1624.13	254.54	1687.59	555.47
20	Rd 304 01	5	2	3	0	2:3:0	1673.95	0	1673.95	123.96	1668.58	850.25
21	Rd 602 01	17	1	13	3	1:13:3	1848.96	2589.46	1766.13	217.88	1718.35	687.64
24	Rd 787 02	7	1	5	1	1:5:1	1725.78	2929.97	1653.42	294.43	1714.26	772.55
27	St Benedict 01	23	1	20	2	1:20:2	1708.27	2588.69	1664.25	233.31	1699.48	536.18

4.4 Summary

In Chapter 3, the geomorphological aspect of the Paleo-ice Stream Criteria was demonstrated. In this chapter, the compositional data were tested to verify the concept of assemblages and the distinct boundary between them and paleo-ice stream corridors. This was demonstrated in various areas of the province:

1. The difference between the Maskwa geochemistry and the Battleford geochemistry can be seen in the carbonate data and the $^{40}\text{Ar}/^{39}\text{Ar}$ ages. The Maskwa paleo-ice stream came from the northeast, and has higher carbonate content in its till compared to the low content in the Battleford tributary that originated from the west, in Alberta. The Maskwa system also carries Archean grains in its till but none were found in the Battleford tributary. This difference in composition reflects distinct boundaries between these two systems that were preserved.
2. The ratio of Archean-aged grains to Proterozoic grains in the southern portion of the Buffalo system, between sites #21 (Rd 602 01) and #16 (Moose 02) suggest that the till sampled at the Moose 02 site was deposited by southwest-flowing ice (bringing material from the Superior Province) and that this till was not significantly reworked by the subsequent southern and southeastern ice flow phases. These ice flows were focused along the Buffalo Corridor, reworking the till and bringing more Proterozoic grains southeastward along the corridor (Rd 602 01 site). These results are thus consistent with the idea that some assemblages like 10, record older SW ice flow phases better because they were preserved beneath Buffalo inter-ice stream areas. This distinction warrants further expansion with this technique to further define the compositional boundaries within Saskatchewan.

Chapter 5 Interpretation and Discussion

No new age controls for deglaciation were introduced in this work, but a better understanding of ice sheet dynamics can be understood in a chronologic sequence. The Table 5.1 below summarizes the chronology proposed in Ross et al. (2009) and the new details provided by this research. Discussed in this chapter is the sequence of ice flow in Saskatchewan based on the paleo-ice stream model and landscape reconstruction.

5.1 Westward Ice Flow Phase

The earliest Late Wisconsinan ice advance occurred around 36 ¹⁴C ka BP ago (Klassen, 1994). A westward ice flow, as seen with Hudson Bay erratics and carbonate distribution, suggest early late Wisconsinan (Prest et al., 2000). However this phase is poorly constrained and not widely found in the landform record, so it could be from an earlier glaciation. The Last Glacial Maximum occurred during relatively stable climate and low global sea level, approximately 18 ¹⁴C ka BP (Dyke et al., 2002).

5.1.1 Dispersal of Omars

Omars are distinct Proterozoic erratics derived from the Belcher Group in southeastern Hudson Bay. They are massive dark siliceous greywacke that contains light-toned (weathered) calcareous concretions that are subspherical (Prest et al., 2000). These erratics were dispersed northwestward and westward across the Hudson Bay Paleozoic Basin by the Labrador Ice sector, than later south and southeastward by the Keewatin Ice sector, over southwestern Manitoba, southern Saskatchewan and Alberta, and thus most of the omars have been redeposited (Prest et al., 2000). Probably constrained by the Keewatin ice lobe, the omars extend westward across Saskatchewan along 55° Latitude, into Alberta. A striated omar boulder was found in a boulder pavement east of Saskatoon, where it was at the lower contact of the Battleford Till. Omars are also found in older tills throughout the central and southern portion of the province, as well as in stone piles and surface tills (Prest et al., 2000).

Table 5.1: Regional chronology based on geomorphology, Dyke (2003) radiocarbon chronology, and mosaic landsystem model.

Date	Event
36 ¹⁴ C ka BP	The earliest Late Wisconsinan advance.
18 ¹⁴ C ka BP	The Last Glacial Maximum occurred during relatively stable climate and low global sea level (Dyke et al., 2002).
15 ¹⁴ C ka BP	The ice readvance had strong southerly flow in Alberta from the Keewatin ice dome, to the limit west of the Cypress Hills uplands (Klassen, 1994). The south-western flow from the Hudson ice dome occurred at the same time around the Alberta-Saskatchewan boundary to the limit of the eastern Cypress Hills and Wood Mountain area (Klassen, 1994).
15 - 14 ¹⁴ C ka BP	In the Clayton and Moran (1982) reconstruction, there is a regional shift from southwest trending ice flow at Last Glacial Maximum (LGM) to southward flow and finally to southeast trending ice flow.
14 ¹⁴ C ka BP	Maskwa south-southwest flow is no longer feeding ice to the Cypress Hills. The Laurentide Ice Sheet had significantly thinned over the Interior Plains since LGM, and its southern lobes had low surface profiles. Large reduction of ice volume, but not extent, is thought to be representative of regional change in flow pattern over the prairies, when the conditions changed from non-deforming to deforming bed conditions, i.e. Maskwa subglacial bed conditions to Battleford subglacial bed conditions (Dyke and Prest, 1987). The James Lobe was initially fed by southwestern flow from Manitoba, but the shift in ice flow direction in the Keewatin dome changed the catchment area of the Lobe. This is when the Buffalo system developed, in a progressive expansion north-westward from the James Lobe. The James lobe advanced along the James River valley in the Dakotas, and its associated ice stream along the Missouri Coteau, reaching its maximum (Patterson, 1997).
13 - 12.5 ¹⁴ C ka BP	The capturing of subglacial water shut down the western limb (Weyburn Lobe) by the eastern limb (Moose Mountain Lobe) of the Buffalo Corridor. This is similar to what is proposed for Ice Stream C in Antarctica that has been stagnated for 250 years (Patterson, 1997).
13.5 ¹⁴ C ka BP	Complete shut-off of the Maskwa paleo-ice stream occurred when the ice stream went from fast ice flow to sluggish/stagnant conditions rapidly. This change increased fast flow and subglacial erosion within the Buffalo Corridor, and inter-ice stream areas of the system saw little erosion and sedimentation, preserving the Maskwa landscape.
13 ¹⁴ C ka BP	The Weyburn Lobe of the Buffalo Corridor starts to recede and create end moraines.
12.5 ¹⁴ C ka BP	The James Lobe readvances when Weyburn Lobe is shut off and eastern Buffalo limb (later becomes the Moose Mountain Lobe) surges. By 11.5 ¹⁴ C ka BP the Moose Mountain Lobe is gone, with miniature lobate features seen between the Manitoba Escarpment highland mountains.
12.5 - 12 ¹⁴ C ka BP	Glacial lake Regina replaced the Weyburn Lobe.
12.5 - 10 ¹⁴ C ka BP	The Buffalo Corridor contained small outlet lobes after the last major surge of the James lobe and the continuous thinning of ice, till the ice eventually retreated onto the Canadian Shield (Dyke et al., 2003).
12 ¹⁴ C ka BP	The eastern limb of Buffalo Corridor has thinned and receded north, ending its James Lobe feeding.
11.5 ¹⁴ C ka BP	The Cold Lake Corridor creates end moraines. The Prince Alberta late readvance lobe occurs when Cold Lake and Churchill corridors retreating, no remnant ice lobes in the Macklin or Battleford Corridors suggesting they were shut off before or during the shut off of the Weyburn Lobe of the Buffalo Corridor. Total retreat of tributary corridor ice occurs within 500 years of each other. The beginning of the corridors fast ice flow is probably contemporaneous with each other, even though the Buffalo paleo-ice streams we are interested in do not represent a steady state system.
11 - 10.5 ¹⁴ C ka BP	Flow along the Shield last occurred.

5.1.2 Dispersal of Carbonates

Carbonates are located to the east in Manitoba and the northeast of Saskatchewan (Figure 5.1). Based on the source area of carbonates, the occurrence of carbonates in west-central Saskatchewan requires a westward ice sheet flow. The regional westward decrease of carbonate content has also been recognized by various researchers (Shetson, 1984; Klassen, 1989; Thorleifson and Garrett, 1993). Pebble lithology from field sites is consistent with this distribution. The till sampled by Thorleifson and Garrett (1993) is unconfirmed as Battleford, but is noted as the youngest till exposed. The till unit that the pebble lithology is from is the Battleford Till based on field observations.

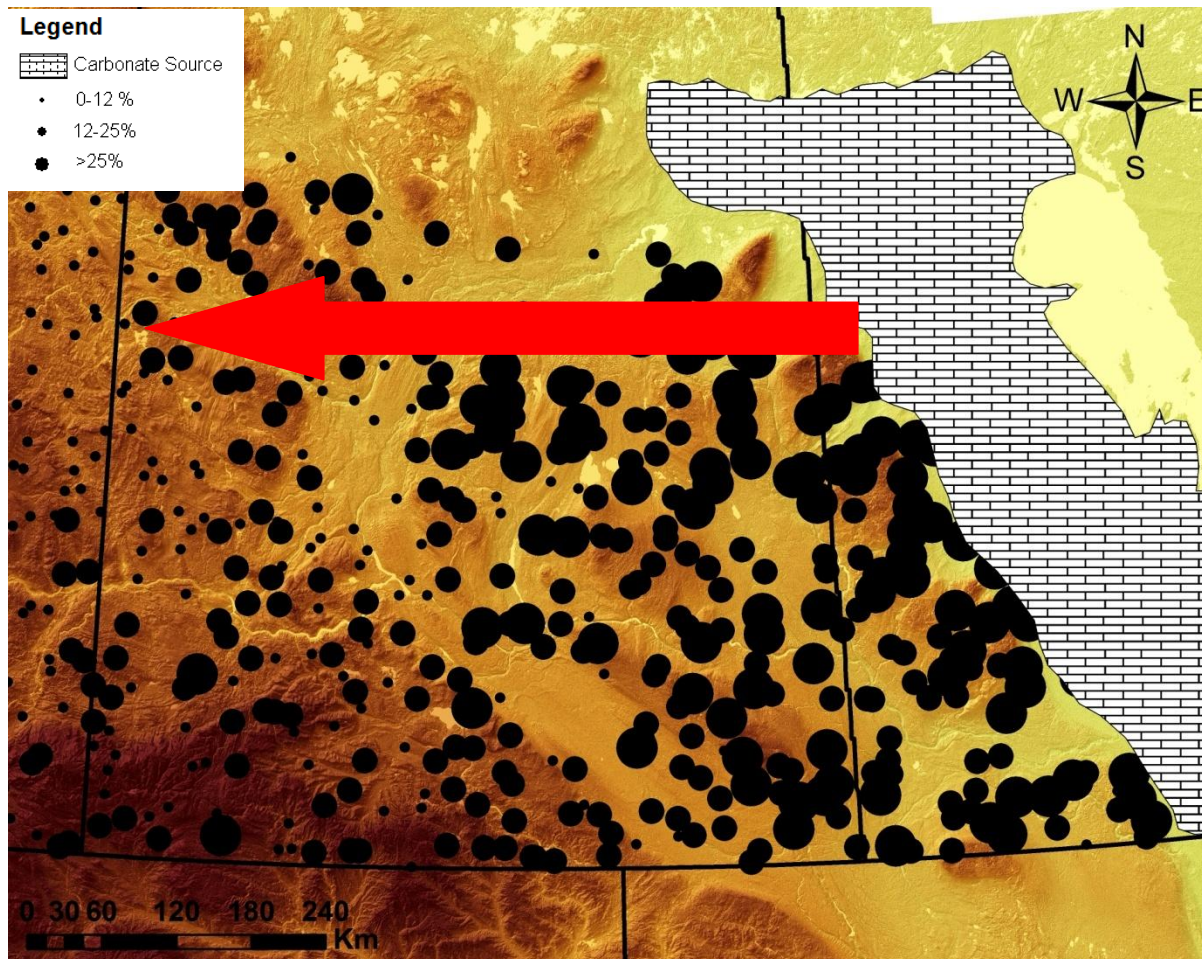


Figure 5.1: Westward dispersal of carbonates from source area in Manitoba.

5.1.3 Other Evidence and Supporting Data

Some of the northern $^{40}\text{Ar}/^{39}\text{Ar}$ tested sites have Archean grains; this is consistent with westward ice flow over the Superior Province that would have carried Archean aged grains across Saskatchewan (Figure 5.2). There is no landform evidence preserved to show westward flow, but site #10 (Hwy 14 to Biggar) has fabric data of 232° and two boulder striations of 254° (both westward orientations). This site is located within the hummocky terrain of Assemblage 6, and is the only westward-trending site found.

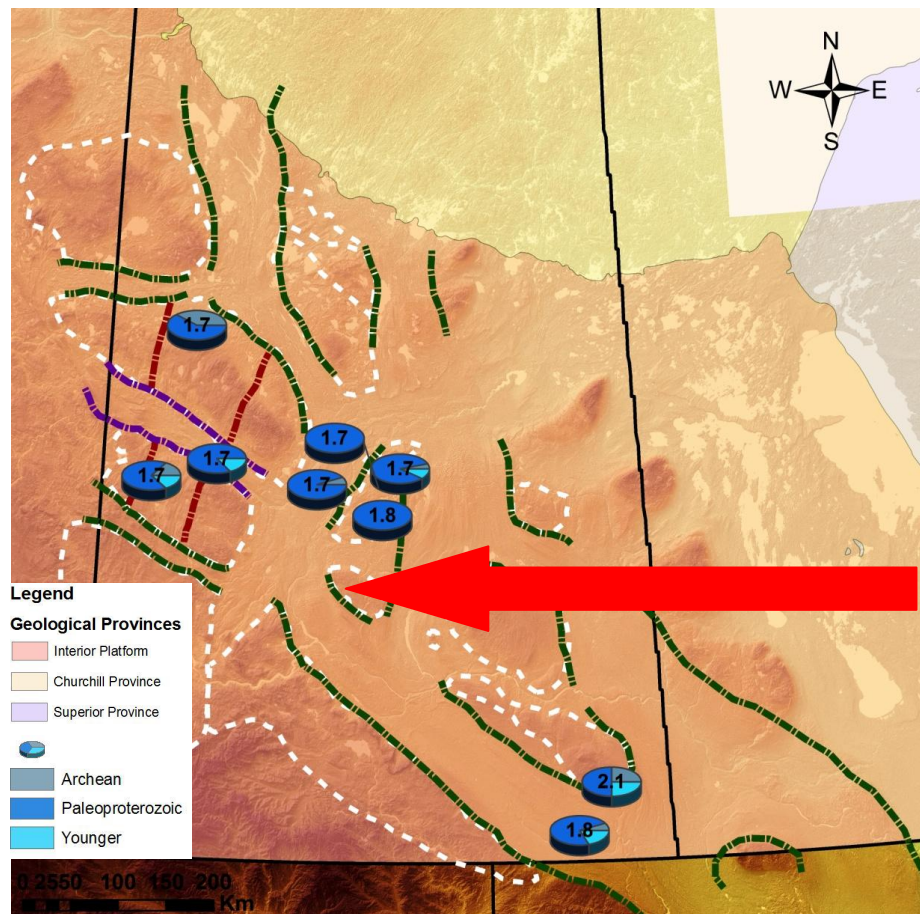


Figure 5.2: Westward shift of Archean-aged grains from Superior Province. Signature preserved in assemblages with more abundant Archean-aged grains.

Although the exact age of the westward flow is unknown, it is estimated to be of Late Wisconsinan age. Most, if not all, of the subglacial landscape in Saskatchewan is Late Wisconsinan in age.

5.2 Southwestward Ice Flow Phase

5.2.1 Summary of evidence

Assemblage 2 may be the oldest assemblage. The landform evidence is trending southwest but these landforms are not all necessarily MSGs (low length to width ratios) and are thus not necessarily formed by ice streaming. Fabric data is consistent with the landforms (field site St Benedicts). However, a lodged boulder at a site south of the landforms is striated 174°. This may reflect the migration from southwestern flow to southeaster flow.

The high proportion of Archean ages in Assemblage 10 suggests southwest flow increased the number of Archean-aged grains in the sample. The sample was found in an area mapped as hummocky terrain, on Moose Mountain. The southwest Archean signature preserved in this hummocky terrain has implications for the origin of hummocky terrain. Hummocky terrain (moraines and till) origin is still widely debated, some possible origins include erosion in subglacial floods, squeezing of subglacial material up into holes through stagnant glacial ice, slumping of supraglacial material down into holes through stagnant glacial ice (Clayton et al., 2008). A preserved signature within hummocky terrain, from an older flow system (not the youngest), provides important insights into hummocky terrain origin, and provide support to the idea that the till was first brought by southwest flowing ice and that the hummocky aspect of the terrain formed subglacially in an inter-ice stream zone due to sluggish ice.

There are southwest trending mega-scale glacial lineations in the Primrose and Cold Lake areas (Assemblage 8). These MSGs need to be further analyzed, but they are consistent with a possible Maskwa-age or older southwest ice stream flow system. These fields are discontinuous and are cross-cut by the Battleford tributary catchment area (Figure 5.3).

5.2.2 The Maskwa paleo-ice stream

Mega-scale glacial lineations are characteristic of paleo-ice streams and those in the Maskwa system are discussed in detail in Chapter 3. The MSGs have a distinct boundary of hummocky terrain on

either side, as seen in Assemblages 6 and 7. There are no striation data within the Maskwa Corridor. As mentioned before, fabric data is used in conjunction with other evidence, due to the poor size and clast content of the tills. The fabric data along the Maskwa Corridor is relatively consistent with the landform evidence, although more sample sites and stronger fabrics would be ideal.

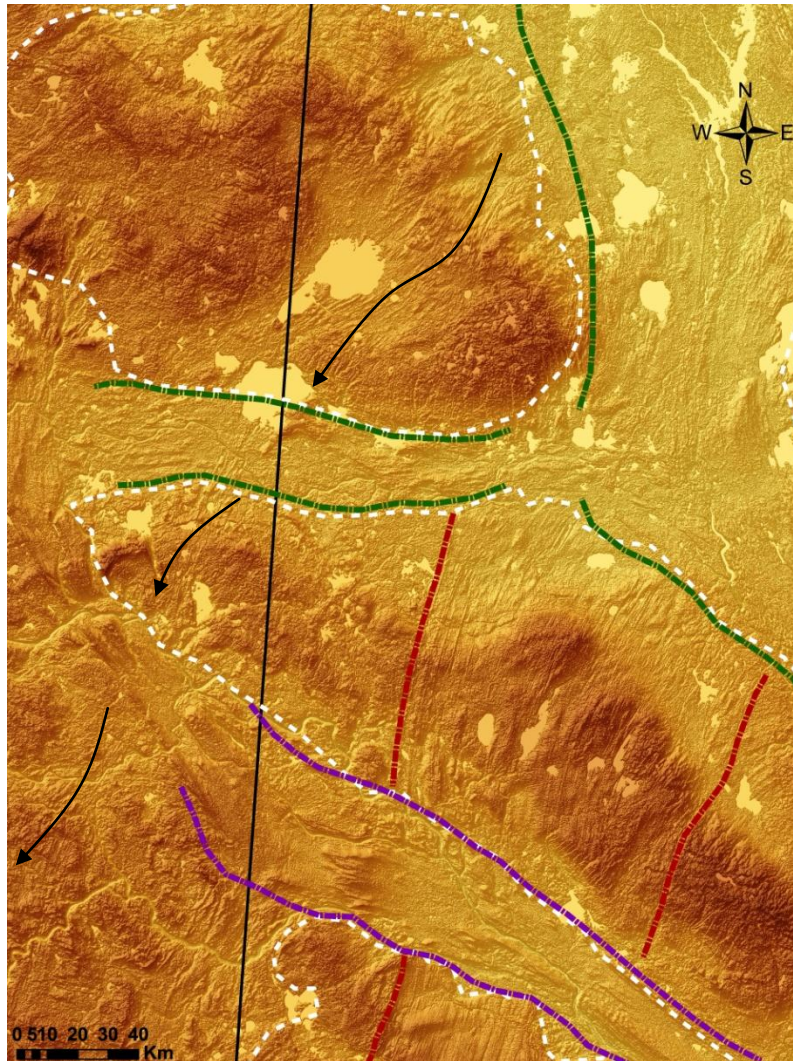


Figure 5.3: Southwest-trending MSGLs in Primrose and Cold Lake area, cross-cut by Battleford Corridor and extending into Alberta. More work needs to be done to delimit extent but initial observations suggest the possibility it is contemporaneous to the Maskwa paleo-ice stream. Black arrows follow MSGLs.

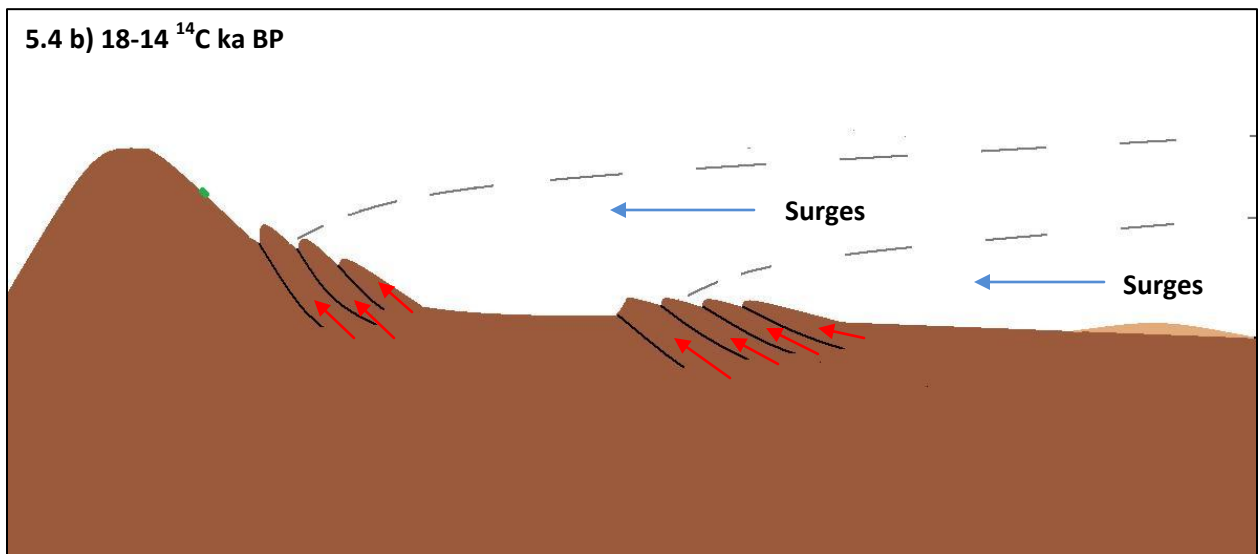
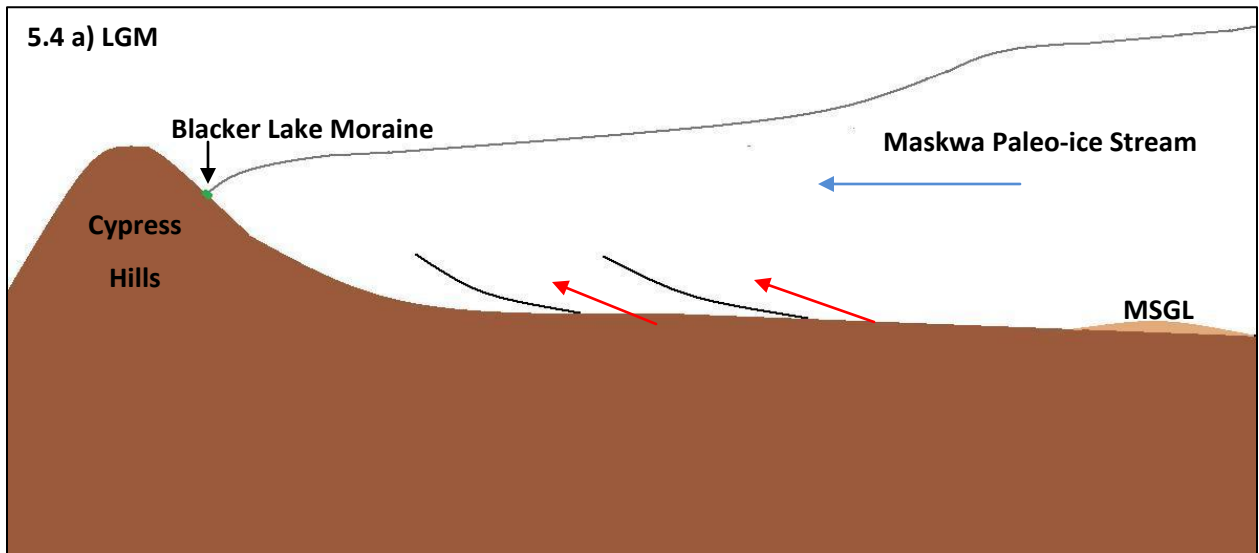
In terms of till compositions, relatively low carbonate content and strong crystalline pebble lithology is consistent with the southwestern flow from the Shield. A large proportion of Proterozoic ages are also consistent with the Churchill Province, most likely from the northeast.

The recessional features (potential end moraines) and transverse ridges of the Maskwa paleo-ice stream roughly correlate with the Lethbridge Moraine in Alberta outlined in Assemblage 5. The extent of Maskwa ice stream was to the southwest corner of Saskatchewan, and can be seen by following the MSGL as far south as the South Saskatchewan River (Ross et al., 2009). It is possible that it may have acted as a feeder to glacial lobes that flowed around the Cypress Hills and Wood Mountain uplands toward the LGM limit in Montana (Ross et al., 2009).

The series of transverse ridges that extend from the South Saskatchewan River to the base of the Cypress Hills were developed along the regional slope (Figure 3.6), with field evidence indicating ice thrusting towards the south-southwest (Kupsch, 1962). Mahaney and Stalker (1988) identified an area north-northwest of Swift Current that exhibited eight different tills based on physical characteristics and composition. Metal content (molybdenum, iron and uranium) generally increase with younger tills, and the top two tills are the only tills not weathered, jointed or stained (Mahaney and Stalker, 1988). This suggests that the top two tills are contemporaneous with the Battleford Till and their high metal contents are consistent with a Canadian Shield source. The stacking of tills is explained by the readvance and succession of eight till compositions that span back the beginning of the Quaternary (Mahaney and Stalker, 1988). Kupsch (1962) proposed the initial ice sheet thrust model, but it was not discussed in Mahaney and Stalker (1988).

Figure 5.4 describes a conceptual model of an alternative explanation for the driving mechanism that created the transverse ridges and till stacks in Assemblage 5. Assemblage 5 is the location of the terminal zone of the Maskwa paleo-ice stream, where thick sequences of stacked till units forming large transverse ridges are expected to form in the terminal zone of a terrestrial ice stream. Ice thrusting from the Maskwa paleo-ice stream, possibly through surges, is thus proposed to explain the thick till sequences found in that area. This till stacking is likely due to glaciotectonic thrusting along the regional slope over a short period of time by the Maskwa paleo-ice stream, as

opposed to persistent glacial thrusting at the margin by the ice sheet itself, or normal stratigraphic build-up through multiple glaciations. This alternative explanation uses a different driving force for the same ice thrusting mechanism that created these features (short term paleo-ice streams as opposed to ice sheet margin changes over long periods of time).



5.4 c) Bird's Eye

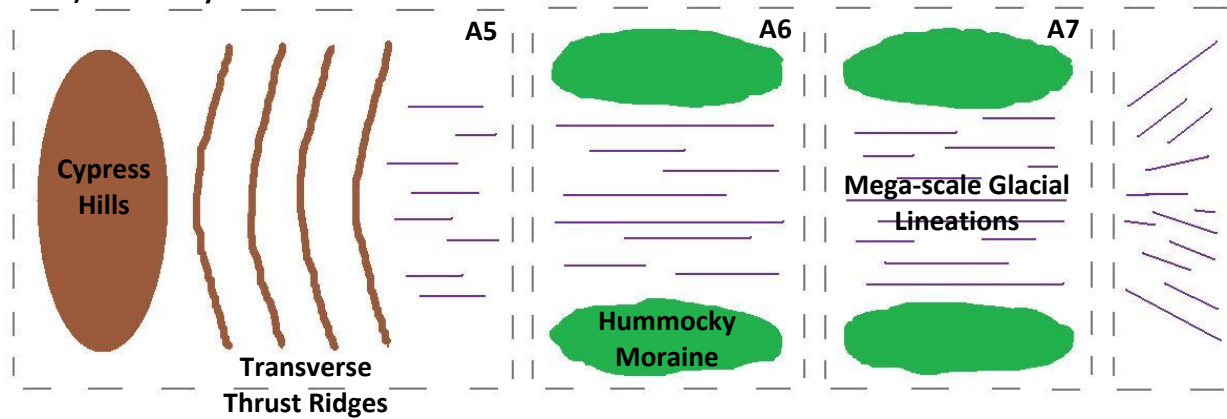


Figure 5.4: Conceptual Model where Maskwa paleo-ice stream created transverse ridges north of the Cypress Hills. (a) In the terminal zone of the Maskwa system (Assemblage 5), transverse ridges are perpendicular to ice flow, and are created when ice thrusts till to create stacks; (b) Continuous surging creates thick sequences of stacked tills throughout the assemblage; (c) A simplified bird's eye view of the Maskwa system shows similarities to the time-transgressive model for terrestrial ice streams in Stokes and Clark (1999). However this new model expects there to be thrust ridges due to the regional slope and surges, while hummocky terrain represents almost stagnant conditions outside of the corridor during ice streaming.

Maskwa south-southwest flow is probably still going at 15 ¹⁴C ka BP because of the ice around Cypress Hills but by 15-14 ¹⁴C ka BP the southern lobes became more unstable and this is marked by multiple ice readvances (e.g. Clark 1994). This is thought to reflect the start of the Buffalo system in the south with the ice stream flowing along the regional slope. Ross et al. (2009) suggested that the lack of similar features north of (Maskwa terminal zone) suggests a complete shutdown of the paleo-ice stream around 13.5 ¹⁴C ka BP occurred when the ice stream went from fast ice flow to sluggish/stagnant conditions rapidly. This change increased fast flow and subglacial erosion within the Buffalo Corridor, and inter-ice stream areas of the system saw little erosion and sedimentation, preserving the Maskwa landscape, after 14 ¹⁴C ka BP.

5.3 Southeastward Ice Flow Phase

In the Clayton and Moran (1982) reconstruction, there is a regional shift from southwest trending ice flow at Last Glacial Maximum (LGM) to southward flow at 15 ¹⁴C ka BP and, finally to southeast trending ice flow at 14 ¹⁴C ka BP. In this research, this shift is thought to be linked to the shut-down of the Maskwa system and replacement by the Buffalo paleo-ice stream.

5.3.1 The Buffalo paleo-ice stream

5.3.1.1 Landform Evidence

The Buffalo paleo-ice stream systems consists of multiple inter-ice stream areas and large corridors of MSGs that trend southeast. Fabric data is inconsistent due to pebble conditions, but striation data is consistent with the landform evidence. The Buffalo system includes tributaries from the west that were contemporaneous, as seen in the convergent flow patterns. The fields of attenuated bedforms and their large length to width ratios suggest rapid velocity occurred along the corridors towards the southeast. The corridors were bounded by topographic and bedrock highs, but the system was dynamic and shifts in lateral margins and overprinting of some assemblages are evidence of this instability. Shear margin moraines are also found throughout the system. Transverse ridges within the corridors suggest increased friction causing sticky spots. Glacial thrusting features and glacial lineations found in North Dakota are consistent with paleo-ice stream features (Bluemle and Clayton, 1984). Their location, east of the Missouri Coteau is also consistent with the proposed paleo-ice stream path to the southeast that ended with the surging glacial James Lobe.

Within Assemblage 1, there are two sets of flow directions, one to the south-southwest (consistent with the Maskwa system) and the other set is to the southeast, overprinting the southwest flow, and is most likely early Buffalo catchment flow, as it shifts to the east towards Prince Albert.

Assemblages 3a and 3b are most likely sticky spots forming small inter-ice stream zones during the Buffalo system. They are topographic highs covered by hummocky terrain that have no landform

evidence of ice flow direction, but they both have high carbonate contents. The southwest flow phase (Sect. 5.2) thus seems to be well recorded and that supports the interpretation that these assemblages are remnant landscape patches not reworked by the Buffalo system. No sampling was done on these assemblages and further investigation is needed.

Assemblages 9 and 10 are topographic highs that are contemporaneous. Assemblage 9 has some landform evidence of previous ice flow, but due to its curvilinear nature, is believed to be due to the shifts in Buffalo ice stream stability. Assemblage 10 is hummocky in nature but ridge moraines dominate its western boundary. These ridge moraines are analogous to lateral shear margin moraines, and were most likely created over multiple shifts in Buffalo paleo-ice stream margin due to its instabilities or could be polygenic due to later Weyburn ice lobe surging.

5.3.1.2 Dispersal of Omars

Omars are sparse in the United States except for North Dakota, eastern South Dakota and Minnesota, where their distribution has been noted for assigning provenance to glacial deposits in Canada, as they are found in the Des Moines and James Lobes (Biek, 1994; Prest et al., 2000). These omars are from the Belcher Islands, and no other source has been identified. A single source area better accounts for the omar dispersal, where southeast flowing ice over the Prairies from the Keewatin sector accounts for the James and Des Moines Lobes omar content (Prest et al., 2000). In Saskatchewan, the omars extend across the province along the 55° Latitude, where the omar content increases to the south-southeast, which is consistent with reworking of the till by the southeast Keewatin sector ice flow (Buffalo paleo-ice stream).

5.3.1.3 Till Composition

The carbonate content of the till varies along the Buffalo track. The carbonate originally from the east, is later re-entrained to the southeast, creating a fan-shaped dispersal train (Figure 5.5). This is evident from the high carbonate content to the east (close to the source area), the low carbonate content to the northwest, and moderate content in the western limb of the Buffalo Corridor. There

is also low carbonate content within and from the western (Alberta carbonate poor) tributaries feeding the Buffalo system. This is consistent and supports the Ross et al. (2009) model. There is a similar dispersal trend with Ca/Al ratios and pebble lithology (Figure 5.6)

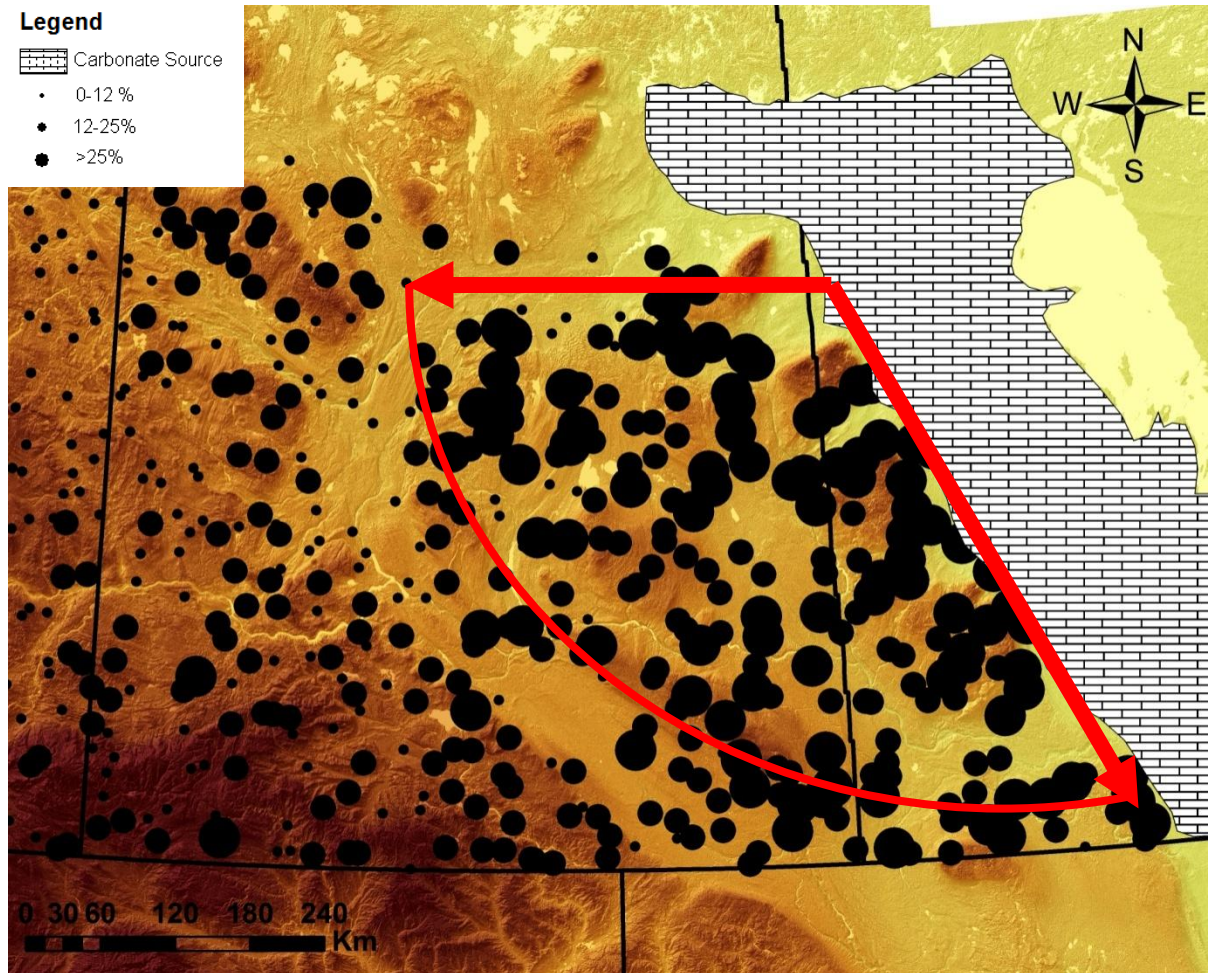


Figure 5.5: Fan-shaped dispersal of carbonates due to reworking of till by two separate ice flow events. The first was the westward flow, and then followed by the south-eastward flow, that decreased the carbonate content along the western limb of the Buffalo paleo-ice stream.

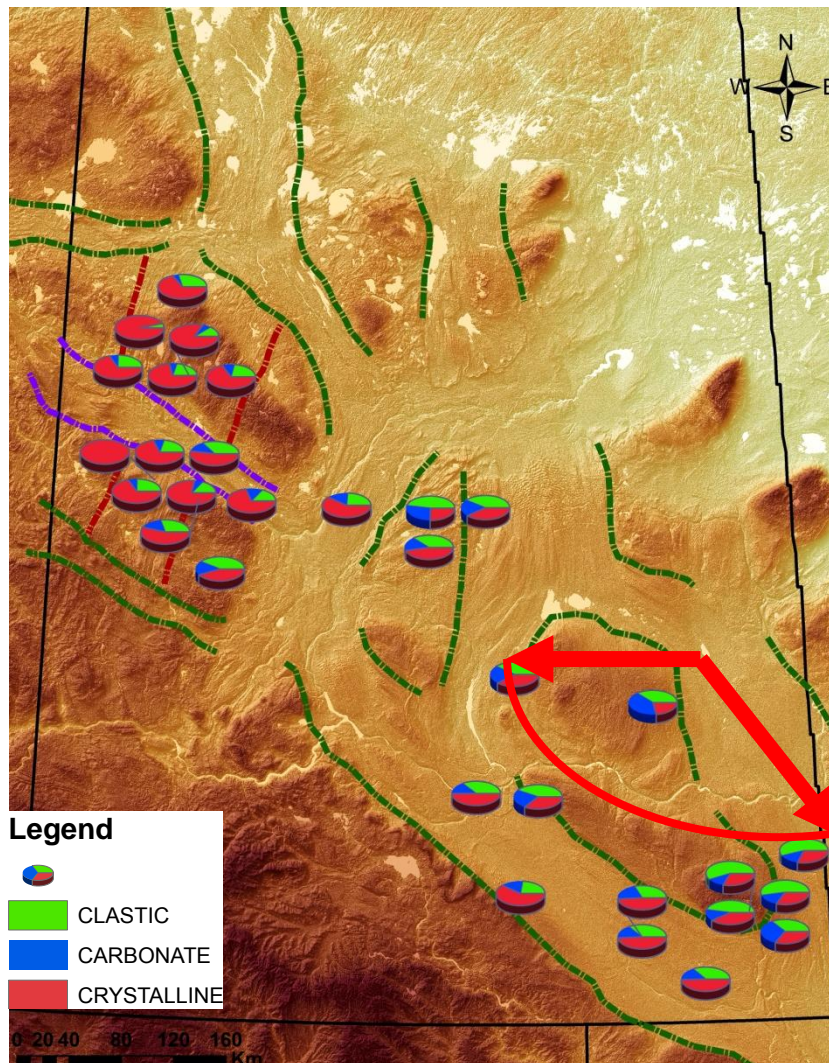


Figure 5.6: Similar fan dispersal pattern as seen with the carbonate content, the carbonate pebble lithology is higher in the southeast due to proximity to source and reworking of the till. High abundance of crystalline lithology is found along the Maskwa paleo-ice stream.

The $^{40}\text{Ar}/^{39}\text{Ar}$ data also reflects a similar change in ice flow direction but is not as extensive as the other methods of analysis due to limited sample sites. Within the Battleford Corridor, there are no Archean-aged grains (site # 18 North B 01), and this suggests a western origin, entering into the Buffalo system (Figure 5.7). Site #21 (Rd 602 01) in the western limb of the Buffalo system contains a sample with some Archean grains, but mostly Proterozoic grains. The sample to the east of it on Moose Mountains (site # 16) contains more Archean grains; this is consistent with the interpretation

that the Moose Mountain site was preserved during the Buffalo system and reflects the initial westward or southwestward flow that introduced the Archean grains from the Superior Province to the area (Figure 4.8). The increase in Proterozoic grains at the Rd 602 01 site is due to the reworking of till within the Buffalo system, which increased the amount of Proterozoic grains in the till, from the north. More sampling is needed within the corridor to confirm the model, but the samples provided are consistent with the proposed model of Ross et al. (2009).

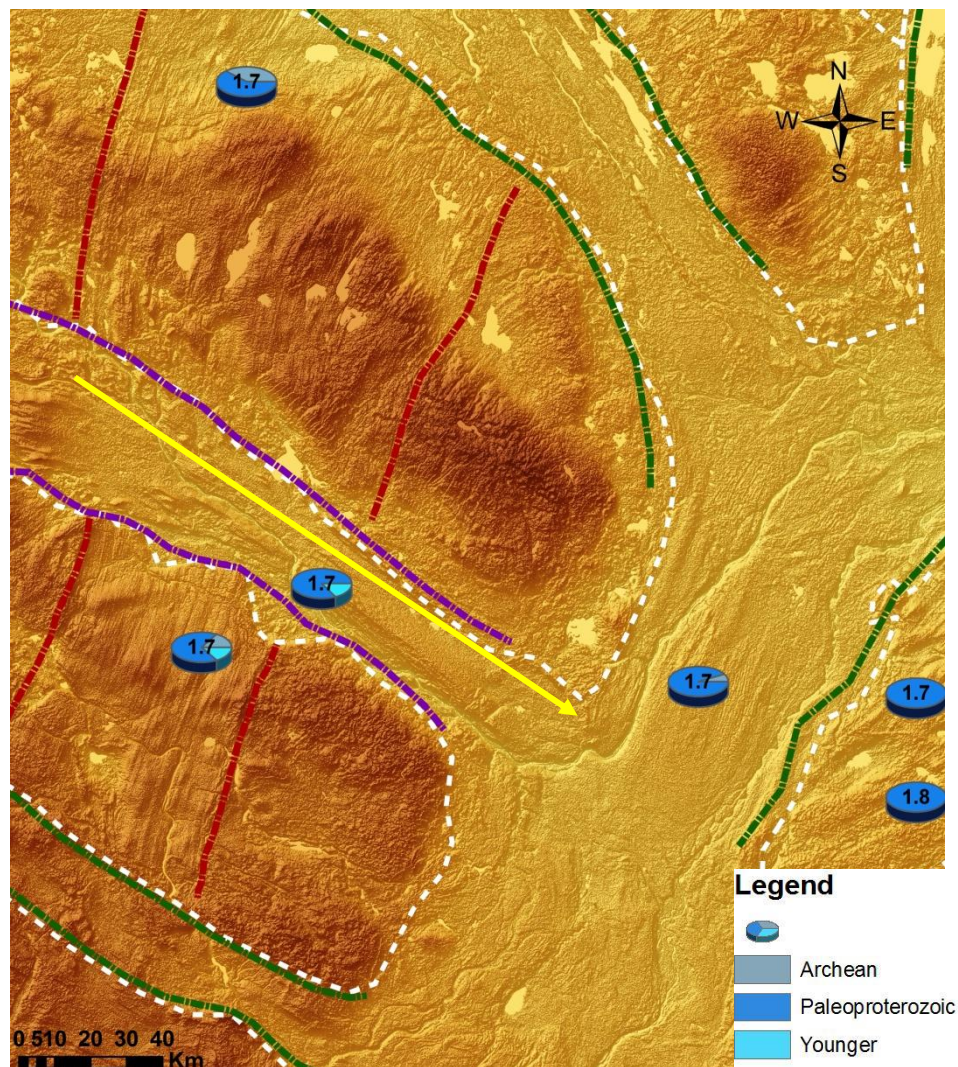
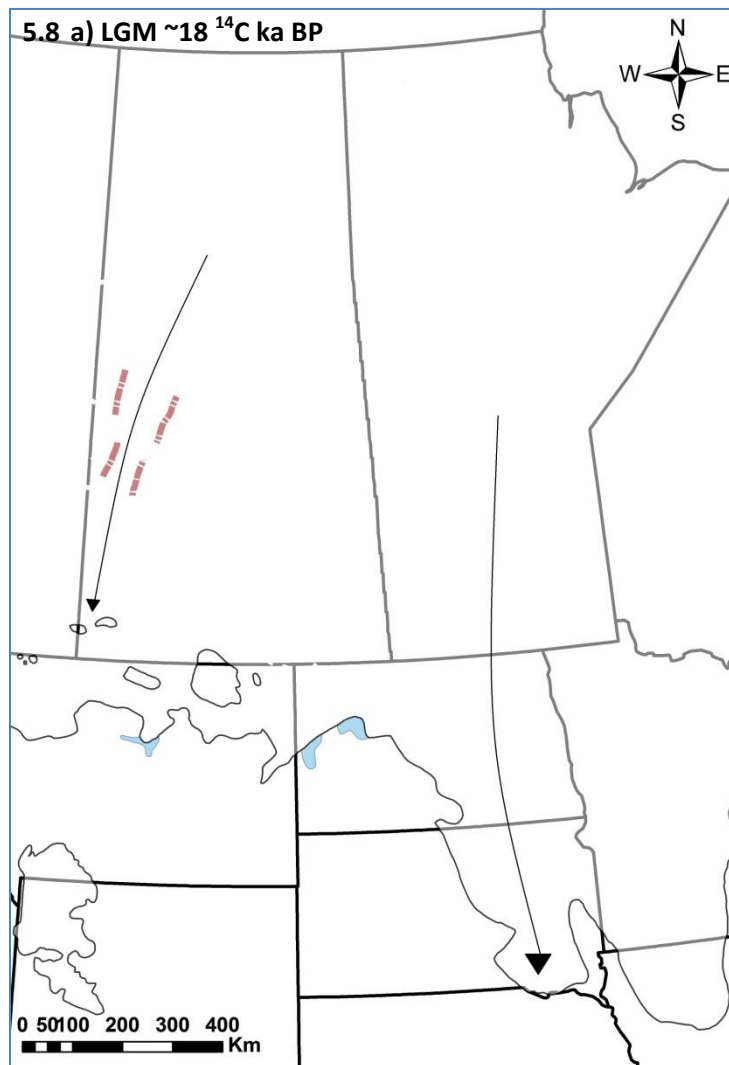
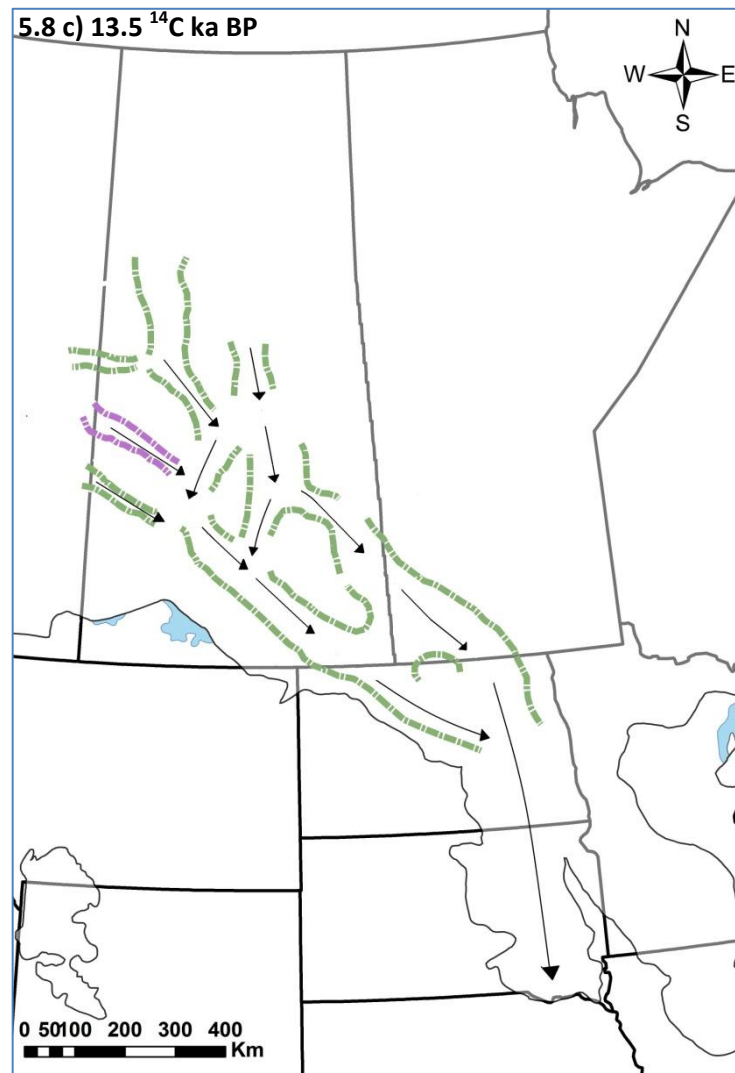


Figure 5.7: Lack of Archean-aged grains found within the Battleford Corridor is consistent with landform evidence suggesting southeastern flow along the corridor, into the Buffalo system. Yellow area shows ice flow direction along Battleford Corridor based on landform evidence.

5.4 Shift between Maskwa and Buffalo Systems

A conceptual model is proposed herein to explain how the shift from the Maskwa paleo-ice stream to the Buffalo system might have happened. The model is based on the landform and till composition evidence, as well as glacial theory. Figure 5.8 outlines the conceptual model of the transition between Maskwa and Buffalo systems.





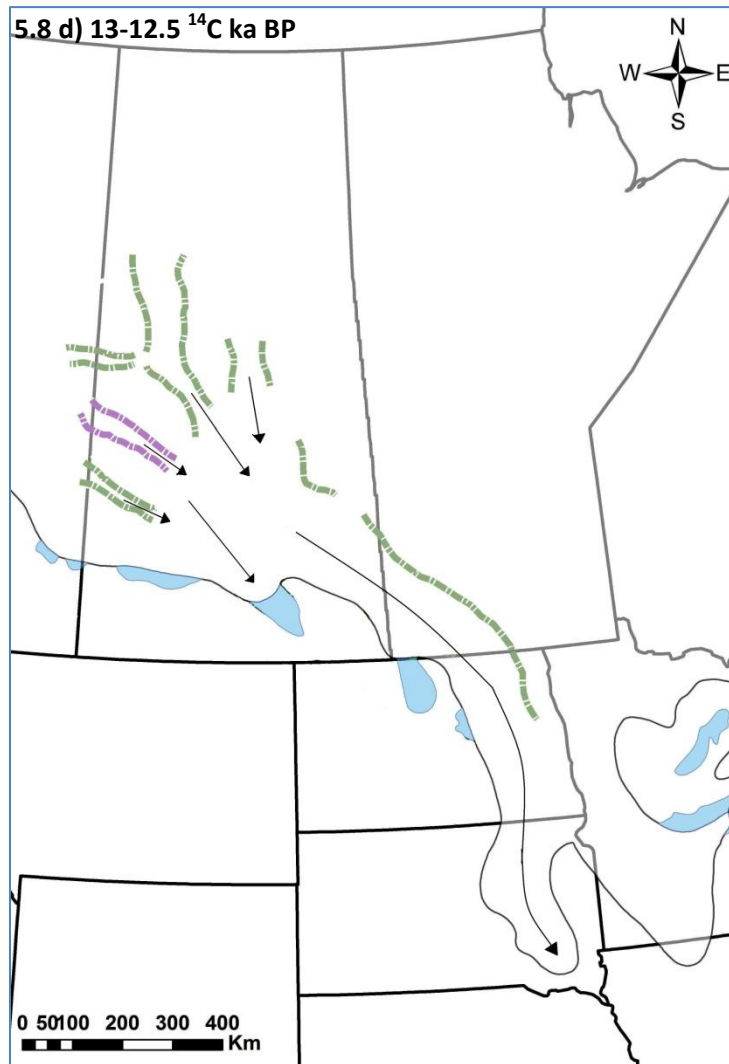


Figure 5.8: Conceptual model of the shift between Maskwa and Buffalo paleo-ice stream systems. (a) at LGM the Maskwa paleo-ice stream was flowing southwest, and the James Lobe was fed by a system in Manitoba; (b) around 14 ¹⁴C ka BP the ice sheet had thinned and regional flow patterns changed to the southeast, changing the catchment area for the James Lobe, thus initiating the Buffalo system in Saskatchewan; (c) by 13.5 ¹⁴C ka BP, inter-ice stream areas had developed and the Maskwa system was shut off due to the Buffalo system capturing its subglacial water, and thus stagnating it and preserving the landscape; (d) the last major surge of the James Lobe happened around 12.5 ¹⁴C ka BP, and at this time the eastern limb had captured most of the subglacial water from the western limb, causing it to develop into a outlet lobe, while the western tributaries continued to feed the whole Buffalo system.

By 14 ¹⁴C ka BP, the Laurentide Ice Sheet had significantly thinned over the Interior Plains since LGM, and its southern lobes had low surface profiles (Mathews, 1974). This change was triggered by “controlling factors (warming trend, subglacial conditions) [that] had brought the glacial system across a threshold [and the] timing for the glacial dynamics shift is also consistent with many paleoclimatic records indicating accelerating warming trends after 14 ¹⁴C ka BP” (Ross et al., 2009). Large reduction of ice volume, but not extent, before 14 ¹⁴C ka BP is thought to be representative of regional change in flow pattern over the prairies, with a thinner ice sheet becoming more sensitive to the regional slope (Dyke and Prest, 1987). Dyke and Prest (1987) proposed that the high basal shear stresses at LGM (linked to thick ice) were balanced out by a regionally frozen subglacial bed. At the time, the steady state equilibrium profile of the ice sheet suggested unfavorable conditions for subglacial bed deformation.

The James Lobe was initially fed by southwestern flow from Manitoba, but the shift in ice flow direction changed the catchment area of the Lobe. In order to explain how the Maskwa landscape was preserved despite the shift in glacial dynamics a two-phase model is used. First, the Buffalo system started to form in the southern lobes as a result of thinning ice and increasing meltwater lubrication. Initially, the ice stream was relatively small but its onset zone progressively expanded northwestward from the James Lobe around 14 ¹⁴C ka BP (Figure 5.8b). This is the start of phase 2. The James lobe advanced along the James River valley in the Dakotas, and its associated ice stream along the Missouri Coteau, reaching its maximum around 14 ¹⁴C ka BP (Patterson, 1997). The Buffalo catchment expanded, developing inter-ice stream areas in Saskatchewan (e.g. Assemblage 10), until it captured the subglacial water from the Maskwa system, which led to the eventual shutdown and stagnation of the Maskwa paleo-ice stream around 13.5 ¹⁴C ka BP (Figure 5.8c). This change increased fast flow and subglacial erosion within the Buffalo Corridor, and inter-ice stream areas of the system saw little erosion and sedimentation, preserving the Maskwa landscape after 14 ¹⁴C ka BP. The stagnation of the Maskwa system followed by the progressive migration of the Buffalo onset zone and associated tributaries explains well the sharp contact relationship between the Buffalo tributaries and the Maskwa assemblages. The capturing of subglacial water might also explain why, later, the western limb (Weyburn Lobe) retreated while the eastern limb (Moose Mountain Lobe) of the Buffalo Corridor readvanced significantly (surged) around 13-12.5 ¹⁴C ka BP (Figure 5.8d).

Chapter 6 Conclusion

“One of the most important controls on the stability of these ice sheets is the location and vigour of ice streams; they are typically several hundred kilometers long, tens of kilometers wide and are characterized by rapid flow surrounded by comparatively stagnant or slower flow ice” (Bennett, 2003). Through decades of research into ice stream mechanisms and behaviour, rapid changes in ice stream velocity and configuration are still not fully understood. Paleo-ice streams provide insight into the ice bed interface that allows analogies between contemporary and paleo systems to be used as mutually inclusively.

6.1 The subglacial landscape of the southern Interior Plains

Maps and literature have for decades shown complex ice flow patterns across the Interior Plains, where large areas of flow lines at right angles, across various topography, could not be explained (Prest et al., 1968). However, it is difficult to reconstruct this without invoking a complex system. The uniform flow model explains the major ice flow shifts, but cannot explain satisfactorily the complexity of the glacial maps (Christiansen, 1979; Shilts et al., 1979; Shilts, 1980; Clayton and Moran, 1982; Klassen, 1989). Around the late 1980s and early 1990s, the soft-bed paradigm shift had occurred, where the identification of conditions for dynamic ice sheet behaviour could occur, was taking place. Several researchers had identified the Prairies as a critical spot for soft bed deformation, sliding and ice sheet instability (Clayton et al., 1985; Clark, 1994; Marshall et al., 1996). The fine-grain material made conditions ideal for low permeability and high subglacial pressures.

Around the same time, a two-way relationship had evolved between modern and paleo-ice stream research. An understanding of Antarctic ice stream systems had evolved to include potential paleo-ice stream systems, where the use of paleo-landscapes could be used to gain information about subglacial conditions and processes that were unavailable for observation in Antarctica. And modern ice stream understanding was used to guide paleo-ice stream research. From this new understanding, a shift occurred towards paleo-ice stream research in the late 1990s. Stokes and Clark (1999) proposed a list of criteria to the identification and reanalysis of the glacial landscape

(with emphasis on the landform evidence), and Patterson (1997, 1998) provoked the idea of detailed analysis for potential terrestrial ice streams in the Prairies. The simultaneous release of new SRTM datasets along with new Antarctic research provoked a flurry of analysis and theory. Jennings (2006) combined field observations with Antarctic knowledge to suggest that the James and Des Moines Lobes were part of a complex ice stream system that needed to be researched up ice (Canada). Using Ice Stream B in Antarctica as an approximation, Patterson (1997) showed that in about 900 years, a 70 km wide 900km long ice stream of approximately 850m thick, could have enough discharge to create the Des Moines Lobe. This approximation holds true for the James Lobe as well. The reason that the Des Moines and James lobes could advance much farther than the rest of the ice sheet had to do with the subglacial conditions and the clay-rich bed mentioned above. The reason that not all southern Laurentide lobes advanced and retreated synchronously was probably due to internal ice stream dynamics (Patterson, 1997; Jennings, 2006). Since then, Evans et al. (2008) and Ross et al. (2009) have suggested ice stream models for Alberta and Saskatchewan, respectively.

Ross et al. (2009) proposed a new landsystem model for the glacial landscape of Saskatchewan. The preliminary assessment used SRTM images and the Stokes and Clark (1999) geomorphologic criteria as well as available surface till compositional data to predict potential sediment-landform relationships. This model was consistent with other paleo-ice stream models in Canada and deglacial models of the Mid-West United States (i.e. North Dakota, Minnesota) (Jennings, 2006; Clayton et al., 2008). However, new data were needed to test the model. Gaining new information and further constraining the model was the purpose of this MSc. Thesis.

The prairie landscape (specifically Alberta) is also central to the development of the controversial Megaflood hypothesis. “The meltwater [megaflood] hypothesis attributes some subglacial landforms to erosion and deposition by outburst floods larger than any floods within historical time” (Shaw, 2002) where massive subglacial outburst floods are viewed as a major subglacial landscape-forming process. The methods of bedform genesis have direct consequences on ice sheet behaviour and climatic history; this is why it is important to understand under which process a bedform has been created. The majority of Megaflood research has been concentrated in Alberta (Shaw et al.,

1989, 2000; Shaw, 2002; Beaney and Shaw, 2000; Munro and Shaw, 1997), where it has also been extensively challenged (Evans et al., 2006; Evans et al., 2008). To date, in Saskatchewan there has been no published research regarding the megaflood hypothesis, except for a M.Sc. Thesis by Grant (1997). In this research, the goal was not to explicitly test or challenge this hypothesis. The main goals were to update and refine the subglacial landscape mosaic assemblage map and test the paleo-ice stream model and the landscape reconstruction of Ross et al. (2009). This model allows a number of predictions to be made. The test focuses on predictions of properties that are link to ice flow and that are unlikely to have been influenced by meltwater such as till compositional data, and glacial structures. But it also uses more subjective geomorphologic observations (the list of paleo-ice stream criteria). Therefore, if the data agrees with the predictions and the landscape fits the criteria, the analysis provides additional support to the model.

According to the Ross et al. (2009) model, the Saskatchewan landscape during the Late Wisconsinan was the scene for two different ice stream systems. The Maskwa paleo-ice stream was a long curvilinear system, not topographically bound, trending southwest from the Canadian Shield to the Cyprus Hills foothills. It was driven by high basal shear stresses under the thick LGM ice, producing fast ice flow indicators such as fields of mega-scale glacial lineations and long-narrow dispersal trains. The second ice stream system, Buffalo, was topographically bounded, trending south and southeast, with as many as four tributary ice streams feeding it. The Buffalo system was formed beneath a thinner ice sheet. Fast flow was achieved by a deformable or sliding bed. It was very similar in size and character as those seen on the Siple Coast of West Antarctica.

The Maskwa ice stream was shut off around 13.5 ¹⁴C ka BP when a shift in glacial dynamics from southwest to southeast flowing ice occurred by about 14 ¹⁴C ka BP. The Buffalo system served as a feeder to the outlet James Lobe until about 12.5 ¹⁴C ka BP. The system evolved into small outlet lobes before receding to the Shield at the position of the Cree Lake Moraine by 10 ¹⁴C ka BP.

6.2 Thesis Contributions

The main goals of the thesis were to update and refine the subglacial landscape mosaic assemblage map and test the paleo-ice stream model and the landscape reconstruction of Ross et al. (2009). This was done over a series of contributions and is defined below:

First: Update and refine the landscape-assemblage map of Ross et al. (2009). This included delineation of new assemblages (assemblages 3b, 9, and 10), and refining the boundaries of previous assemblages through GIS analysis of landforms. Mapping of mega-scale glacial lineations and other features of interest (ice flow direction indicators), that could be used in the analysis of the landscape. The above-mentioned features were used with a compilation of literature review (previous research throughout the area) and entered into GIS for extensive spatial analysis. An alternative explanation was used to understand previously mapped terrain elements (transverse ice thrust ridges in Assemblage 5) and other unexplained observations (Mahaney and Stalker, 1988) as being associated with the Maskwa paleo-ice stream system. This type of terminal zone is now integrated into the terrestrial paleo-ice stream landsystem model. A new conceptual model was introduced to explain the sharp transitions between the Maskwa and Buffalo systems, and the associated landform preservation and genesis.

Through this work, it was realized that the original list of criteria to identify and characterize paleo-ice streams (Stokes and Clark 1999) needed to be expanded to include evidence for tributary-type flow systems as well as a description of what may define an inter-ice stream zone in other settings than the Canadian Arctic. Tributaries are now included in the convergent flow pattern criteria. This is recognized in the landscape by narrow converging corridors connected to the main corridor of MSGs. They contain streamlined ridges that are slightly shorter than typical MSGs due to intermediate ice flow velocities. The compositional signature of the surface till should reflect the source material of its catchments. Finally, they should not contain extensive ice stream shear margin moraines. The general characteristic of inter-ice stream areas in the prairies is that they are isolated terrain elements bounded by fields of MSGs. They may consist of hummocky terrain or fragments of various landforms cross-cut by the younger surrounding MSGs. These terrains may have a compositional signature consistent with previous ice flow phases.

Second: Field test sediment-landform relationship through till fabrics and field observations. It was important to determine if the surface till was most likely the youngest till linked to the landform record, in order to determine a sediment-landform relationship. This was done by field observations of the till units sampled and comparison to other descriptions and first-hand knowledge from the area. This was important because of the potential complex stratigraphy, and to enhance the confidence of external data, such as the use of the Thorleifson and Garrett (1993) carbonate database. Other sediment-landform relationships were explored by observing striations on shallow boulder pavements, and till fabric samples. There was a good correlation between striation observations and the landforms, but due to the nature of the till, fabric data are not as reliable and should be used in conjunction with other data

Third: Compositional data and clast lithology. Geochemistry was analyzed on all till samples and ratios of Ca/Al and Mg/Al were used to verify crystalline or carbonate source material. Clast lithology of till samples was determined through visual examination to determine the distribution of lithologies across the area. When integrated with the geochemistry data into the GIS analysis, it was fairly consistent with the proposed model. This integrated approach allowed to better establish the signature of individual assemblages versus the surrounding corridors and to confidently link the various assemblages to the main ice flow phases.

Fourth: The use of $^{40}\text{Ar}/^{39}\text{Ar}$ dating to further test model predictions. The initial hypothesis was that the Buffalo Corridor should contain a higher proportion of Churchill (Proterozoic-age) grains than in the assemblages, because these assemblages would consist of pre-existing glacial sediments preserved as Buffalo inter-ice stream areas. These assemblages should contain more Archean-age grains because older ice flow phases are west and southwest trending. This would have brought more material from the Superior Province (Archean-age). Although a limited number of sites were tested, the results are in good agreement with the predictions. Further sampling throughout the province, in corridors and assemblages needs to be done to further refine this model and increase the confidence of the interpretation, but the results yield enough evidence to proceed with further

testing at a later date. This is the kind of sediment-landform relationship that is not easily explained by subglacial meltwater erosion.

Overall the new data confirmed the spatial patterns predicted by Ross et al. (2009) fit well within the structure of the mosaic landscape. Landforms, striations, compositional data and $^{40}\text{Ar}/^{39}\text{Ar}$ dating were analyzed in GIS to provide a spatial analysis of Saskatchewan that was formed by complex glacial transport processes. This integrated approach has provided a better understanding of the regional subglacial landscape and evolution and provides evidence of ice streaming and associated major glacial dynamics shifts.

6.3 Implications of Work

The results of this work will not only be useful for both paleo and contemporary ice stream research, but they also have implications in other areas of geology, the understanding of the complex relationship between sediments, landforms and geochemistry. The concept of a mosaic landscape, of ice streaming and preserved inter-ice stream areas in the prairies, offers a new perspective on ice sheet reconstruction, and ice sheet dynamics of the southwestern LIS. It also has implications in provenance studies and mineral exploration, soil sampling and geotechnical engineering and, potentially, regional hydrogeology.

1. Ice sheet reconstruction and dynamics

- The documentation and characterization of large paleo-ice streams are changing the way we view the Laurentide Ice Sheet and how we understand its dynamic response to internal instabilities or external (climate) forcing. It provides information on their potential controlling factors and on how these systems may behave over long periods of time. It also provides knowledge on ice stream systems that may not have modern analogues (e.g. the Maskwa system) but that are still essential to understand ice sheets and their response to other earth systems. This will provide geologic constraints to the new generation of ice sheet numerical models.

2. Provenance studies and mineral exploration

- If indicator minerals are found in an area delineated as an assemblage i.e. Assemblage 2, the geologist has to determine the direction of ice flow and trace the mineral back to its source. By using a mosaic model, as opposed to a uniform landscape model, it will change the sampling strategy significantly such as the grid-type and search pattern as well as interpretation of results. This could help a company look in the right direction, making it save both time and money, and potentially increase the chances of mineral discoveries in the Prairies.

3. Hydrogeology

- Links between and the extent of aquifers and aquitards can be discontinuous across assemblages, corridors and their boundaries. Delineation of these boundaries can aid in groundwater modeling. The model can also aid in development of a hydro-stratigraphic conceptual model and help target subsurface investigations. For example, the Maskwa system now includes a terminal zone consisting of major transverse ridges. These ridges may be the location of kilometer-scale and deep-seated thrust planes which may act as preferential pathways for groundwater.

References

- Aber, J. S., (Ed.) (1993). Glaciotectonics and Mapping Glacial Deposits. Regina, Canadian Plains Research Center.
- Aber, J. S. and K. Apolzer (2004). Pre-Wisconsinan glacial database and ice limits in the central United States. Quaternary Glaciations- Extent and Chronology 2. J. Ehlers and P. L. Gibbard, Elsevier: 83-88.
- Adams, R. S., M. Ross, J.E. Campbell, and S.R. Hemming (2009). Investigation of Large Paleo-Ice Stream Systems in the Canadian Prairies. CANQUA-CGRG Biennial Meeting, Simon Fraser University, Burnaby Campus, B.C.
- Alberta Geological Survey (AGS) (2009). "Geology of Alberta Interactive Maps." from http://www.ags.gov.ab.ca/GIS/download_gis.htm.
- Altuhafi, F. N., B. A. Baudet, and P. Sammonds. (2009). "On the time-dependent behaviour of glacial sediments: a geotechnical approach." Quaternary Science Reviews **28**(7-8): 693-707.
- Andrews, J. T. (1971). Methods in the Analysis of Till Fabrics. Till A Symposium. S. L. Goldstein, Ohio State University Press: 321-327.
- Andrews, J. T. (1971). Techniques of Till Fabric Analysis. Norwich, British Geomorphological Group.
- Andrews, J. T., P. Clark, and J.A. Stavers. (1985). The patterns of glacial erosion across the eastern Canadian Arctic. Quaternary Environments. J. T. Andrews: 69-92.
- Andrews, J.T. and Tedesco, K. 1992. Detrital carbonate rich sediments, Northwestern Labrador Sea- Implications for ice-sheet dynamics and iceberg rafting (Heinrich) events in the North Atlantic. Geology, **20 (12)**: 1087-1090.
- Ansdell, K. M. (2005). "Tectonic evolution of the Manitoba-Saskatchewan segment of the Paleoproterozoic Trans-Hudson Orogen, Canada." Canadian Journal of Earth Sciences **42**(4): 741-759.
- Bamber, J. L., D. G. Vaughan, and I. Joughin. (2000). "Widespread complex flow in the interior of the Antarctic ice sheet." Science **287**(5456): 1248-1250.
- Barendregt, R. W. and E. Irving (1998). "Changes in the extent of North American ice sheets during the late Cenozoic." Canadian Journal of Earth Sciences **35**(5): 504-509.

- Barendregt, R. W., E. Irving, E.A. Christiansen, E.K. Sauer, and B.T. Schreiner. (1998). "Stratigraphy and paleomagnetism of Late Pliocene and Pleistocene sediments in the Wellsch Valley and Swift Current Creek areas, southwestern Saskatchewan, Canada." Canadian Journal of Earth Sciences **35**(12): 1347-1361.
- Beaney, C. L. and J. Shaw (2000). "The subglacial geomorphology of southeast Alberta: evidence for subglacial meltwater erosion." Canadian Journal of Earth Sciences **37**(1): 51-61.
- Benn, D. I. (1994). "Fabric shape and the interpretation of sedimentary fabric data." Journal of Sedimentary Research Section a-Sedimentary Petrology and Processes **64**(4): 910-915.
- Benn, D. I. (2006). Interpreting glacial sediments. Glacier Science and Environmental Change. P. G. Knight, Blackwell Publishing: 434-439.
- Benn, D. I. and D. J. A. Evans (2006). Glaciers and Glaciation. London, Arnold.
- Benn, D. I. and D. J. A. Evans (2006). Subglacial megafloods: outrageous hypothesis or just outrageous? Glacier Science and Environmental Change. P. G. Knight, Blackwell Publishing: 44-50.
- Bennett, M. R. (2003). "Ice streams as the arteries of an ice sheet: their mechanics, stability and significance." Earth-Science Reviews **61**(3-4): 309-339.
- Bennett, M. R., R. I. Waller, N.F. Glasser, M.J. Hambrey and D. Huddart. (1999). "Glacigenic clast fabrics: genetic fingerprint or wishful thinking?" Journal of Quaternary Science **14**(2): 125-135.
- Bentley, C. R. (1987). "Antarctica Ice Streams - A Review." Journal of Geophysical Research-Solid Earth and Planets **92**(B9): 8843-8858.
- Biek, R. F. (1994). "Concretions and nodules in North Dakota; cannonballs, logs, and other oddities." North Dakota Geological Survey Newsletter **21**(2): 6-11.
- Bluemle, J. P. and L. Clayton (1984). "Large-Scale Glacial Thrusting and Related Processes in North Dakota." Boreas **13**(3): 279-299.
- Bluemle, J. P., J. R. Reid, and K.J.R. Mitchell. (2004). Glaciation of North Dakota U.S.A. Quaternary Glaciations: Extent and Chronology 2. J. Ehlers and P. L. Gibbard: 207-212.
- Boone, S. J. and N. Eyles (2001). "Geotechnical model for great plains hummocky moraine formed by till deformation below stagnant ice." Geomorphology **38**(1-2): 109-124.

- Bougamont, M. and S. Tulaczyk (2003). Glacial erosion beneath ice streams and ice-stream tributaries: constraints on temporal and spatial distribution of erosion from numerical simulations of a West Antarctic ice stream, Taylor & Francis As.
- Boulton, G. and M. Hagdorn (2006). "Glaciology of the British Isles Ice Sheet during the last glacial cycle: form, flow, streams and lobes." Quaternary Science Reviews **25**(23-24): 3359-3390.
- Boulton, G. S. and C. D. Clark (1990). The Laurentide Ice-Sheet through the Last Glacial Cycle - The Topology of Drift Lineations as a key to the Dynamic Behaviour of former Ice Sheets, Royal Soc Edinburgh.
- Briner, J. P. (2007). "Supporting evidence from the New York drumlin field that elongate subglacial bedforms indicate fast ice flow." Boreas **36**(2): 143-147.
- Camfield, P. A. and D. I. Gough (1977). "Possible Proterozoic Plate Boundary in North America." Canadian Journal of Earth Sciences **14**(6): 1229-1238.
- Campbell, J. E. (2007). Quaternary geology of the eastern Athabasca Basin, Saskatchewan. EXTECH IV: Geology and Uranium Exploration TECHNOLOGY of the Proterozoic Athabasca Basin, Saskatchewan and Alberta. C. W. Jefferson and G. Delaney. Ottawa, Geological Survey of Canada. **Bulletin 588**: 211-228.
- Campbell, J. E., R. W. Klassen, and R.B.K. Shives. (2007). Integrated field investigation of airborne radiometric data and drift composition, Nuclear Energy Agency-International Atomic Energy Athabasca test area, Saskatchewan. EXTECH IV: Geology and Uranium Exploration TECHNOLOGY of the Proterozoic Athabasca Basin, Saskatchewan and Alberta. C. W. Jefferson and G. Delaney. Ottawa, Geological Survey of Canada. **Bulletin 588**: 533-554.
- Carlson, A. E., J. W. Jenson, and P.U.Clark. (2007). "Modeling the subglacial hydrology of the James Lobe of the Laurentide Ice Sheet." Quaternary Science Reviews **26**(9-10): 1384-1397.
- Christiansen, E. A. (1956). Glacial Geology of the Moose Mountain Area Saskatchewan. Regina, Government of Saskatchewan Department of Mineral Resources. **Report 21**: 1-35.
- Christiansen, E. A. (1959). Glacial Geology of the Swift Current Area Saskatchewan. Regina, Government of Saskatchewan Department of Mineral Resources. **Report 32**: 1-62.
- Christiansen, E. A. (1960). Geology and Ground-Water Resources of the Qu'Appelle Area Saskatchewan. Regina, Saskatchewan Research Council. **Report 1**: 1-53.

- Christiansen, E. A. (1968). "A thin till in West-Central Saskatchewan, Canada." Canadian Journal of Earth Sciences **5**(1): 329-336.
- Christiansen, E. A. (1971). Tills in Southern Saskatchewan, Canada. Till A Symposium. S. L. Goldstein, Ohio State University Press: 167-183.
- Christiansen, E. A. (1972). Southern Saskatchewan in Quaternary Geology and Geomorphology between Winnipeg and the Rocky Mountains. XXIV International Geological Congress. D. J. Glass. Montreal, Quebec: 24-30.
- Christiansen, E. A. (1973). Geology and Groundwater Resources of the Prince Albert Area (73-H) Saskatchewan, Saskatchewan Research Council.
- Christiansen, E. A. (1977). Engineering Geology of Glacial Deposits in Southern Saskatchewan. 13th Canadian Geotechnical Conference. Saskatoon, Saskatchewan.
- Christiansen, E. A. (1979). "The Wisconsin Deglaciation of Southern Saskatchewan and Adjacent Areas." Canadian Journal of Earth Sciences **16**(4): 913-938.
- Christiansen, E. A. (1980). "The Wisconsin Deglaciation of Southern Saskatchewan and Adjacent Areas - Reply." Canadian Journal of Earth Sciences **17**(4): 541-541.
- Christiansen, E. A. (1983). "The Denholm Landslide, Saskatchewan 1. Geology." Canadian Geotechnical Journal **20**(2): 197-207.
- Christiansen, E. A. (1987). "Verendrye Valley and the Glidden esker, Saskatchewan - Subglacial and ice walled features in southwestern Saskatchewan, Canada." Canadian Journal of Earth Sciences **24**(1): 170-176.
- Christiansen, E. A. (1992). "Pleistocene Stratigraphy of the Saskatoon area, Saskatchewan, Canada - An Update." Canadian Journal of Earth Sciences **29**(8): 1767-1778.
- Christiansen, E. A., D. J. Gendzwill, and W.A. Meneley. (1982). "Howe Lake - A Hydrodynamic Blowout Structure." Canadian Journal of Earth Sciences **19**(6): 1122-1139.
- Christiansen, E. A. and E. K. Sauer (1988). "Age of the Frenchman Valley and associated drift of the Cypress Hills, Saskatchewan, Canada." Canadian Journal of Earth Sciences **25**(10): 1703-1708.
- Christiansen, E. A. and E. K. Sauer (1988). "Fire Lake Depression - A Glacially eroded feature in southwestern Saskatchewan, Canada." Canadian Journal of Earth Sciences **25**(12): 2130-&.

- Christiansen, E. A. and E. K. Sauer (1993). "Red Deer Hill - a drumlinized, glaciotectonic feature near Price Albert Saskatchewan, Canada." Canadian Journal of Earth Sciences **30**(6): 1224-1235.
- Christiansen, E. A. and E. K. Sauer (1997). "The Dirt Hills structure: An ice-thrust feature in southern Saskatchewan, Canada." Canadian Journal of Earth Sciences **34**(1): 76-85.
- Christiansen, E. A. and E. K. Sauer (2001). "Stratigraphy and structure of a Late Wisconsinan salt collapse in the Saskatoon Low, south of Saskatoon, Saskatchewan, Canada: an update." Canadian Journal of Earth Sciences **38**(11): 1601-1613.
- Christiansen, E. A. and E. K. Sauer (2002). "Stratigraphy and structure of Pleistocene collapse in the Regina Low, Saskatchewan, Canada." Canadian Journal of Earth Sciences **39**(9): 1411-1423.
- Christiansen, E. A. and B. T. Schreiner (1987). Trip 7 Quaternary Geology and Geotechnology Field Trip Guide Book. GAC-MAC 1987. University of Saskatchewan Saskatoon Campus: 1-27.
- Clark, C. D. (1993). "Mega-scale glacial lineations and cross-cutting ice flow landforms." Earth Surface Processes and Landforms **18**(1): 1-29.
- Clark, C. D. (1997). "Reconstructing the evolutionary dynamics of former ice sheets using multi-temporal evidence, remote sensing and GIS." Quaternary Science Reviews **16**(9): 1067-1092.
- Clark, C. D., A. L. C. Hughes, S.L. Greenwood, M. Spagnolo, and F.S.L. Ng. (2009). "Size and shape characteristics of drumlins, derived from a large sample, and associated scaling laws." Quaternary Science Reviews **28**(7-8): 677-692.
- Clark, C. D., S. M. Tulaczyk, C.R. Stokes and M. Canals. (2003). "A groove-ploughing theory for the production of mega-scale glacial lineations, and implications for ice-stream mechanics." Journal of Glaciology **49**(165): 240-256.
- Clark, P. U., J. M. Licciardi, D.R. MacAyeal, and J.W. Jenson. (1996). "Numerical reconstruction of a soft-bedded laurentide ice sheet during the last glacial maximum." Geology **24**(8): 679-682.
- Clarke, G. K. C. (1987). "Subglacial till - a physical framework for its properties and processes." Journal of Geophysical Research-Solid Earth and Planets **92**(B9): 9023-9036.
- Clarke, G. K. C., D. W. Leverington, J.T. Teller, and A.S. Dyke. (2004). "Paleohydraulics of the last outburst flood from glacial Lake Agassiz and the 8200 BP cold event." Quaternary Science Reviews **23**(3-4): 389-407.

- Clarke, G. K. C., D. W. Leverington, J.T.Teller, A.S. Dyke, and S.J. Marshall. (2005). "Fresh arguments against the Shaw megaflood hypothesis. A reply to comments by David Sharpe on "Paleohydraulics of the last outburst flood from glacial Lake Agassiz and the 8200 BP cold event". " Quaternary Science Reviews **24**(12-13): 1533-1541.
- Clayton, L., J. W. Attig, N.R. Ham, M.D. Johnson, C.E. Jennings, and K.M. Syverson. (2008). "Ice-walled-lake plains: Implications for the origin of hummocky glacial topography in middle North America." Geomorphology **97**(1-2): 237-248.
- Clayton, L. and S. R. Moran (1982). "Chronology of Late Wisconsinan Glaciation in Middle North America." Quaternary Science Reviews **1**: 55-82.
- De Angelis, H. and J. Kleman (2005). Paleo-ice streams in the northern Keewatin sector of the Laurentide ice sheet, International Geological Society.
- De Angelis, H. and J. Kleman (2007). "Paleo-ice streams in the Foxe/Baffin sector of the Laurentide Ice Sheet." Quaternary Science Reviews **26**(9-10): 1313-1331.
- De Angelis, H. and J. Kleman (2008). "Paleo-ice-stream onsets: examples from the north-eastern Laurentide Ice Sheet." Earth Surface Processes and Landforms **33**(4): 560-572.
- Denton, G. H. and T. J. Hughes, (Eds). (1981). The Last Great Ice Sheets. New York, John Wiley & Sons.
- Dowdeswell, J. A. and A. Elverhoi (2002). "The timing of initiation of fast-flowing ice streams during a glacial cycle inferred from glacial marine sedimentation." Marine Geology **188**(1-2): 3-14.
- Dowdeswell, J. A., D. Ottesen, J. Evans, C.O. Cofaigh, and J.B. Anderson. (2008). "Submarine glacial landforms and rates of ice-stream collapse." Geology **36**(10): 819-822.
- Dowdeswell, J. A., D. Ottesen, L. Rise and J. Craig. (2007). "Identification and preservation of landforms diagnostic of past ice-sheet activity on continental shelves from three-dimensional seismic evidence." Geology **35**(4): 359-362.
- Dowdeswell, J. A. and M. J. Sharp (1986). "Characterization of pebble fabrics in modern terrestrial glacial sediments." Sedimentology **33**(5): 699-710.
- Dreimanis, A. and U. J. Vagners (1971). Bimodal Distribution of Rock and Mineral Fragments in Basal Tills. Till A Symposium. R. P. Goldthwait, Ohio State University Press: 237-250.

- Dyke, A. S. (2004). An outline of North American deglaciation with emphasis on central and northern Canada. Quaternary Glaciations: Extent and Chronology 2. J. Ehlers and P. L. Gibbard, Elsevier: 373-424.
- Dyke, A. S., J. T. Andrews, P.U. Clark, J.H. England, G.H. Miller, J. Shaw, and J.J. Veillette. (2002). "The Laurentide and Innuitian ice sheets during the Last Glacial Maximum." Quaternary Science Reviews **21**(1-3): 9-31.
- Dyke, A. S., L. A. Dredge, and J. Vincent. (1982). "Configuration and Dynamics of the Laurentide Ice Sheet during the Late Wisconsin Maximum." Geographie Physique Et Quaternaire **XXXVI**(1-2): 5-14.
- Dyke, A. S., A. Moore, and L. Robertson. (2003). Deglaciation of North America. http://geopub.nrcan.gc.ca/moreinfo_e.php?id=214399, Natural Resources Canada, Ottawa.
- Dyke, A. S. and T. F. Morris (1988). "Canadian Landform Examples 7: Drumlin fields, dispersal trains and ice streams in Arctic Canada." Canadian Geographer-Geographe Canadien **32**(1): 86-90.
- Dyke, A. S., T. F. Morris, D.E.C. Green, and J. England. (1992). Quaternary Geology of Prince of Wales Island, Arctic Canada. Ottawa, Geological Survey of Canada. **Memoir 433**: 1-142.
- Edmunds, F. H. (1962). Recession of Wisconsinan Glacier. Regina, Government of Saskatchewan Department of Mineral Resources. **Report 67**: 1-23.
- Engelhardt, H.F., N. Humphrey, B. Kamb, and M. Fahnestock. 1990. Physical conditions at the base of a fast moving Antarctic ice stream. Science, **248**, 57-59.
- Engelhardt, H. and B. Kamb (1998). "Basal sliding of Ice Stream B, West Antarctica." Journal of Glaciology **44**(147): 223-230.
- Evans, D. J. A. (2006). Glacial landsystems. Glacier Science and Environmental Change. P. G. Knight, Blackwell Publishing: 83-88.
- Evans, D. J. A. (2009). "Special theme: Modern analogues in Quaternary paleoglaciological reconstruction." Quaternary Science Reviews **28**(3-4): 181-182.
- Evans, D. J. A., C. D. Clark, and B.R. Rea. (2008). "Landform and sediment imprints of fast glacier flow in the southwest Laurentide Ice Sheet." Journal of Quaternary Science **23**(3): 249-272.
- Evans, D. J. A. and J. F. Hiemstra (2005). "Till deposition by glacier submarginal, incremental thickening." Earth Surface Processes and Landforms **30**(13): 1633-1662.

- Evans, D. J. A., J. F. Hiemstra, and C. O’Cofaigh. (2007). "An assessment of clast macrofabrics in glacial sediments based on A/B plane data." Geografiska Annaler Series a-Physical Geography **89A**(2): 103-120.
- Evans, D. J. A., D. S. Lemmen, and B.R. Rea. (1999). "Glacial landsystems of the southwest Laurentide Ice Sheet: modern Icelandic analogues." Journal of Quaternary Science **14**(7): 673-691.
- Evans, D. J. A., E. R. Phillips, J.F. Hiemstra and C.A. Auton. (2006). "Subglacial till: Formation, sedimentary characteristics and classification." Earth-Science Reviews **78**(1-2): 115-176.
- Evans, D. J. A., B. R. Rea, J.F. Hiemstra, and C. O’Caofaigh. (2006). "A critical assessment of subglacial mega-floods: a case study of glacial sediments and landforms in south-central Alberta, Canada." Quaternary Science Reviews **25**(13-14): 1638-1667.
- Evans, J., C. O’Cofaigh, J.A. Dowdeswell, and P. Wadhams. (2009). "Marine geophysical evidence for former expansion and flow of the Greenland Ice Sheet across the north-east Greenland continental shelf." Journal of Quaternary Science **24**(3): 279-293.
- Fenton, M. M. (1974). The Quaternary Stratigraphy of a Portion of Southeastern Manitoba, Canada. Department of Earth Sciences, University of Western Ontario. PhD Dissertation: 286.
- Fisher, T. G., N. Waterson, T.V. Lowell and I. Hajdas. (2009). "Deglaciation ages and meltwater routing in the Fort McMurray region, northeastern Alberta and northwestern Saskatchewan, Canada." Quaternary Science Reviews **IN PRESS**: 1-17.
- Fricker, H. A., T. Scambos, R. Bindshadler, and L. Padman. (2007). "An active subglacial water system in West Antarctica mapped from space." Science **315**(5818): 1544-1548.
- Frost, D. B. (1972). Route: Regina-Chaplin-Gardiner Dam in Southern Prairies Field Excursion. 22nd International Geographical Congress. E. H. Dale, A. H. Paul and H. Schlichtmann. University of Saskatchewan Regina Campus, University of Saskatchewan: 1-250.
- Fullerton, D. S., E. A. Christiansen, B.T. Schreiner, R.B. Colton, and L. Clayton. (2007). Quaternary Geologic Map of the Regina 4 x 6 Quadrangle, United States and Canada. Quaternary Geological Atlas of the United States, Miscellaneous Investigations Series, USGS: MAP I-1420 (NM-13).

- Fullerton, D. S., E. A. Christiansen, B.T. Schreiner, R.B. Colton, and L. Clayton. (2007). Quaternary Geologic Map of the Regina 40x60 Quadrangle, United States and Canada. U. S. G. S. U.S. Department of the Interior. Madison, Wisconsin, USGS: 1-37.
- Fullerton, D. S., R. B. Colton, and C.A. Bush. (2004). Limits of mountain and continental glaciations east of the Continental Divide in northern Montana and north-western North Dakota, U.S.A. Quaternary Glaciations: Extent and Chronology 2. J. Ehlers and P. L. Gibbard: 131-150.
- Fulton, R. J. (1995). Surficial Materials of Canada, Geological Survey of Canada.
- Geirsdottir, A., G. H. Miller, and J.T. Andrews. (2007). Glaciation, erosion, and landscape evolution of Iceland, Pergamon-Elsevier Science Ltd.
- Geological Survey of Canada (GSC) (2008). "Geomagnetism- Magnetic Declination Calculator." from <http://geomag.nrcan.gc.ca/apps/mdcal-eng.php>.
- Geological Survey of Canada (GSC) (2008). Geoscience Data Repository. http://gdr.nrcan.gc.ca/index_e.php, Natural Resources Canada, Ottawa.
- Goldthwait, R. P., (Ed). (1971). Till A Symposium, Ohio State University Press.
- Graham, A. G. C., L. Lonergan, and M.S. Stoker. (2007). "Evidence for Late Pleistocene ice stream activity in the Witch Ground Basin, central North Sea, from 3D seismic reflection data." Quaternary Science Reviews **26**(5-6): 627-643.
- Grant, N. M. (1997). Genesis of the North Battleford Fluting Field, West-Central Saskatchewan. Department of Earth and Atmospheric Sciences. Edmonton, University of Alberta. **Masters of Science: 212.**
- Grasby, S., K. Osadetz, R. Betcher, F. Render. (2000). "Reversal of the regional-scale flow system of the Williston basin in response to Pleistocene glaciation." Geology **28**(7): 635-638.
- Gwyn, Q. H. J. and A. Dreimanis (1979). "Heavy mineral assemblages in tills and their use indistinguishing glacial lobes in the Great-Lakes region." Canadian Journal of Earth Sciences **16**(12): 2219-2235.
- Hajnal, Z., J. Lewry, D. White, K. Ashton, R. Clowes, M. Stauffer, I. Gyorfi and E. Takacs . (2005). "The Sask Craton and Hearne Province margin: seismic reflection studies in the western Trans-Hudson Orogen." Canadian Journal of Earth Sciences **42**(4): 403-419.

- Hallberg, G. R. and T. J. Kemmis (1986). "Stratigraphy and correlation of the glacial deposits of the Des Moines and James Lobes and adjacent areas in North Dakota, South Dakota, Minnesota, and Iowa." Quaternary Science Reviews **5**: 65-&.
- Harper, C. T. (2003). Geology, and Mineral and Petroleum Resources of Saskatchewan. Regina, Saskatchewan Industry and Resources. **Miscellaneous Report 2003-7**: 171.
- Hart, J. K. and G. S. Boulton (1991). "The interrelation of glaciotectonic and glaciodepositional processes within the glacial environment." Quaternary Science Reviews **10**(4): 335-350.
- Hart, J. K., K. C. Rose, K. Martinez, and R. Ong. (2009). "Subglacial clast behaviour and its implication for till fabric development: new results derived from wireless subglacial probe experiments." Quaternary Science Reviews **28**(7-8): 597-607.
- Hegner, E., J. C. Roddick, S.M. Fortier, and L. Hulbert. (1995). "Nd, Sr, Ph, Ar, AND O isotopic systematics of Sturgeon Lake Kimberlite, Saskatchewan, Canada - Constraints on emplacement age, alteration and source composition." Contributions to Mineralogy and Petrology **120**(2): 212-222.
- Heim Jr., G. E. and W. B. Howe (1963). Pleistocene Drainage and Depositional History in Northwestern Missouri. Transactions of the Academy of Science, Kansas Academy of Science.
- Hemming, S. R., G. C. Bond, W.S. Broecker, W.D. Sharp, and M. Klas-Mendelson. (2000). "Evidence from Ar-40/Ar-39 ages of individual hornblende grains for varying Laurentide sources of iceberg discharges 22,000 to 10,500 yr BP." Quaternary Research **54**(3): 372-383.
- Hemming, S. R., T. van de Flierdt, S.L. Goldstein, A.M. Franzese, M. Roy, G. Gastineau, and G. Landrot. (2007). "Strontium isotope tracing of terrigenous sediment dispersal in the Antarctic Circumpolar Current: Implications for constraining frontal positions." Geochemistry Geophysics Geosystems **8**: 13.
- Hicock, S. R. and E. A. Fuller (1995). "Lobal interactions, rheologic superposition, and implications for a Pleistocene ice stream on the continental shelf of British Columbia." Geomorphology **14**(2): 167-184.
- Hicock, S. R., J. R. Goff, O.B. Lian, and E.C. Little. (1996). "On the interpretation of subglacial till fabric." Journal of Sedimentary Research **66**(5): 928-934.

- Hildes, D. H. D., G. K. C. Clarke, G.E. Flowers, S.J. Marshall. (2004). "Subglacial erosion and englacial sediment transport modelled for North American ice sheets." Quaternary Science Reviews **23**(3-4): 409-430.
- Hindmarsh, R. C. A. and C. R. Stokes (2008). "Formation mechanisms for ice-stream lateral shear margin moraines." Earth Surface Processes and Landforms **33**(4): 610-626.
- Hubbard, T. D. and J. R. Reid (2006). "Analysis of flute forming conditions using ice sheet reconstructions and field techniques." Geomorphology **74**(1-4): 137-151.
- Iverson, N.R., B. Hanson, R.L. Hooke, and P. Jansson. (1995). "Flow Mechanism of Glaciers on Soft Beds." Science **267**(5194): 80-81.
- Jennings, C. E. (2006). Terrestrial ice streams - a view from the lobe, Elsevier Science Bv.
- Joughin, I. and S. Tulaczyk (2002). "Positive Mass Balance of the Ross Ice Streams, West Antarctica." Science **295**: 476-480.
- Joughin, I., S. Tulaczyk, R. Bindshadler, and S.F. Price. (2002). "Changes in west Antarctic ice stream velocities: Observation and analysis." Journal of Geophysical Research-Solid Earth **107**(B11): 22.
- Kamb, B. 1991. Rheological Nonlinearity and flow instability in the deforming bed mechanism of ice stream motion. Journal of Geophysical Research, **96 (B10)**: 16585-16595.
- Kehew, A. E. and J. T. Teller (1994). "History of late glacial runoff along the southwestern margin of the Laurentide Ice Sheet." Quaternary Science Reviews **13**(9-10): 859-877.
- Klassen, R. W. (1972). "Wisconsin Events and Assiniboine and Qu'Appelle Valleys of Manitoba and Saskatchewan." Canadian Journal of Earth Sciences **9**(5): 544-&.
- Klassen, R. W. (1989). Quaternary Geology of the Southern Canadian Interior Plains. Quaternary Geology of Canada and Greenland. R. J. Fulton, Geological Survey of Canada: 138-173.
- Klassen, R. W. (1992). "Nature, origin and age relationships of landscape complexes in southwestern Saskatchewan." Geographie Physique Et Quaternaire **46**(3): 361-388.
- Klassen, R. W. (1994). "Late Wisconsinan nad Holocene History of southwestern Saskatchewan." Canadian Journal of Earth Sciences **31**(12): 1822-1837.
- Kleman, J. and N. F. Glasser (2007). "The subglacial thermal organisation (STO) of ice sheets." Quaternary Science Reviews **26**(5-6): 585-597.
- Knight, P. G., (Ed). (2006). Glacier Science and Environmental Change, Blackwell Publishing.

- Knight, P. G., C. E. Jennings, R.I. Waller and Z.P. Robinson. (2007). "Changes in ice-margin processes and sediment routing during ice-sheet advance across a marginal moraine." Geografiska Annaler Series a-Physical Geography **89A**(3): 203-215.
- Kupsch, W. O. (1955). "Drumlins with jointed boulders near Dollard, Saskatchewan." Geological Society of America Bulletin **66**(3): 327-&.
- Kupsch, W. O. (1962). "Ice thrust ridges in western Canada." Journal of Geology **70**(5): 582-&.
- Lane, D. M. (1964). Souris River Formation in Southern Saskatchewan. Regina, Government of Saskatchewan Department of Mineral Resources. **Report 92**: 1-72.
- Langford, F. F. (1973). The Geology of the Wapawekka Area Saskatchewan. Regina, Province of Saskatchewan Department of Mineral Resources. **Report 147**: 1-36.
- Larsen, N. K. and J. A. Piotrowski (2003). "Fabric pattern in a basal till succession and its significance for reconstructing subglacial processes." Journal of Sedimentary Research **73**(5): 725-734.
- Larter, R. D., A. G. C. Graham, K. Gohl, G. Kuhn, C.D. Hillenbrand, J.A. Smith, T.J. Deen, R.A. Livermore, and H.W. Schenke. (2009). "Subglacial bedforms reveal complex basal regime in a zone of paleo-ice stream convergence, Amundsen Sea embayment, West Antarctica." Geology **37**(5): 411-414.
- Laymon, C. A. (1992). "Glacial Geology of Western Hudson Strait, Canada, with reference to Laurentide ice sheet dynamics." Geological Society of America Bulletin **104**(9): 1169-1177.
- Lemieux, J. M., E. A. Sudicky, W.R. Peltier and L. Tarasov. (2008). "Dynamics of groundwater recharge and seepage over the Canadian landscape during the Wisconsinian glaciation." Journal of Geophysical Research-Earth Surface **113**(F1): 18.
- Lian, O. B., S. R. Hicock, A. Dreimanis. (2003). Laurentide and Cordilleran fast ice flow: some sedimentological evidence from Wisconsinan subglacial till and its substrate, Taylor & Francis As.
- Licciardi, J. M., P. U. Clark, J.W. Jenson, and D.R. MacAyeal. (1998). "Deglaciation of a soft-bedded Laurentide Ice Sheet." Quaternary Science Reviews **17**(4-5): 427-448.
- Lord, M. L. (1991). "Depositional record of a glacial lake outburst - Glacial Lake Souris, North Dakota." Geological Society of America Bulletin **103**(2): 290-299.
- Lowe, J. J. and M. J. C. Walker (1997). Reconstructing Quaternary Environments. London, Longman.

- Mahaney, W. C. and A. M. Stalker (1988). "Stratigraphy of the North Cliff section, Wellsch Valley site, Saskatchewan." Canadian Journal of Earth Sciences **25**(2): 206-214.
- Manitoba Geological Survey (MGS) (2009). "Geology of Manitoba GIS Map Gallery." from <http://www.gov.mb.ca/stem/mrd/geo/gis/index.html>.
- Majorowicz, J. A., F. W. Jones, and K.G. Osadetz. (1988). "Heat-flow environment of the electrical-conductivity anomalies in the Williston Basin, and occurrence of hydrocarbons." Bulletin of Canadian Petroleum Geology **36**(1): 86-90.
- Marshall, S. J. and G. K. C. Clarke (1997). "A continuum mixture model of ice stream thermomechanics in the Laurentide Ice Sheet .1. Theory." Journal of Geophysical Research-Solid Earth **102**(B9): 20599-20613.
- Marshall, S. J. and G. K. C. Clarke (1997). "A continuum mixture model of ice stream thermomechanics in the Laurentide Ice Sheet .2. Application to the Hudson Strait Ice Stream." Journal of Geophysical Research-Solid Earth **102**(B9): 20615-20637.
- Marshall, S. J., G. K. C. Clarke, A.S. Dyke and D.A. Fisher. (1996). "Geologic and topographic controls on fast flow in the Laurentide and Cordilleran Ice Sheets." Journal of Geophysical Research-Solid Earth **101**(B8): 17827-17839.
- Mathews, W. H. (1974). "Surface Profiles of the Laurentide Ice Sheet in its Marginal Areas." Journal of Glaciology **13**(67): 37-43.
- Maxeiner, R. O. (2002). Geological Highway Map of Saskatchewan. Regina, Saskatchewan Geological Society: Special Publication 15.
- Meneley, W. A. (1964). Geology of the Melfort Area (73-A) Saskatchewan. Department of Geology. Urbana, University of Illinois. **PhD Dissertation**: 148.
- Meneley, W. A. (1967). Geology and Groundwater Resources of the Melfort Area (73-A) Saskatchewan, Saskatchewan Research Council.
- Meneley, W. A., E. A. Christiansen, and W.O. Kupsch. (1957). "Preglacial Missouri River in Saskatchewan." Journal of Geology **65**(4): 441-&.
- Misfeldt, G. A., E. K. Sauer, and E.A. Christiansen. (1991). "The Hepburn Landslide- an interactive slope-stability and seepage analysis." Canadian Geotechnical Journal **28**(4): 556-573.
- Mooers, H. D. (1997). "Numerical reconstruction of a soft-bedded laurentide ice sheet during the last glacial maximum: Comment." Geology **25**(4): 379-380.

- Moran, S. R. and L. Clayton (1984). "Chronology of Late Wisconsinan glaciation in middle North America - Reply." Quaternary Science Reviews **3**(2-3): R1-R6.
- Moran, S. R., L. Clayton, R.L. Hooke, M.M. Fenton and L.D. Andriashek. (1980). "Glacier bed landforms of the Prairie Region of North America." Journal of Glaciology **25**(93): 457-476.
- Munro, M. and J. Shaw (1997). "Erosional origin of hummocky terrain in south-central Alberta, Canada." Geology **25**(11): 1027-1030.
- Munro-Stasiuk, M. J. and D. Sjogren (2006). The erosional origin of hummocky terrain, Alberta, Canada. Glacier Science and Environmental Change. P. G. Knight, Blackwell Publishing: 33-36.
- Murray, T., H. Corr, A. Forieri and A.M. Smith. (2008). "Contrasts in hydrology between regions of basal deformation and sliding beneath Rutford Ice Stream, West Antarctica, mapped using radar and seismic data." Geophysical Research Letters **35**(12): 5.
- Napleralski, J., Y. K. Li, and J. Harbor. (2006). "Comparing predicted and observed spatial boundaries of geologic phenomena: Automated Proximity and Conformity Analysis applied to ice sheet reconstructions." Computers & Geosciences **32**(1): 124-134.
- North Dakota Geological Survey (NDGS) (2009). "North Dakota Geographic Information Systems." from <http://web.apps.state.nd.us/hubexplorer/generalinfo/viewer.html>.
- Nygaard, A., H. P. Sejrup, H. Hafliðason, W.A.H. Lekens, C.D. Clark, and GR. Bigg. (2007). "Extreme sediment and ice discharge from marine-based ice streams: New evidence from the North Sea." Geology **35**(5): 395-398.
- O'Cofaigh, C., J. A. Dowdeswel, J. Evans, and R.D. Larter. (2008). "Geological constraints on Antarctic paleo-ice-stream retreat." Earth Surface Processes and Landforms **33**(4): 513-525.
- O'Cofaigh, C., J. Evans, J.A. Dowdeswell, and R.D. Larter. (2007). "Till characteristics, genesis and transport beneath Antarctic paleo-ice streams." Journal of Geophysical Research-Earth Surface **112**(F3): 16.
- O'Cofaigh, C., C. J. Pudsey, J.A. Dowdeswell, and P. Morris. (2002). "Evolution of subglacial bedforms along a paleo-ice stream, Antarctic Peninsula continental shelf." Geophysical Research Letters **29**(8): 4.
- Oppenheimer, M. (1998). "Global warming and the stability of the West Antarctic Ice Sheet." Nature **393**(6683): 325-332.

- Parizek, R. R. (1964). *Geology of the Willow Bunch Lake Area (72-H) Saskatchewan*. Regina, Saskatchewan Research Council. **Report 4**: 1-48.
- Paterson, W. S. B. (1994). *The Physics of Glaciers*. New York, Elsevier Science, Inc.
- Patterson, C. J. (1997). "Southern Laurentide ice lobes were created by ice streams: Des Moines lobe in Minnesota, USA". *Sedimentary Geology* **111**(1-4): 249-261.
- Patterson, C. J. (1998). "Laurentide glacial landscapes: The role of ice streams." *Geology* **26**(7): 643-646.
- Pilcher, J. R. (1991). Radiocarbon Dating. *Quaternary Dating Methods- A User's Guide*. P. L. Smart and P. D. Frances. Nottingham, M1 Press Ltd. **4**: 16-36.
- Piotrowski, J. A., N. K. Larsen, and F.W. Junge. (2004). "Reflections on soft subglacial beds as a mosaic of deforming and stable spots." *Quaternary Science Reviews* **23**(9-10): 993-1000.
- Prest, V. K., J. A. Donaldson, and H.D. Moores. (2001). "The omar story: The role of omars in assessing glacial history of west-central north America." *Geographie Physique Et Quaternaire* **54**(3): 257-270.
- Ramsden, J. and J. A. Westgate (1971). Evidence for Reorientation of a Till Fabric in the Edmonton Area, Alberta. *Till A Symposium*. S. L. Goldstein, Ohio State University Press: 335-344.
- Raymond, C.F., Echelmeyer, K.A., Whillans, I.M., and Doake, C.S.M. 2001: Ice stream shear margins. *In* Alley, R. B. & Bindschadler, R. A. (Eds.): *The West Antarctic Ice Sheet : behavior and environment*, 137-155. *American Geophysical Union*, Washington, D.C..
- Richards, D. A. and P. L. Smart (1991). Potassium Argon and Argon-Argon Dating. *Quaternary Dating Methods- A User's Guide*. P. L. Smart and P. D. Frances. Nottingham, M1 Press Ltd. **4**: 37-44.
- Rockware Earth Science and GIS Software (2008). StereoStat.
- Ross, M., J. E. Campbell, M. Parent, and R.S. Adams. (2009). "Paleo-ice streams and the subglacial landscape mosaic of the North American mid-continental prairies." *Boreas* **38**: 421-439.
- Ross, M., M. Parent, B. Benjumea and J. Hunter. (2006). "The late Quaternary stratigraphic record northwest of Montreal: regional ice-sheet dynamics, ice-stream activity, and early deglacial events." *Canadian Journal of Earth Sciences* **43**(4): 461-485.
- Roy, M., P. U. Clark, R.A. Duncan and S.R. Hemming. (2007). "Insights into the late Cenozoic configuration of the Laurentide Ice Sheet from Ar-40/Ar-39 dating of glacially transported minerals in midcontinent tills." *Geochemistry Geophysics Geosystems* **8**: 12.

- Roy, M., T. V. van de Flierdt, S.R. Hemming and S.L Goldstein. (2007). "Ar-40/Ar-39 ages of hornblende grains and bulk Sm/Nd isotopes of circum-Antarctic glacio-marine sediments: Implications for sediment provenance in the Southern Ocean." Chemical Geology **244**(3-4): 507-519.
- Saskatchewan Geological Survey (SGS) (2003). Geology and Mineral and Petroleum Resources of Saskatchewan. Regina, Saskatchewan Industry and Resources. **Miscellaneous Report 2003-7: 1-173.**
- Saskatchewan Water Authority (SWA) (2009). "Groundwater Mapping." from <http://www.swa.ca/WaterManagement/Groundwater.asp?type=Mapping>.
- Sauchyn, D. J., (Ed). (1993). Quaternary and Late Tertiary Landscapes of Southwestern Saskatchewan and Adjacent Areas. Regina, Canadian Plains Research Center.
- Sauer, E. K. (1973). Geological Techniques Applied to Engineering Practice in Southern Saskatchewan in An Excursion Guide to Geology of Saskatchewan. F. Simpson. Regina, Saskatchewan Geological Society. **Special Publication Number 1: 126-154.**
- Sauer, E. K. and E. A. Christiansen (1985). "A landslide in till near Warman, Saskatchewan, Canada." Canadian Geotechnical Journal **22**(2): 195-&.
- Sauer, E. K., A. K. Egeland, E.A. Christiansen. (1993). "Compression Characteristics and Index Properties of tills and intertill clays in southern Saskatchewan, Canada." Canadian Geotechnical Journal **30**(2): 257-275.
- Schneider, D. A., M. T. Heizler, M.E. Bickford, G.L. Wortman, K.C. Condie, and S. Perilli. (2007). "Timing constraints of orogeny to cratonization: Thermochronology of the paleoproterozoic trans-hudson orogen, Manitoba and Saskatchewan, Canada." Precambrian Research **153**(1-2): 65-95.
- Segev, A. (2009). "Ar-40/Ar-39 and K-Ar geochronology of Berriasian-Hauterivian and Cenomanian tectonomagmatic events in northern Israel: implications for regional stratigraphy." Cretaceous Research **30**(3): 810-828.
- Shaw, J. (2002). "The meltwater hypothesis for subglacial bedforms." Quaternary International **90**: 5-22.
- Shaw, J. (2006). A glimpse at meltwater effects associated with continental ice sheets. Glacier Science and Environmental Change. P. G. Knight, Blackwell Publishing: 25-32.

- Shaw, J. (2009). "In defence of the meltwater (megaflood) hypothesis for the formation of subglacial bedform fields." Journal of Quaternary Science **IN PRESS**: 12.
- Shaw, J., D. M. Faragini, D.R. Kvill, and R.B. Rains. (2000). "The Athabasca fluting field, Alberta, Canada: implications for the formation of large-scale fluting (erosional lineations)." Quaternary Science Reviews **19**(10): 959-980.
- Shaw, J. and D. Kvill (1984). "A glaciofluvial origin for drumlins of the Livingstone Lake area, Saskatchewan." Canadian Journal of Earth Sciences **21**(12): 1442-1459.
- Shaw, J., D. J. W. Piper, G.B.J. Fader, E.L. King, B.J. Todd, T. Bell, M.J. Batterson, and D.G.E. Liverman. (2006). "A conceptual model of the deglaciation of Atlantic Canada." Quaternary Science Reviews **25**(17-18): 2059-2081.
- Shaw, J., A. Pugin, and R.R. Young. (2008). "A meltwater origin for Antarctic shelf bedforms with special attention to megalineations." Geomorphology **102**(3-4): 364-375.
- Shetsen, I. (1984). "Application of till pebble lithology to the differentiation of glacial lobes in southern Alberta." Canadian Journal of Earth Sciences **21**(8): 920-933.
- Shetsen, I. (1987). Quaternary Geology, Southern Alberta, Alberta Research Council.
- Shetsen, I. (1990). Quaternary Geology, Central Alberta, Alberta Research Council.
- Shilts, W. W. (1980). "Flow patterns in the Central North American Ice Sheet." Nature **286**(5770): 213-218.
- Shilts, W. W., C. M. Cunningham, and C.A. Kasycki. (1979). "Keewatin Ice Sheet - Re-evaluation of the traditional concept of the Laurentide Ice Sheet." Geology **7**(11): 537-541.
- Shumway, J. R. and N. R. Iverson (2009). "Magnetic fabrics of the Douglas Till of the Superior lobe: exploring bed-deformation kinematics." Quaternary Science Reviews **28**(1-2): 107-119.
- Simpson, M. A. (1997). Surficial Geology Map of Saskatchewan, Saskatchewan Energy and Mines, Saskatchewan Research Council.
- Simpson, M. A. (2004). Geology and Ground-Water Resources of the Regina Area (72I), Saskatchewan. Regina, Saskatchewan Research Council. **SRC Publication 10420-1E04**: 1-24.
- Simpson, M. A. and B. T. Schreiner (1999). Geology and Hydrostratigraphy of the Melville Region (62L,K), Saskatchewan. Regina, Saskatchewan Research Council. **SRC Publication 10416-1C99**: 1-39.

- Slimmon, W. L. (2007). Geological Atlas of Saskatchewan. DVD. Regina, Saskatchewan Industry and Resources. **Version 10**.
- Smith, A. M. (2006). "Microearthquakes and subglacial conditions." Geophysical Research Letters **33**(24): 5.
- Smith, A. M. and T. Murray (2009). "Bedform topography and basal conditions beneath a fast-flowing West Antarctic ice stream." Quaternary Science Reviews **28**(7-8): 584-596.
- Smith, A. M., T. Murray, K.W. Nichollas, K. Makinson, G. Aoalgeirsdottir, A.E. Behar and D.G. Vaughan. (2007). "Rapid erosion, drumlin formation, and changing hydrology beneath an Antarctic ice stream." Geology **35**(2): 127-130.
- Stauffer, M. R., D. J. Gendzwill, and E.K. Sauer. (1990). "Ice-thrust features and the Maymont landslide in the North Saskatchewan River Valley." Canadian Journal of Earth Sciences **27**(2): 229-242.
- Stauffer, M. R., A. C. Mukherjee, and J. Koo. (1975). "Amisk Group - Aphebian (Questionable) Island Arc Deposit." Canadian Journal of Earth Sciences **12**(12): 2021-2035.
- Steiger, J. R. and N. Holowaychuk (1971). Particle-Size and Carbonate Analysis of Glacial Till and Lacustrine Deposits in Western Ohio. Till A Symposium. S. L. Goldstein, Ohio State University Press: 275-288.
- Stevenson, R. K., X. W. Meng, and C. Hillarie-Marcel. (2008). "Impact of melting of the Laurentide Ice Sheet on sediments from the upper continental slope off southeastern Canada: evidence from Sm-Nd isotopes." Canadian Journal of Earth Sciences **45**(11): 1243-1252.
- Stokes, C. R. and C. D. Clark (1999). Geomorphological criteria for identifying Pleistocene ice streams, Int Glaciological Soc.
- Stokes, C. R. and C. D. Clark (2002). "Are long subglacial bedforms indicative of fast ice flow?" Boreas **31**(3): 239-249.
- Stokes, C. R. and C. D. Clark (2002). "Ice stream shear margin moraines." Earth Surface Processes and Landforms **27**(5): 547-558.
- Stokes, C. R. and C. D. Clark (2003). The Dubawnt Lake paleo-ice stream: evidence for dynamic ice sheet behaviour on the Canadian Shield and insights regarding the controls on ice-stream location and vigour, Taylor & Francis As.

- Stokes, C. R. and C. D. Clark (2003). "Laurentide ice streaming on the Canadian Shield: A conflict with the soft-bedded ice stream paradigm?" Geology **31**(4): 347-350.
- Stokes, C. R. and C. D. Clark (2006). What can the 'footprint' of a paleo-ice stream tell us? Interpreting the bed of the Dubawnt Lake Ice Stream, Northern Keewatin, Canada. Glacier Science and Environmental Change. P. G. Knight, Blackwell Publishing.
- Stokes, C. R., C. D. Clark, D.A. Darby and D.A. Hodgson. (2005). "Late pleistocene ice export events into the Arctic Ocean from the M'Clure Strait Ice Stream, Canadian Arctic Archipelago." Global and Planetary Change **49**(3-4): 139-162.
- Stokes, C. R., C. D. Clark, O.B. Lian, and S. Tulaczyk. (2007). "Ice stream sticky spots: A review of their identification and influence beneath contemporary and paleo-ice streams." Earth-Science Reviews **81**(3-4): 217-249.
- Stokes, C. R., C. D. Clark, R. Storrar. (2009). "Major changes in ice stream dynamics during deglaciation of the north-western margin of the Laurentide Ice Sheet." Quaternary Science Reviews **28**(7-8): 721-738.
- St'Onge, D. A. (1980). "The Wisconsinan Deglaciation of Southern Saskatchewan and Adjacent Areas - Discussion." Canadian Journal of Earth Sciences **17**(2): 287-288.
- Stroeven, A. P. and D. A. Swift (2008). "Glacial landscape evolution - Implications for glacial processes, patterns and reconstructions." Geomorphology **97**(1-2): 1-4.
- Tarasov, L. and W. R. Peltier (2004). "A geophysically constrained large ensemble analysis of the deglacial history of the North American ice-sheet complex." Quaternary Science Reviews **23**(3-4): 359-388.
- Tarasov, L. and W. R. Peltier (2006). "A calibrated deglacial drainage chronology for the North American continent: evidence of an Arctic trigger for the Younger Dryas." Quaternary Science Reviews **25**(7-8): 659-688.
- Teller, J. T., S. R. Moran, and L. Clayton. (1980). "The Wisconsinan Deglaciation of Southern Saskatchewan and Adjacent Areas - Discussion." Canadian Journal of Earth Sciences **17**(4): 539-541.
- Thomas, G. S. P. and R. C. Chiverrell (2007). "Structural and depositional evidence for repeated ice-marginal oscillation along the eastern margin of the Late Devensian Irish Sea Ice Stream." Quaternary Science Reviews **26**(19-21): 2375-2405.

- Thorleifson, H. and R. G. Garrett (1993). Prairie Kimberlite Study - Till matrix geochemistry and preliminary indicator mineral data. http://geopub.nrcan.gc.ca/moreinfo_3.php?id=192437, Geological Survey of Canada, Ottawa. **Open File Report 2745**.
- Todd, B. J., P. C. Valentine, O. Longva, and J. Shaw. (2007). "Glacial landforms on German Bank, Scotian Shelf: evidence for Late Wisconsinan ice-sheet dynamics and implications for the formation of De Geer moraines." *Boreas* **36**(2): 148-169.
- Tulaczyk, S. (2006). Fast glacier flow and ice streaming. *Glacier Science and Environmental Change*. P. G. Knight, Blackwell Publishing: 353-359.
- Tulaczyk, S. M., R. P. Scherer, and C.D. Clark. (2001). A ploughing model for the origin of weak tills beneath ice streams: a qualitative treatment, Pergamon-Elsevier Science Ltd.
- United States Geological Survey (2008). Shuttle Radar Topography Mission; Mapping the World in 3 Dimensions. <http://srtm.usgs.gov>, United States Geological Survey.
- University of Waterloo (2007a). Hydrometer Analysis; Sieve Analysis. Department of Earth and Environmental Science: 1-11.
- University of Waterloo (2007b). Pebble Lithology. Department of Earth and Environmental Science: 1-2.
- Van Schmus, W. R., D. A. Schneider, D.K. Holm, S. Dodson, and B.K. Nelson. (2007). "New insights into the southern margin of the Archean-Proterozoic boundary in the north-central United States based on U-Pb, Sm-Nd, and Ar-Ar geochronology." *Precambrian Research* **157**(1-4): 80-105.
- Wellner, J. S., A. L. Lowe, S.S. Ship and J.B. Anderson. (2001). "Distribution of glacial geomorphic features on the Antarctic continental shelf and correlation with substrate: implications for ice behavior." *Journal of Glaciology* **47**(158): 397-411.
- Whitaker, S. H. and E.A. Christiansen (1972). "Empress Group in Southern Saskatchewan." *Canadian Journal of Earth Sciences* **9**(4): 353-&.
- Winberry, J. P., S. Anandakrishnan, R.B. Alley, R.A. Bindschadler and M.A. King. (2009). "Basal mechanics of ice streams: Insights from the stick-slip motion of Whillans Ice Stream, West Antarctica." *Journal of Geophysical Research-Earth Surface* **114**: 11.

Appendices

Appendix A Site Data

The following is field site images and fabric data from applicable field sites. Analysis of fabric data can be found in Appendix B.

Site # 1 RD 642 01



Figure A. 1: RD 642 01, linear feature, west of Regina SK. Boulder pavement divides younger Battleford till from older Floral Formation.



Figure A. 2: One of eleven boulders, creating a pavement, with striations in the 114° direction.

Table A. 1: Fabric data for field site #1.

A-axis		AB plane	
Trend	Plunge	Strike	Dip
141	7	134	46
114	9	42	9
23	11	319	12
108	4	316	9
42	2	299	2
88	2	271	31
26	13	208	80
70	21	23	28
72	47	11	51
76	23	344	23

Site # 2 Battleford 01



Figure A. 3: Linear feature along the Maskwa Corridor.

Site # 3 Birch Lake 01



Figure A. 4: Subdued feature along the Maskwa Corridor.

Table A. 2: Fabric data for field site #3.

Trend	Plunge	Strike	Dip
239	14	218	34
23	44	279	45
249	52	217	28
71	14	259	60
127	16	326	41
260	17	208	21
242	16	108	22
30	14	14	42
50	35	43	81
273	35	269	84
133	32	87	41

42	26	299	27
47	12	231	70
113	41	326	58
95	34	311	49
209	2	32	35
40	41	263	52
67	23	52	58
278	27	276	85
149	34	127	61
346	26	318	46
66	21	47	50
310	26	276	41
272	30	269	85
40	21	248	39
112	36	338	45
10	7	352	22
61	26	294	31
272	19	177	19
17	15	254	18

Site # 4 Cutknife 01



Figure A. 5: Linear feature along the Maskwa Corridor, few kilometers long.

Table A. 3: Fabric data for field site #4.

Trend	Plunge	Strike	Dip
274	1	273	46
311	4	136	41
232	9	203	18
134	11	101	20
207	11	53	24
316	15	276	23
188	2	186	49
333	6	166	25
108	14	345	17
266	9	108	23
131	16	53	16

107	34	39	36
198	23	56	35
53	31	30	57
162	24	5	49
65	46	24	58
252	9	135	10
324	6	316	37
344	31	251	31
221	5	67	11
73	35	17	40
232	26	219	65
218	16	146	17
233	27	118	29
121	3	107	12
238	14	211	29
228	29	90	40
272	31	124	49
26	18	313	19
282	17	242	26

Site # 5 Dana 01



Figure A. 6: Large exposure within Assemblage 2.

Site # 6 Glaslyn 01



Figure A. 7: Subdued linear feature transverse to flow along the Maskwa Corridor.

Table A. 4: Fabric data for field site #6.

Trend	Plunge	Strike	Dip
98	41	65	58
9	6	335	11
182	14	131	18
202	19	45	41
321	13	302	35
234	9	63	44
118	23	47	24
102	17	53	22
351	6	194	15
325	34	162	67
216	11	193	26
257	27	154	28
57	44	35	69
262	52	139	57
359	2	181	49
333	14	157	75
244	32	82	64
292	18	115	82
230	36	209	64
216	11	89	14
72	18	274	41
147	43	114	59
351	44	325	66
39	8	255	14
131	44	348	58
173	7	128	10
106	34	79	56
183	14	18	44
194	23	138	27
258	24	84	77

Site # 7 Hepburn 01



Figure A. 8: Long attenuated landforms along the Buffalo Corridor.

Table A. 5: Fabric data for field site #7.

Trend	Plunge	Strike	Dip
293	14	178	15
130	4	319	24
293	6	142	12
201	17	108	17
4	14	192	60
195	7	186	39
264	51	159	52
15	59	15	90
40	36	237	68
269	7	105	23
304	37	190	40

209	29	134	30
267	51	113	71
261	14	160	14
304	39	166	50
25	31	260	36
353	39	270	39
248	14	98	27
222	31	164	35
308	8	161	15
81	11	56	24
244	15	91	31
310	32	280	52
47	22	3	30
135	44	122	77
342	34	194	52
172	27	149	52
259	17	203	20
223	21	205	52
206	21	157	27

Site # 8 Hwy 02 01



Figure A. 9: Subdued landform, part of extensive field in Assemblage 2, trending southwest.

Site # 9 Hwy 13 01



Figure A. 10: Exposure along road, in southeastern limb of Buffalo Corridor.

Table A. 6: Fabric data for field site #9.

Trend	Plunge	Strike	Dip
217	40	134	40
191	43	77	46
182	44	117	47
207	8	119	8
146	23	17	29
14	23	195	88
195	26	96	26
75	35	343	35
170	41	65	42
42	34	242	64
34	11	232	32
88	28	38	35
223	21	184	31
168	16	9	38
48	26	234	79
222	24	195	45
176	19	10	55
179	36	104	37
351	22	335	55
163	44	128	60
60	24	302	27
18	14	243	19
304	14	169	19
193	36	127	38

Site # 10 Hwy 14 to Biggar



Figure A. 11: Railway cut through lineation in Maskwa Corridor.

Table A. 7: Fabric data for field site #10.

Trend	Plunge	Strike	Dip
339	46	282	51
45	16	262	25
49	49	303	50
17	41	342	56
354	49	348	85
0	32	286	33
318	7	293	16
328	19	177	35
322	16	251	17
24	36	0	61
181	11	51	14

90	10	293	24
79	15	69	58
354	40	318	55
90	19	348	19
295	4	118	52
347	14	318	27
333	32	255	33
332	10	265	11
297	11	163	15
121	24	79	34
19	40	4	73
33	27	359	42
143	9	336	34
319	12	216	12
293	13	160	18
134	17	335	41
330	27	312	59
112	26	98	63
134	17	330	49

Site # 11 Hwy 15 02



Figure A. 12: Subdued landform west of Assemblage 9 in the Buffalo Corridor.

Table A. 8: Fabric data for field site #11.

Trend	Plunge	Strike	Dip
52	15	41	54
215	31	38	85
212	10	79	14
7	31	337	50
3	22	354	68
333	22	193	32
338	39	304	56
44	25	5	36
105	2	93	9
125	51	67	55
251	18	242	65
25	22	355	39
9	55	266	56
50	38	3	47

91	44	50	56
350	20	329	46
174	70	64	71
156	27	122	43
153	36	103	43
208	20	83	24
100	21	62	32
192	10	163	20
36	18	252	29
151	17	343	55
152	1	149	16
332	24	316	59
340	29	282	33
11	19	343	37
205	17	188	46
326	19	309	49
183	26	45	36
85	36	10	37
209	9	35	56
50	42	358	49
13	42	257	45
289	30	250	43
22	23	358	46
353	60	251	61
179	1	174	11
355	19	181	72
352	11	200	23
290	8	282	46
312	35	272	48
8	30	346	57
110	3	292	53
31	42	252	54
210	24	170	35
39	28	234	64
85	44	46	57
10	45	265	46

Site # 12 Hwy 21 01



Figure A. 13: Lineation located on the edge of Assemblage 7 boundary with Battleford Corridor.

Table A. 9: Fabric data for field site #12.

Trend	Plunge	Strike	Dip
341	22	243	22
302	13	155	23
252	32	201	39
208	27	192	62
303	19	269	32
351	46	275	47
100	14	90	55
161	24	45	26
314	39	179	49
114	35	114	90
57	55	328	55

48	29	21	50
216	10	56	27
330	56	208	60
53	38	14	51
243	31	198	40
29	53	291	53
253	6	100	13
38	30	237	61
42	24	349	29
343	41	248	41
84	33	311	42
20	30	277	31
272	45	137	55
0	27	259	27
18	16	241	23
190	17	162	33
12	27	254	30
345	29	307	42
68	22	281	37

Site # 13 Hwy 52 01



Figure A. 14: Subdued landforms along Assemblage 9.

Site # 14 Maymont 01



Figure A. 15: Elongated features along the Battleford Corridor.

Site # 15 Moose 01A



Figure A. 16: Hummocky terrain on Moose Mountain.

Site # 16 Moose 02



Figure A. 17: Large exposure of hummocky terrain, Moose Mountain.

Site # 17 Moosomin 01



Figure A. 18: Dugout outside of Moosomin, SK, south eastern limb of Buffalo Corridor. Some exposed boulders were found and striations measured.

Table A. 10: Fabric data for field site #17.

Trend	Plunge	Strike	Dip
344	13	189	29
105	19	342	22
180	15	165	46
78	37	20	42
27	40	293	40
127	11	325	33
184	35	80	36
332	9	168	29

349	16	207	25
21	9	214	35
5	17	210	36
229	22	149	22
269	26	133	35
180	14	154	30
119	23	351	28
47	32	334	33
289	34	272	66
348	56	213	64
219	49	48	82
120	2	119	53
52	41	17	57
53	24	252	54
170	23	54	25
59	28	41	60
96	3	94	62
57	29	272	44
245	52	322	55
102	50	302	74
65	47	347	48
341	50	188	69
277	27	97	89
39	47	346	53
327	44	237	44
322	45	204	48
330	31	263	33
50	20	260	36
285	11	279	61

Site # 18 North B 01



Figure A. 19: Dugout outside of North Battleford, SK.

Table A. 11: Fabric data for field site #18.

Trend	Plunge	Strike	Dip
341	59	233	60
203	29	56	45
59	19	353	21
197	31	190	79
182	39	161	67
31	15	21	58
34	25	252	37
252	27	183	29
149	54	36	56
213	6	49	21
347	7	340	45

323	36	180	51
171	46	152	72
258	33	205	39
281	72	141	78
203	27	50	48
134	57	116	79
268	27	157	29
100	74	340	76
239	22	67	70
58	1	57	60
180	21	2	86
261	45	228	61
273	54	192	54
194	9	55	14
81	1	262	61
152	49	90	53
260	6	119	9
277	17	182	17
160	44	97	47

Site # 19 Qu'Appelle 01



Figure A. 20: Large exposure at top of Qu'Appelle Valley, southwest of Melville.

Site # 20 RD 304 01



Figure A. 21: Northern most field site, along Maskwa Corridor in Assemblage 7.

Table A. 12: Fabric data for field site #20.

Trend	Plunge	Strike	Dip
32	21	346	28
299	4	296	49
228	65	108	68
143	13	124	36
91	21	319	27
46	19	286	22
320	7	296	17
147	5	140	35
11	6	2	35
177	36	9	74
122	1	305	20
124	35	321	68
54	20	311	21
197	4	24	31
318	22	179	32
318	0	318	27
57	21	353	23
196	13	182	44
254	18	224	33
56	7	13	10
287	18	268	45
174	38	75	38
21	17	8	54
67	5	49	16
165	32	10	56
121	34	16	35
65	13	328	13
248	59	214	71
197	5	133	6
108	9	309	24

Site # 21 RD 602 01



Figure A. 22: Subdued landforms along southwestern limb of Buffalo Corridor.

Table A. 13: Fabric data for field site #21.

Trend	Plunge	Strike	Dip
298	52	243	55
357	2	338	6
97	67	31	69
177	30	48	37
104	27	75	46
358	52	357	89
45	43	33	77
329	68	260	69
242	50	233	82
336	42	307	61
28	30	19	74

277	38	258	67
8	41	305	44
314	62	188	67
58	6	275	10
164	12	15	23
49	45	317	45
232	13	56	72
347	28	269	29
82	9	288	20
72	3	37	5
76	44	311	50
341	42	259	42
297	43	220	44
307	15	133	70
148	21	38	22
349	28	225	33
312	42	203	44
75	13	293	20
262	18	241	42
270	58	178	58
279	90	2	90
15	26	330	35

Site # 22 RD 687 01



Figure A. 23: Large exposure along Maskwa Corridor.

Site # 23 RD 734 01



Figure A. 24: Subdued ridges north of Regina.

Table A. 14: Fabric data for field site #23.

Trend	Plunge	Strike	Dip
158	81	50	81
327	43	278	51
165	57	90	58
68	26	22	34
79	35	50	55
331	62	236	62
285	14	220	15
254	78	151	78
351	11	181	49
323	36	297	59
65	45	13	52
227	16	58	57
288	17	139	30
188	19	45	30
320	63	191	69
109	25	296	75
293	3	249	4
289	14	159	18
321	7	297	17
106	60	3	61
283	59	197	59
135	60	65	61
150	13	130	33
327	5	270	6
354	19	331	41
21	20	352	37
311	2	134	33
135	20	333	50
200	43	119	43
220	25	76	38

Site # 24 RD 787 02



Figure A. 25: Elongated ridge along Maskwa Corridor.

Table A. 15: Fabric data for field site # 24.

Trend	Plunge	Strike	Dip
30	6	224	24
291	75	191	75
328	27	236	27
145	31	119	54
172	1	20	2
302	26	240	29
164	34	99	37
203	40	58	55
203	9	184	25
109	1	292	20
308	29	150	56

311	4	159	9
73	2	259	19
345	27	255	27
324	39	264	43
332	64	222	65
249	48	157	48
273	4	132	6
335	8	306	16
304	14	243	16
316	27	244	28
21	14	329	18
202	23	148	28
153	45	3	63
165	4	354	25
319	9	294	21
274	44	245	63
241	28	181	32
12	39	286	39
335	43	320	74

Site # 25 RD 26 Good Sect



Figure A. 26: Large exposure along the Maskwa Corridor.

Site # 26 RD 26 Cln Rd Cut



Figure A. 27: Subdued elongated feature along Maskwa Corridor.

Table A. 16: Fabric data for field site #26.

Trend	Plunge	Strike	Dip
324	10	177	18
113	8	331	13
114	3	90	7
298	20	139	45
190	57	96	57
336	16	303	28
353	9	265	9
291	17	156	23
185	2	179	19
162	4	160	68
261	3	230	6
349	11	176	57
102	22	320	33
320	5	159	15
49	30	274	39
260	23	187	24
216	15	203	50
352	18	223	23
328	13	282	18
37	20	242	41
11	43	260	45
211	30	98	32
172	7	58	8
305	4	138	17
69	3	62	22
264	13	225	20
237	25	148	25
2	3	190	21
350	2	198	4
292	12	247	17

Site # 27 St Benedict 01



Figure A. 28: Exposure west of Basin Lake Ridge in Assemblage 2.

Table A. 17: Fabric data for field site #27.

Trend	Plunge	Strike	Dip
75	28	356	28
24	35	238	51
78	3	259	73
206	35	152	41
59	22	249	68
314	40	242	41
64	11	254	48
81	28	356	28
325	70	253	71
35	57	273	61
358	20	214	32
52	31	322	31

75	5	32	7
72	46	355	47
115	28	319	53
79	41	2	42
107	9	323	15
171	12	6	40
102	22	56	30
68	44	268	70
24	75	307	75
305	7	144	21
89	58	345	59
118	42	353	48
128	26	326	58
85	65	306	73
89	54	279	83
129	36	1	43
71	41	304	47
70	34	288	48
140	39	353	56
294	69	190	70
211	60	123	60
126	66	87	74
131	42	81	50
101	40	330	48
265	49	256	83
135	30	353	43
61	15	252	53
104	22	302	52
275	17	145	22
260	21	258	85
120	23	308	71
117	26	304	77
141	15	347	32
114	29	313	60
19	58	310	60
99	64	93	87
72	19	28	26
178	41	36	54

Site # 28 Sweetgrass 01



Figure A. 29: Exposure along Maskwa Corridor.

Site # 29 West of 6



Figure A. 30: Shale bedrock fragments (yellow arrows) found in till, southwestern Buffalo Corridor.

Table A. 18: Fabric data for field site #29.

Trend	Plunge
270	25
282	12
244	8
298	24
151	24

Site # 30 Yorkton 01

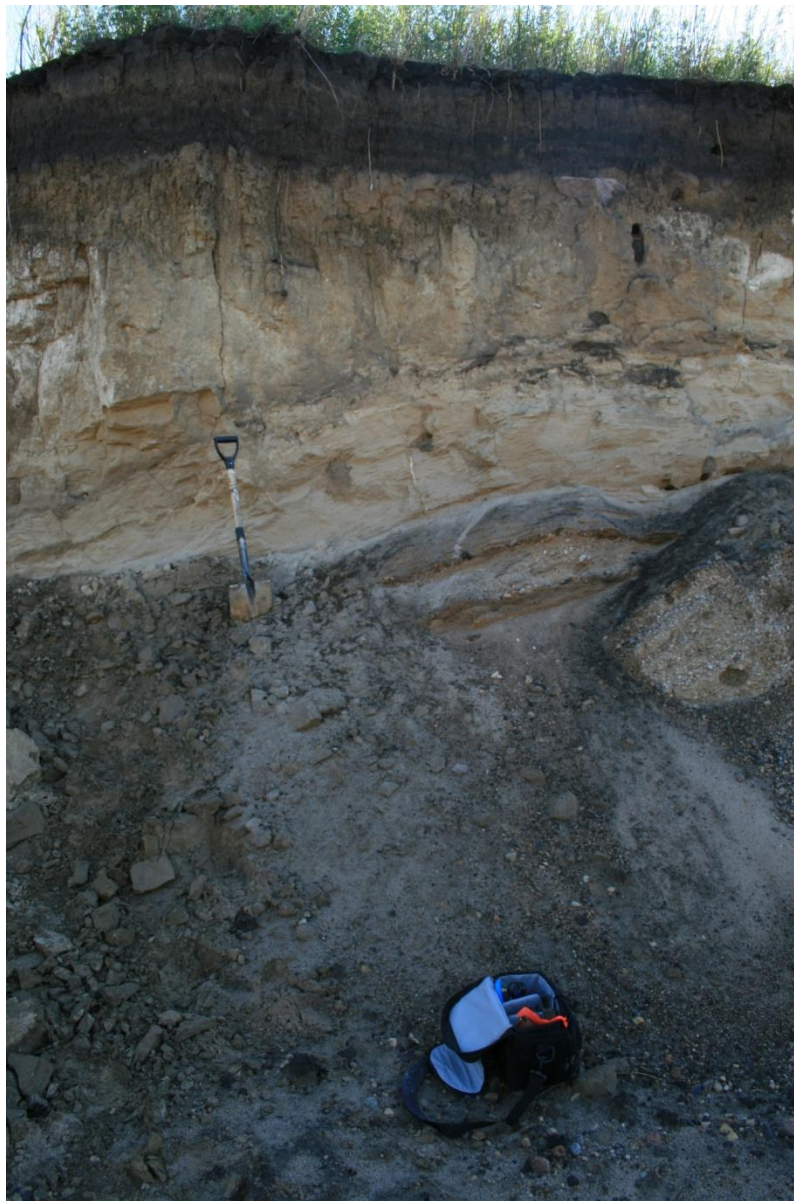


Figure A. 31: Drumlinoid feature in Buffalo Corridor with large sand deposits.

Site # 31 Griffin B and F



Figure A. 32: Two exposed tills along Buffalo Corridor.

Table A. 19: Fabric data for field site #31, Battleford till.

Trend	Plunge
234	5
61	45
78	55
173	25
191	10
206	42
241	60
78	15
98	50
54	38
181	17
221	30
46	37
196	40
184	75
145	60
213	55
158	25

Table A. 20: Fabric data for field site # 31, Floral Formation till.

Trend	Plunge
66	25
216	44
73	32
58	45
53	32
21	14
16	8
121	32
98	75
73	30
166	15
183	24

Appendix B Laboratory Data

The following is the laboratory data from field sampling, including geochemistry and $^{40}\text{Ar}/^{39}\text{Ar}$ dating.

Table B. 1: Grain size curve values for all sampled sites. Values were determined from seive and hydrometer analysis.

Site	Lat	Long	Q1	MEDIAN	Q3	Sorting Coefficient	Skewness	62u	2u	Amt Sand	Amt Silt	Amt Clay
Rd 687 01	52.69628	-108.866	0.02	0.09	0.5	5	1.234568	0.35	0.14	0.65	0.21	0.14
Cutknife 01	52.60952	-109.058	0.0025	0.07	0.15	7.745967	0.076531	0.47	0.23	0.53	0.24	0.23
rd 304 01	54.03195	-108.658	0.0017	0.0175	0.33	13.93261	1.831837	0.48	0.26	0.52	0.22	0.26
Moose 02	49.74369	-102.281	0.0017	0.08	0.33	13.93261	0.087656	0.48	0.26	0.52	0.22	0.26
Rd26Cln rd CUT	53.73349	-109.133	0.0015	0.06	0.45	17.32051	0.1875	0.5	0.27	0.5	0.23	0.27
St Benedict 01	52.56521	-105.386	0.005	0.06	0.25	7.071068	0.347222	0.5	0.19	0.5	0.31	0.19
Glaslyn 01	53.43168	-108.537	0.0016	0.055	0.34	14.57738	0.179835	0.52	0.27	0.48	0.25	0.27
Rd 787 02	52.60954	-108.724	0.00175	0.053	0.27	12.42118	0.168209	0.52	0.26	0.48	0.26	0.26
Hwy 02 01	52.5509	-105.725	0.0045	0.053	0.8	13.33333	1.281595	0.52	0.2	0.48	0.32	0.2
Hwy 21 01	53.45351	-109.357	0.0015	0.05	0.375	15.81139	0.225	0.54	0.27	0.46	0.27	0.27
Hwy 15 02	51.41646	-104.779	0.0053	0.042	0.5	9.712859	1.502268	0.54	0.19	0.46	0.35	0.19
Moosomin 01	50.1538	-101.673	0.0028	0.04	0.4	11.95229	0.7	0.57	0.23	0.43	0.34	0.23
Birch Lake 01	53.42852	-108.046	0.0013	0.04	0.4	17.54116	0.325	0.57	0.27	0.43	0.3	0.27
Rd 734 01	50.57171	-104.528	0.002	0.023	0.37	13.60147	1.398866	0.58	0.25	0.42	0.33	0.25
Hwy 52 01	51.21027	-103.259	0.0017	0.032	0.38	14.9509	0.630859	0.58	0.26	0.42	0.32	0.26
Hepburn 01	52.57002	-106.675	0.0019	0.043	0.27	11.92079	0.277447	0.58	0.26	0.42	0.32	0.26
Maymont 01	52.58053	-107.755	0.0009	0.022	0.3	18.25742	0.557851	0.58	0.31	0.42	0.27	0.31
Dana 01	52.28966	-105.737	0.0019	0.02	0.25	11.47079	1.1875	0.6	0.26	0.4	0.34	0.26
North B 01	52.7837	-108.242	0.00125	0.023	0.35	16.7332	0.827032	0.6	0.29	0.4	0.31	0.29
Sweetgrass 01	52.76709	-108.811	0.001	0.025	0.25	15.81139	0.4	0.61	0.31	0.39	0.3	0.31
Griffin F	49.59666	-103.431	0.00175	0.022	0.35	14.14214	1.265496	0.62	0.28	0.38	0.34	0.28
Griffin B	49.59666	-103.431	0.0013	0.02	0.16	11.094	0.52	0.62	0.29	0.38	0.33	0.29
Moose 01 A	49.75452	-102.284	0.0007	0.007	0.15	14.6385	2.142857	0.65	0.35	0.35	0.3	0.35
Hwy 13 01	49.60349	-101.911	0.0175	0.019	0.15	2.9277	7.271468	0.65	0.26	0.35	0.39	0.26

642 Rd 01 above	50.59596	-105.199	0.00095	0.028	0.18	13.76494	0.218112	0.65	0.32	0.35	0.33	0.32
West Of 6 01	49.90649	-104.721	0.00125	0.0175	0.325	16.12452	1.326531	0.66	0.29	0.34	0.37	0.29
Hwy 14 To Bigr	52.10304	-108.076	0.0012	0.0185	0.07	7.637626	0.245435	0.68	0.31	0.32	0.37	0.31
Rd26 GOOD SECT	53.40942	-108.991	0.0018	0.0125	0.07	6.236096	0.8064	0.71	0.26	0.29	0.45	0.26
Battleford 01	52.58025	-108.352	0.0006	0.0065	0.5	28.86751	7.100592	0.71	0.37	0.29	0.34	0.37
Rd 602 01	49.29416	-102.769	0.00075	0.013	0.067	9.451631	0.297337	0.72	0.36	0.28	0.36	0.36
642 Rd 01 below	50.59596	-105.199	0.000475	0.01	0.035	8.583951	0.16625	0.93	0.38	0.07	0.55	0.38
Moose 01 B	49.75452	-102.284	0.00027	0.0025	0.01	6.085806	0.432	0.95	0.47	0.05	0.48	0.47

Table B. 2: Summary of Fabric Data for all field sites where fabric measurements were taken.

	Site #	Site	Location		Field Measurements			Fabric Calculations									
					Pebble Count	Mean Dip Direction	Mean Dip Angle	axis or plane	S1	S2	S3	V1 (plunge-trend)	V1 Trend	V1 Plunge	V1 Trend2 (-180)	Isotropy S3/S1	Elongation 1-(S2/S1)
			Lat	Long													
FABRIC	6	Glaslyn 01	53.43168	-108.53693	30	202	23	A	0.47	0.35	0.18	10-197	197	10	17	0.38	0.26
	6	Glaslyn 01	53.43168	-108.53693	30	150	44	AB	0.56	0.24	0.21	69-007	7	69	187	0.38	0.57
	20	rd 304 01	54.03195	-108.65835	30	155	19	A	0.44	0.42	0.14	12-137	137	12	317	0.32	0.05
	20	rd 304 01	54.03195	-108.65835	30	186	35	AB	0.68	0.19	0.13	75-248	248	75	68	0.19	0.72
	26	Rd26Cln rd CUT	53.73349	-109.13298	30	218	15	A	0.54	0.37	0.09	07-328	328	7	148	0.17	0.31
	26	Rd26Cln rd CUT	53.73349	-109.13298	30	197	27	AB	0.79	0.13	0.08	78-105	105	78	285	0.10	0.84
	10	Hwy 14 To Bigr	52.10304	-108.07569	30	194	23	A	0.6	0.34	0.06	17-349	349	17	169	0.10	0.43
	10	Hwy 14 To Bigr	52.10304	-108.07569	30	232	39	AB	0.66	0.21	0.13	67-232	232	67	52	0.20	0.68
	1	642 Rd 01 above	50.59596	-105.19902	10	76	14	A	0.66	0.3	0.04	17-075	75	17	255	0.06	0.55
	1	642 Rd 01 above	50.59596	-105.19902	10	197	29	AB	0.74	0.18	0.08	78-265	265	78	85	0.11	0.76
	31	Griffin B	49.59666	-103.43098	18	153	38	A	0.53	0.38	0.09	47-187	187	47	7	0.17	0.28
	31	Griffin F	49.59666	-103.43098	12	95	31	A	0.57	0.36	0.07	31-054	54	31	234	0.12	0.37
	29	West Of 6 01	49.90649	-104.72139	5	249	19	A	0.74	0.22	0.04	15-280	280	15	100	0.05	0.70
	23	Rd 734 01	50.57171	-104.52784	30	223	33	A	0.44	0.33	0.24	09-315	315	9	135	0.55	0.25
	23	Rd 734 01	50.57171	-104.52784	30	168	45	AB	0.51	0.26	0.23	75-323	323	75	143	0.45	0.49
	21	Rd 602 01	49.29416	-102.76859	33	203	35	A	0.48	0.32	0.19	49-346	346	49	166	0.40	0.33
	21	Rd 602 01	49.29416	-102.76859	33	193	48	AB	0.51	0.33	0.16	65-181	181	65	1	0.31	0.35
	9	Hwy 13 01	49.60349	-101.91140	24	153	27	A	0.61	0.28	0.11	16-195	195	16	15	0.18	0.54
	9	Hwy 13 01	49.60349	-101.91140	24	155	41	AB	0.58	0.24	0.17	77-002	2	77	182	0.29	0.59
	17	Moosomin 01	50.15380	-101.67263	37	174	28	A	0.43	0.37	0.2	30-018	18	30	198	0.47	0.14
17	Moosomin 01	50.15380	-101.67263	37	204	46	AB	0.52	0.25	0.23	73-169	169	73	349	0.44	0.52	

11	Hwy 15 02	51.41646	-104.77922	50	159	27	A	0.55	0.27	0.18	20-010	10	20	190	0.33	0.51
11	Hwy 15 02	51.41646	-104.77922	50	196	45	AB	0.54	0.29	0.18	70-241	241	70	61	0.33	0.46
27	St Benedict 01	52.56521	-105.38622	50	131	35	A	0.61	0.21	0.19	39-094	94	39	274	0.31	0.66
27	St Benedict 01	52.56521	-105.38622	50	233	52	AB	0.56	0.28	0.16	48-217	217	48	37	0.29	0.50
24	Rd 787 02	52.60954	-108.72448	30	228	26	A	0.54	0.31	0.15	19-326	326	19	146	0.28	0.43
24	Rd 787 02	52.60954	-108.72448	30	207	35	AB	0.68	0.18	0.14	76-141	141	76	321	0.21	0.74
18	North B 01	52.78370	-108.24214	30	196	32	A	0.52	0.26	0.23	33-220	220	33	40	0.44	0.50
18	North B 01	52.78370	-108.24214	30	152	51	AB	0.44	0.35	0.2	69-046	46	69	226	0.45	0.20
4	Cutknife 01	52.60952	-109.05846	30	205	17	A	0.5	0.38	0.12	04-256	256	4	76	0.24	0.24
4	Cutknife 01	52.60952	-109.05846	30	147	32	AB	0.71	0.18	0.11	83-351	351	83	171	0.15	0.75
3	Birch Lake 01	53.42852	-108.04555	30	41	25	A	0.56	0.27	0.17	13-063	63	13	243	0.30	0.52
3	Birch Lake 01	53.42852	-108.04555	30	217	46	AB	0.57	0.29	0.14	61-197	197	61	17	0.25	0.49
12	Hwy 21 01	53.45351	-109.35652	30	170	30	A	0.52	0.32	0.16	30-022	22	30	202	0.31	0.38
12	Hwy 21 01	53.45351	-109.35652	30	201	42	AB	0.61	0.21	0.18	70-166	166	70	346	0.30	0.66
7	Hepburn 01	52.57002	-106.67542	30	207	25	A	0.48	0.37	0.16	21-256	256	21	76	0.33	0.23
7	Hepburn 01	52.57002	-106.67542	30	161	39	AB	0.68	0.17	0.15	66-079	79	66	259	0.22	0.75

Table B. 3: Field sites where only samples were taken.

	Site #	Site	Location	
			Lat	Long
SAMPLE ONLY	15	Moose 01 A	49.75452	-102.28353
	25	Rd26 GOOD SECT	53.40942	-108.99109
	1	642 Rd 01 below	50.59596	-105.19902
	15	Moose 01 B	49.75452	-102.28353
	16	Moose 02	49.74369	-102.28125
	13	Hwy 52 01	51.21027	-103.25893
	8	Hwy 02 01	52.55090	-105.72492
	2	Battleford 01	52.58025	-108.35225
	28	Sweetgrass 01	52.76709	-108.81116
	14	Maymont 01	52.58053	-107.75542

Table B. 4: Field sites where bedding plane measurements or boulder striations were taken. Yorkton and Qu'Appelle field sites do not have samples.

	Site #	Site	Location		Field Measurements			
			Lat	Long	Pebble Count	Mean Dip Direction	Mean Dip Angle	
BOULDERS AND BEDDING	5	Dana 01	52.28966	-105.73654	2	150		striations
	5	Dana 01	52.28966	-105.73654	2	197		striations
	22	Rd 687 01	52.69628	-108.86569	1	135		striations
	17	Moosomin 01	50.15380	-101.67263	6	151		striations
	17	Moosomin 01	50.15380	-101.67263	6	148		striations
	17	Moosomin 01	50.15380	-101.67263	6	154.5		striations
	17	Moosomin 01	50.15380	-101.67263	6	118		striations
	17	Moosomin 01	50.15380	-101.67263	6	183		striations
	17	Moosomin 01	50.15380	-101.67263	6	113		striations
	1	642 Rd 2007	50.59596	-105.19902	4	106		striations
	1	642 Rd 2007	50.59596	-105.19902	4	104		striations
	1	642 Rd 2007	50.59596	-105.19902	4	104		striations
	1	642 Rd 2007	50.59596	-105.19902	4	116		striations
	10	Hwy 14 To Bigr	52.10304	-108.07569	2	244		striations
	10	Hwy 14 To Bigr	52.10304	-108.07569	2	263		striations
	27	St Benedict 01	52.56521	-105.38622	2	268	27	bedding planes
	27	St Benedict 01	52.56521	-105.38622	2	292	40	bedding planes
	29	West Of 6 01	49.90649	-104.72139	1	279	30	bedrock bedding plane
	30	Yorkton 01	51.30549	-102.45080	3	208	50	bedding planes
	30	Yorkton 01	51.30549	-102.45080	3	211	54	bedding planes
30	Yorkton 01	51.30549	-102.45080	3	235	50	bedding planes	
19	Qu'appelle 01	50.52443	-102.25931	2	250	22	bedding planes	

Table B. 5: Modality classification from fabric data. Numerical values related to graphing.

Site #	Site	Location		Modality	
		Lat	Long	Modality Classification	Numerical Modality
6	Glaslyn 01	53.43168	-108.53693	su	2
20	rd 304 01	54.03195	-108.65835	mm	5
20	rd 304 01	54.03195	-108.65835	sb	4
26	Rd26Cln rd CUT	53.73349	-109.13298	mm	5
26	Rd26Cln rd CUT	53.73349	-109.13298	mm	5
10	Hwy 14 To Bigr	52.10304	-108.07569	bi	3
10	Hwy 14 To Bigr	52.10304	-108.07569	su	2
1	642 Rd 01 above	50.59596	-105.19902	bi	3
1	642 Rd 01 above	50.59596	-105.19902	bi	3
31	Griffin B	49.59666	-103.43098	bi	3
31	Griffin F	49.59666	-103.43098	bi	3
29	West Of 6 01	49.90649	-104.72139	bi	3
23	Rd 734 01	50.57171	-104.52784	mm	5
23	Rd 734 01	50.57171	-104.52784	un	1
21	Rd 602 01	49.29416	-102.76859	bi	3
21	Rd 602 01	49.29416	-102.76859	su	2
9	Hwy 13 01	49.60349	-101.91140	bi	3
9	Hwy 13 01	49.60349	-101.91140	su	2
17	Moosomin 01	50.15380	-101.67263	mm	5
17	Moosomin 01	50.15380	-101.67263	su	2
11	Hwy 15 02	51.41646	-104.77922	sb	4
11	Hwy 15 02	51.41646	-104.77922	su	2

27	St Benedict 01	52.56521	-105.38622	su	2
27	St Benedict 01	52.56521	-105.38622	su	2
24	Rd 787 02	52.60954	-108.72448	sb	4
24	Rd 787 02	52.60954	-108.72448	su	2
18	North B 01	52.78370	-108.24214	mm	5
18	North B 01	52.78370	-108.24214	un	1
4	Cutknife 01	52.60952	-109.05846	mm	5
4	Cutknife 01	52.60952	-109.05846	mm	5
3	Birch Lake 01	53.42852	-108.04555	bi	3
3	Birch Lake 01	53.42852	-108.04555	un	1
12	Hwy 21 01	53.45351	-109.35652	su	2
12	Hwy 21 01	53.45351	-109.35652	su	2
7	Hepburn 01	52.57002	-106.67542	sb	4
7	Hepburn 01	52.57002	-106.67542	su	2

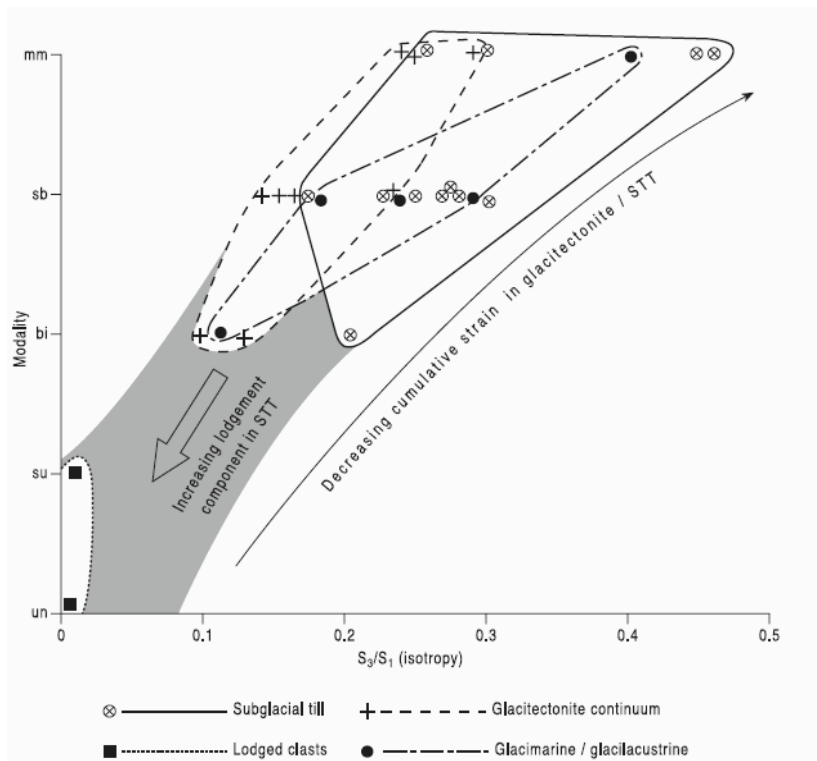


Figure B. 1: Modality Classification Curve, from Evans et al. (2007)

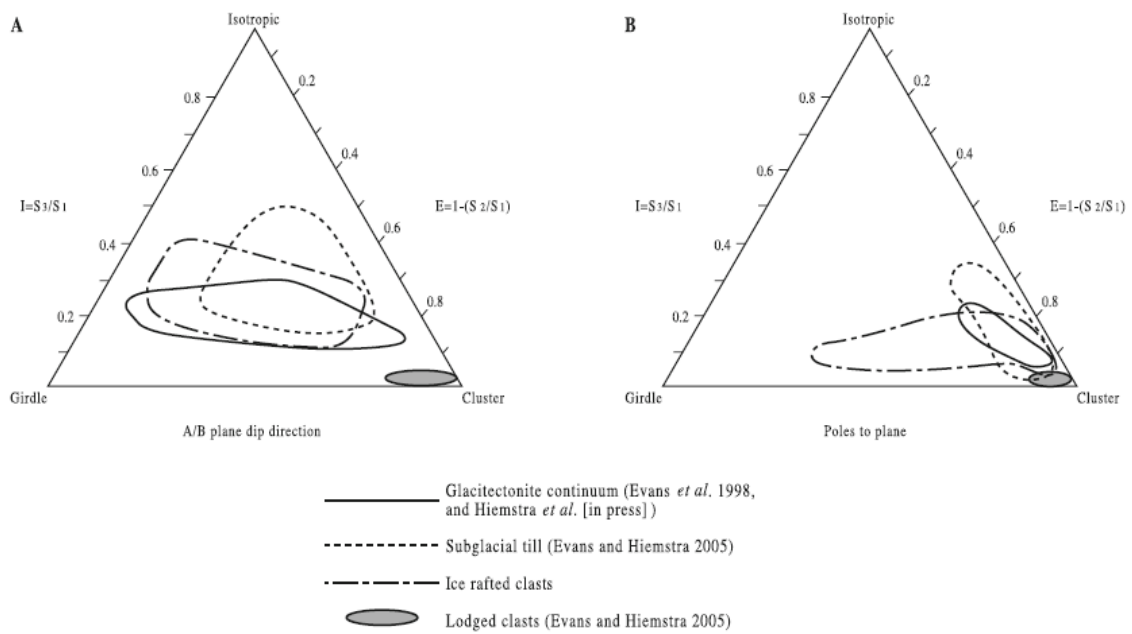


Figure B. 2: Ternary Plot classification for fabrics, from Evans et al. (2007).

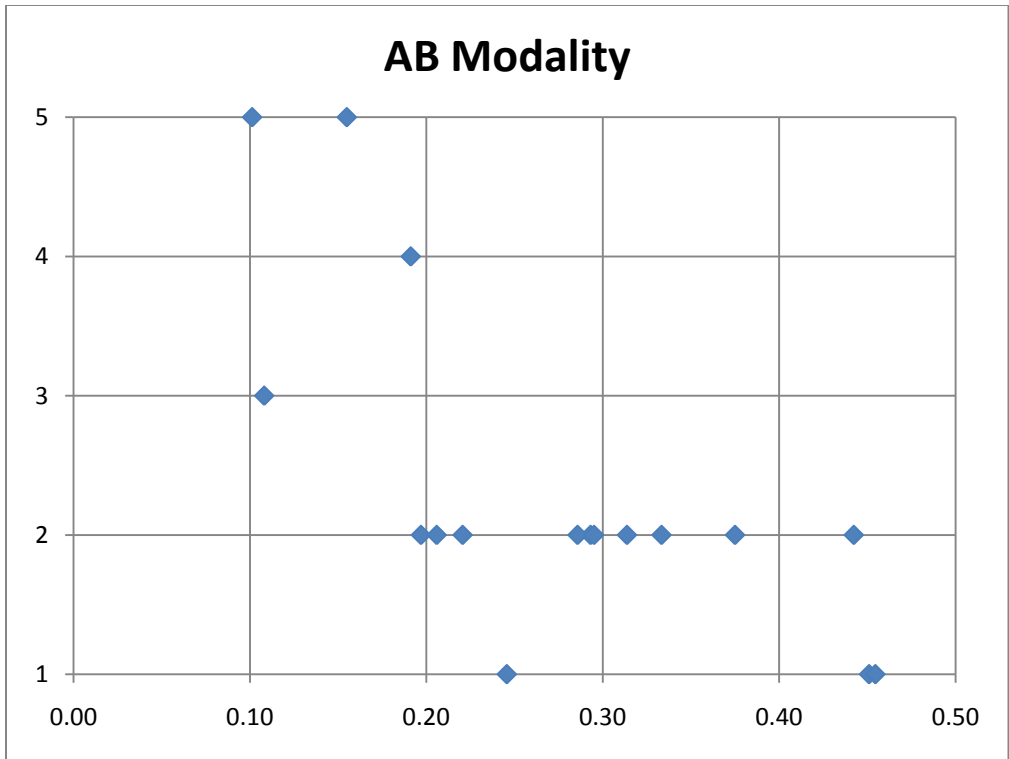


Figure B. 3: A/B Plane Modality.

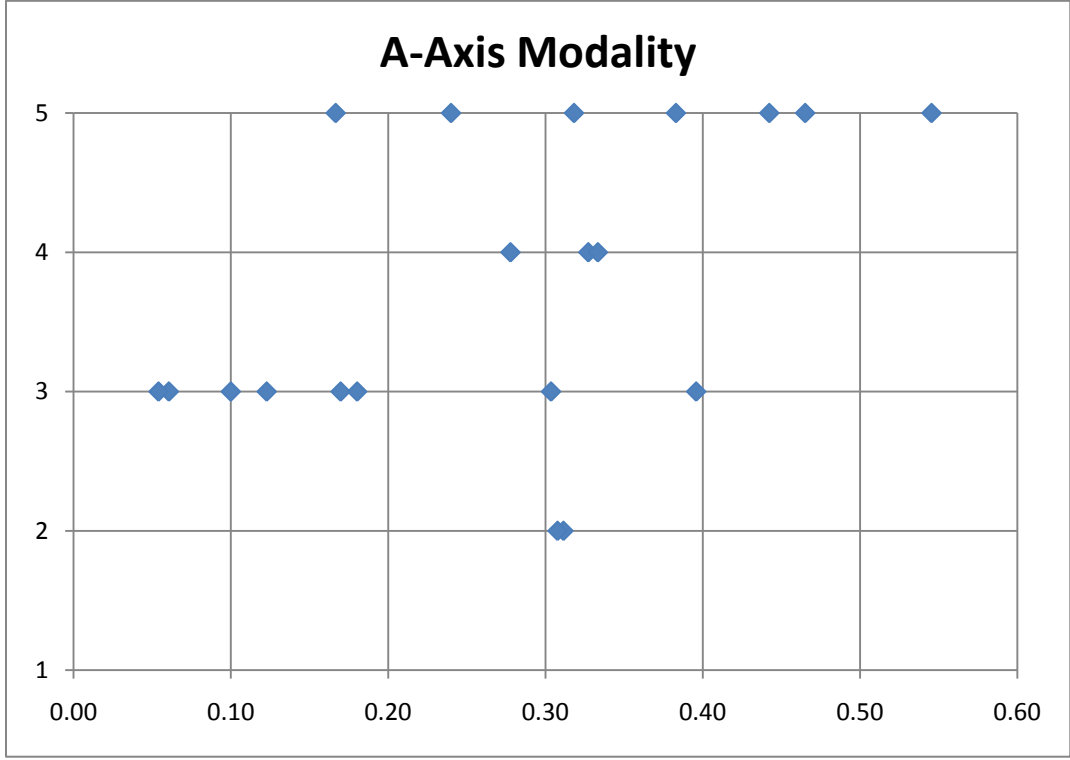


Figure B. 4: A-axis modality.

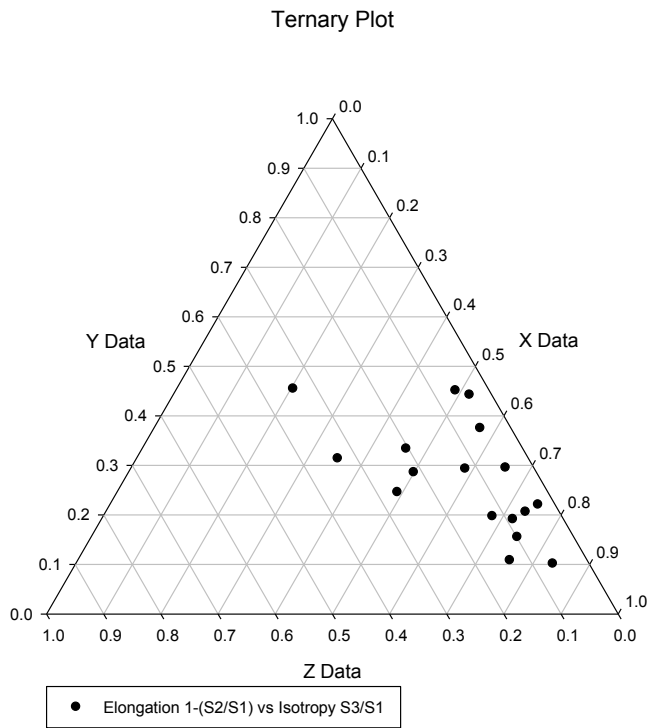


Figure B. 5: Ternary Plot of A/B plane data.

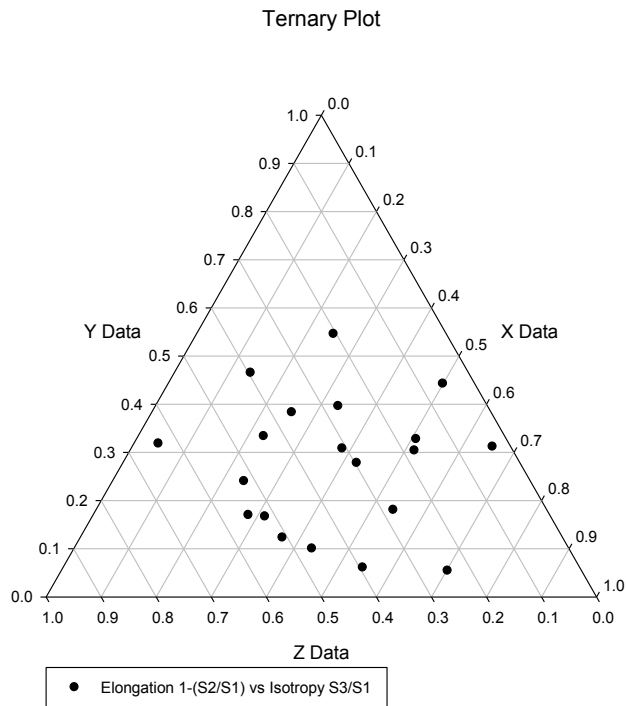


Figure B. 6: Ternary Plot of A-axis data.

Table B. 6: Geochemistry Set (1)

Site #	Sample Name	Latitude	Longitude	Ca/Al	Mg/Al	Ag ppb	Al %	As ppm	Au ppb	Ba ppm	Be ppm	Bi ppm	Br ppm	Ca %
1	642 Rd 01 below	50.59596	-105.19902	0.6323268	0.2095915	138	5.63	5	-2	800	1	0.17	1.1	3.56
1	642 Rd 01 above	50.59596	-105.19902	0.5813953	0.2724252	126	6.02	8.9	2	630	1	0.15	1.7	3.5
2	Battleford 01	52.58025	-108.35225	0.9801325	0.3609272	126	6.04	7.4	4	580	1	0.17	5.5	5.92
3	Birch Lake 01	53.42852	-108.04555	0.8579137	0.3561151	86	5.56	4.6	3	550	1	0.14	2.8	4.77
4	Cutknife 01	52.60952	-109.05846	0.5623902	0.2864675	102	5.69	5.4	2	690	1	0.14	2.9	3.2
5	Dana 01	52.28966	-105.73654	1.4294872	0.6709402	135	4.68	8.3	3	540	1	0.17	3	6.69
6	Glaslyn 01	53.43168	-108.53693	0.727451	0.2666667	87	5.1	4.2	4	580	1	0.13	3.5	3.71
7	Hepburn 01	52.57002	-106.67542	1.4816415	0.4946004	99	4.63	5.2	3	540	1	0.13	4.2	6.86
8	Hwy 02 01	52.5509	-105.72492	2.7979798	1.2424242	115	3.96	3.5	3	340	<1	0.09	3.6	11.08
9	Hwy 13 01	49.60349	-101.9114	1.7711111	0.5533333	128	4.5	7.9	3	610	<1	0.14	13	7.97
10	Hwy 14 To Biggar	52.10304	-108.07569	0.9771863	0.3821293	129	5.26	7	4	610	1	0.15	3.9	5.14
11	Hwy 15 02	51.41646	-104.77922	1.2522727	0.5181818	105	4.4	6.4	3	610	1	0.12	3.3	5.51
12	Hwy 21 01	53.45351	-109.35652	0.8745247	0.2376426	197	5.26	5.3	5	570	1	0.14	4.2	4.6
13	Hwy 52 01	51.21027	-103.25893	2.3808354	0.5479115	121	4.07	6.4	3	520	1	0.14	8.6	9.69
14	Maymont 01	52.58053	-107.75542	0.5462795	0.1869328	96	5.51	7.9	-2	750	1	0.14	2.9	3.01
15	Moose 01 B	49.75452	-102.28353	1.1121495	0.471028	150	5.35	11	4	500	1	0.25	2.9	5.95
15	Moose 01 A	49.75452	-102.28353	1.3305785	0.5082645	148	4.84	11	4	500	1	0.2	3	6.44
16	Moose 02	49.74369	-102.28125	1.7577938	0.6019185	147	4.17	12	9	490	1	0.19	3.5	7.33
17	Moosomin 01	50.1538	-101.67263	1.6456876	0.5407925	136	4.29	7.7	3	580	1	0.14	3.5	7.06
18	North B 01	52.7837	-108.24214	0.7049743	0.3447684	120	5.83	6.5	6	590	1	0.16	2.8	4.11
20	rd 304 01	54.03195	-108.65835	0.6716418	0.2425373	93	5.36	4.4	3	570	1	0.14	2.2	3.6
21	Rd 602 01	49.29416	-102.76859	1.166998	0.4691849	108	5.03	9	2	980	1	0.17	15	5.87
22	Rd 687 01	52.69628	-108.86569	0.2796209	0.1469194	66	4.22	3.7	-2	500	1	0.07	1.6	1.18
23	Rd 734 01	50.57171	-104.52784	1.8975501	0.3518931	135	4.49	7.6	4	580	1	0.15	7.8	8.52
24	Rd 787 02	52.60954	-108.72448	0.7684211	0.2842105	100	5.7	6.2	6	590	2	0.14	7	4.38
25	Rd26 GOOD SECT	53.40942	-108.99109	0.5345528	0.2886179	116	4.92	6.3	3	590	2	0.13	1.8	2.63

26	Rd26Cln rd CUT	53.73349	-109.13298	0.1381958	0.1170825	121	5.21	6.3	3	530	2	0.15	1.7	0.72
27	St Benedict 01	52.56521	-105.38622	1.5255474	0.6326034	133	4.11	8	3	520	<1	0.13	3	6.27
28	Sweetgrass 01	52.76709	-108.81116	0.4973638	0.2073814	90	5.69	6.9	4	700	1	0.16	2.8	2.83
29	West Of 6 01	49.90649	-104.72139	0.3771791	0.2139461	135	6.31	11	3	820	1	0.19	2.6	2.38
31	Griffin F	49.59666	-103.43098	0.5302491	0.2811388	120	5.62	10	4	730	1	0.19	2.7	2.98
31	Griffin B	49.59666	-103.43098	0.8624754	0.3516699	90	5.09	10	-2	710	1	0.15	4.8	4.39

Table B. 7: Geochemistry Set (2)

Site #	Sample Name	Latitude	Longitude	Cd ppm	Ce ppm	Co ppm	CO2 %	Cr ppm	Cs ppm	Cu ppm	Dy ppm	Er ppm	Eu ppm	Fe %
1	642 Rd 01 below	50.59596	-105.19902	0.27	56	8	4.25	64	3.2	16.6	2.8	1.4	0.7	2
1	642 Rd 01 above	50.59596	-105.19902	0.41	63	10	4.6	69	3.6	21.59	3.8	1.7	0.9	2.9
2	Battleford 01	52.58025	-108.35225	0.39	58	13	7.66	73	3.5	24.61	3.4	1.6	0.9	2.9
3	Birch Lake 01	53.42852	-108.04555	0.36	64	11	6.76	62	2.4	20.42	3.1	1.6	0.8	2.5
4	Cutknife 01	52.60952	-109.05846	0.34	66	11	3.9	59	2.8	19.17	3.5	1.6	0.9	2.5
5	Dana 01	52.28966	-105.73654	0.63	57	12	9.82	63	2.7	22.06	3.2	1.7	0.8	2.6
6	Glaslyn 01	53.43168	-108.53693	0.26	64	10	4.21	58	2.5	17.32	3	1.5	0.8	2.4
7	Hepburn 01	52.57002	-106.67542	0.37	57	9	9.13	49	2.2	16.92	2.9	1.4	0.7	2.3
8	Hwy 02 01	52.5509	-105.72492	0.09	37	11	19.33	49	1.2	20.3	2	1.2	0.6	2.1
9	Hwy 13 01	49.60349	-101.9114	0.44	51	10	11.01	55	2.7	18.67	2.9	1.5	0.8	2.2
10	Hwy 14 To Biggar	52.10304	-108.07569	0.37	53	10	6.51	53	3.2	20.62	2.9	1.5	0.8	2.5
11	Hwy 15 02	51.41646	-104.77922	0.53	51	10	7.52	55	2	14.96	2.6	1.3	0.7	2
12	Hwy 21 01	53.45351	-109.35652	0.36	69	11	5.29	61	2.8	19.04	2.9	1.7	0.8	2.5
13	Hwy 52 01	51.21027	-103.25893	0.39	53	9	11.56	49	2.3	17.2	2.6	1.5	0.7	2.1
14	Maymont 01	52.58053	-107.75542	0.23	53	11	3.07	77	3.4	18.09	2.8	1.4	0.7	2.6
15	Moose 01 B	49.75452	-102.28353	0.5	51	12	9.23	66	4.1	24.79	3.3	1.7	0.8	2.8
15	Moose 01 A	49.75452	-102.28353	0.5	50	11	9.82	62	3.6	22.45	3.2	1.6	0.8	2.6
16	Moose 02	49.74369	-102.28125	0.51	44	11	11.5	58	3	22.19	2.8	1.4	0.7	2.4
17	Moosomin 01	50.1538	-101.67263	0.58	49	10	10.03	50	2.4	17.66	2.8	1.5	0.8	2.1
18	North B 01	52.7837	-108.24214	0.49	66	12	5.78	66	2.8	21.7	3.4	1.7	0.9	2.7
20	rd 304 01	54.03195	-108.65835	0.38	62	12	4.28	56	2.5	18.03	3.6	1.7	0.9	2.4
21	Rd 602 01	49.29416	-102.76859	0.33	57	12	7.77	65	3.5	18.65	2.7	1.6	0.7	2.5
22	Rd 687 01	52.69628	-108.86569	0.21	54	9	0.86	35	1.7	10.05	2.6	1.3	0.7	1.7
23	Rd 734 01	50.57171	-104.52784	0.4	49	11	9.65	66	2.8	24.95	2.9	1.4	0.7	2.3
24	Rd 787 02	52.60954	-108.72448	0.34	72	12	4.95	59	2.7	18.64	3.3	1.8	0.9	2.5

25	Rd26 GOOD SECT	53.40942	-108.99109	0.31	60	10	3.73	62	2.5	18.2	3.3	1.5	0.8	2.5
26	Rd26Cln rd CUT	53.73349	-109.13298	0.15	72	10	<0.02	62	2.7	19.51	4.5	2.2	1.1	2.8
27	St Benedict 01	52.56521	-105.38622	0.56	52	10	9.65	48	1.9	18.66	2.9	1.5	0.7	2.2
28	Sweetgrass 01	52.76709	-108.81116	0.44	64	10	3.2	65	3.2	19.73	3.1	1.5	0.7	2.7
29	West Of 6 01	49.90649	-104.72139	0.31	53	12	2.32	65	3.9	21.29	3.5	1.9	0.8	2.8
31	Griffin F	49.59666	-103.43098	0.32	63	12	3.22	74	3.8	19.91	3.4	1.8	0.8	2.9
31	Griffin B	49.59666	-103.43098	0.29	54	10	6.17	69	3.1	16.79	3.2	1.6	0.8	2.6

Table B. 8: Geochemistry Set (3)

Site #	Sample Name	Latitude	Longitude	Ga ppm	Gd ppm	Hf ppm	Hg ppb	Ho ppm	Ir ppb	K %	La ppm	Li ppm	Lu ppm	Mg %
1	642 Rd 01 below	50.59596	-105.19902	11.51	3.1	6	<10	0.5	-50	1.68	27	28.7	0.2	1.18
1	642 Rd 01 above	50.59596	-105.19902	13.49	4.4	6	32	0.6	-50	1.56	32	31	0.2	1.64
2	Battleford 01	52.58025	-108.35225	14.66	4.1	4	32	0.6	-50	1.5	29	34.3	0.2	2.18
3	Birch Lake 01	53.42852	-108.04555	11.91	3.7	6	17	0.6	-50	1.7	30	30.7	0.2	1.98
4	Cutknife 01	52.60952	-109.05846	13.42	4.5	6	28	0.6	-50	1.67	32	33.3	0.2	1.63
5	Dana 01	52.28966	-105.73654	10.44	3.6	6	27	0.6	-50	1.56	28	31.8	0.2	3.14
6	Glaslyn 01	53.43168	-108.53693	12.17	3.3	6	14	0.6	-50	1.66	32	28.1	0.2	1.36
7	Hepburn 01	52.57002	-106.67542	10.58	3.3	6	13	0.5	-50	1.52	28	26.1	0.2	2.29
8	Hwy 02 01	52.5509	-105.72492	8.9	2.4	3	24	0.4	-50	1.58	18	24.3	0.2	4.92
9	Hwy 13 01	49.60349	-101.9114	11.11	4	5	26	0.5	-50	1.28	24	30.8	0.2	2.49
10	Hwy 14 To Biggar	52.10304	-108.07569	11.95	3.5	5	26	0.5	-50	1.38	25	29.5	0.2	2.01
11	Hwy 15 02	51.41646	-104.77922	8.96	3	6	20	0.5	-50	1.55	26	25.8	0.2	2.28
12	Hwy 21 01	53.45351	-109.35652	11.51	3.5	7	21	0.6	-50	1.65	33	28.7	0.2	1.25
13	Hwy 52 01	51.21027	-103.25893	9.44	2.9	6	38	0.5	-50	1.39	27	25.9	0.2	2.23
14	Maymont 01	52.58053	-107.75542	12.96	2.9	5	38	0.5	-50	1.58	26	26.9	0.2	1.03
15	Moose 01 B	49.75452	-102.28353	12.31	3.5	4	37	0.6	-50	1.5	27	33.3	0.2	2.52
15	Moose 01 A	49.75452	-102.28353	11.53	4	5	41	0.5	-50	1.25	26	28.6	0.2	2.46
16	Moose 02	49.74369	-102.28125	9.92	3	6	42	0.5	-50	1.3	23	27.1	0.2	2.51
17	Moosomin 01	50.1538	-101.67263	10.03	3.7	5	26	0.5	-50	1.31	25	24.4	0.2	2.32
18	North B 01	52.7837	-108.24214	13.02	4.1	6	23	0.7	-50	1.83	32	35.8	0.3	2.01
20	rd 304 01	54.03195	-108.65835	12.23	4.3	7	19	0.6	-50	1.77	33	29.8	0.3	1.3
21	Rd 602 01	49.29416	-102.76859	11.28	3.3	5	49	0.6	-50	1.51	28	38.2	0.2	2.36
22	Rd 687 01	52.69628	-108.86569	9.31	3	6	16	0.5	-50	1.66	27	21.8	0.2	0.62
23	Rd 734 01	50.57171	-104.52784	10.3	3.3	5	31	0.6	-50	1.35	26	26.5	0.2	1.58
24	Rd 787 02	52.60954	-108.72448	12.84	4.1	7	20	0.7	-50	1.8	35	32	0.3	1.62

25	Rd26 GOOD SECT	53.40942	-108.99109	10.89	3.6	7	34	0.6	-50	1.58	30	28.8	0.2	1.42
26	Rd26Cln rd CUT	53.73349	-109.13298	13.16	5.9	7	27	0.7	-50	1.47	38	29.7	0.3	0.61
27	St Benedict 01	52.56521	-105.38622	9.08	3.4	6	34	0.5	-50	1.45	26	23.7	0.2	2.6
28	Sweetgrass 01	52.76709	-108.81116	12.65	3.7	6	32	0.6	-50	1.81	32	32.8	0.2	1.18
29	West Of 6 01	49.90649	-104.72139	13.64	4.1	5	47	0.7	-50	1.74	29	46.8	0.2	1.35
31	Griffin F	49.59666	-103.43098	13.31	3.9	6	38	0.7	-50	1.88	30	41.3	0.3	1.58
31	Griffin B	49.59666	-103.43098	11.55	3.6	5	37	0.6	-50	1.7	28	37.3	0.2	1.79

Table B. 9: Geochemistry Set (4).

Site #	Sample Name	Latitude	Longitude	Mn ppm	Mo ppm	Na %	Nb ppm	Nd ppm	Ni ppm	P %	Pb ppm	Pr ppm	Rb ppm	S %	Sb ppm	Sc ppm	Se ppm
1	642 Rd 01 below	50.59596	-105.19902	360	0.75	1	8.45	21.9	19.9	0.059	12.01	5.6	70	<0.04	0.8	8.2	-5
1	642 Rd 01 above	50.59596	-105.19902	466	1.88	0.86	10.59	28.7	28.6	0.058	17.18	7.1	72	<0.04	0.8	10	-5
2	Battleford 01	52.58025	-108.35225	537	0.85	0.78	10.55	27	35.8	0.052	12.95	6.4	73	<0.04	0.8	10	-5
3	Birch Lake 01	53.42852	-108.04555	558	0.69	0.92	8.45	25.6	26.1	0.062	13.81	6.7	67	<0.04	0.5	8.4	-5
4	Cutknife 01	52.60952	-109.05846	474	1.21	1	9.91	30.3	26.7	0.054	12.54	7.2	73	<0.04	0.5	9	-5
5	Dana 01	52.28966	-105.73654	636	2.08	0.75	8.02	24.8	28.8	0.065	13.51	6.4	65	<0.04	0.9	8.4	-5
6	Glaslyn 01	53.43168	-108.53693	486	0.52	1	8.54	26.5	26.3	0.05	14	6.8	62	<0.04	0.5	8.7	-5
7	Hepburn 01	52.57002	-106.67542	444	0.66	0.91	7.77	23.8	21.7	0.055	14.52	6.3	60	<0.04	0.5	7.7	-5
8	Hwy 02 01	52.5509	-105.72492	425	0.83	0.88	4.95	17.7	17.9	0.045	10.27	4.4	45	<0.04	0.3	7.9	-5
9	Hwy 13 01	49.60349	-101.9114	707	1.98	0.7	8.39	23.8	27.2	0.052	12.36	5.7	61	<0.04	0.8	7.4	-5
10	Hwy 14 To Biggar	52.10304	-108.07569	488	4	0.87	8.52	23.9	28.1	0.052	11.2	5.6	69	0.91	0.7	8.6	-5
11	Hwy 15 02	51.41646	-104.77922	732	2.78	0.94	6.94	21.7	25.3	0.059	13.35	5.5	54	0.69	0.6	6.9	-5
12	Hwy 21 01	53.45351	-109.35652	493	0.7	0.89	8.83	27.5	25.8	0.062	13.74	7.4	70	<0.04	0.6	9.1	-5
13	Hwy 52 01	51.21027	-103.25893	609	1.28	0.79	7.11	22	23.5	0.061	12.63	5.6	56	<0.04	0.7	7	-5
14	Maymont 01	52.58053	-107.75542	409	0.84	1.1	8.28	20	26	0.051	13.11	5	63	<0.04	0.8	9.1	-5
15	Moose 01 B	49.75452	-102.28353	1103	2.83	0.53	9.53	25	36.1	0.06	15.7	6.5	65	<0.04	0.9	8.7	-5
15	Moose 01 A	49.75452	-102.28353	958	2.48	0.56	10.24	26.1	34.1	0.053	12.81	6.1	60	<0.04	0.9	8.3	-5
16	Moose 02	49.74369	-102.28125	1329	4.78	0.5	7.78	20.4	33.2	0.057	14.98	5	59	<0.04	1	6.9	-5
17	Moosomin 01	50.1538	-101.67263	789	2.48	0.76	8.55	24.9	28.9	0.051	12.02	5.7	55	<0.04	0.8	6.8	-5
18	North B 01	52.7837	-108.24214	596	2.48	1	8.98	28.2	30.6	0.068	15.39	7.6	76	<0.04	0.6	10	-5
20	rd 304 01	54.03195	-108.65835	527	0.84	1	9.34	32.4	25.7	0.06	14.98	8.3	68	<0.04	0.5	8.6	-5
21	Rd 602 01	49.29416	-102.76859	457	0.84	0.94	8.74	25	26.6	0.056	13.94	6.4	68	0.22	0.8	9	-5
22	Rd 687 01	52.69628	-108.86569	377	0.33	1	7.14	20.8	16.3	0.048	11.75	5.4	64	<0.04	0.3	6.1	-5
23	Rd 734 01	50.57171	-104.52784	512	0.96	0.69	7.33	24	29.7	0.058	12.72	5.9	54	<0.04	0.7	7.9	-5
24	Rd 787 02	52.60954	-108.72448	513	0.5	1	9.45	29.5	25.3	0.058	15.35	7.8	71	<0.04	0.4	9.1	-5

25	Rd26 GOOD SECT	53.40942	-108.99109	426	0.86	0.88	8.99	25.2	22.7	0.055	12.98	6.5	66	<0.04	0.5	8.7	-5
26	Rd26Cln rd CUT	53.73349	-109.13298	401	0.55	0.82	10.13	37.8	26.3	0.035	12.97	8.4	66	<0.04	0.5	9.3	-5
27	St Benedict 01	52.56521	-105.38622	610	2.37	0.83	6.58	22.9	24.6	0.064	12.89	6.2	50	<0.04	0.8	6.9	-5
28	Sweetgrass 01	52.76709	-108.81116	474	1.82	1	8.95	24.7	26.4	0.062	14.76	6.1	77	<0.04	0.8	10	-5
29	West Of 6 01	49.90649	-104.72139	586	1.35	1	9.98	26.8	31	0.071	16.77	7	70	0.17	0.8	10	-5
31	Griffin F	49.59666	-103.43098	465	1.97	1	9.51	27.8	27.7	0.065	16.47	7.1	73	0.34	0.8	10	-5
31	Griffin B	49.59666	-103.43098	467	1.13	1	10.22	23.7	24.6	0.059	14.46	6.3	70	<0.04	0.7	8.8	-5

Table B. 10: Geochemistry Set (5).

Site #	Sample Name	Latitude	Longitude	Sm ppm	Sn ppm	Sr ppm	Ta ppm	Tb ppm	Te ppm	Th ppm	Ti %	Tm ppm	U ppm	V ppm	W ppm	Y ppm	Yb ppm	Zn ppm	Zr ppm	Zr ppm
1	642 Rd 01 below	50.59596	-105.19902	4.4	1.3	201	0.8	0.4	-10	8	0.248	0.2	2.4	75	0.7	14.2	1.4	62	230	70.7
1	642 Rd 01 above	50.59596	-105.19902	5	7.4	170	0.8	0.5	-10	10	0.288	0.2	2.5	108	0.9	16.4	1.9	75.9	-200	104.4
2	Battleford 01	52.58025	-108.35225	4.6	1.4	184	0.8	0.5	-10	9.2	0.283	0.2	2.1	108	0.9	15.3	1.8	73.3	230	106.4
3	Birch Lake 01	53.42852	-108.04555	5.4	1.2	192	0.8	0.5	-10	10	0.241	0.2	2.1	76	0.6	15.6	1.5	55.1	280	108.9
4	Cutknife 01	52.60952	-109.05846	5	1.1	200	0.7	0.5	-10	10	0.271	0.2	2.2	83	0.8	15.9	1.8	59.3	-200	119.2
5	Dana 01	52.28966	-105.73654	4.5	1.2	177	0.6	0.5	-10	8.4	0.218	0.2	2.6	98	0.7	16.2	1.5	62.3	-200	85.4
6	Glaslyn 01	53.43168	-108.53693	4.9	1.5	180	0.8	0.4	-10	10	0.231	0.2	1.9	70	0.6	14.1	1.5	52.1	210	107
7	Hepburn 01	52.57002	-106.67542	4.4	1.5	187	0.9	0.5	-10	8.6	0.216	0.2	1.9	67	0.5	14	1.5	46.8	-200	98.2
8	Hwy 02 01	52.5509	-105.72492	3.1	0.8	171	0.6	0.4	-10	5.3	0.168	0.2	1.3	48	0.4	10.4	1.1	34.4	-200	78.8
9	Hwy 13 01	49.60349	-101.9114	3.8	1	219	0.7	0.5	-10	7.4	0.221	0.2	3.2	94	0.8	13.8	1.6	59.5	200	87.2
10	Hwy 14 To Biggar	52.10304	-108.07569	4.1	1	187	0.8	0.4	-10	7.7	0.237	0.2	3.1	92	0.8	13.9	1.6	63	-200	85.1
11	Hwy 15 02	51.41646	-104.77922	4	0.9	206	0.6	0.4	-10	7.6	0.198	0.2	3.7	70	0.5	14	1.3	50.9	-200	76.7
12	Hwy 21 01	53.45351	-109.35652	5.2	1.5	169	0.8	0.5	-10	10	0.25	0.2	2.1	78	0.6	16.2	1.5	49.9	340	115
13	Hwy 52 01	51.21027	-103.25893	4.1	1.1	217	0.6	0.5	-10	8.2	0.208	0.2	3.3	79	0.6	13.6	1.3	55.2	-200	79.6
14	Maymont 01	52.58053	-107.75542	4.2	1.2	240	0.8	0.4	-10	7.6	0.267	0.2	1.8	89	0.8	13.1	1.4	63.3	-200	73.8
15	Moose 01 B	49.75452	-102.28353	4.2	2.1	150	0.8	0.5	-10	7.8	0.247	0.3	2.5	131	0.8	16	1.6	81.1	-200	84.2
15	Moose 01 A	49.75452	-102.28353	4.2	1.2	143	0.8	0.5	-10	8.1	0.247	0.2	2.5	123	1	15.2	1.7	74	-200	92.7
16	Moose 02	49.74369	-102.28125	4.1	1.3	152	0.9	0.4	-10	7.3	0.199	0.2	2.9	102	0.6	13.8	1.5	70.2	260	84.4
17	Moosomin 01	50.1538	-101.67263	4	0.9	179	0.7	0.4	-10	7.5	0.23	0.2	3	86	0.7	13.7	1.5	59.9	-200	87.8
18	North B 01	52.7837	-108.24214	5	1.5	203	0.9	0.6	-10	10	0.264	0.3	2.9	93	0.7	17.4	1.7	68.2	350	114.7
20	rd 304 01	54.03195	-108.65835	5.1	1.3	181	0.8	0.6	-10	10	0.246	0.2	2	75	0.6	17	1.7	49.9	210	125.1
21	Rd 602 01	49.29416	-102.76859	4.4	1.5	274	1	0.5	-10	8.1	0.246	0.2	2	100	0.7	15.3	1.5	61.3	210	89.9
22	Rd 687 01	52.69628	-108.86569	4.2	1	153	0.6	0.4	-10	8.4	0.2	0.2	1.5	46	0.4	12.3	1.2	36.5	240	97.5
23	Rd 734 01	50.57171	-104.52784	4.2	1.4	178	0.8	0.5	-10	7.5	0.22	0.2	2	86	0.6	13.9	1.4	54.7	210	77.7
24	Rd 787 02	52.60954	-108.72448	5.4	2.6	203	0.7	0.5	-10	11	0.254	0.3	2.1	76	0.6	16.8	1.8	53.8	250	130.2

25	Rd26 GOOD SECT	53.40942	-108.99109	4.8	1.2	158	0.8	0.5	-10	8.6	0.261	0.2	1.9	73	0.6	15.6	1.6	54.7	340	110.2
26	Rd26Cln rd CUT	53.73349	-109.13298	6.9	1.1	133	1	0.6	-10	10	0.263	0.3	1.9	83	0.8	21.1	2.3	51.7	350	126.3
27	St Benedict 01	52.56521	-105.38622	4.1	0.9	176	0.6	0.4	-10	7.3	0.195	0.2	2.8	75	0.5	14.8	1.4	54.4	220	77.2
28	Sweetgrass 01	52.76709	-108.81116	5.1	1.5	200	0.8	0.4	-10	10	0.267	0.2	2.9	95	0.7	14.4	1.6	69.4	-200	93.1
29	West Of 6 01	49.90649	-104.72139	4.5	1.4	255	0.7	0.5	-10	8.6	0.3	0.2	3.3	109	1	17.1	1.7	78.9	240	96.3
31	Griffin F	49.59666	-103.43098	5	1.7	226	0.9	0.5	-10	9.1	0.28	0.2	3.5	107	0.8	16.6	1.7	74.7	290	97.3
31	Griffin B	49.59666	-103.43098	4.6	1.6	240	0.8	0.5	-10	8	0.253	0.2	2.2	94	0.7	15.7	1.7	64.8	260	87.2

Table B. 11: $^{40}\text{Ar}/^{39}\text{Ar}$ dated hornblend grains, batch results.

	Run ID	Ca/K	Mol 39Ar	%40Ar*	Age (Ma) ± Age	
Moose 02	<i>1-7 batch 1, 8-12 batch 2</i>					
	12981-12	0.22249	0.085	12.5	95.59572	3.58376
	12981-02	0.40518	0.034	64.6	176.7397	1.9222
	12981-11	-0.03839	0.041	17	182.7586	4.78847
	12981-05	0.05426	0.144	96.4	1026.672	2.33874
	12981-07	0.05724	0.338	99.4	1641.773	2.53741
	1 12981-09	1.93355	0.05	7.4	1011.058	44.22008
	2 12981-10	30.33467	0.142	95.9	1710.683	4.09109
	3 12981-03	7.17335	0.078	98.7	1756.695	3.69465
	4 12981-04	10.7341	0.02	98.3	2294.718	8.56424
	5 12981-06	14.37035	0.053	98.7	2589.541	7.19289
	6 12981-08	18.08291	0.131	82.7	2597.934	5.92686
	7 12981-01	18.13405	0.068	99.4	2932.723	6.32722
Total Average Age	1501.408					
Average Age	2127.622					
Count	12					
Archean grains (4-2.5 Ga)	3					
Proterozoic grains (2.5-.57 Ga)	6					
Younger < 570 Ma	3					
Avg Archean	2706.733					
Avg Proterozoic	1573.6					
Avg Younger	151.698					
Median	1676.228					
Standard Deviation	1005.837					
Kurtosis	-1.3293					
Skewness	-0.16656					
	Run ID	Ca/K	Mol 39Ar	%40Ar*	Age (Ma) ± Age	
Hwy 2 01						
	1 12982-04	21.63705	0.021	89.4	1390.357	7.83086
	2 12982-02	6.20487	0.025	98	1708.232	6.35968
	3 12983-04	10.89972	0.029	97.2	1709.18	6.31813
	4 12982-06	28.30011	0.013	92.4	1712.097	9.46427
	5 12982-07	8.90423	0.02	97.9	1714.01	5.88815
	6 12982-03	18.20663	0.019	91.9	1727.424	8.35643
	8 12982-05	8.33744	0.024	93.8	1757.187	6.25104
	9 12982-01	7.3437	0.084	98	1782.85	3.57041

Total Average Age	1687.667
Average Age	
Count	8
Archean grains (4-2.5 Ga)	0
Proterozoic grains (2.5-.57 Ga)	8
Younger < 570 Ma	0
Avg Archean	0
Avg Proterozoic	1687.667
Avg Younger	0
Median	1713.053
Standard Deviation	123.0813
Kurtosis	6.936082
Skewness	-2.55058

Run ID	Ca/K	Mol 39Ar	%40Ar*	Age (Ma) ± Age
--------	------	----------	--------	----------------

Dana 01

1	12983-01	12.19391	0.057	99.5	1745.267	4.2706
2	12983-02	7.37156	0.034	97.1	1974.2	6.03022
	12983-03	0.49583	0.183	99.5	1708.598	2.3664
3	12983-04	10.89972	0.029	97.2	1709.18	6.31813
4	12983-05	25.68472	0.043	97.5	1863.325	5.07376

Total Average Age	1800.114
Average Age	1822.993
Count	5
Archean grains (4-2.5 Ga)	0
Proterozoic grains (2.5-.57 Ga)	5
Younger < 570 Ma	0
Avg Archean	0
Avg Proterozoic	1800.114
Avg Younger	0
Median	1745.267
Standard Deviation	116.1402
Kurtosis	-0.56632
Skewness	1.022683

Run ID	Ca/K	Mol 39Ar	%40Ar*	Age (Ma) ± Age
--------	------	----------	--------	----------------

St Benedict 01

1-8 batch 1, 9-23 batch 2

	12985-16	0.28101	0.13	15.2	209.6987	5.55902
	12985-11	0.15261	0.073	9.7	310.1691	12.57666
	12985-15	0.04292	0.056	62.1	1512.745	8.04277
	1 12985-05	18.80698	0.009	95.7	1619.75	13.81538
	2 12985-19	1.25311	1.454	97.7	1667.974	3.53203
	3 12985-06	13.54778	0.016	99.3	1716.893	9.24084
	4 12985-07	10.37699	0.021	99.3	1717.236	7.7473
	5 12985-14	11.98707	0.209	99.3	1718.348	2.78076
	6 12985-17	8.99853	0.14	98.2	1734.502	4.02461
	7 12985-04	9.42175	0.055	98.6	1746.928	4.50481
	8 12985-13	9.0224	0.326	98.1	1750.675	3.43232
	9 12985-01	22.05654	0.034	96.8	1752.139	7.09005
	10 12985-10	36.25635	0.101	91.8	1788.821	5.19875
	11 12985-03	17.56267	0.034	94	1809.462	6.39396
	12 12985-12	14.72383	0.173	99.2	2424.251	4.45617
	13 12985-18	11.47897	0.088	97.1	2589.465	7.01868
Total Average Age		1541.342				
Average Age		1848.957				
Count		17				
Archean grains (4-2.5 Ga)		1				
Proterozoic grains (2.5-.57 Ga)		13				
Younger < 570 Ma		3				
Avg Archean		2589.465				
Avg Proterozoic		1766.133				
Avg Younger		217.8772				
Median		1718.348				
Standard Deviation		687.6356				
Kurtosis		0.905489				
Skewness		-1.10864				
	Run ID	Ca/K	Mol 39Ar	%40Ar*	Age (Ma) ± Age	
	Hepburn 01	<i>1-7 batch 1, 8-17 batch 2</i>				
	1 12987-15	25.69035	0.018	63.2	1071.504	10.12195
	2 12987-13	5.20838	1.007	97.2	1397.235	2.4689
	3 12987-04	18.49823	0.016	94.9	1603.541	10.33842
	4 12987-06	102.9249	0.005	90.1	1609.124	23.51247
	5 12987-12	18.7923	0.357	97.5	1631.267	3.37117
	6 12987-11	25.03212	0.465	98.3	1686.19	2.62357
	7 12987-03	7.94246	0.048	98.3	1686.526	5.37328
	8 12987-01	8.8724	0.091	97.8	1686.93	3.88686

9	12987-17	30.92412	0.081	95.2	1687.466	6.33914
10	12987-09	11.10272	0.197	96.1	1693.856	3.89758
11	12987-07	12.99991	0.056	96.6	1696.753	4.47624
12	12987-16	10.14385	0.846	98.5	1703.101	2.85491
13	12987-05	11.02187	0.063	91.6	1708.284	3.96109
14	12987-02	11.15158	0.04	98	1729.539	5.88741
15	12987-08	6.60599	0.47	99.2	1739.719	2.80072
16	12987-14	7.9452	0.447	99.4	1762.092	2.59579
17	12987-10	8.83297	0.154	99.4	2569.767	4.67272
Total Average Age		1686.053				
Average Age						
Count		17				
Archean grains (4-2.5 Ga)		1				
Proterozoic grains (2.5-.57 Ga)		16				
Younger < 570 Ma		0				
Avg Archean		2569.767				
Avg Proterozoic		1630.82				
Avg Younger		0				
Median		1687.466				
Standard Deviation		281.6559				
Kurtosis		7.335432				
Skewness		1.374144				
	Run ID	Ca/K	Mol 39Ar	%40Ar*	Age (Ma) ± Age	
	Rd 787 02					
	12988-07	0.25505	0.029	41.1	294.4313	3.80028
	12988-05	0.37827	0.01	87.7	1363.981	15.96194
	12988-03	0.46871	0.07	95.1	2929.972	5.44609
	1 12988-02	14.46242	0.048	97.9	1712.077	4.7743
	2 12988-04	8.618	0.082	91.3	1714.259	4.64607
	3 12988-06	9.58649	0.323	98.9	1728.386	3.17027
	4 12988-01	10.3913	0.157	99	1748.393	2.63616
Total Average Age		1641.643				
Average Age		1725.779				
Count		7				
Archean grains (4-2.5 Ga)		1				
Proterozoic grains (2.5-.57 Ga)		5				
Younger < 570 Ma		1				
Avg Archean		2929.972				

Avg Proterozoic	1653.419
Avg Younger	294.4313
Median	1714.259
Standard Deviation	772.5521
Kurtosis	2.532807
Skewness	-0.16477
Run ID Ca/K Mol 39Ar %40Ar* Age (Ma) ± Age	
North B 01	<i>1-8 batch 1, 9-20 batch 2</i>
12989-04	0.77272 0.087 48 189.456 1.55133
12989-09	0.13647 0.465 84.8 258.9145 0.75921
12989-10	0.60433 0.103 25.9 315.245 4.59443
12989-15	0.88498 0.056 15.1 1008.151 21.12137
12989-06	0.08067 0.213 98.8 1970.645 3.22964
1 12989-12	3.43246 0.004 13.9 1444.625 60.79594
2 12989-14	19.9496 0.133 97.4 1575.463 3.74064
3 12989-13	16.69858 0.103 92.7 1618.44 5.0692
4 12989-05	19.13795 0.081 97 1674.55 3.99334
5 12989-03	11.80859 0.094 99 1686.578 4.26054
6 12989-08	15.41736 0.522 97.1 1688.6 2.72524
7 12989-19	11.38768 0.097 73.5 1697.059 5.48345
8 12989-07	12.53322 0.149 98.3 1697.675 3.24385
9 12989-11	29.34226 0.13 92.4 1709.368 4.59989
10 12989-20	17.50577 0.034 98.1 1710.42 9.09916
11 12989-18	20.8168 0.058 96.8 1717.207 7.09368
12 12989-16	8.24671 0.169 98.7 1717.678 3.11297
13 12989-02	11.3806 0.057 98.6 1794.1 4.98601
14 12989-01	16.81637 0.055 98.9 1893.675 5.32688
12989-17	902.7612 0.009 5.5 1005.918 73.55721
Total Average Age	1418.688
Average Age	1687.531
Count	20
Archean grains (4-2.5 Ga)	0
Proterozoic grains (2.5-.57 Ga)	17
Younger < 570 Ma	3
Avg Archean	0
Avg Proterozoic	1624.127
Avg Younger	254.5385
Median	1687.589
Standard Deviation	555.4734

Kurtosis	0.903673					
Skewness	-1.48721					
		Run ID	Ca/K	Mol 39Ar	%40Ar*	Age (Ma) ± Age
Rd 304 01						
		12990-01	0.77232	0.018	14.7	58.1603 6.6668
		12990-04	0.09968	0.015	21.4	189.7537 7.33067
		1 12990-03	11.9679	0.062	98	1668.58 4.12597
		2 12990-05	30.46543	0.037	98	1676.465 6.61786
		3 12990-02	27.74793	0.037	98.3	1676.8 7.3028
Total Average Age	1053.952					
Average Age	1673.949					
Count	5					
Archean grains (4-2.5 Ga)	2					
Proterozoic grains (2.5-.57 Ga)	3					
Younger < 570 Ma	0					
Avg Archean	0					
Avg Proterozoic	1673.949					
Avg Younger	123.957					
Median	1668.58					
Standard Deviation	850.2456					
Kurtosis	-3.25358					
Skewness	-0.62216					

Appendix C Bedrock Geology

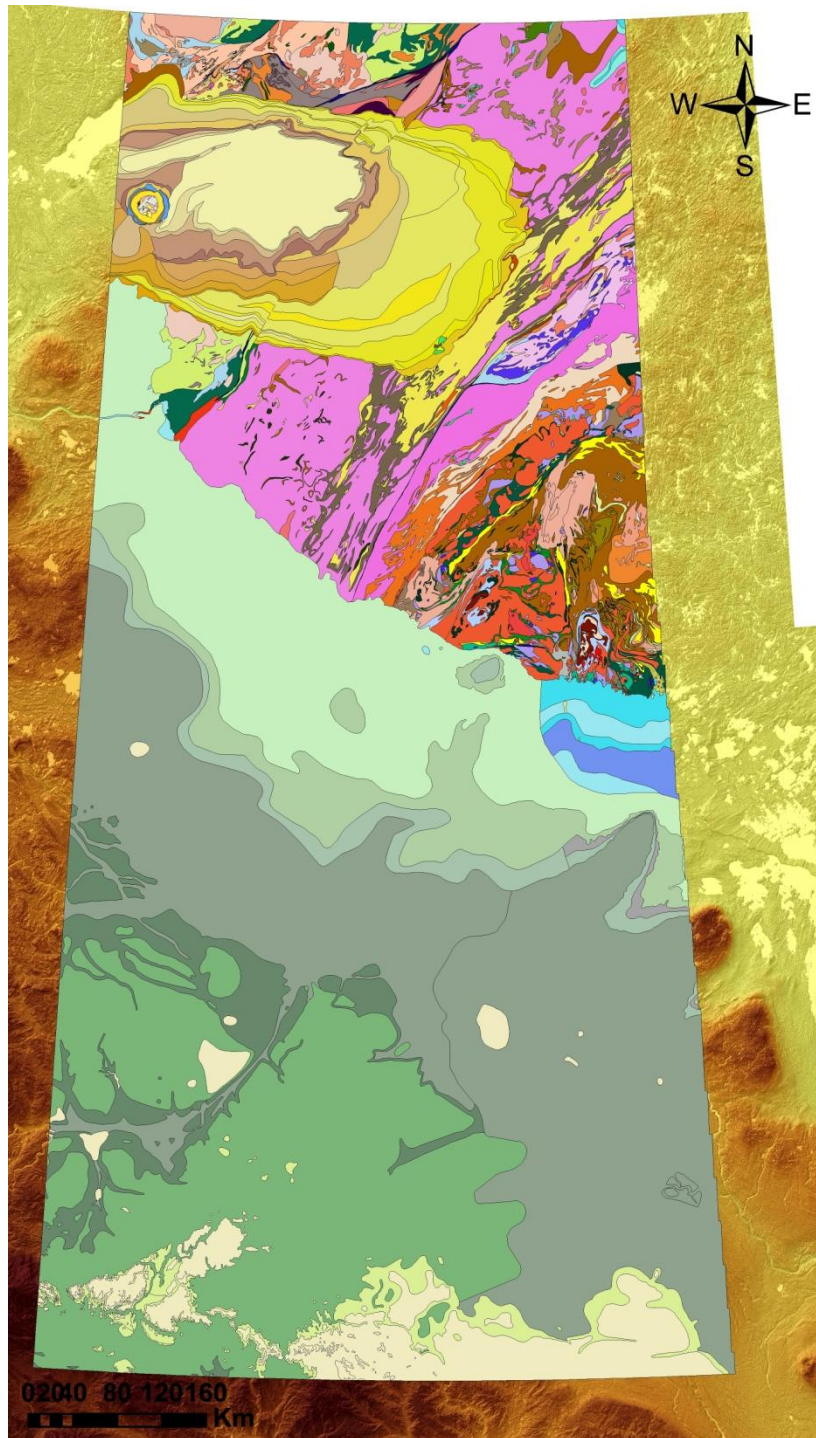
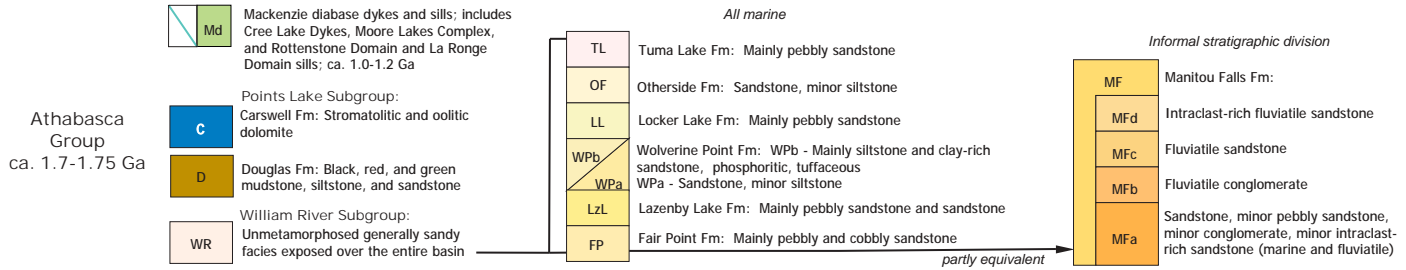


Figure C. 1: Bedrock Geology of Saskatchewan (Slimmon, 2007).

Unmetamorphosed Terrains



Metamorphosed Terrains

Rae Province		Hearne Province		Reindeer Zone	
<p>Forcie, Zemiak, Nolan, Ena, Black Bay, Beaverlodge, Nevins, Train, Dodge, Clearwater, and Western Granulite domains (R); and Tantato Domain (T)</p>		<p>Mudjatik and Virgin River domains (M), and Wollaston Domain (W)</p>		<p>Peter Lake (P), Wathamam (PW), and Rottenstone domains (PR)</p>	
<p>RM Martin Group: Arkose, sandstone, siltstone, and conglomerate; ca. 1.75-1.9 Ga?; local basic flows (RMB)</p> <p>RT Biotite-sericite schist, polymictic conglomerate, arkose, quartzite, phyllite, and basalt: Thluicho Lake Group and Waugh Lake Group</p> <p><i>unconformity</i></p> <p>RJ Junction Granite and other megacrystic granite; ca. 1.82 Ga</p> <p>Ran Clearwater Anorthosite</p> <p>Rgd Granite-granodiorite; includes Colin Granodiorite and North Shore Plutons</p> <p>Rbq Tonalite-diorite</p>	<p>Mg/Wg Late granitoid</p> <p>MH Many Islands Group (Hurwitz Group): Calcareous rock, siliceous siltstone</p> <p>MHc Dolomitic marble</p> <p><i>unconformity</i></p> <p>Wollaston Group: (Assumed to be Proterozoic)</p> <p>WH Hidden Bay Assemblage: Quartzite, amphibolite, calc-silicate rock</p> <p>Wr Calcareous arkose, arkose, minor psammopelite, and calc-silicate rock</p> <p>WJ Janice Lake Formation: Funglomerate, conglomerate, arkose</p> <p>Wp Pelitic gneiss, psammopelite</p> <p>Wd Slate, phyllite, mica schist</p> <p>Wq Quartzite-pelite assemblage, minor quartz-pebble conglomerate</p> <p><i>unconformity</i></p> <p>Wo Conglomerate, arkose, bimodal volcanics</p>	<p>Pz Sheared and refoliated rocks of the Peter Lake Complex</p> <p>Pgl Late granitoid, including the Middle Lake Granite</p> <p>PW Wathamam Granite: generally megacrystic monzogranite; ca. 1.85 Ga</p> <p>PRT Trondjhemite-tonalite derived as melts of unit PRp</p> <p>PRp Biotitic and hornblende gneiss</p> <p>PC Campbell River Group: Slate, phyllite, minor chert, psammite, mafic volcanics</p> <p>PL Peter Lake Complex: Felsic to mafelsic plutons, including the Lueza River Granite</p> <p>Pf Quartzofeldspathic granite gneiss, possibly supracrustal (Zengle Lake Gneisses)</p> <p>Pv Volcanic rocks, mainly mafic (Zangeza Bay area)</p> <p>Pbb Gabbro and diorite, including the Swan River Gabbro</p>	<p>J Late to post-tectonic aplogranite to pegmatite, including the Jan Lake Granite suite</p> <p>g Granite to tonalite</p> <p>r Arkose, polymictic conglomerate and psammite gneiss of the Amisk molasse, including Missi, Sickle, McLennan, Oorum, and Wapawekka groups</p> <p><i>unconformity</i></p> <p>Mainly post-Amisk intrusions, including "stitching" plutons of the Amisk Collage 1.88-1.83 Ga</p> <p>gd Granite-granodiorite-tonalite</p> <p>bq Tonalite-diorite</p> <p>bb (Diorite)-gabbro-(ultramafic)</p> <p>bg Gneissic gabbro-diorite</p> <p>"Amisk Collage" and equivalents: Arc to MORB volcanogenic rocks and syn-volcanic intrusions including rocks originally termed Amisk Group in the Flin Flon region and the Central Metavolcanic Belt in the La Ronge Domain; ca. 1.92-1.87 Ga</p> <p>w Greywacke, local conglomerate, iron formation, etc.</p> <p>s Schist, phyllite, siltstone</p> <p>v Volcanics, undivided</p> <p>va Acid volcanics</p> <p>vi Acid to intermediate volcanics</p> <p>vb Basic to intermediate volcanics, local ultramafics</p> <p>f Felsic gneiss, including those derived from acid volcanics</p> <p>h Felsic-mafelsic gneiss, hornblende gneiss, largely volcanogenic</p> <p>m Basite, amphibolite, and other mafic gneisses, largely volcanogenic</p> <p>sg Interlayered supracrustals and orthogneiss, undivided</p> <p>fn Felsic orthogneiss, undivided</p> <p>gs Gneiss complex, mainly plutonic with supracrustals, undivided</p>	<p>e Enderbite sill; ca. 1.83-1.82 Ga</p> <p>gg Granodiorite and related rocks, including diatexitic wacke with >70 percent melt</p> <p>wg Diatexitic greywacke and related rocks, derived from unit wn</p> <p>wn Gneissic greywacke, psammopelite to pelite, conglomerate, garnet-biotite-sillimanite-cordierite gneiss</p> <p>c Calc-silicate rock, generally psammopelitic, locally carbonaceous and sulphide-rich</p>	
<p>Rz Gneiss complex with abundant cataclases and mylonites</p> <p>Rs Supracrustal assemblage of uncertain age; includes the "Tazin Series"</p> <p>Rsm Murmac Bay Group: Mixed sediments, mafic volcanics, mafic and ultramafic sills</p> <p>Rw Greywacke, pelitic gneiss, minor psammite</p> <p>Rgg Mobilized and migmatitic rocks, including the Donaldson Lake Gneiss; ca. 2.2 Ga</p> <p>Rf Unclassified quartzofeldspathic gneiss, mainly of plutonic origin</p> <p>Rgn Granite-granodiorite gneiss</p>	<p>Mv Volcanics, predominantly basic, minor sediments, including the Virgin River Schists</p> <p>Ms Undivided, mainly sediments</p> <p>Mrp Psammite to psammopelitic gneiss</p> <p>Mp Mainly pelitic gneiss, with iron formation</p> <p>Mb Basite, including amphibolite, pyrobitite, and minor ultramafic</p> <p>Mc Calc-silicate rock, minor marble; including possible Hurwitz Group</p>	<p>Pf Quartzofeldspathic granite gneiss, possibly supracrustal (Zengle Lake Gneisses)</p> <p>Pv Volcanic rocks, mainly mafic (Zangeza Bay area)</p>	<p>va Acid volcanics</p> <p>vi Acid to intermediate volcanics</p> <p>vb Basic to intermediate volcanics, local ultramafics</p> <p>f Felsic gneiss, including those derived from acid volcanics</p> <p>h Felsic-mafelsic gneiss, hornblende gneiss, largely volcanogenic</p> <p>m Basite, amphibolite, and other mafic gneisses, largely volcanogenic</p> <p>sg Interlayered supracrustals and orthogneiss, undivided</p> <p>fn Felsic orthogneiss, undivided</p> <p>gs Gneiss complex, mainly plutonic with supracrustals, undivided</p>	<p>AS, AI Sahli and McMillan Point granites (AS): Gneissic charnockite; Iskwtikan and Hunter Bay domes (AI): gneissic granodiorite; ca. 2.45 Ga?</p> <p>Az Strongly deformed to mylonitic gneiss of the Pelican Décollement Zone and Guncoat Gneiss</p> <p>Ap Migmatitic pelite</p> <p>AQ Strongly foliated leucogranodiorite and tonalite ("Q Gneiss"); ca. 3.0 Ga?</p>	
<p>RNg Nolan Complex: Largely felsic plutons; ca. 2.65 Ga</p> <p>RFG Foot Bay Gneiss: Granitoid gneiss; ca. 2.5 Ga</p> <p>RLg Lodge Bay Granite; ca. 3.0 Ga</p> <p>Various retrograded granulite facies rocks, probably largely Archean:</p> <p>Ra Felsic-mafelsic gneiss, largely interpreted as metaplutonic</p> <p>Rb Mafic-mafelsic gneiss, largely interpreted as metaplutonic, "blue quartz" gneiss</p> <p>Rm Basite, including pyrobitite, amphibolite, and ultramafics</p> <p>Rhf Hypersthene-feldspar gneiss</p> <p>Rgf Garnet-feldspar rock, minor quartzite and iron formation; largely diatexitic (Rgf(m) = retrometamorphosed)</p> <p>Rp Mainly psammopelitic-psammite sediment</p>	<p>MR Rankin-Ennadai Greenstone Belt: basic volcanics, minor felsics, greywacke and iron formation; ca. 2.68 Ga</p> <p>Mf Felsic gneiss, mainly plutonic</p> <p>Wf Felsic orthogneiss ("Wollaston Basement inliers")</p>	<p>Pv Volcanic rocks, mainly mafic (Zangeza Bay area)</p>	<p>va Acid volcanics</p> <p>vi Acid to intermediate volcanics</p> <p>vb Basic to intermediate volcanics, local ultramafics</p> <p>f Felsic gneiss, including those derived from acid volcanics</p> <p>h Felsic-mafelsic gneiss, hornblende gneiss, largely volcanogenic</p> <p>m Basite, amphibolite, and other mafic gneisses, largely volcanogenic</p> <p>sg Interlayered supracrustals and orthogneiss, undivided</p> <p>fn Felsic orthogneiss, undivided</p> <p>gs Gneiss complex, mainly plutonic with supracrustals, undivided</p>	<p>AS, AI Sahli and McMillan Point granites (AS): Gneissic charnockite; Iskwtikan and Hunter Bay domes (AI): gneissic granodiorite; ca. 2.45 Ga?</p> <p>Az Strongly deformed to mylonitic gneiss of the Pelican Décollement Zone and Guncoat Gneiss</p> <p>Ap Migmatitic pelite</p> <p>AQ Strongly foliated leucogranodiorite and tonalite ("Q Gneiss"); ca. 3.0 Ga?</p>	
<p>Tg Late syntectonic and largely mylonitized granite; ca. 2.6 Ga</p> <p>Td Garnet-pyroxene diatexitic; ca. 2.6 Ga</p> <p>Tb Mafic granulite (Fond-du-Lac and Bohica Mafic complexes); ca. 2.6 Ga</p>	<p>Tp Hornblende-garnet-pyroxene orthogneiss; ca. 2.62 Ga</p> <p>Tbs Chipman Sill swarm; ca. 3.1 Ga (not shown on map)</p> <p>Tt Chipman Tonalite; ca. 3.2-3.4 Ga</p>	<p>Uncategorized and undated, all domains:</p> <p>Z Flinty mylonite, typically separating terrains</p>	<p>va Acid volcanics</p> <p>vi Acid to intermediate volcanics</p> <p>vb Basic to intermediate volcanics, local ultramafics</p> <p>f Felsic gneiss, including those derived from acid volcanics</p> <p>h Felsic-mafelsic gneiss, hornblende gneiss, largely volcanogenic</p> <p>m Basite, amphibolite, and other mafic gneisses, largely volcanogenic</p> <p>sg Interlayered supracrustals and orthogneiss, undivided</p> <p>fn Felsic orthogneiss, undivided</p> <p>gs Gneiss complex, mainly plutonic with supracrustals, undivided</p>	<p>AS, AI Sahli and McMillan Point granites (AS): Gneissic charnockite; Iskwtikan and Hunter Bay domes (AI): gneissic granodiorite; ca. 2.45 Ga?</p> <p>Az Strongly deformed to mylonitic gneiss of the Pelican Décollement Zone and Guncoat Gneiss</p> <p>Ap Migmatitic pelite</p> <p>AQ Strongly foliated leucogranodiorite and tonalite ("Q Gneiss"); ca. 3.0 Ga?</p>	

* Domain names are not all currently in use to describe geological terrains, but are included here as a historic literature reference. The Precambrian legend only attempts to indicate horizontal age equivalence in the broadest terms. Plutonic units in the Reindeer Zone are only partially dated and are not generally categorized by age at the 1:1 000 000 scale.

Appendix D Methodology

The following pages outline the methodology used in the laboratory analysis.

Hydrometer Analysis

References: ASTM Procedure for testing soils.
T.W. Lambe, Soil testing for engineers

Equipment Required

One hydrometer cylinder per sample analysed (1000 ml.).

One hydrometer cylinder for a reference column.

Thermometer to hang in reference cylinder.

Rubber stopper to fit hydrometer cylinder (# 13).

Wash bottle of DI water.

Clock with minute hand.

Mechanical stirrer.

Cylinder or beaker with 1000 ml. DI water per sample.

Hydrometer.

Preparations (Day before)

1. Weigh 10 g. of air dry sample.
Dry in oven, overnight, at 110°C.
Determine % moisture in the air dry sample.
Use this value in the calculation of "W" (do not apply "W" to sand alone).
2. Weigh 50 g. of air dry clayey soil (all tills in S. Ont.)
or
100 g. of sandy soil.
3. Place in a (250 ml or larger) beaker and add 125 ml sodium hexametaphosphate
(4% sol'n, i.e. 40 g/l).
Stir.
Let stand overnight.

4. Fill out times on Hydrometer analysis data sheet.

Readings will be taken at:	15sec.	30 min.
	30 sec.	1 hr.
	1 min.	2 hr.
	2 min.	4 hr.
	4 min.	8 hr.
	8 min.	24 hr.
	15 min.	

5. Prepare reference cylinder:

- pour 125 ml sodium hexametaphosphate into cylinder.
- add DI water until level reaches 1000 ml. mark..
- place thermometer in solution (hang it from a pencil or wire) so that it is easily read through the cylinder.
- place hydrometer (very gently) into cylinder. This is its resting place between readings. Be very careful not to drop it in, as it will hit bottom and break.

Procedure

1. Pour dispersed sample into mechanical stirrer.
Wash all sediment into stirring cup.
Add DI water until cup is just over half full.
Stir for at least one minute.
2. Pour stirred sample into hydrometer cylinder (wash all of sample in).
Add DI until within approx. 1 cm. of 1000 ml. mark.
3. Insert rubber stopper securely into top of cylinder.
Invert cylinder (with one hand on each end) vigorously for one minute (approx. 30 times minimum).
4. Quickly set cylinder down at end of one minute.
Remove stopper.
Wash any sediment off of the stopper and off of the sides of the cylinder.
Bring the water/sediment level up to the 1000 ml. mark.
5. Take timed readings.
Time zero is the moment the cylinder is set down and the stopper removed (step 4 above).
Read the temperature in the storage cylinder.
Read the composite correction (i.e. the hydrometer reading in the reference cylinder).

Notes on readings:

- Insert hydrometer very gently (do not let it twist or bob).
 - Read top of meniscus.
 - Insert hydrometer 20 sec. before reading, to allow it to stabilize.
 - When returning hydrometer to reference cylinder:
 - give it a gentle twist to remove adhered sediment, then release it (carefully) in the cylinder
 - for the first 4 readings, the hydrometer may be left in the sample cylinder
 - when recording readings be sure to record the actual time the readings were taken, if not exactly at 1 min. 2 min. etc.
6. When all readings are taken (i.e. after 24 hrs):
Insert stopper, mix suspension for one minute and repeat 15 sec, 30 sec, 1 min. and 2 min. readings.
These should be consistent with the original readings (if not - repeat until consistent readings obtained).
7. Fill out chart and do calculations.
8. For reach sample cylinder:
Wash sediment mixture through a (clean) 230 mesh sieve.
Rinse retained sediment into filter paper.
Retain and dry this filter paper.
Use this sediment for the sieve analysis.
9. Use data from sieve analysis and hydrometer calculations to plot cumulative curve.

Hydrometer calculations:

1.
$$P = \frac{Ra}{W} (100)$$

P = percentage of soil particles remaining in suspension at time of hydrometer reading.

R = corrected hydrometer reading. It is found by subtracting the composite hydrometer correction (obtained from the reading in the storage cylinder) from the hydrometer reading.

a = correction factor for variance of soil specific gravity from the assumed value of 2.65. Factors are given in Table I, p. 102, ASTM. We will assume S.G. of 2.65 so factor is 1.

W = oven-dry weight of <2 mm. soil sample. Calculate from air dry weight of original sample by deducting moisture content determined from oven drying in step 1, and weight of material coarser than screen no. 10 (2 mm.)

2.
$$D = K\sqrt{\frac{L}{T}}$$

D = diameter of particle in mm.

K = constant depending on temperature of suspension and specific gravity of soil particles. Values are given in Table III, p. 104, ASTM, a copy of which is attached.

L = effective depth. Values given in Table II, p. 103, ASTM, for various corrected hydrometer readings. A copy is attached.

T = interval of time from beginning of sedimentation to the taking of the reading in minutes.

* Hydrometer readings should be taken at 15 sec., 30 sec., 1 min., 2, 4, 8, 15, 30 min. 1 hr., 2, 4, 8 and 24 hrs.

University of Waterloo
Department of Earth Sciences

Earth 440 Quaternary Geology
Sieve Analysis

1. Put dried sediment sample from hydrometer analysis into top of series of sieves nos. 10, 18, 35, 60, 120, 230, and pan, coarsest screen at the top. Place sieves in shaker and clamp firmly. Let sieves be agitated by shaker for 15 minutes.
2. Carefully remove sediment from each screen in turn and weigh. Record weight of sediment on number 10 screen and subtract from original weight adjusted to oven dry weight to get corrected weight. Calculate percentage for each screen fraction of oven dry sample.

_____ Grain Size Analysis Sample # _____.

Sample Data:

Location _____ Depth _____ Date Begun _____.

Description _____ Tested by _____.

Mechanical Analysis:

Dry Sample Weight _____ gm.

Correction Factor _____ (% moisture)

Weight retained on # 10 sieve _____ gm.

Corrected Weight _____ gm.

Sieve #	Wt. Retained	% W. retained	Cum. % W. retained	Cum. % passing
18				
35				
60				
120				
230				
Pan				

Plotting Cumulative Curve

1. Plot the size distribution cumulative curve of the till on semi-log graph paper. Plot sieve data on the basis of percent passing (finer than) a given size. Label axes clearly. All curves should plot 100% at 2 mm. (# 10 sieve). Plot data points clearly so they show well after curve drawn in. *See example on separate sheet.*

Both sieve and hydrometer results should be plotted on the same sheet to yield a single curve. Plot P from hydrometer data.

2. Determine the % sand, % silt, and % clay from the curve at the 62 μ and 2 μ intersections. Also determine the first and third quartiles and median diameter where possible - i.e. some tills are so rich in clay that the curve does not intersect all quartiles.
3. Determine Trask's sorting and skewness values according to the following formulae:

$$s_o = \sqrt{Q_3/Q_1} \quad S_k = \frac{Q_1 Q_3}{Md^2} \quad \text{where} \quad S_o = \text{sorting coefficient}$$
$$S_k = \text{skewness}$$
$$Md = \text{median diameter } 50\%$$
$$Q_1 = 25\% \quad Q_3 = 75\%$$

4. Where there is a large gap (5 % or more) between hydrometer and sieve portions of curve the analysis should be repeated.

TABLE II.—VALUES OF EFFECTIVE DEPTH BASED ON HYDROMETER AND SEDIMENTATION CYLINDER OF SPECIFIED SIZES.*

Hydrometer 151H		Hydrometer 152H			
Actual Hydrometer Reading	Effective Depth, L, cm	Actual Hydrometer Reading	Effective Depth, L, cm	Actual Hydrometer Reading	Effective Depth, L, cm
1.000	16.3	0	16.3	31	11.2
1.001	16.0	1	16.1	32	11.1
1.002	15.8	2	16.0	33	10.9
1.003	15.5	3	15.8	34	10.7
1.004	15.2	4	15.6	35	10.6
1.005	15.0	5	15.5		
1.006	14.7	6	15.3	36	10.4
1.007	14.4	7	15.2	37	10.2
1.008	14.2	8	15.0	38	10.1
1.009	13.9	9	14.8	39	9.9
1.010	13.7	10	14.7	40	9.7
1.011	13.4	11	14.5	41	9.6
1.012	13.1	12	14.3	42	9.4
1.013	12.9	13	14.2	43	9.2
1.014	12.8	14	14.0	44	9.1
1.015	12.3	15	13.8	45	8.9
1.016	12.1	16	13.7	46	8.8
1.017	11.8	17	13.5	47	8.6
1.018	11.5	18	13.3	48	8.4
1.019	11.3	19	13.2	49	8.3
1.020	11.0	20	13.0	50	8.1
1.021	10.7	21	12.9	51	7.9
1.022	10.5	22	12.7	52	7.8
1.023	10.2	23	12.5	53	7.6
1.024	10.0	24	12.4	54	7.4
1.025	9.7	25	12.2	55	7.3
1.026	9.4	26	12.0	56	7.1
1.027	9.2	27	11.9	57	7.0
1.028	8.9	28	11.7	58	6.8
1.029	8.6	29	11.5	59	6.6
1.030	8.4	30	11.4	60	6.5
1.031	8.1				
1.032	7.8				
1.033	7.6				
1.034	7.3				
1.035	7.0				
1.036	6.8				
1.037	6.5				
1.038	6.2				

* Values of effective depth are calculated from the formula:

$$L = L_1 + \frac{1}{2} \left[L_2 - \frac{V_B}{A} \right]$$

where:

- L = effective depth, in centimeters,
 L₁ = distance along the stem of the hydrometer from the top of the bulb to the mark for a hydrometer reading, in centimeters,
 L₂ = overall length of the hydrometer bulb, in centimeters,
 V_B = volume of hydrometer bulb, in cubic centimeters,
 A = cross-sectional area of sedimentation cylinder, in square centimeters.

Values used in calculating the values in Table II are as follows:

For both hydrometers, 151H and 152H:

- L₂ = 14.0 cm
 V_B = 67.0 cu cm
 A = 27.8 sq cm

For hydrometer 151H:

- L₁ = 10.5 cm for a reading of 1.000
 = 2.3 cm for a reading of 1.031

For hydrometer 152H:

- L₁ = 10.5 cm for a reading of 0 g per liter
 = 2.3 cm for a reading of 50 g per liter

P = percentage of soil remaining in suspension at the level at which the hydrometer measures the density of the suspension,
R = hydrometer reading with composite correction applied (Section 6),
 be calculated according to Stokes' law (Note 14), on the basis that a particle of this diameter was at the surface of the suspension at the beginning of sedimentation and had settled to the level at which the hydrometer is measuring the density of the suspension.

TABLE III.—VALUES OF *K* FOR USE IN FORMULA FOR COMPUTING DIAMETER OF PARTICLE IN HYDROMETER ANALYSIS.

Temperature, deg C	Specific Gravity of Soil Particles								
	2.45	2.50	2.55	2.60	2.65	2.70	2.75	2.80	2.85
16.....	0.01510	0.01505	0.01481	0.01457	0.01435	0.01414	0.01394	0.01374	0.01356
17.....	0.01511	0.01486	0.01462	0.01439	0.01417	0.01396	0.01376	0.01356	0.01338
18.....	0.01492	0.01467	0.01443	0.01421	0.01399	0.01378	0.01359	0.01339	0.01321
19.....	0.01474	0.01449	0.01425	0.01403	0.01382	0.01361	0.01342	0.01323	0.01305
20.....	0.01456	0.01431	0.01408	0.01386	0.01365	0.01344	0.01325	0.01307	0.01289
21.....	0.01438	0.01414	0.01391	0.01369	0.01348	0.01328	0.01309	0.01291	0.01273
22.....	0.01421	0.01397	0.01374	0.01353	0.01332	0.01312	0.01294	0.01276	0.01258
23.....	0.01404	0.01381	0.01358	0.01337	0.01317	0.01297	0.01279	0.01261	0.01243
24.....	0.01388	0.01365	0.01342	0.01321	0.01301	0.01282	0.01264	0.01246	0.01229
25.....	0.01372	0.01349	0.01327	0.01306	0.01286	0.01267	0.01249	0.01232	0.01215
26.....	0.01357	0.01334	0.01312	0.01291	0.01272	0.01253	0.01235	0.01218	0.01201
27.....	0.01342	0.01319	0.01297	0.01277	0.01258	0.01239	0.01221	0.01204	0.01188
28.....	0.01327	0.01304	0.01283	0.01264	0.01244	0.01225	0.01208	0.01191	0.01175
29.....	0.01312	0.01290	0.01269	0.01249	0.01230	0.01212	0.01195	0.01178	0.01162
30.....	0.01298	0.01276	0.01256	0.01236	0.01217	0.01199	0.01182	0.01165	0.01149

W = oven-dry weight of soil in a total test sample represented by weight of soil dispersed (Paragraph (b)) in grams,

G = specific gravity of the soil particles, and

*G*₁ = specific gravity of the liquid in which soil particles are suspended. Use numerical value of one in both instances in the formula. In the first instance any possible variation produces no significant effect, and in the second instance, the composite correction for *R* is based on a value of one for *G*₁.

Diameter of Soil Particles

14. (a) The diameter of a particle corresponding to the percentage indicated by a given hydrometer reading shall

According to Stokes' law:

$$D = \sqrt{\frac{30\pi}{980(G - G_1)} \times \frac{L}{T}}$$

where:

D = diameter of particle, in millimeters,

n = coefficient of viscosity of the suspending medium (in this case water) in poises (varies with changes in temperature of the suspending medium),

L = distance from the surface of the suspension to the level at which the density of the suspension is being measured, in centimeters.

(For a given hydrometer and sedimentation cylinder, values vary according to the hydrometer

University of Waterloo

Department of Earth Sciences

Earth Sciences 440 Quaternary Geology

Pebble lithology

1. Collect 105 pebbles in the field. During collection, if any rotten pebbles are encountered, their number and lithology should be noted so they can be included in the count. Collect pebbles 1 - 2" diam. If possible. Pebbles must be collected from fresh exposure, not on weathered surface.
2. Two methods of pebble identification are currently in use. If the count is done outdoors, the pebbles are each broken open with a hammer. In this case a flat boulder may be used as an anvil.

The second method is used in the laboratory and involves thorough washing of the pebbles to remove any mud or calcareous cement.

3. With either cracked or washed pebbles, identification proceeds on 100 pebbles. The extra 5 pebbles collected are insurance in case of a miscount in the field. Pebbles for lithology must be collected separately from fabric pebbles.

Crystallines:

Many possible categories. Identify as closely as possible initially; later they may be lumped together as one or two groups. This group will include all Precambrian rocks of igneous and metamorphic origin. Only marble will effervesce with acid.

Carbonates:

Limestone - strong effervescence with acid. Easily scratched by knife. May be initially subdivided into black, white, crystalline (but not Precambrian), lithographic, fossiliferous.

Dolostone - little or no effervescence until powdered by scratching with a knife. Easily scratched by knife. May be initially subdivided into petroliferous (oily smell when cracked), porous, crinoidal, white, gray, buff, brown, sugary.

Clastics:

Shale - shaly parting or fissility; may be calcareous or non-calcareous. May be initially subdivided by fossil content, color, and acid reaction.

Siltstone - usually moderately strong effervescence with acid. Finely gritty feel and makes fine scratches on knife blade. Weathers brown and may be fissile. May be initially subdivided by color and acid reaction.

Sandstone - gritty feel, looks sandy, and may or may not be calcareous. Note color, acid reaction, degree of cementing.

Others:

Chert - may have calcareous coating but inside is non-calcareous, scratches knife blade, has conchoidal fracture. Class by color.

4. Results of detailed classification should be summarized -

e.g.	Limestone	48%
	Dolostone	25%
	Shale and Siltstone	16%
	Chert	5%
	Igneous and metamorphic	6%

The categories used in the summary will depend on lithologies encountered.